NASA CR-121008
FR-5212

NTIS: HC $10.00

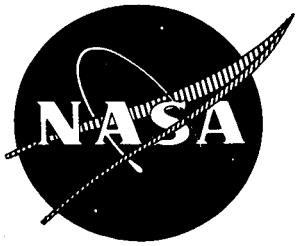

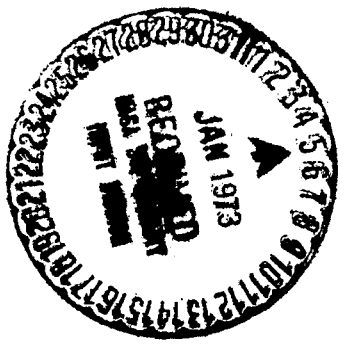

SINGLE-STAGE EXPERIMENTAL EVALUATION OF TANDEM-AIRFOIL ROTOR AND STATOR BLADING FOR COMPRESSORS

PART V - ANALYSIS AND DESIGN OF STAGES D AND E

December, 1972

by J. A. Brent, J. G. Cheatham, and D. R. Clemmons

PRATT & WHITNEY AIRCRAFT
DIVISION OF UNITED AIRCRAFT CORPORATION
FLORIDA RESEARCH AND DEVELOPMENT CENTER

Prepared for
NATIONAL AERONAUTICS AND SPACE ADMINISTRATION

NASA Lewis Research Center
Contract NAS3-11158

Reproduced by
NATIONAL TECHNICAL
INFORMATION SERVICE
U.S Department of Commerce
Springfield VA 22151

(NASA-CR-121008) SINGLE-STAGE EXPERIMENTAL EVALUATION OF TANDEM-AIRFOIL ROTOR AND STATOR BLADING J.A. Brent, et al (Pratt and Whitney Aircraft) 15 Dec. 1972 157 p CSCL 21E G3/28

N73-13779

Unclas
50248

1. Report No.	2. Government Accession No.	3. Recipient's Catalog No.
NASA CR-121008		

4. Title and Subtitle	5. Report Date
"SINGLE-STAGE EXPERIMENTAL EVALUATION OF TANDEM-AIRFOIL ROTOR AND STATOR BLADING FOR COMPRESSORS," PART V - ANALYSIS AND DESIGN OF STAGES D AND E	15 December 1972
	6. Performing Organization Code
7. Author(s)	8. Performing Organization Report No.
J. A. Brent, J. G. Cheatham, and D. R. Clemmons	FR-5212
	10. Work Unit No.
9. Performing Organization Name and Address	11. Contract or Grant No.
Pratt & Whitney Aircraft Florida Research and Development Center West Palm Beach, Florida 33402	NAS3-11158
	13. Type of Report and Period Covered
12. Sponsoring Agency Name and Address	Contractor Report
National Aeronautics and Space Administration Washington, D. C. 20546	14. Sponsoring Agency Code

15. Supplementary Notes

Project Manager, Everett E. Bailey, Fluid System Components Division, NASA-Lewis Research Center, Cleveland, Ohio 44135

16. Abstract

A conventional and a tandem bladed stage were designed for a comparative experimental evaluation in a 0.8 hub/tip ratio single-stage compressor. Based on a preliminary design study, a radially constant work input distribution was selected for the rotor designs. Velocity diagrams and blade leading and trailing edge angles selected for the conventional rotor and stator were used in the design of the tandem blading. The effects of axial velocity ratio and secondary flow on turning were included in the selection of blade leading and trailing edge angles. Design values of rotor tip velocity and stage pressure ratio were 757 ft/sec and 1.26, respectively.

Pt 1 ATS 31374
Pt 2 31375
pt ? 36764
Non others

17. Key Words (Suggested by Author(s))	18. Distribution Statement
Tandem Blading Compressor	Unclassified-Unlimited

19. Security Classif. (of this report)	20. Security Classif. (of this page)	21. No. of Pages	22. Price*
Unclassified	Unclassified	157	$3.00

* For sale by the National Technical Information Service, Springfield, Virginia 22151

FOREWORD

This report was prepared by the Pratt & Whitney Aircraft Division of United Aircraft Corporation, West Palm Beach, Florida, to describe the aerodynamic and mechanical design work conducted under Contract NAS3-11158, Task III, Single-Stage Experimental Evaluation of Tandem-Airfoil Rotor and Stator Blading for Compressors. Mr. Everett E. Bailey, NASA-Lewis Research Center, Fluid System Components Division, was Project Manager.

The requirements of NASA Policy Directive NPD 2220.4 (September 14, 1970) regarding the use of SI Units have been waived in accordance with the provisions of paragraph 5d of that Directive by the Director of Lewis Rearch Center.

CONTENTS

ILLUSTRATIONS v

TABLES ix

SUMMARY 1

INTRODUCTION 2

AERODYNAMIC DESIGN 3

Design Guidelines 3

SELECTION OF DESIGN PRESSURE RATIO AND ROTOR WORK DISTRIBUTION 4

METAL GEOMETRY SELECTION 6

Stage D 6
Stage E 13

MECHANICAL DESIGN 19

Rotor Steady-State Stress Analysis 19

Rotor D 19
Rotor E 19

Rotor Vibratory Analysis 19

Rotor D 19
Rotor E 20

Rotor Flutter Analysis 21

Rotor D 21
Rotor E 21

Rotor Attachment 22

Rotor Disk and Carrier 22

Stator Steady-State Stress Analysis 22

Stator Vibratory Analysis 24

Stator Flutter Analysis 24

Stator Attachment 25

CONTENTS (Continued)

APPENDIX A - Definition of Symbols. 109

APPENDIX B - Stage D Airfoil Coordinates 115

APPENDIX C - Stage E Airfoil Coordinates 123

APPENDIX D - References 141

ILLUSTRATIONS

FIGURE		PAGE
1	Rotor Loss Parameter vs Diffusion Factor, 10% Span From Tip	26
2	Rotor Loss Parameter vs Diffusion Factor, 30% Span From Tip	27
3	Rotor Loss Parameter vs Diffusion Factor, 50% Span	28
4	Rotor Loss Parameter vs Diffusion Factor, 70% Span From Tip	29
5	Rotor Loss Parameter vs Diffusion Factor, 90% Span From Tip	30
6	Stator Loss Parameter vs Diffusion Factor, 10% Span From Tip	31
7	Stator Loss Parameter vs Diffusion Factor, 30% Span From Tip	32
8	Stator Loss Parameter vs Diffusion Factor, 50% Span	33
9	Stator Loss Parameter vs Diffusion Factor, 70% Span From Tip	34
10	Stator Loss Parameter vs Diffusion Factor, 90% Span From Tip	35
11	Design Flowpath Dimensions for Stages D and E	36
12	Rotor Inlet Absolute Velocity Distribution	37
13	Effect of Rotor Inlet Velocity Profile on Rotor Inlet Relative Air Angle	38
14	Effect of Compressor Inlet Velocity on Rotor and Stator Performance	39
15	Effect of Rotor Work Distribution on Rotor Loading, Stator Loading, and Stage Exit Axial Velocity for Rotor Pressure Ratio of 1.28	40
16	Effect of Rotor Work Distribution on Rotor Loading, Stator Loading, and Stage Exit Axial Velocity for Rotor Pressure Ratio of 1.32	41
17	Effect of Pressure Ratio on Constant Work Stages	42
18	Stage Inlet and Exit Axial Velocity Distributions for Stages D and E	43
19	Rotor and Stator Diffusion Factor Distributions for Stages D and E	44
20	Rotor and Stator Loss Distributions for Stages D and E	45

ILLUSTRATIONS (Continued)

FIGURE		PAGE
21	Rotor and Stator Exit Pressure Profiles for Stages D and E	46
22	Effect of Axial Velocity Ratio and Secondary Flow Corrections on Rotor Exit Air Angle	47
23	Effect of Axial Velocity Ratio and Secondary Flow Corrections on Stator Exit Air Angle	48
24	Predicted Values of Rotor Exit Air Angle and Axial Velocity Ratio for Stages D and E	49
25	Rotors D and E Incidence and Deviation Angle Distributions	50
26	Rotor D Camber Angle Distribution	51
27	Comparison of Stator Camber Angle Distributions	52
28	Stators D and E Incidence and Deviation Angle Distributions	53
29	Stator D Camber Angle Distribution	54
30	Description of Technique Used to Modify Two-Dimensional Potential Flow Solution for Streamtube Convergence Through the Blade Row	55
31	Rotor E Camber Angle Distributions	56
32	Stator E Camber Angle Distributions	57
33	Rotor E Static Pressure Coefficient Distribution, 0% Span From Tip	58
34	Rotor E Blade Surface Velocities, 0% Span From Tip	59
35	Rotor E Static Pressure Coefficient Distribution, 2.5% Span From Tip	60
36	Rotor E Blade Surface Velocities, 2.5% Span From Tip	61
37	Rotor E Static Pressure Coefficient Distribution, 9.3% Span From Tip	62
38	Rotor E Blade Surface Velocities, 9.3% Span From Tip	63
39	Rotor E Static Pressure Coefficient Distribution, 12.2% Span From Tip	64
40	Rotor E Blade Surface Velocities, 12.2% Span From Tip	65
41	Rotor E Static Pressure Coefficient Distribution, 39.8% Span From Tip	66

ILLUSTRATIONS (Continued)

FIGURE		PAGE
42	Rotor E Blade Surface Velocities, 39.8% Span From Tip	67
43	Rotor E Static Pressure Coefficient Distribution, 66.5% Span From Tip	68
44	Rotor E Blade Surface Velocities, 66.5% Span From Tip	69
45	Rotor E Static Pressure Coefficient Distribution, 91.0% Span From Tip	70
46	Rotor E Blade Surface Velocities, 91.0% Span From Tip	71
47	Stator E Static Pressure Coefficient Distribution, 2.5% Span From Tip	72
48	Stator E Vane Surface Velocities, 2.5% Span From Tip	73
49	Stator E Static Pressure Coefficient Distribution, 5% Span From Tip	74
50	Stator E Vane Surface Velocities, 5% Span From Tip	75
51	Stator E Static Pressure Coefficient Distribution, 9.1% Span From Tip	76
52	Stator E Vane Surface Velocities, 9.1% Span From Tip	77
53	Stator E Static Pressure Coefficient Distribution, 20% Span From Tip	78
54	Stator E Vane Surface Velocities, 20% Span From Tip	79
55	Stator E Static Pressure Coefficient Distribution, 50% Span	80
56	Stator E Vane Surface Velocities, 50% Span	81
57	Stator E Static Pressure Coefficient Distribution, 80% Span From Tip	82
58	Stator E Vane Surface Velocities, 80% Span From Tip	83
59	Stator E Static Pressure Coefficient Distribution, 91.1% Span From Tip	84
60	Stator E Vane Surface Velocities, 91.1% Span From Tip	85
61	Stator E Static Pressure Coefficient Distribution, 95% Span From Tip	86

ILLUSTRATIONS (Continued)

FIGURE		PAGE
62	Stator E Vane Surface Velocities, 95% Span From Tip	87
63	Stator E Static Pressure Coefficient Distribution, 97.5% Span From Tip	88
64	Stator E Blade Surface Velocities, 97.5% Span From Tip	89
65	Tandem Airfoil Geometry, Simulated Double-Circular-Arc Airfoils	90
66	Calculated Rotor D Stress Distribution	91
67	Graphic Description of Tandem Rotor Analytical Model	92
68	Calculated Rotor E Stress Distributions	93
69	Rotor D Resonance Diagram for First Bending and First Torsional Mode Vibration	94
70	Rotor D Goodman Diagram	95
71	Rotor E Resonance Diagram for First Bending and First Torsional Mode Vibration	96
72	Rotor E Goodman Diagram	97
73	Calculated Rotor D First Bending and First Torsional Mode Flutter Characteristics	98
74	Calculated Rotor E First Bending and First Torsional Mode Flutter Characteristics	99
75	Calculated Stator D Stress Distribution	100
76	Calculated Stator E Stress Distributions	101
77	Stator D Resonance Diagram for First Bending and First Torsional Mode Vibration	102
78	Stator E Resonance Diagram for First Bending and First Torsional Mode Vibration	103
79	Stator D Goodman Diagram	104
80	Stator E Goodman Diagram	105
81	Calculated Stator D First Torsional Mode Flutter Characteristics	106
82	Calculated Stator E First Torsional Mode Flutter Characteristics	107
B-1	Stage D Airfoil Coordinates	115
C-1	Stage E Airfoil Coordinates	123

TABLES

TABLE		PAGE
I	Design Guidelines	3
II	Summary of Predicted Overall Performance	5
III	Rotor Vector Diagram Calculation Results	7
IV	Stator Vector Diagram Calculation Results	8
V	Effect of Axial Velocity Ratio and Secondary Flow Corrections on Rotor Exit Air Angle	10
VI	Rotor D Geometry Data	12
VII	Stator Gap-Averaged Tangential Secondary Velocity and Two-Dimensional Exit Air Angle	13
VIII	Stator D Geometry Data	14
IX	Tandem Airfoil Geometry Data	17
X	Tandem Airfoil Design Summary	18
XI	Blade Attachment Stress (6000 rpm)	23
XII	Disk and Carrier Stress (6000 rpm)	24
B-1	Stage D Airfoil Coordinates	116
C-1	Stage E Airfoil Coordinates	124

SUMMARY

Two compressor stages were designed for a comparative experimental evaluation in a 0.8 hub/tip ratio single-stage compressor. One stage was comprised of a conventional rotor and stator, and the other stage was comprised of a tandem rotor (two airfoils in series) and a tandem stator. The conventional and tandem rotors were both designed to produce a pressure ratio of 1.28 at a rotor tip velocity of 757 ft/sec. The stage pressure ratio at design flow and rotor speed was 1.26 for both stages. Predicted rotor and stage adiabatic efficiencies at design flow and rotor speed were 90% and 85%, respectively.

A preliminary design study was performed to examine the effects of work input level and distribution on the rotor and stator diffusion factors, stage exit velocity profile, and overall efficiency. Based on this study, a radially constant work input distribution and an average rotor pressure ratio of 1.28 were selected for the rotor designs. Velocity diagrams and blade leading and trailing edge angles selected for the conventional rotor and stator blading were used in the design of the tandem blading. The effects of axial velocity ratio and secondary flow on turning were included in the selection of blade leading and trailing edge angles.

Stress analyses were performed for the selected blading. These included analysis of blade attachment and disk stresses, vibratory stresses, and flutter. Materials that would provide adequate stress margins were selected for blade fabrication.

INTRODUCTION

The effectiveness of tandem airfoils as a means for increasing the loading limit and stable operating range of highly loaded compressor blade rows was investigated for the National Aeronautics and Space Administration at the Florida Research and Development Center of Pratt & Whitney Aircraft under Task I of Contract NAS3-11158 (References 1 through 3). During this program, tandem rotors demonstrated higher pressure rise and efficiency than a conventional single airfoil rotor with identical inlet and exit airfoil angles. The performance of the conventional stage was controlled to a large extent by three-dimensional flow effects associated with high losses near the walls. The three-dimensional flows resulted even though the blading was designed with increased work input near the walls to compensate for the high losses in these regions and, thereby, maintain a constant radial pressure distribution. In principle, tandem rotors improved the performance by distributing the overall aerodynamic loading between the airfoils in tandem and effectively reduced the three-dimensional flows near the walls that were present with the highly loaded conventional rotor.

Based on these results, a single-stage compressor investigation was initiated to evaluate the potential of tandem blading for improving the performance of a conventional stage designed with a selected radial work distribution that had lower work input at the walls. The radial work gradient was selected on the basis of rotor and stator diffusion factors in the end wall regions, stage exit flow profiles, and stage efficiency. The lower work input near the walls should reduce the three-dimensional flows and high wall losses that are characteristic of highly loaded blade rows and provide a comparison between a tandem stage and a conventional stage that is not characterized by a highly three-dimensional flow and associated poor performance. The aerodynamic and mechanical design of a conventional and a tandem airfoil stage is the subject of this report. The conventional single airfoil rotor and stator were designated Rotor D and Stator D. The tandem-blade rotor and stator were designated Rotor E and Stator E.

AERODYNAMIC DESIGN

Design Guidelines

The selection of the design velocity diagrams was accomplished within the range of the design guidelines given in table I.

Table I. Design Guidelines

Rotor Tip Diameter	30 in. (Minimum)
Hub/Tip Ratio	0.7 to 0.8
Rotor Tip Speed	800 ft/sec (Maximum)
Rotor Tip Diffusion Factor	Less than 0.55
Rotor Tip Solidity	1.4 to 1.5
Stator Hub Diffusion Factor	Less than 0.60
Stator Hub Solidity	1.5 or greater

In addition to the guidelines specified in table I, the following criteria were specified for the design:

1. No inlet guide vanes (axial inlet flow)
2. Axial discharge flow at the stator exit
3. Common flowpath for both stages (same as used for Reference 1 program)
4. Double-circular-arc blade sections.

To ensure a valid comparison between the conventional Stage D and the tandem blade Stage E, the velocity diagrams selected for Rotor and Stator D were used to design the tandem blading.

SELECTION OF DESIGN PRESSURE RATIO AND ROTOR WORK DISTRIBUTION

A preliminary design study of the effect of the radial distribution of work input on rotor diffusion factor, stator diffusion factor, stage exit flow profile, and efficiency was conducted to select the design rotor work distribution and pressure ratio for Stages D and E. Velocity diagrams were calculated for rotor pressure ratios of 1.28 and 1.32 for the following three radial distributions of work input: (1) constant spanwise, (2) that required to produce a constant rotor exit total pressure, and (3) parabolic (i.e., reduced work input near the walls). Velocity diagrams were also calculated for constant spanwise rotor work input at pressure ratios of 1.20 and 1.24.

The initial phase of the design study involved an updating of the loss parameter vs diffusion factor correlation presented in Reference 1. To better define the radial loss profile, the loss correlation was expanded from three span locations (10, 50, and 90%) to five span locations (10, 30, 50, 70, and 90%). The 30 and 70% span data were obtained from the same data references that were used in the three-span loss correlation (Reference 1). The five-span loss correlation was then updated by adding data from NASA-sponsored programs (References 3 through 10) and unpublished loss data from in-house single-stage compressor programs performed at FRDC. The design loss curves selected to represent the data at each percent span are shown in figures 1 through 10. The two-dimensional cascade data from figure 149 of Reference 11 and the range of compressor data shown in figure 192 of Reference 11 are included for comparison with the selected loss curves at 10, 50 and 90% span from the tip.

The velocity diagrams were calculated by means of an iteration procedure using an axisymmetric flow field calculation and the loss correlations shown in figures 1 through 10. The calculation procedure solved the continuity, energy, and radial equilibrium equations, which included the effects of streamline curvature and radial gradients of enthalpy and entropy. The Reference 1 flowpath dimensions (figure 11), a rotor tip speed of 757 ft/sec, and an equivalent flow of 110 lb/sec were maintained for the velocity diagram calculations. These values of rotor tip speed and flow are consistent with the design values used in the Reference 1 program and result in a rotor tip inlet Mach number of approximately 0.8 and a specific flow of 33 lb/sec-ft^2; these values are generally representative of current design practice for compressor middle stages.

The rotor inlet total pressure distribution from the data of the Reference 1 program was used for the velocity diagram calculations. The resulting inlet velocity distribution is shown in figure 12. This velocity distribution represents an equivalent blockage of 3.0% of the total annulus area, and no additional blockage allowance was used at the rotor inlet. Figures 13 and 14 illustrate the differences in rotor inlet relative air angle and rotor and stator diffusion factors, respectively, which are associated with the measured rotor inlet total pressure (i.e., velocity) and a constant rotor inlet total pressure for an average rotor pressure ratio of 1.28 and constant rotor work. If the higher relative

air angles near the walls for the measured total pressure (i.e., velocity) profile are ignored during the metal geometry selection, the blade sections near the walls will be operating at high incidence angles. As discussed in Reference 12, these high incidence angles can stall the blade sections near the walls and affect the blade row performance over a large portion of the blade span. As shown in figure 14, ignoring the inlet total pressure gradients near the walls also results in substantial errors in the estimated values of rotor and stator diffusion factors near the walls. A blockage allowance of 5% of the local annulus area was assumed at both the rotor exit and stator exit to account for boundary layer growth on the flowpath walls at these locations.

The resulting radial distributions of rotor diffusion factor, stator diffusion factor, and stator exit axial velocity are shown in figures 15 and 16 for the three radial distributions of work input investigated for rotor pressure ratios of 1.28 and 1.32. Rotor diffusion factor, stator diffusion factor, and stage exit axial velocity are shown in figure 17 for the three pressure ratios (i.e., 1.20, 1.24, and 1.28) investigated for constant spanwise rotor work input. The stator tip region diffusion factor and exit axial velocity are not shown in figure 16 for the parabolic rotor work condition at a rotor pressure ratio of 1.32 because as the tip region loading was increased, the total pressure losses increased at a faster rate, and the iteration between the axisymmetric flow field calculation and the loss correlation would not converge. The overall performance in terms of pressure ratio and efficiency for the eight combinations of pressure ratio and radial distribution of rotor work input are summarized in table II.

Table II. Summary of Predicted Overall Performance

Work Distribution	Rotor		Stage	
	Pressure Ratio	Adiabatic Efficiency	Pressure Ratio	Adiabatic Efficiency
Constant Work	1.204	91.6	1.196	88.3
Constant Work	1.246	90.5	1.235	86.6
Constant Work	1.282	89.9	1.265	84.8
Constant Pressure	1.295	88.1	1.272	81.1
Parabolic Work	1.283	91.9	1.271	87.6
Constant Work	1.319	88.6	1.294	82.5
Constant Pressure	1.318	87.3	1.290	80.2
Parabolic Work	1.323	88.8	*	*

*Values not available because the axisymmetric flow field calculation and loss correlation would not converge in the tip region as discussed above.

The radial diffusion factor distributions shown in figures 15 through 17 indicate that too much rotor work input near the walls causes high rotor diffusion factors, whereas, too little work input results in high stator diffusion factors and a very nonuniform stage exit axial velocity (and flow). Although the parabolic rotor work profile design resulted in the highest predicted stage efficiency, the stator end wall diffusion factors, shown in figures 15 and 16, were considerably higher than would be considered acceptable for design. Based on these results and the rotor and stator diffusion factor levels specified in table I, an average rotor pressure ratio of 1.28 with a constant radial distribution of work input was selected for the Stages D and E design. These design conditions result in a rotor diffusion factor of 0.50 at 10% span from the tip and a stator diffusion factor of 0.45 at 90% span, both of which are well within the respective maximum allowable values specified in the design guidelines shown in table I. The radial distributions of stage inlet and exit velocity for the selected rotor pressure ratio of 1.28 with constant rotor work input are shown in figure 18. As shown in figure 18, the radial distribution of the stage exit velocity is slightly more nonuniform than the inlet velocity distribution. However, a secondary objective of this program is to evaluate the impact that a stage designed with constant work input would have on other stages.

The velocity diagram calculation results selected for the Stage D and E design are shown in tables III and IV for the rotors and stators, respectively, along streamlines that pass through 5, 10, 15, 30, 50, 70, 85, 90, and 95% span at the rotor exit. The diffusion factor, loss coefficient, and exit total pressure distributions are also presented in figures 19 through 21. The predicted average rotor pressure ratio and adiabatic efficiency are 1.28 and 89.8%, respectively, at a rotor tip speed of 757 ft/sec. The predicted average pressure ratio and efficiency for the stage at design rotor speed are 1.26 and 84.8%, respectively.

METAL GEOMETRY SELECTION

Stage D

Simulated double-circular-arc airfoils (i.e., the mean camber line and the suction and pressure surface lines of each blade element are lines with a constant rate of angle change with path distance on a specified conical surface), having constant chord length were selected for the rotor and stator. The thickness-to-chord ratio distributions, chord lengths, number of blades, and the number of vanes used in the design of the Reference 1 blading were used in the design of the Stage D blading. (See pages 12 and 14.)

A study performed by Pratt & Whitney Aircraft has revealed better agreement between predicted and measured rotor and stator exit air angles when the cascade turning is modified to include the effects of axial velocity ratio and secondary flow. The predicted values both with and without the corrections for axial velocity ratio and secondary flow for the Reference 3 blading are compared with the measured values in figures 22 and 23. Therefore, this technique was used in combination with equations 286 and 288 presented in Reference 11 to select the Stage D camber and incidence angles.

Table III. Rotor Vector Diagram Calculation Results

Equivalent Rotor Speed = 4210 rpm

Equivalent Weight Flow = 110 lb/sec

	Percent Span From Tip												
	Leading Edge	Trailing Edge	V'_{1e} (ft/sec)	V_{z1e} (ft/sec)	$V'_{\theta 1e}$ (ft/sec)	β'_{1e} (deg)	U_{1e} (ft/sec)	V'_{te} (ft/sec)	V_{zte} (ft/sec)	$V'_{\theta te}$ (ft/sec)	β'_{te} (deg)	U_{te} (ft/sec)	α (deg)
Hub	96.8	95.0	758.6	458.8	608.7	53.31	608.7	416.8	371.3	193.5	27.95	610.5	1.52
	92.0	90.0	787.8	488.5	615.8	51.49	615.8	493.9	448.9	204.8	24.55	617.6	1.37
	86.9	85.0	800.7	500.5	623.8	51.21	623.8	535.6	491.5	215.9	23.72	624.7	0.89
	71.0	70.0	819.8	501.1	642.9	52.18	642.9	575.8	519.6	249.0	25.70	645.9	-1.17
	49.5	50.0	844.3	499.9	680.6	53.63	680.6	603.1	525.8	293.7	29.35	674.3	-4.21
	28.1	30.0	869.4	496.5	713.2	55.05	713.2	622.8	521.1	339.8	32.95	702.6	-7.16
	12.0	15.0	877.9	473.4	737.8	57.29	737.8	596.0	464.2	370.0	38.35	723.9	-9.37
	7.1	10.0	861.4	428.7	745.3	59.71	745.3	553.0	400.9	379.7	43.48	730.9	-9.64
Tip	3.0	5.0	837.2	375.1	751.5	64.71	751.5	483.5	270.0	388.9	53.00	738.0	-9.07

	Percent Span From Tip									
	Leading Edge	Trailing Edge	M'_{1e}	D	$\bar{\omega}'$	Loss Parameter	P_{1e} (psia)	T_{1e} (°R)	P_{te} (psia)	T_{te} (°R)
Hub	96.8	95.0	0.697	0.604	0.236	0.0604	14.427	518.7	17.765	561.14
	92.0	90.0	0.719	0.530	0.162	0.0432	14.659	518.7	18.361	561.15
	86.9	85.0	0.732	0.484	0.106	0.0288	14.694	518.7	18.735	561.14
	71.0	70.0	0.750	0.453	0.064	0.0177	14.699	518.7	19.000	561.34
	49.5	50.0	0.774	0.436	0.046	0.0129	14.693	518.7	19.063	561.34
	28.1	30.0	0.796	0.426	0.056	0.0158	14.701	518.7	19.010	561.07
	12.0	15.0	0.801	0.461	0.123	0.0335	14.602	518.7	18.465	561.28
	7.1	10.0	0.783	0.504	0.150	0.0382	14.308	518.7	17.915	561.14
Tip	3.0	5.0	0.757	0.567	0.201	0.0428	13.820	518.7	17.130	561.38

Note: $\beta_{1e} = 0$ and is constant with radius.

Table IV. Stator Vector Diagram Calculation Results

Equivalent Rotor Speed = 4210 rpm

Equivalent Weight Flow = 110 lb/sec

	Percent Span From Tip										
	Leading Edge	Trailing Edge	V_{le} (ft/sec)	V_{zle} (ft/sec)	$V_{\theta le}$ (ft/sec)	β_{le} (deg)	V_{te} (ft/sec)	V_{zte} (ft/sec)	$V_{\theta te}$ (ft/sec)	β_{te} (deg)	α (deg)
Hub	95.0	95.0	569.9	383.9	417.7	47.43	395.1	395.1	0.0	0.0	-0.29
	90.0	90.0	616.8	456.9	412.8	42.17	472.2	472.2	0.0	0.0	-0.57
	85.0	85.0	645.3	501.1	407.9	39.08	514.3	514.3	0.0	0.0	-0.86
	70.0	70.0	659.8	526.2	396.8	37.01	543.9	543.9	0.0	0.0	-1.72
	50.0	50.0	655.9	533.7	380.5	35.51	554.2	554.2	0.0	0.0	-2.86
	30.0	30.0	642.5	529.8	362.9	34.41	547.8	547.8	0.0	0.0	-4.00
	15.0	15.0	595.2	471.9	354.3	36.59	486.2	486.2	0.0	0.0	-4.86
	10.0	10.0	538.1	407.2	349.0	40.58	417.2	417.2	0.0	0.0	-5.14
Tip	5.0	5.0	450.2	208.1	349.1	49.54	298.4	298.4	0.0	0.0	-5.43

	Percent Span From Tip						
	Leading Edge	Trailing Edge	M_{le}	D	$\bar{\omega}$	Loss Parameter	P_{te} (psia)
Hub	95.0	95.0	0.5024	0.540	0.0972	0.02216	17.419
	90.0	90.0	0.5463	0.462	0.0803	0.02027	18.117
	85.0	85.0	0.5751	0.423	0.0712	0.01902	18.472
	70.0	70.0	0.5867	0.389	0.0604	0.01714	18.748
	50.0	50.0	0.5832	0.369	0.0534	0.01610	18.864
	30.0	30.0	0.5709	0.364	0.0587	0.01866	18.762
	15.0	15.0	0.5262	0.418	0.0995	0.03165	18.153
	10.0	10.0	0.4748	0.488	0.1506	0.04575	17.534
Tip	5.0	5.0	0.3958	0.630	0.1634	0.04282	16.738

For Rotor D, the turning that combines with the axial velocity ratio and secondary flow corrections to produce the required work input was calculated using the following procedure:

1. A spanwise distribution of the required axisymmetric two-dimensional rotor exit relative air angle $(\beta_{te})_{2D}$ was assumed. The initial spanwise distribution was selected to be identical to the design rotor exit air angle (β_{te}) distribution shown in table III, and subsequent selections were based on the magnitude of the corrections calculated in step 4, below.

2. The spanwise distribution of the axial velocity ratio (AVR) was calculated using the axisymmetric flow field calculation routine and the loss correlations shown in figures 1 through 10.

3. The secondary velocities due to the blade row exit streamwise vorticity and the trailing edge filament vorticity were calculated. The streamwise vorticity, which includes the distributed passage and trailing shed vorticities, was calculated using the equation for the rate of change of the vorticity given in Reference 13:

$$\left\{\text{i.e., } V' \cdot \nabla \frac{\xi}{V'} = \frac{2}{V'^4}\left[(V' \times \zeta) \times V'\right] \cdot \left[(V' \cdot \nabla)V'\right] + \frac{2}{V'^2}\left[\Omega \cdot (V' \times \zeta)\right]\right\}$$

This equation was integrated to determine the exit streamwise vorticity by making the simplifying assumption that the tangential velocity varied linearly through the blade row. The trailing edge vorticity was calculated using the method of Reference 14.

4. The assumed values of $(\beta_{te})_{2D}$ were corrected for the axial velocity ratio and secondary flow effects to obtain values of β_{te} • i.e.,

$$\beta_{te} = \arctan\left[\frac{V_{z_{te_a}}}{V_{z_{te}}} \tan(\beta_{te_a}) + \bar{v}_\theta / V_{z_{te}}\right]$$

Where: $\beta_{te_a} = \arctan\left[(AVR)_a \tan(\beta_{te})_{2D}\right]$

$V_{z_{te}}$ = exit axial velocity $(V_{z_{te_a}} + \bar{v}_z)$

$V_{z_{te_a}}$ = axisymmetric exit velocity (i.e., flow redistribution due to total pressure losses)

$(AVR)_a$ = axisymmetric axial velocity ratio

$\bar{v}_\theta$ = gap-averaged tangential secondary velocity

$\bar{v}_z$ = axial component of secondary velocity

5. The calculated values of β_{te} were compared to the design velocity diagram angles. If the calculated values of β_{te} did not agree with the design velocity diagram angles, a new spanwise distribution of the axisymmetric two-dimensional rotor exit air angle $(\beta_{te})_{2D}$ was assumed and the procedure repeated.

6. The final values of $(\beta_{te})_{2D}$ were then used, along with the known inlet conditions, to calculate the design two-dimensional turning for use in equations 286 and 288 of Reference 11 to calculate the incidence and camber angles. The three-dimensional connections given in Reference 11 were omitted since the selected turning including the effects of axial velocity ratio and secondary flow. Radial distributions of the final values for the following items are summarized in table V:

   1. Axial secondary velocity at the rotor exit $(\bar{v}_z)$
   2. Gap-averaged tangential secondary velocity at the rotor exit $(\bar{v}_\theta)$
   3. Axisymmetric two-dimensional rotor exit relative air angle $(\beta_{te})_{2D}$
   4. The correction to the rotor exit relative air angle due to secondary flow $(\Delta\beta_{te})_{SF}$
   5. The correction to the rotor exit relative air angle due to the axial velocity ratio $(\Delta\beta_{te})_{AVR}$
   6. Rotor exit relative air angle corrected for secondary flow and axial velocity ratio (β_{te}).

Table V. Effect of Axial Velocity Ratio and Secondary Flow Corrections on Rotor Exit Air Angle

	Trailing Edge Percent Span From Tip	$\bar{v}_z$	$\bar{v}_\theta$	$(\beta_{te})_{2D}$	$(\Delta\beta_{te})_{SF}$	$(\Delta\beta_{te})_{AVR}$	β_{te}
Hub	95.0	9.95	0.95	22.40	-0.49	4.64	26.55
	90.0	9.45	1.35	22.35	-0.29	1.24	23.30
	85.0	8.20	2.40	22.75	-0.12	0.37	23.00
	70.0	5.60	2.50	26.25	-0.02	-0.68	25.55
	50.0	2.55	0.55	30.55	-0.08	-1.27	29.20
	30.0	-1.10	-3.40	34.65	-0.19	-0.86	33.60
	15.0	-7.55	-7.10	38.45	-0.09	0.69	39.05
	10.0	-15.30	-3.70	40.90	0.79	1.31	43.00
Tip	5.0	-29.10	10.50	45.10	3.25	2.35	50.70

The final calculated radial distributions of the axial velocity ratio and the rotor exit relative air angle (β_{te}) are compared with the design velocity diagram values in figure 24. The simulated double-circular-arc airfoil sections selected for the rotor were positioned on conic surfaces that approximate the design streamlines of revolution, and the resulting Rotor D metal geometry on these conic surfaces is summarized in table VI. The radial distributions of camber, incidence, and deviation angles are shown in figures 25 and 26. The design velocity diagram turning given in table III and the camber and incidence angles given in table VI were used to calculate the rotor deviation angle (i.e., $\delta^\circ = \phi - \Delta\beta + i_m$).

The following procedure was used to select the stator metal geometry:

1. The secondary velocities due to the stator exit streamwise vorticity were calculated.

2. The stator exit air angles (β_{te}) were modified to include the effect of secondary flow on turning to obtain the two-dimensional exit air angle that would theoretically result in an axial exit flow (i.e., $\beta_{te} = \arctan \overline{v}_\theta / V_{zte}$).

3. The radial distributions of the gap-averaged tangential secondary velocity ($\overline{v}_\theta$) and two-dimensional exit air angle $(\beta_{te})_{2D}$ are summarized in table VII. The camber angles required to turn the flow from the design velocity diagram inlet angle to the stator exit air angle calculated in item 2 were calculated using equation 288 of Reference 11, except that the three-dimensional corrections for incidence and deviation angles were omitted.

4. The camber angles required to turn the flow from the design velocity diagram inlet angle to the design exit angle (i.e., 0 deg) were calculated using the same method used in item 3.

5. The actual design camber angles were obtained by averaging the camber angles calculated in items 3 and 4. (See figure 27.) This method was arbitrarily selected, since the predicted secondary flow resulted in more overturning near the walls than has been observed from the results of the test programs reported in References 3, 4, 5, 9, and 10.

6. The incidence angles were calculated using equation 286 of Reference 11, except that the three-dimensional correction was omitted.

7. The deviation angles were calculated from the design velocity diagram turning (table IV) and the camber and incidence angles calculated in items 5 and 6, respectively (i.e., $\delta^\circ = \phi - \Delta\beta + i_m$).

The resulting Stator D metal geometry along design streamlines is summarized in table VIII, and the radial distributions of camber, incidence, and deviation angles are shown in figures 28 and 29.

Table VI. Rotor D Geometry Data*

Airfoil: Simulated Double-Circular-Arc **

No. of Blades: 70

Chord Length: 2.57 in.

	Percent Span From Tip									
	Leading Edge	Trailing Edge	κ'_{le}	κ'_{te}	ϕ	$\gamma°$	σ	t/c	i_m	$\delta°$
Hub	96.8	95.0	52.42	15.14	37.27	33.78	1.725	0.0782	0.57	8.35
	92.0	90.0	50.91	14.15	36.75	32.53	1.705	0.0763	0.58	8.09
	86.9	85.0	50.57	14.63	35.94	32.60	1.684	0.0743	0.52	7.91
	71.0	70.0	52.04	18.64	33.40	35.34	1.627	0.0681	0.15	7.60
	49.5	50.0	53.96	23.19	30.77	38.58	1.553	0.0599	-0.36	7.30
	28.1	30.0	55.88	27.50	28.37	41.69	1.485	0.0515	-0.88	6.99
	12.0	15.0	58.51	31.53	26.98	45.02	1.439	0.0454	-1.41	6.91
	7.1	10.0	62.12	33.03	29.09	47.58	1.424	0.0433	-2.32	7.71
Tip	3.0	5.0	68.00	35.87	32.12	51.93	1.412	0.0415	-3.90	9.02

*Information included in this table is defined on planes tangent to the conic surfaces, which approximate design streamlines of revolution.

**Mean camber line and suction and pressure surface lines of each blade element are lines with a constant rate of angle change with path distance on the conic surface, which approximates the design streamline of revolution.

Table VII. Stator Gap-Averaged Tangential Secondary Velocity and Two-Dimensional Exit Air Angle

Trailing Edge Percent Span From Tip		$(\beta_{te})_{2D}$	$\bar{v}_\theta$
Hub	95.0	11.10	-48.5
	90.0	1.00	-11.5
	85.0	-0.75	7.1
	70.0	-0.95	8.9
	50.0	-0.80	7.7
	30.0	-1.35	13.0
	15.0	-0.35	3.0
	10.0	2.00	-25.2
Tip	5.0	22.70	-140.5

Rotor D and Stator D airfoil sections were designed on conic surfaces which approximate streamlines of revolution. For manufacturing purposes, the airfoil coordinates for each blade row were given on planes tangent to cylindrical surfaces normal to a radial line termed the stacking line. The airfoil sections were positioned so that the stacking line passed through the center of gravity of the sections. A computer program provided a smooth fit of the airfoil properties and produced a set of coordinates for manufacturing purposes. Coordinates for the redefined sections, which were used for manufacturing purposes, are given in Appendix B.

Stage E

Tandem Rotor E and tandem Stator E were designed for approximately an equal distribution of loading between the front and rear airfoils; loading is defined as the tangential lift produced by the airfoil. To ensure interchangeability with Stage D, the radial distribution of overall axial chord for the tandem rotor and stator blading were maintained equal to the values selected for the Stage D blading. To minimize the number of variables to be investigated in the selection of metal geometry, the maximum thickness-to-chord ratio for each of the airfoils in tandem was also maintained equal to the corresponding value selected for the Stage D blading. Simulated double-circular-arc sections were selected for both airfoils of the tandem blading. These airfoil sections were selected to closely approximate the type of blade sections used in an in-house study conducted at NASA-Lewis Research Center (Reference 15). The individual chords for the tandem blades were arbitrarily set equal, and the following procedure was used to select the metal geometry. (This procedure was used in the Reference 1 design):

1. Initial values of camber angle were assumed for the front and rear airfoils. The assumed camber angles were selected so that the passage between the blades would be slightly convergent (inlet-to-exit area ratio greater than one) to avoid undue velocity peaks or decelerations in the passage between the airfoils.

Table VIII. Stator D Geometry Data *

Airfoil: Simulated Double-Circular-Arc **

No. of Vanes: 66

Chord Length: 2.35 in.

	Percent Span From Tip									
	Leading Edge	Trailing Edge	$\varkappa_{le}$	$\varkappa_{te}$	ϕ	γ°	σ	t/c	i_m	δ°
Hub	95.0	95.0	50.16	-8.83	59.00	20.66	1.484	0.09	-2.51	8.83
	90.0	90.0	43.38	-11.31	54.70	16.03	1.468	0.09	-1.48	11.31
	85.0	85.0	40.28	-11.31	51.60	14.48	1.453	0.09	-1.08	11.31
	70.0	70.0	38.02	-10.97	49.00	13.52	1.407	0.09	-1.02	10.97
	50.0	50.0	36.68	-11.01	47.70	12.83	1.350	0.09	-1.18	11.01
	30.0	30.0	35.83	-11.66	47.50	12.08	1.298	0.09	-1.43	11.66
	15.0	15.0	38.65	-12.44	51.10	13.10	1.262	0.09	-2.15	12.44
	10.0	10.0	43.11	-12.68	55.80	15.21	1.250	0.09	-3.11	12.68
Tip	5.0	5.0	59.14	-4.85	64.00	27.14	1.238	0.09	-6.64	4.85

*Information included in this table is defined on planes tangent to the conic surfaces, which approximate design streamlines of revolution.

**Mean camber line and suction and pressure surface lines of each blade element are lines with a constant rate of angle change with path distance on the conic surface, which approximates the design streamline of revolution.

2. The individual airfoils were positioned according to the following criteria:

   a. The leading edge metal angle of the front airfoil and the trailing edge metal angle for the rear airfoil were maintained equal to the leading and trailing edge metal angles, respectively, selected for Stage D.

   b. The passage width between the blades was maintained at approximately 10% of the individual airfoil chord. This selection was based on the results of the NASA in-house analytical study of tandem blading described in Reference 15.

   c. Zero axial overlap of the front and rear airfoils was maintained for ease of fabrication; however, this selection was consistent with the cascade results presented in Reference 16 and the rotor results in Reference 17, and yielded a blade passage area ratio in the same range indicated as favorable in the NASA studies (Reference 15).

3. Blade surface pressure and velocity distributions were calculated for two-dimensional, incompressible, inviscid potential flow. For these calculations, the airfoil sections on the conic surfaces that approximate design streamlines of revolution were assumed to be double-circular-arc sections on planes tangent to the conic and rotated to planes tangent to a cylindrical surface. The axis of rotation was defined by the intersection of two planes: one plane tangent to the cylindrical surface and the second plane normal to the compressor centerline. This second plane was located midway between the blade row leading and trailing edges. The potential flow solution involved a computer program that calculated the velocity field of an infinite cascade as governed by Laplace's equation:

$$\nabla^2 \Phi = 0$$

where Φ is the velocity potential. Solutions were obtained for a zero angle of attack, 90-deg angle of attack, and circulatory flow for each airfoil, and the results superimposed in such a way that the design angle of attack was obtained and the Kutta condition satisfied. The method of solution, described in Reference 18, uses a distribution of sources on the airfoil surface and solves a set of linear algebraic equations for the source distribution that forces the total velocity normal to the airfoil surface to be zero. The total velocity is the sum of two velocities: the onset velocity, defined as the velocity field in which the body is immersed, and the disturbance velocity, defined as the velocity field caused by the source distribution. The blade surface pressure and velocity distributions thus obtained were corrected for compressibility by means of the Karman-Tsien equation.

4. The difference in the pressure surface and suction surface pressures were integrated to determine the loading (tangential lift) for each of the two airfoils in tandem.

5. The maximum suction surface-to-exit velocity ratio for each airfoil was calculated to ensure that it was not greater than 2.0. According to the results presented in Reference 19, a velocity ratio in excess of 2.0 may lead to a possible rapid increase in the airfoil boundary layer momentum thickness with a corresponding increase in loss. The maximum velocity on the suction surface was increased to reflect streamtube convergence and radius change through the blade passage that were not accounted for in the two-dimensional analysis. The amount of increase was the local difference between linear distributions of velocity from the inlet values to the exit values obtained from (1) the velocity diagram calculations and (2) the potential flow calculations, as illustrated by LC in figure 30. The velocity ratio of interest was the corrected suction surface velocity divided by the exit velocity obtained in the velocity diagram calculations.

6. The individual camber angles were changed while holding the overall total camber angle constant and the procedure repeated until approximately an equal distribution of loading was obtained between the two airfoils in tandem and no sharp velocity peaks existed in the passage between the airfoils.

The resulting spanwise camber distributions for Rotor E and Stator E are shown in figures 31 and 32, respectively, and the Stage E metal geometry is summarized in table IX.

The static pressure coefficients and velocities at the radial locations used to define the spanwise camber angle distributions are shown in figures 33 through 64 for the final tandem airfoil configurations. The maximum suction surface velocity corrected for streamtube convergence through the blade passage and the design inlet and exit velocities obtained from the velocity diagram calculations are shown on the appropriate figures. The loading splits, camber ratios, and the airfoil maximum suction surface-to-exit velocity ratios are given in table X. The blade passage overlaps, gaps, and convergences (figure 65) are also given in table X.

The Stage E airfoil sections were designed on conic surfaces, and the airfoil coordinates were given on plane surfaces tangent to cylindrical surfaces for manufacturing purposes using the same procedure used for Stage D. The Rotor E airfoil sections were positioned so that the stacking line passes through the centers of gravity of the combined airfoil sections. The Stator E airfoil sections were positioned so that the stacking line passes through the trailing edges of the front airfoil sections. Coordinates for the tandem airfoil sections which were used for manufacturing purposes are given in Appendix C.

Table IX. Tandem Airfoil Geometry Data*

Tandem Rotor E
Airfoils: Simulated Double-Circular-Arc**

Trailing Edge Percent Span From Tip	Front Body				Rear Body				Each Body	
	ϕ	κ'_{le}	κ'_{te}	$\gamma°$	ϕ	κ'_{le}	κ'_{te}	$\gamma°$	σ	t/c
91.0	13.0	51.549	38.549	45.049	27.0	41.052	14.052	27.552	0.914	0.0765
66.5	12.0	52.541	40.541	46.541	24.5	43.844	19.344	31.594	0.824	0.0666
39.8	11.0	55.172	44.172	49.672	21.0	46.486	25.486	35.986	0.815	0.0559
12.2	10.5	59.450	48.950	54.200	19.2	51.300	32.100	41.700	0.747	0.0450
9.3	12.25	62.651	50.401	56.526	19.6	52.876	33.276	43.076	0.744	0.0436
2.5	16.6	69.500	52.900	61.200	20.3	56.100	35.800	45.950	0.750	0.0418
0.0	17.5	73.600	56.100	64.850	21.2	64.000	43.000	53.500	0.727	0.0400

Tandem Stator E
Airfoils: Simulated Double-Circular-Arc**

Trailing Edge Percent Span From Tip	Front Body				Rear Body				Each Body	
	ϕ	κ_{le}	κ_{te}	$\gamma°$	ϕ	κ_{le}	κ_{te}	$\gamma°$	σ	t/c
97.5	26.0	56.207	30.207	43.207	39.0	34.008	-4.992	14.508	0.772	0.09
95.0	25.0	50.160	25.160	37.660	37.0	28.170	-8.830	9.670	0.775	0.09
91.1	24.0	44.479	20.479	32.479	35.0	24.010	-10.990	6.510	0.746	0.09
80.0	21.5	38.500	17.000	27.750	31.0	19.600	-11.400	4.100	0.696	0.09
50.0	20.0	36.680	16.680	26.680	29.5	18.490	-11.010	3.740	0.656	0.09
20.0	20.5	37.000	16.500	26.750	31.0	19.200	-11.800	3.700	0.742	0.09
9.1	25.0	45.003	20.003	32.503	34.0	22.594	-11.406	5.594	0.647	0.09
5.0	32.0	59.140	27.140	43.140	36.5	31.650	-4.850	13.400	0.649	0.09
2.5	35.0	73.000	38.000	55.500	41.0	43.200	2.200	22.700	0.653	0.09

*Information included in this table is defined on planes tangent to the conic surfaces, which approximate design streamlines of revolution.

**Mean camber line and suction and pressure surface lines of each blade element are lines with a constant rate of angle change with path distance on the conic surface, which approximates the design streamline of revolution.

Table X. Tandem Airfoil Design Summary*

Tandem Rotor E

Work Split: 50% - 50%

Trailing Edge Percent Span From Tip	Camber Ratio	Convergence F	Gap G/c	Overlap L/c	Work Split Potential Work Front	Work Split Potential Work Rear	Velocity Ratio Front	Velocity Ratio Rear
91.0	2.077	1.004	0.10	0.103	51.4	48.6	1.341	1.627
66.5	2.042	1.021	0.10	0.110	52.8	47.2	1.342	1.501
39.8	1.909	1.006	0.10	0.120	51.5	48.5	1.267	1.475
12.2	1.829	1.005	0.10	0.139	51.0	49.0	1.254	1.527
9.3	1.600	1.001	0.10	0.148	50.9	49.1	1.229	1.563
2.5	1.222	1.001	0.10	0.167	52.9	47.1	1.343	1.625
0.0	1.211	1.139	0.10	0.217	53.5	46.5	1.451	1.828

Tandem Stator E

Loading Split: 50% - 50%

Trailing Edge Percent Span From Tip	Camber Ratio	Convergence F	Gap G/c	Overlap L/c	Work Split Potential Flow Front	Work Split Potential Flow Rear	Velocity Ratio Front	Velocity Ratio Rear
97.5	1.500	1.007	0.10	0.088	53.3	46.7	1.423	1.668
95.0	1.480	1.003	0.10	0.074	52.2	47.8	1.387	1.619
91.1	1.458	1.014	0.10	0.059	53.6	46.4	1.425	1.576
80.0	1.442	1.008	0.10	0.048	53.9	46.1	1.404	1.575
50.0	1.475	1.000	0.10	0.045	51.9	48.1	1.359	1.562
20.0	1.512	1.009	0.10	0.046	50.3	49.7	1.347	1.511
9.1	1.360	1.004	0.10	0.058	52.3	47.7	1.326	1.608
5.0	1.141	1.018	0.10	0.086	48.0	52.0	1.396	1.314
2.5	1.171	1.001	0.10	0.124	53.1	46.9	1.413	1.823

*Information included in this table is defined on planes tangent to the conic surfaces which approximate design streamlines of revolution.

MECHANICAL DESIGN

Rotor Steady-State Stress Analysis

Rotor D

The stresses due to centrifugal loads and/or gas bending loads were calculated at 13 radial locations for a Rotor D airfoil fabricated from AMS 5616 (stainless steel). The reduction of gas bending stress due to centrifugal load was considered, and the resulting net gas bending stress and centrifugal tensile stress were added to yield the total blade stress at each radial location. The results of this analysis are presented in figure 66. The maximum stress for Rotor D was 12,000 psi in the leading and trailing edges of the hub. This calculated stress is well within the 0.2% yield strength of 110,000 psi for AMS 5616.

Rotor E

Preliminary analysis of the front and rear airfoil natural frequencies for Rotor E indicated that a bridge connecting the two airfoils in tandem was required to increase frequency and stiffness (thus reducing susceptibility to flutter, as will be discussed on page 21) and to ensure dimensional stability during operation. Rotor E, with a 0.060-in. thick interblade bridge at 30% span, was analyzed to determine airfoil and interblade bridge stress due to centrifugal and/or gas bending loads. To minimize centrifugal force stress, titanium (AMS 4973) was selected as the blade material in preference to stainless steel (AMS 5616). An analytical model comprised of statically loaded elastic structures represented by slender prismatic beam members was used to determine tandem blade stress. Figure 67 presents a graphic description of the analytical model. The front and rear airfoils of Rotor E were each divided into 10 elements, and the interblade bridge was divided into 3 elements. The beam members or elements were represented by their centroidal axis and analyzed as line elements. Centrifugal and aerodynamic loads were then applied to each element to yield reactions and displacements of the element or the element end, i.e., joint. These values were then used to calculate the total stress values shown in figure 68 for Rotor E. A maximum stress of 23,000 psi occurred in the leading edge of the front airfoil at the hub. The maximum interblade bridge stress was 17,800 psi. These calculated steady-state blade element stresses are well within the 0.2% yield strength of 104,000 psi for titanium (AMS 4973).

Rotor Vibratory Analysis

Rotor D

Bending and torsional vibratory frequencies were calculated for Rotor D and the results presented in terms of frequency vs rotor speed in figure 69. At design equivalent rotor speed, the calculated bending and torsional vibratory frequencies were 440 Hz and 1370 Hz, respectively. Lines representing multiples of rotor frequency (E) are shown in figure 69 to permit identification of resonant operating conditions that might possibly be encountered during testing due to upstream bearing support struts, rotating stall zones, or upstream instrumentation. As can be seen in figure 69, the first bending mode for Rotor D is close to the 6E line at 100 and 110% design equivalent rotor speed. This indicates a

potential resonance condition because there are six inlet struts. However, no resonance condition is expected because 6E excitation frequencies have not been observed during testing of similar blading in the same compressor. The lack of 6E excitation frequencies is attributed to the unequally spaced struts (t/c = 0.12) being located three chord lengths upstream of the rotor, thus providing sufficient distance for the strut wakes to be substantially dissipated prior to reaching the rotor inlet. No torsional vibratory problem is expected because of the low energy associated with the high multiples of rotor speed, shown in figure 69, required to produce a resonant condition. The excitations due to rotating stall cells would be in the range of 35 to 70 Hz at design speed and are well below any resonance frequency. Because of the relatively high resonant frequencies shown in figure 69 and the large vibratory stress margin available (as indicated by the Goodman diagram of figure 70, i.e., 56,000 psi based on the smooth fatigue strength and 19,500 psi based on the notched fatigue strength), no Rotor D vibratory problem is anticipated.

Rotor E

Bending vibratory frequencies were calculated for the individual front and rear airfoils and the bridged airfoil configuration of tandem Rotor E and the results shown in terms of frequency vs rotor speed in figure 71. The bridged blade bending frequencies were determined by restraining the front and rear airfoils at the bridge location so that bending vibratory motion was permitted in one plane, i.e., at one shroud angle. The shroud angle was then varied until both the front and rear airfoils achieved the same frequency, or theoretically vibrated together. The frequency so calculated for tandem Rotor E at design equivalent rotor speed was approximately 470 Hz. The Rotor E bending frequency approaches the 6E line at 110% design equivalent rotor speed, but, as with Rotor D, no resonance problem is anticipated for this rotor. The same technique was used to calculate the bending frequencies of the Reference 2 tandem blading, and good agreement was obtained between the measured and calculated frequencies.

Torsional vibratory frequencies calculated for the front and rear airfoils of Rotor E at design equivalent rotor speed were 740 and 770 Hz, respectively. A torsional frequency for the bridged blade configuration was not calculated. However, the bridged blade frequency is not expected to deviate substantially from the individual airfoil frequencies. When the frequencies for the Reference 2 tandem blading were recalculated using the same technique used for Rotor E, the frequencies of the individual airfoils were within 11% of the value measured for the bridged blade configurations. No torsional resonance problem is expected since, as shown in figure 71, the individual airfoil frequencies were well above the 6E excitation frequency. To illustrate the vibratory stress margin present in the design of Rotor E, a Goodman diagram for AMS 4973 is presented in figure 72. As shown in figure 72, allowable vibratory stress to failure for Rotor E was 43,500 psi based on the smooth fatigue strength and 27,500 psi based on the notched fatigue strength. Neither configuration indicated a vibratory problem.

Rotor Flutter Analysis

Rotor D

Values of the reduced velocity and incidence parameters were calculated for Rotor D at the design operating conditions and for the estimated negative and positive incidence angle operating limits between 50 and 110% design equivalent rotor speed. These results were compared to correlated flutter data for the first bending and first torsional vibratory frequencies (figure 73). The reduced velocity parameter is defined as:

$$K = \frac{12V}{\pi c \omega}$$

and the incidence parameter is defined as:

$$f(i_m) = \frac{i_m - i_{m_{ref}}}{\text{low-loss incidence range}}$$

where V, c, $i_{m_{ref}}$, and low-loss incidence range are the values for airfoil sections located at 25% span from the tip. The low-loss incidence range and $i_{m_{ref}}$ were determined from an unpublished P&WA cascade data correlation. The bending and torsional mode flutter calculations were made at Mach numbers of 0.4 and 0.6, respectively, so that the values obtained could be compared with the correlated data. No flutter problem is anticipated because, as indicated in figure 73, the operating range is in the safe operating zone. The operating region for the conventional airfoil of Reference 3, which did not encounter a flutter condition, is also shown in figure 73. Since the calculated operating region for Rotor D compares favorably with the operating region for the Reference 3 rotor, this further supports the prior conclusion that no bending or torsional flutter problems are anticipated for Rotor D.

Rotor E

Bending and torsional mode reduced velocity parameters of 2.80 and 1.76, respectively, were calculated for the front airfoil of Rotor E. Because of the high value of the reduced velocity parameter for the front airfoil, a 0.060-in. thick interblade bridge was added to Rotor E at 30% span to increase the blade natural frequency.

Bending and torsional mode reduced velocities and incidence parameters were calculated for the bridged configuration of Rotor E at the design operating point and for the estimated negative and positive incidence angle operating limits between 50 and 110% design equivalent rotor speed and the results compared to correlated flutter data in figure 74. The reduced velocities and incidence parameters for the bridged blade were calculated using the overall chord dimensions and the front airfoil incidence angles and velocities. This was done because the front airfoil of the tandem configuration is subjected to incidence angle variations, while the incidence angle variations on the rear airfoil are expected to be small because of the small variations in exit air angle from the front airfoil. The overall chord was used because the bridged blades will move together in the immediate bridge region. The Rotor E reduced velocity parameters for the bending operating range were based on the calculated bridged blade frequency.

However, since the bridged blade torsional frequency was not available, the rear airfoil frequency was used to calculate the torsional reduced velocity parameter. Because individual airfoil frequencies are expected to be less than the bridged blade frequency, any conclusion based on the individual airfoil should be conservative. Values of the reduced velocity and incidence parameter for tandem Rotor E at the design operating conditions and the estimated negative and positive incidence limits are shown in relation to correlated flutter data in figure 74. No flutter problem is anticipated. The operating region for the Reference 2 tandem blade, which did not encounter flutter, is also shown on figure 74 for comparison with the calculated operating region of Rotor E. Since the operating region for Rotor E is similar to the operating region of the Reference 2 blading, this further supports the prior conclusion that no bending or torsional flutter problems should occur during testing of Rotor E.

Rotor Attachment

Blade spindle tensile, bending, shear, and bearing stresses were calculated considering the airfoil centrifugal forces and gas bending stresses due to aerodynamic loading. The calculations were performed at a rotor speed of 6000 rpm, which is approximately 140% of design speed. The results of the stress calculations for Rotors D and E are presented in table XI. The combined tensile and bending spindle stresses calculated for Rotor D and Rotor E were 67,700 and 30,200 psi, respectively. These calculated stresses are well within the 0.2% yield strengths of 114,000 and 104,000 psi of the stainless steel (AMS 5616) and titanium (AMS 4973) selected for Rotor D and Rotor E, respectively. Similarly, calculated shear and bearing stresses of 12,900 and 84,000 psi for Rotor D and 5,760 and 37,500 psi for Rotor E, respectively, did not exceed the specified material limitation shown in table XI (i.e., allowable shear stress equals 55% of material ultimate tensile strength and allowable bearing stress equals 120% of material 0.2% yield strength). Consequently, no blade attachment stress problems are anticipated.

Rotor Disk and Carrier

The average tangential stress for the AMS 6415 (low alloy steel) rotor disk and carrier was determined through the use of a computer disk analysis program and found to be well within design practice for AMS 6415 (0.2% yield strength of 140,000 psi). The results of this analysis are presented in table XII.

Stator Steady-State Stress Analysis

The gas bending stresses in the leading and trailing edge and on the concave surface at the point of maximum thickness were calculated for Stator D and the front and rear airfoils of Stator E. Calculations were made assuming (1) the vanes would be fabricated from AMS 5613, a stainless steel that has a 0.2% yield strength of 110,000 psi and (2) the vanes were beams that would deflect as guided cantilevers about the tip. The guided cantilever about the tip condition was selected, even though the stator vanes are attached to the shrouds by trunnions at both the hub and tip, to provide a conservative estimate of the vane stresses.

Table XI. Blade Attachment Stress (6000 rpm)

Type Stress, psi	Tensile	Bending	Combined Tensile and Bending	Shear	Bearing
Rotor D AMS 5616 Stainless Steel	37,000	30,700	67,700	12,900	84,000
Maximum Allowable Stress for AMS 5616 at 200°F	114,000*	114,000*	114,000*	75,000**	136,000***
Rotor E AMS 4973 Titanium	16,500	13,700	30,200	5,760	37,500
Maximum Allowable Stress for AMS 4973 at 200°F	104,000*	104,000*	104,000*	65,000**	124,000***

*0.2% Yield Strength at 200°F
**Allowable Shear Stress = 0.55 x Ultimate Tensile Strength at 200°F
***Allowable Bearing Stress = 1.2 x 0.2% Yield Strength at 200°F

Table XII. Disk and Carrier Stress (6000 rpm)

Configuration	Rotor D	Rotor E
Disk (AMS 6415) Stress, psi	94,000	42,000
Carrier (AMS 6415) Stress, psi	62,000	27,700
0.2% Yield Strength of AMS 6415 at 100°F, psi	140,000	140,000

Some movement of the vane at the hub is possible. These stress values are shown in figure 75 for Stator D and in figure 76 for Stator E. The maximum bending stress of 2,000 psi occurred in the leading edge tip of Stator D. A maximum Stator E front airfoil bending stress of 7,300 psi (compressive) was calculated for the convex surface at the tip. The maximum rear airfoil stress was 8,300 psi and occurred in the leading edge at the tip. None of the calculated stator stresses were prohibitive because of the high yield strength of the vane material and no stress problem is anticipated.

Stator Vibratory Analysis

Bending and torsional vibratory frequencies were calculated for Stator D and Stator E front and rear airfoils and the results presented in terms of frequency vs rotor speed in figures 77 and 78. The vibratory analysis was made assuming the stators to be beams with both ends fixed (fixed-fixed mode). This assumption was permissible because stator hub and tip trunnions are held in inner and outer diameter shrouds. Lines representing multiples of rotor passing frequency (70E) are shown in the figures to permit the identification of any excitation frequencies within the operating range. Stator D bending and torsional frequencies in the fixed-fixed mode were 4650 and 4050 Hz, respectively. Stator E front and rear airfoil bending frequencies were 1820 and 1870 Hz, respectively, while the torsional frequency of the front and rear airfoils were 4200 and 4000 Hz, respectively. No vibratory fatigue problems are anticipated for either Stator D or Stator E. Because of the low steady-state stress present in these vanes, a large vibratory stress margin is available, as indicated by the Goodman diagram of figure 79 for Stator D and figure 80 for Stator E. As shown in figure 79, Stator D can withstand 56,000 psi vibratory stress based on the smooth fatigue strength and 21,000 psi based on the notched fatigue strength. Similarly shown in figure 80, both Stator E front and rear airfoils can withstand 53,000 psi vibratory stress based on the smooth fatigue strength; and 20,000 psi, based on the notched fatigue strength.

Stator Flutter Analysis

Stator D and Stator E front and rear airfoil torsional stall flutter characteristics were calculated and presented for comparison with correlated flutter

data in figures 81 and 82. The flutter variables are a reduced velocity parameter K, as defined in the rotor flutter analysis section, page 24 and an average row pressure ratio, defined as:

$$\frac{\frac{P_{le} + P_{te}}{2}}{P_{le}}$$

The values of velocity and chord used to calculate the stator reduced velocity parameter are the values at 50% span. Torsional frequencies for the stators in a fixed-fixed configuration were used in the calculations. As shown in figures 81 and 82, no flutter problems are anticipated for Stator D or the front and rear airfoils of Stator E.

Stator Attachment

Stator assembly is achieved by tack welding the cylindrical trunnions at each end of the vane into the inner and outer diameter shrouds. The cross section of primary interest for stator stress evaluation is the junction of the airfoils and trunnion. For this cross sectional area of Stator D, the calculated bending stress due to aerodynamic loading was 6,530 psi. For Stator E front and rear airfoils, this stress was 15,700 psi and 14,600 psi. These trunnion-airfoil stress values are well within the 0.2% yield strength of 110,000 psi for the AMS 5613 stainless steel material selected for stator fabrication, and no stress problems are anticipated.

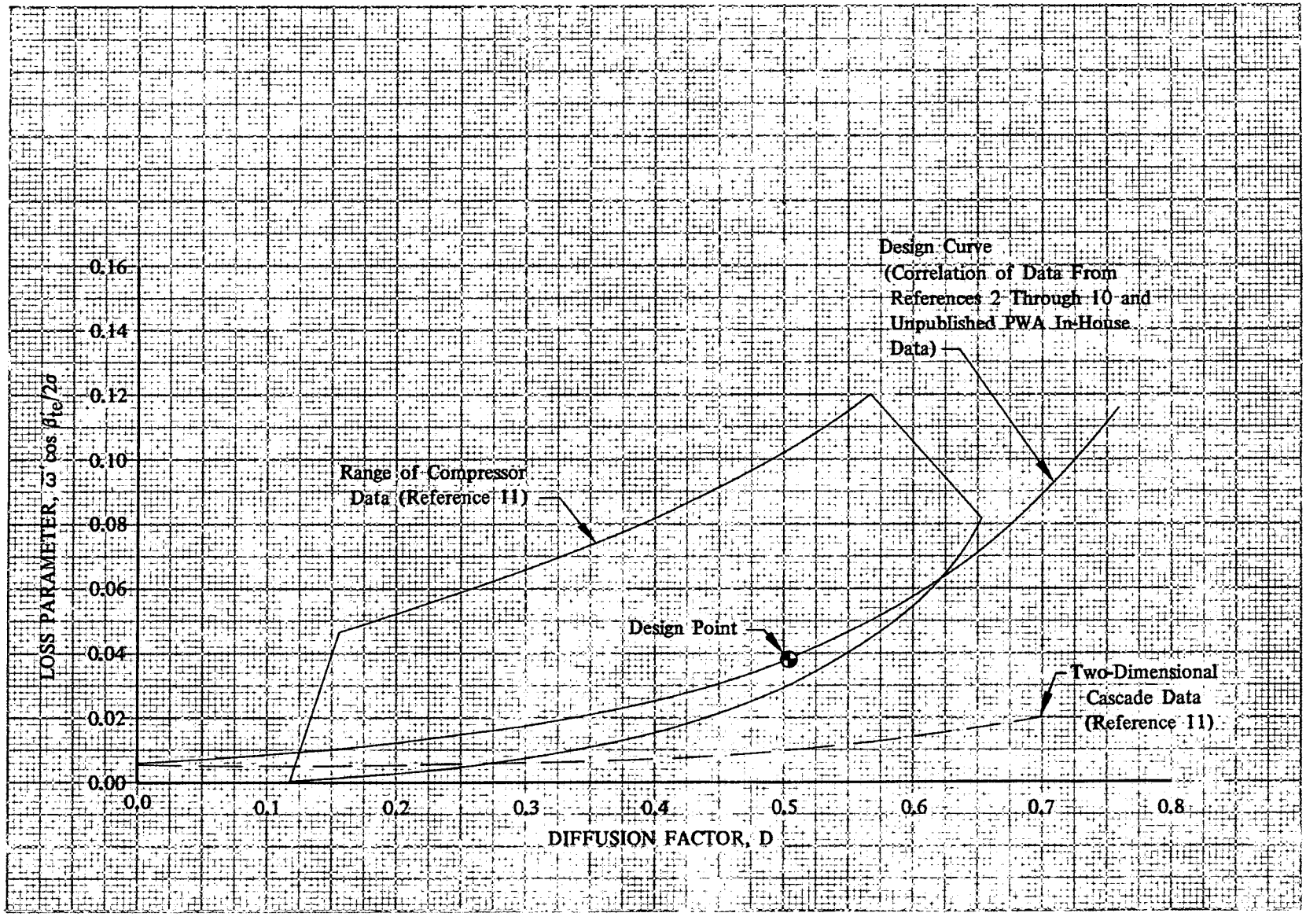

Figure 1. Rotor Loss Parameter vs Diffusion Factor, 10% Span From Tip DF 93388

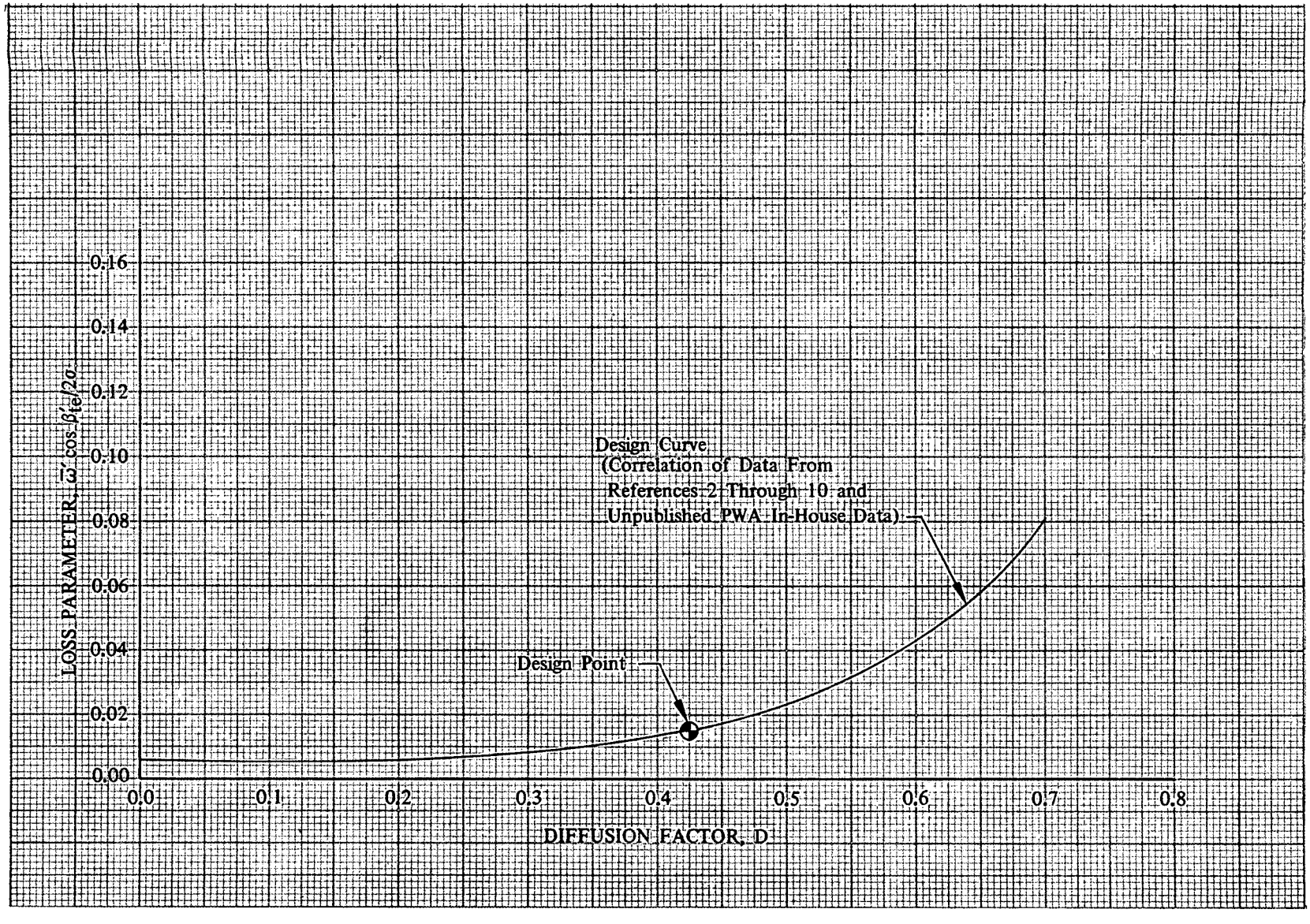

Figure 2. Rotor Loss Parameter vs Diffusion Factor, 30% Span From Tip

DF 93389

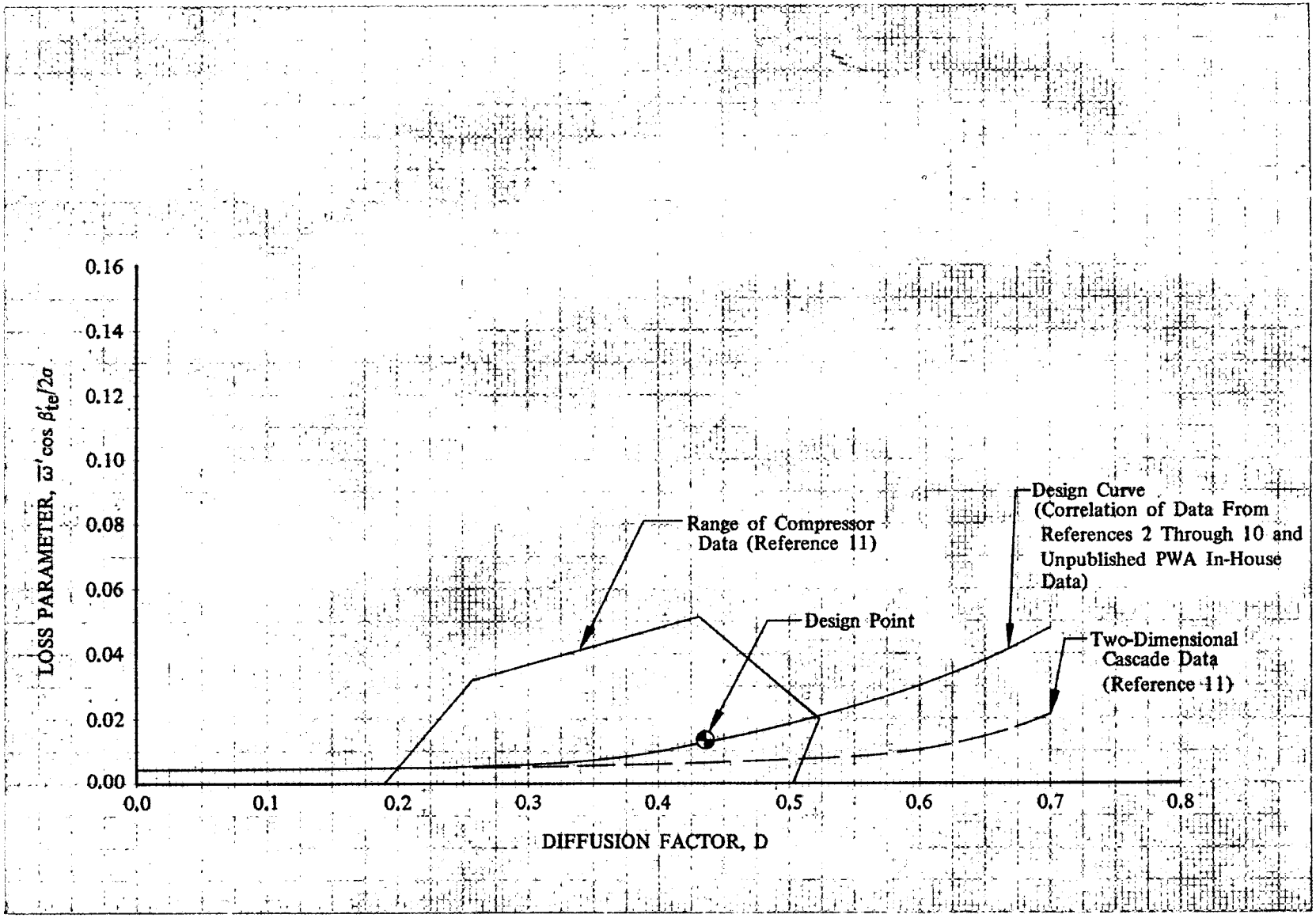

Figure 3. Rotor Loss Parameter vs Diffusion Factor, 50% Span

DF 93390

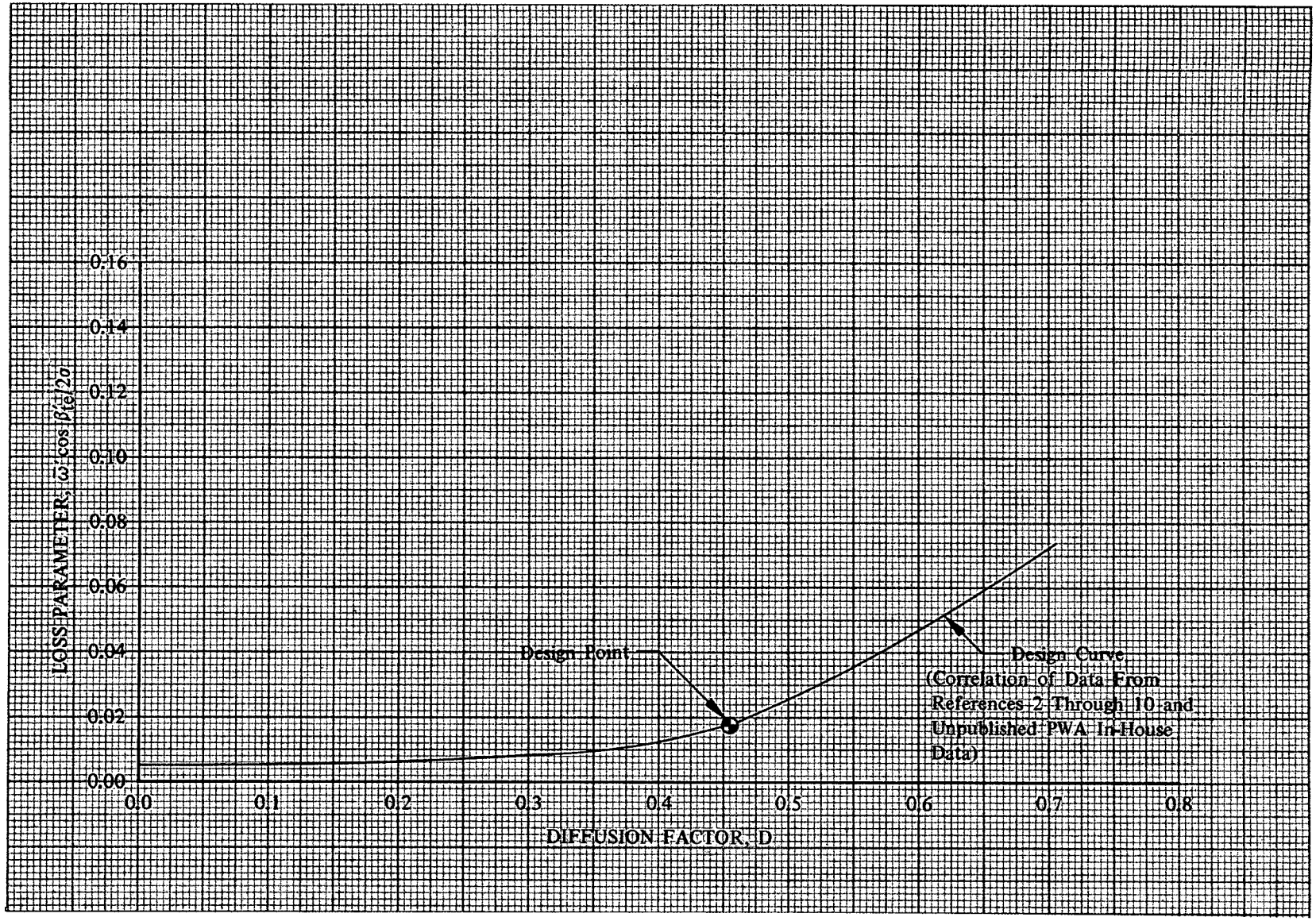

Figure 4. Rotor Loss Parameter vs Diffusion Factor, 70% Span From Tip

DF 93391

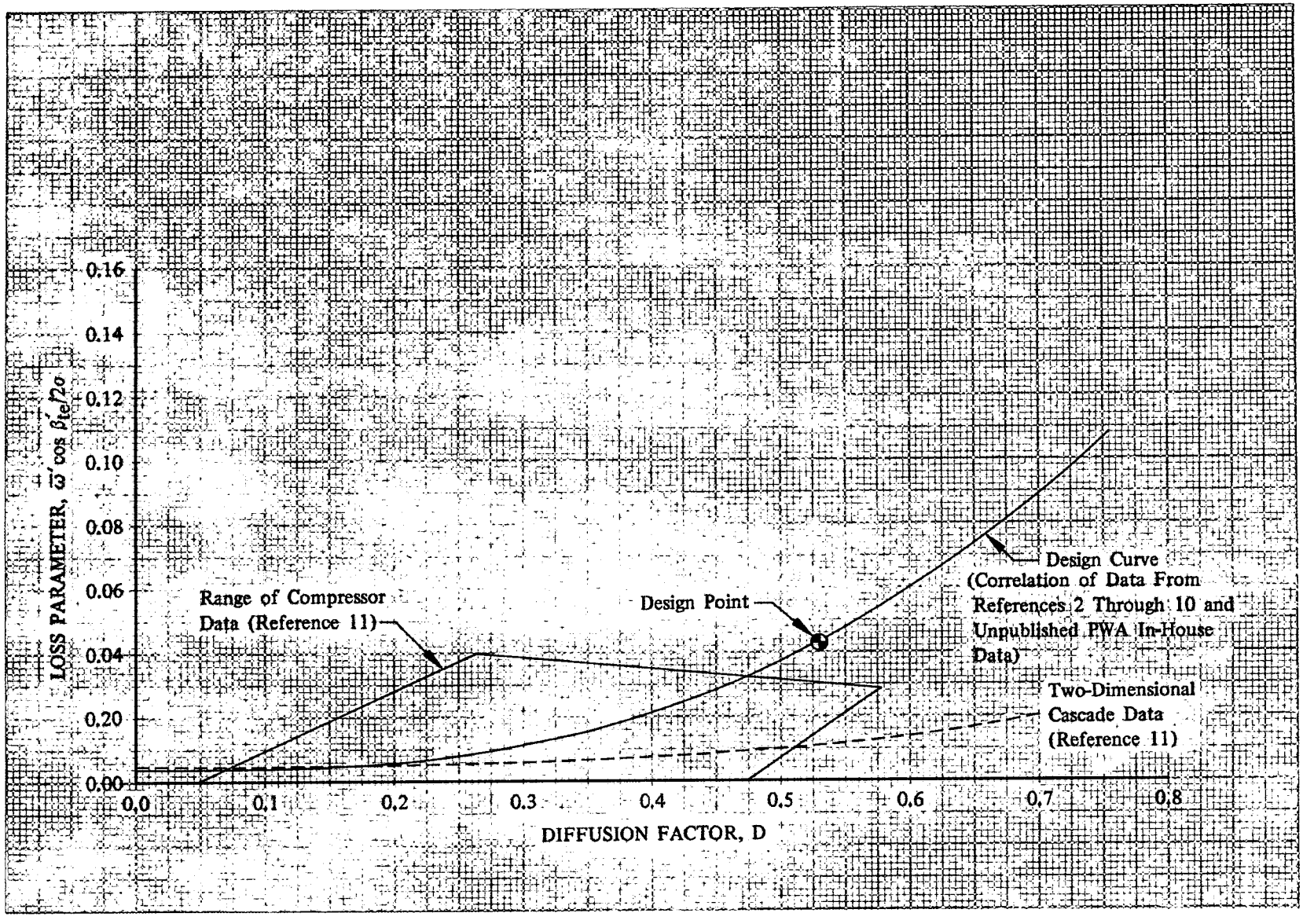

Figure 5. Rotor Loss Parameter vs Diffusion Factor, 90% Span From Tip

DF 93392

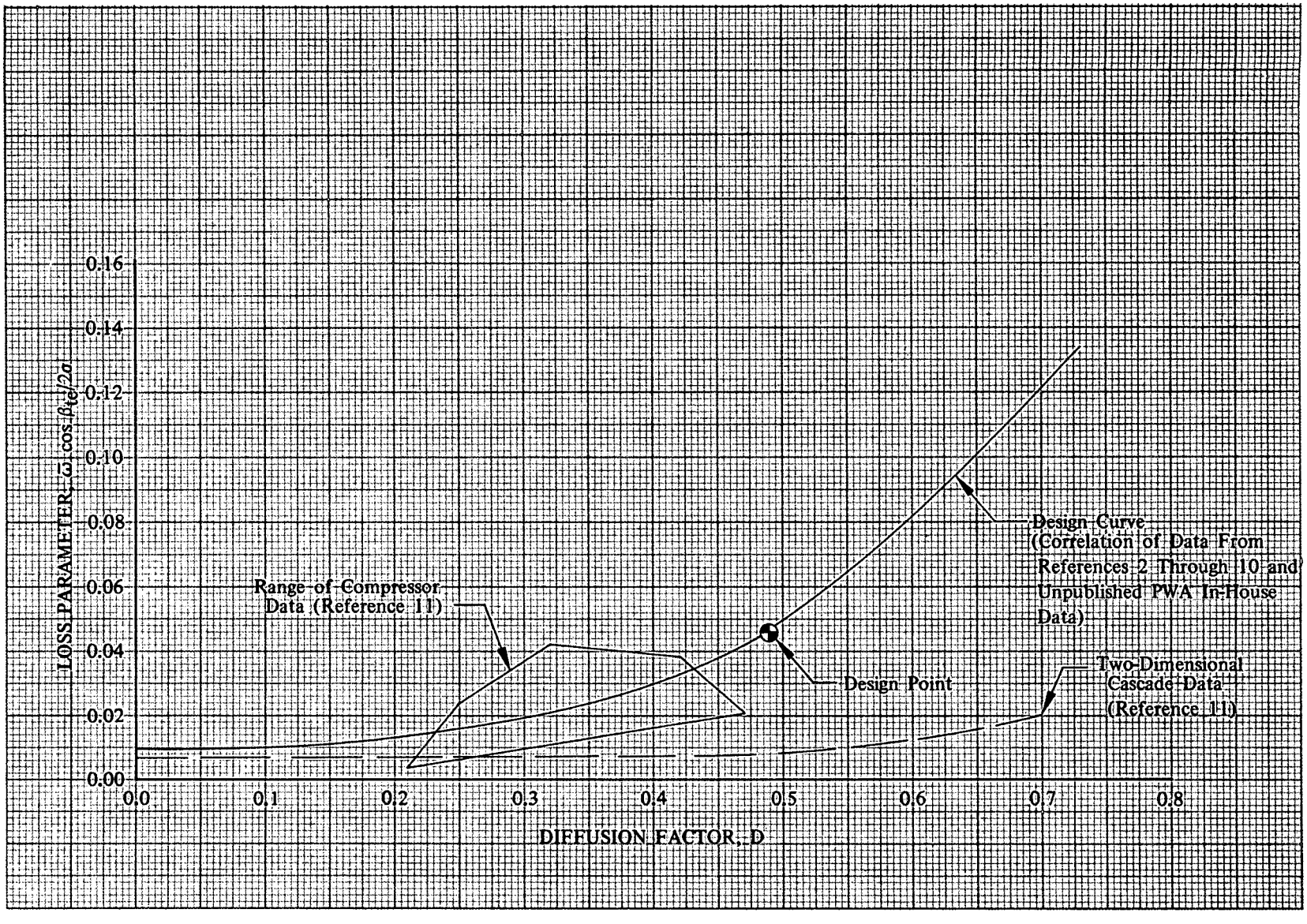

Figure 6. Stator Loss Parameter vs Diffusion Factor, 10% Span From Tip

DF 93393

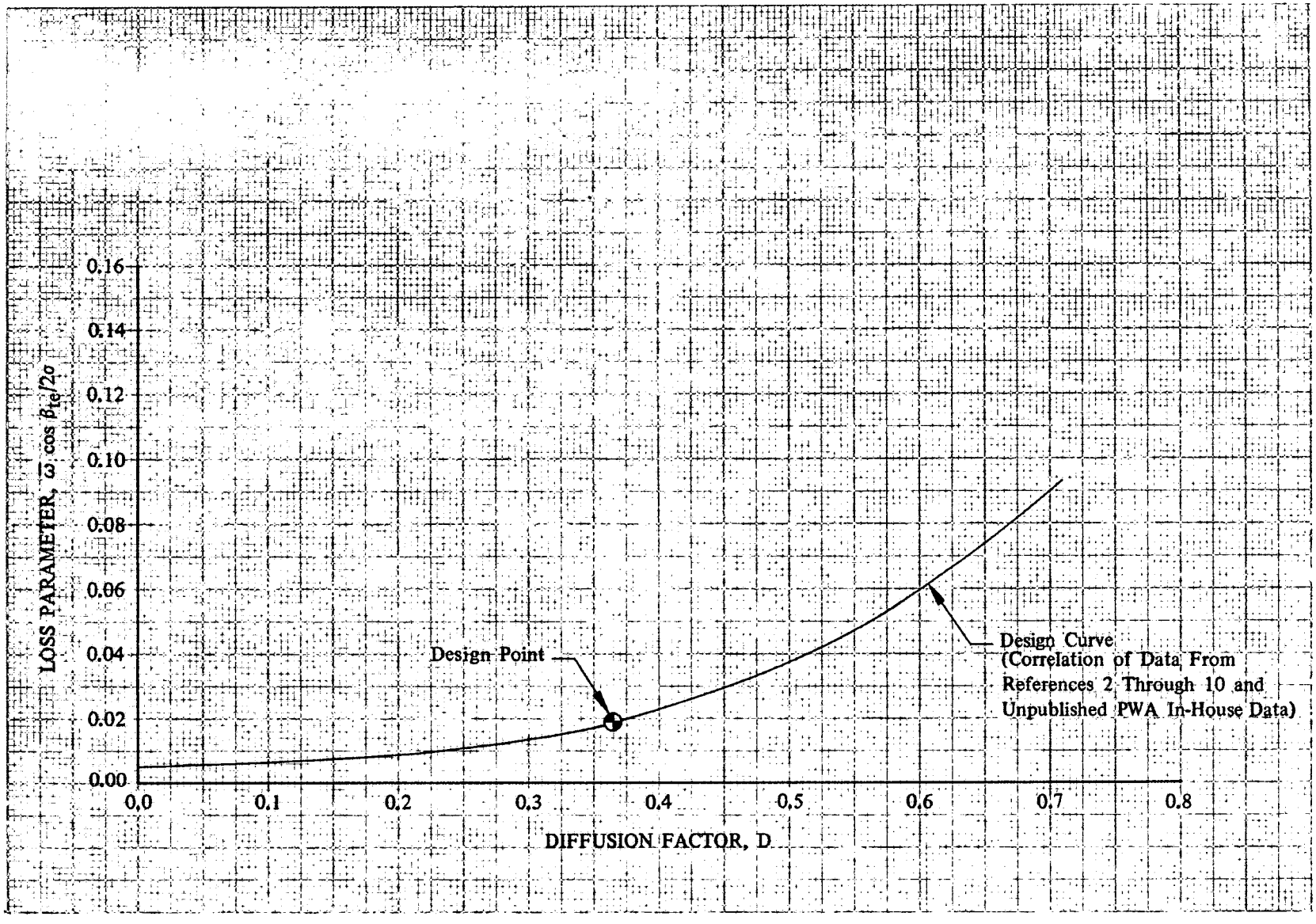

Figure 7. Stator Loss Parameter vs Diffusion Factor, 30% Span From Tip

DF 93394

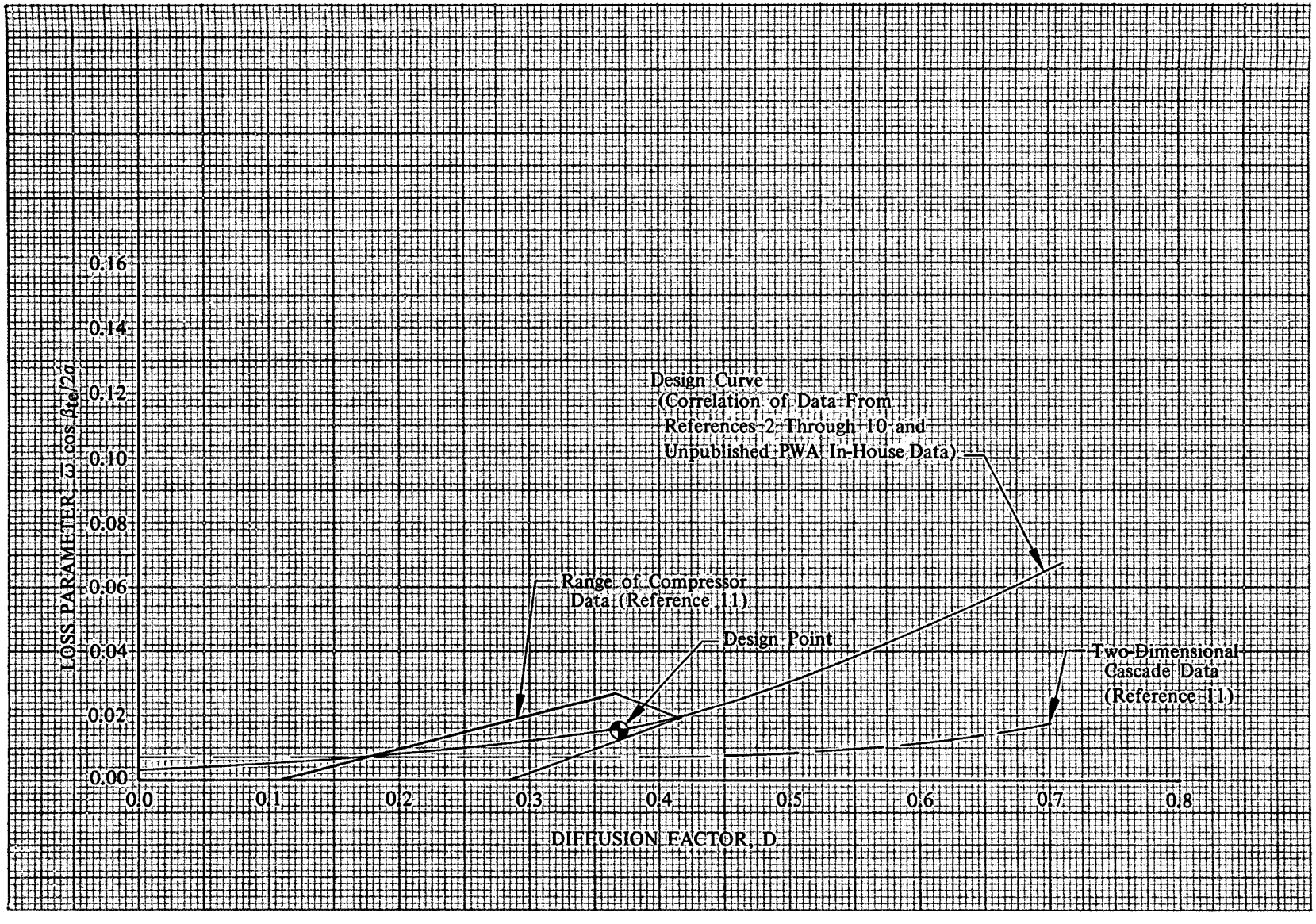

Figure 8. Stator Loss Parameter vs Diffusion Factor, 50% Span

DF 93395

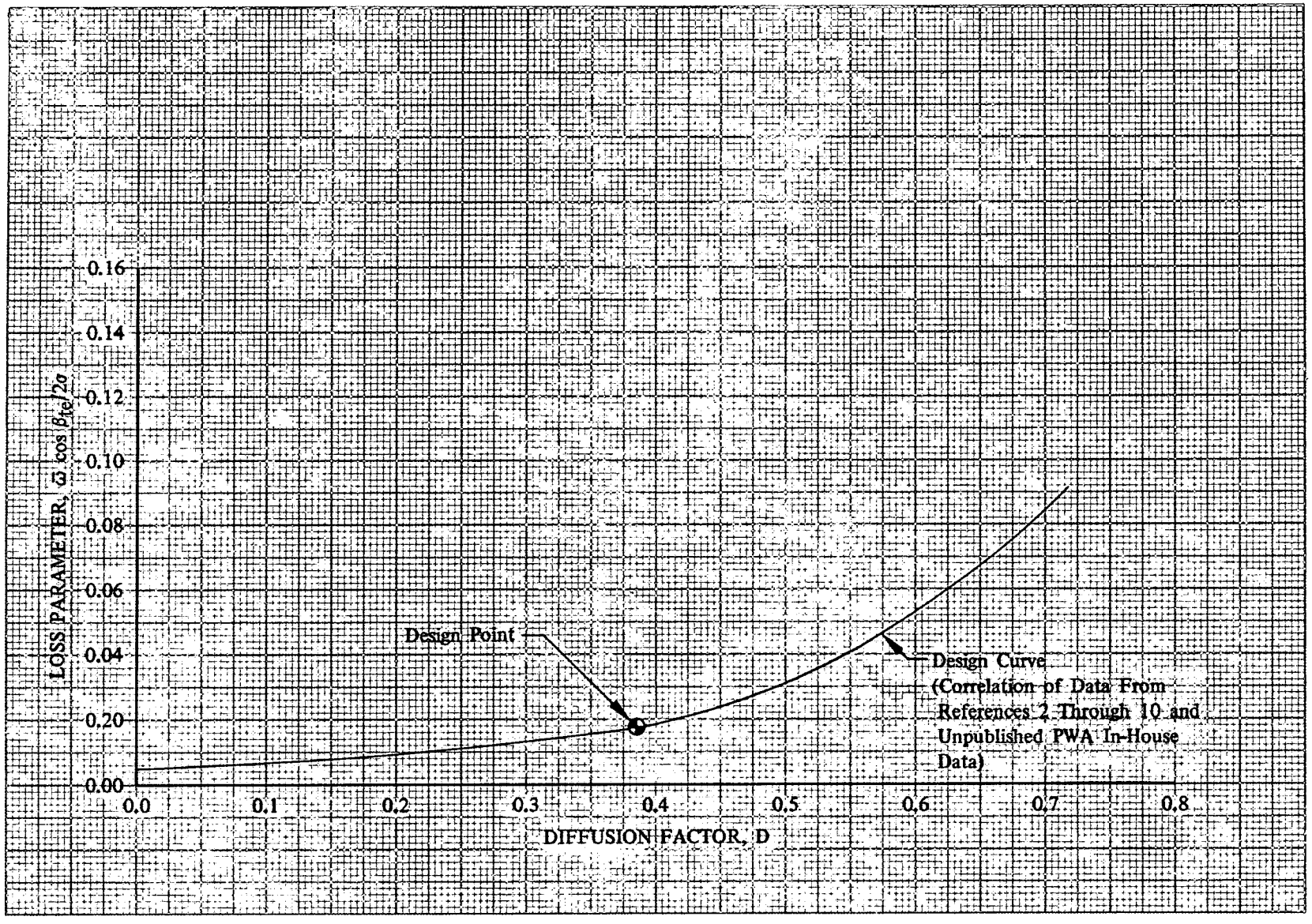

Figure 9. Stator Loss Parameter vs Diffusion Factor, 70% Span From Tip

DF 93396

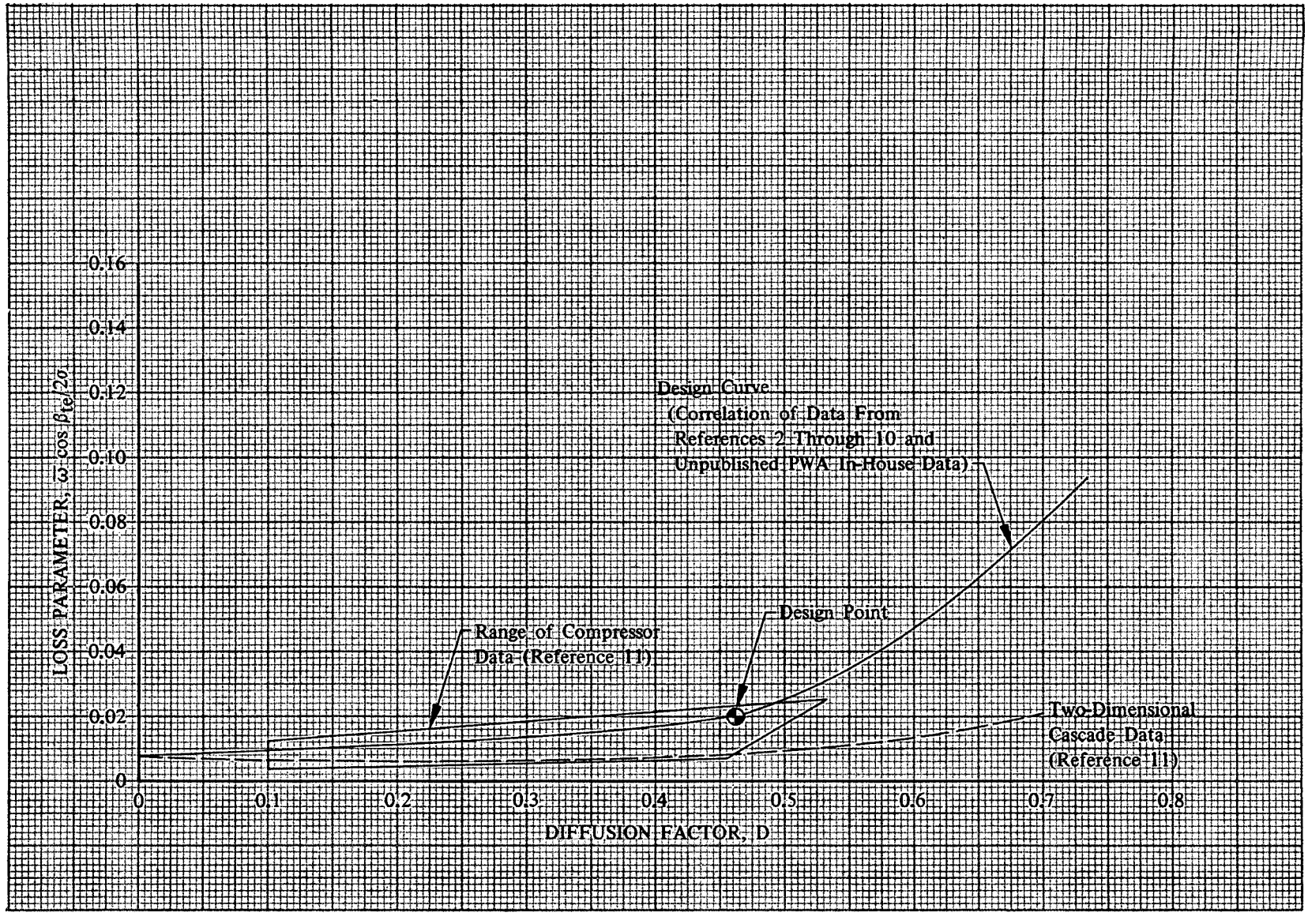

Figure 10. Stator Loss Parameter vs Diffusion Factor, 90% Span From Tip

DF 93397

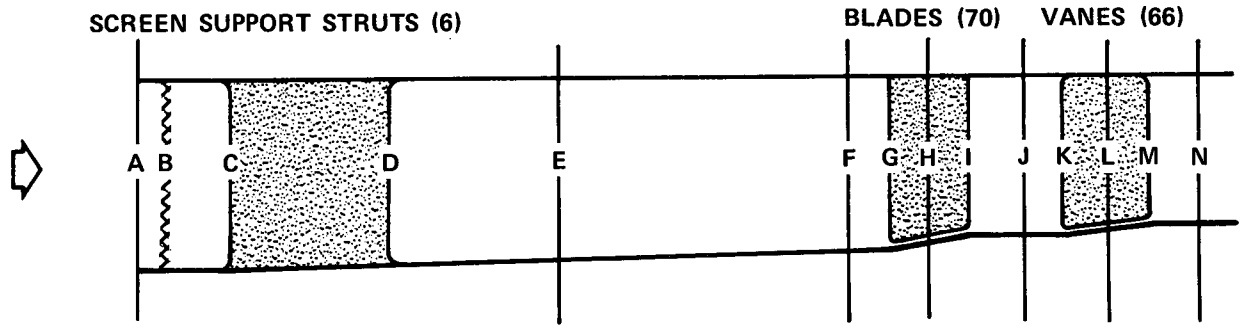

FLOWPATH LOCATION	LOCATION DESCRIPTION	INNER DIAMETER, in.	OUTER DIAMETER, in.	AXIAL DISTANCE FROM REFERENCE PLANE, in.
A	REFERENCE PLANE	32.850	41.790	0.0
B	DISTORTION SCREEN	32.850	41.790	1.500
C	SUPPORT STRUT LEADING EDGE	32.850	41.744	2.440
D	SUPPORT STRUT TRAILING EDGE	32.850	41.744	6.265
E	INSTRUMENTATION STATION 0	32.850	41.340	10.248
F	INSTRUMENTATION STATION 1	32.850	41.226	17.188
G	ROTOR INLET STATION	32.850	41.145	18.061
H	ROTOR D AND E STACKING LINE	32.850	40.860	19.188
I	ROTOR EXIT STATION	32.850	40.562	20.315
J	INSTRUMENTATION STATION 2	32.850	40.520	21.368
K	STATOR INLET STATION	32.850	40.450	22.163
L	STATOR D STACKING LINE	32.850	40.220	23.293
	STATOR E STACKING LINE AND FRONT BODY TRAILING EDGE	32.850	40.228	23.276
M	STATOR EXIT STATION	32.850	39.990	24.468
N	INSTRUMENTATION STATION 2A	32.850	39.990	25.418

NOTE: ALL DIMENSIONS ARE IN INCHES.

Figure 11. Design Flowpath Dimensions for Stages D and E

FD 64415

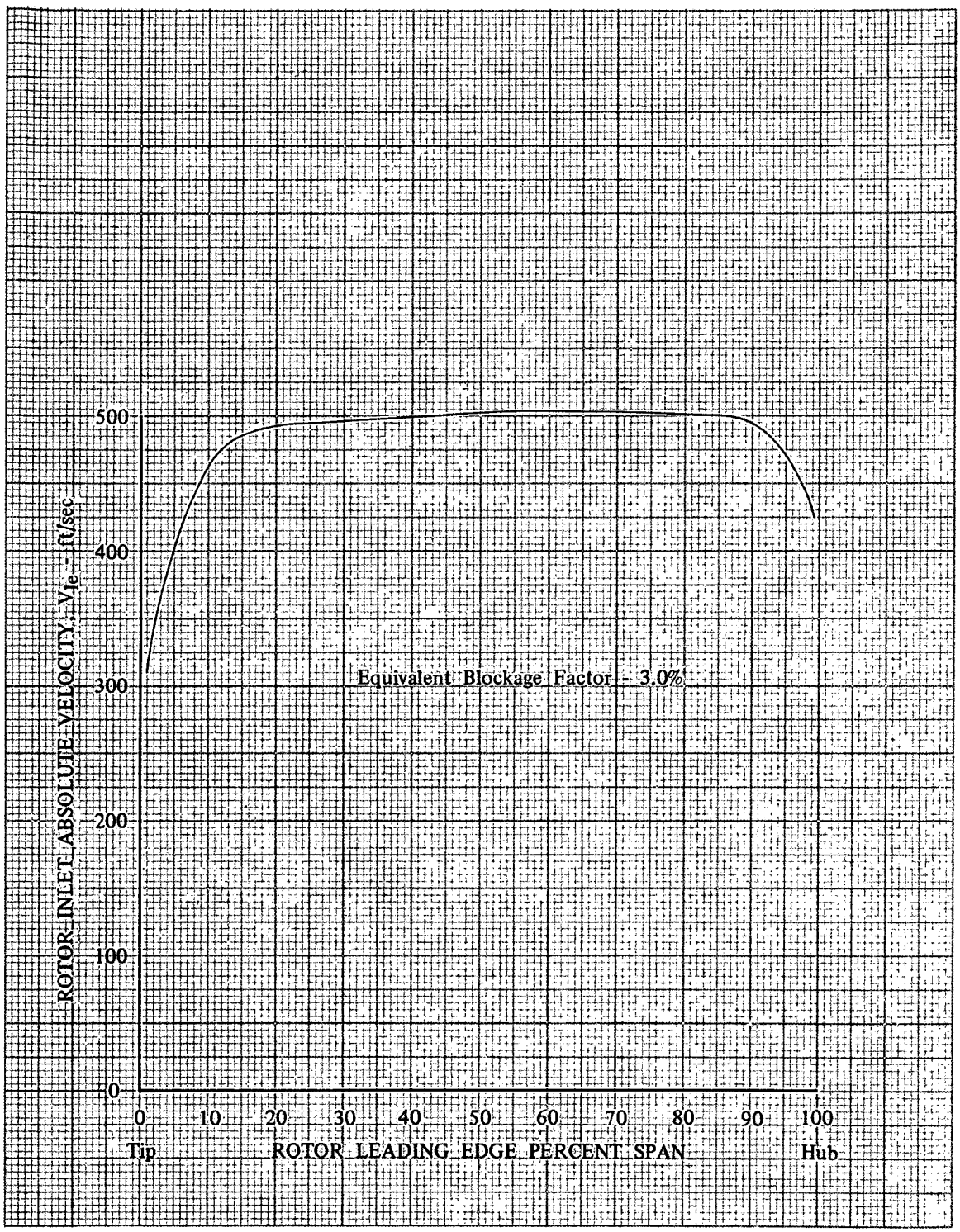

Figure 12. Rotor Inlet Absolute Velocity Distribution DF 93398

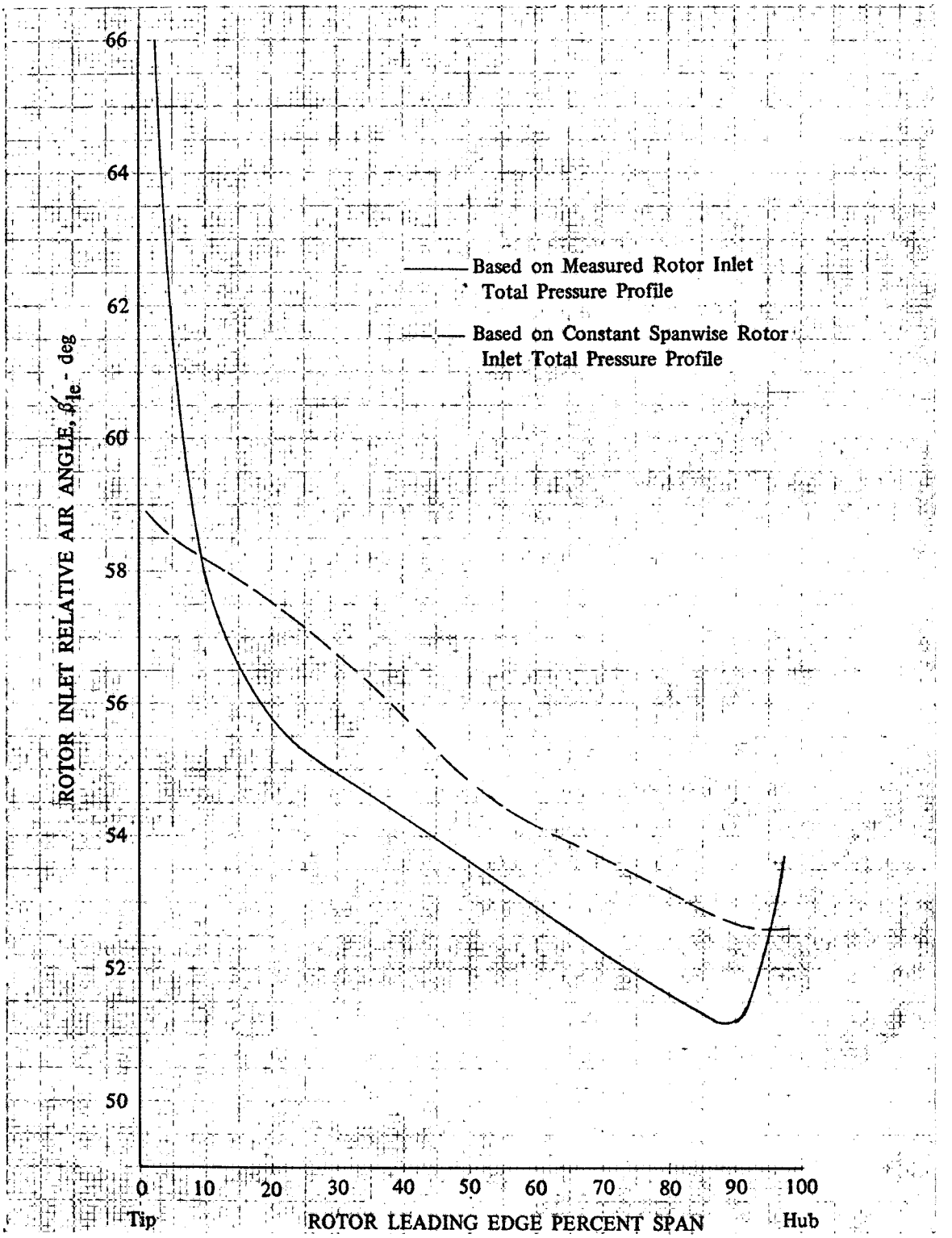

Figure 13. Effect of Rotor Inlet Velocity Profile on Rotor Inlet Relative Air Angle

DF 93399

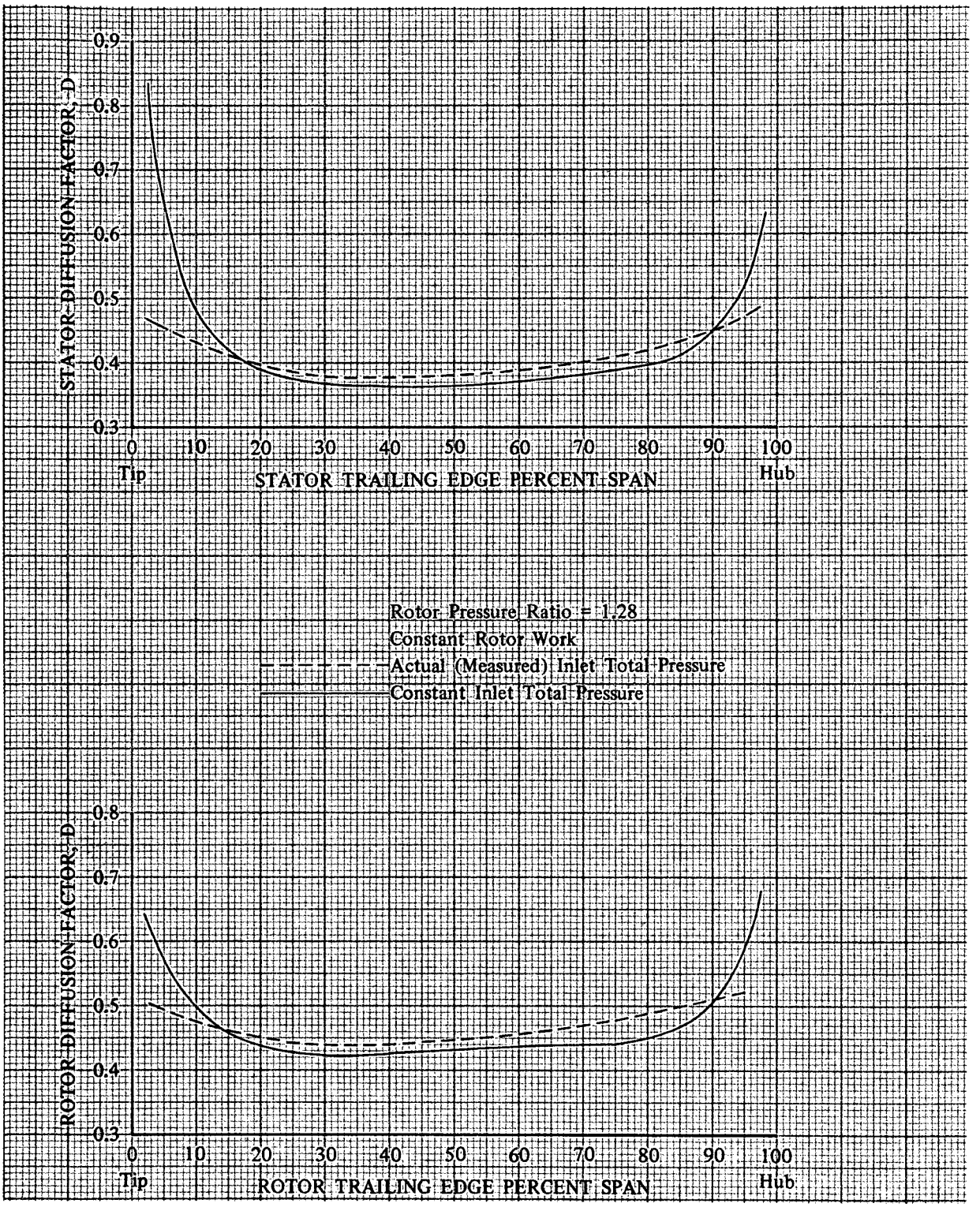

Figure 14. Effect of Compressor Inlet Velocity on Rotor and Stator Performance

DF 93400

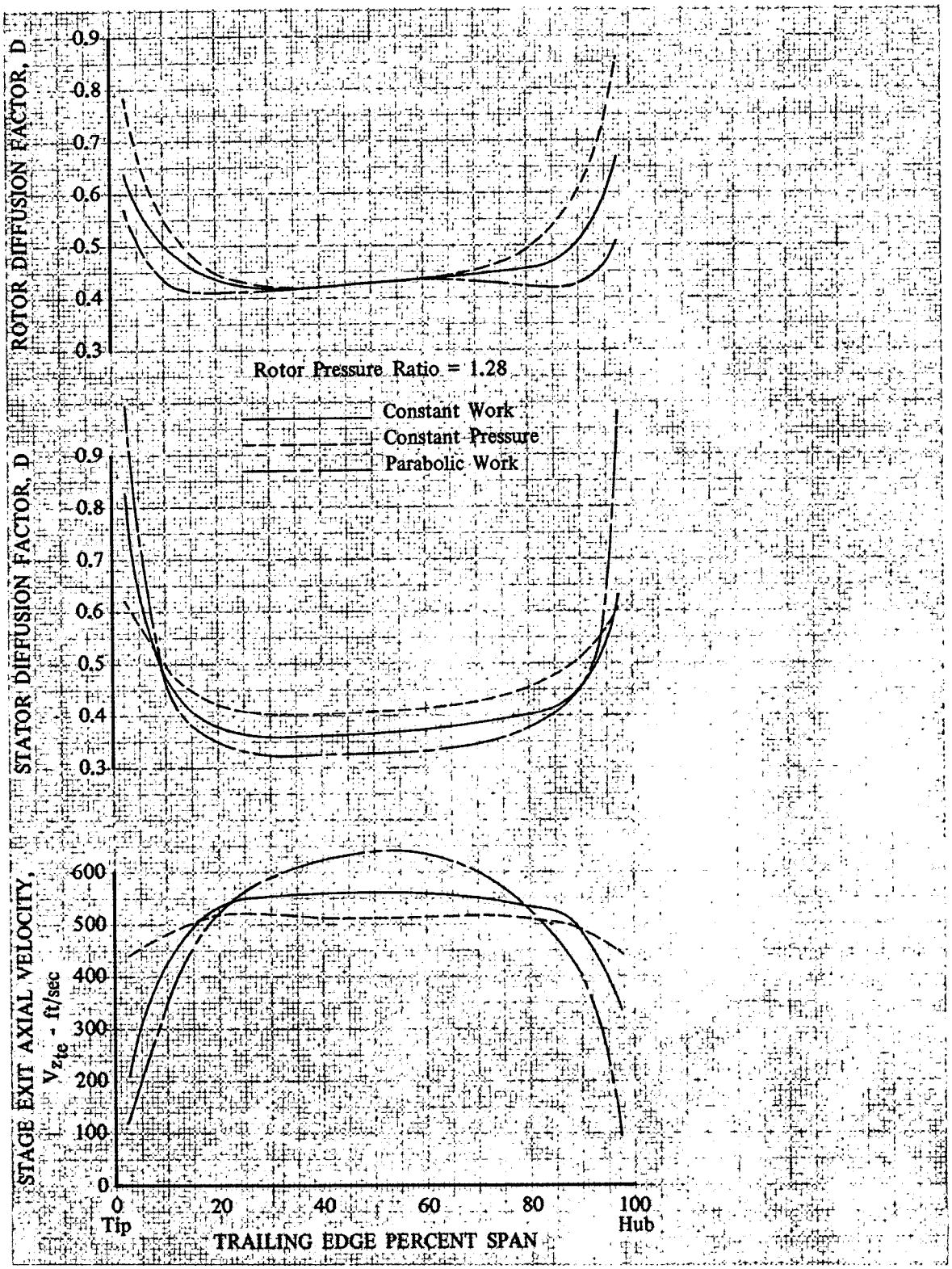

Figure 15. Effect of Rotor Work Distribution on Rotor Loading, Stator Loading, and Stage Exit Axial Velocity for Rotor Pressure Ratio of 1.28

DF 93401

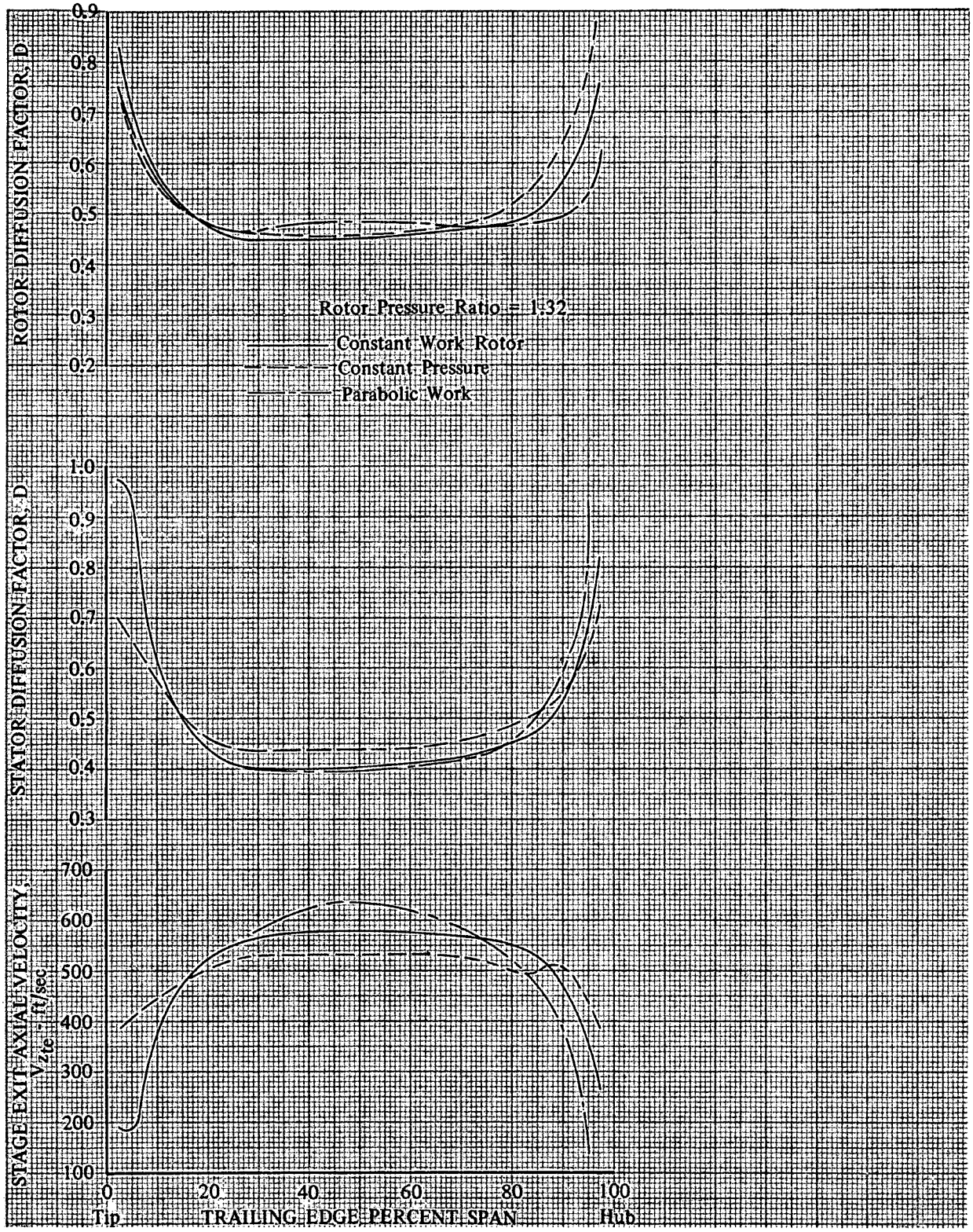

Figure 16. Effect of Rotor Work Distribution on Rotor Loading, Stator Loading, and Stage Exit Axial Velocity for Rotor Pressure Ratio of 1.32 DF 93402

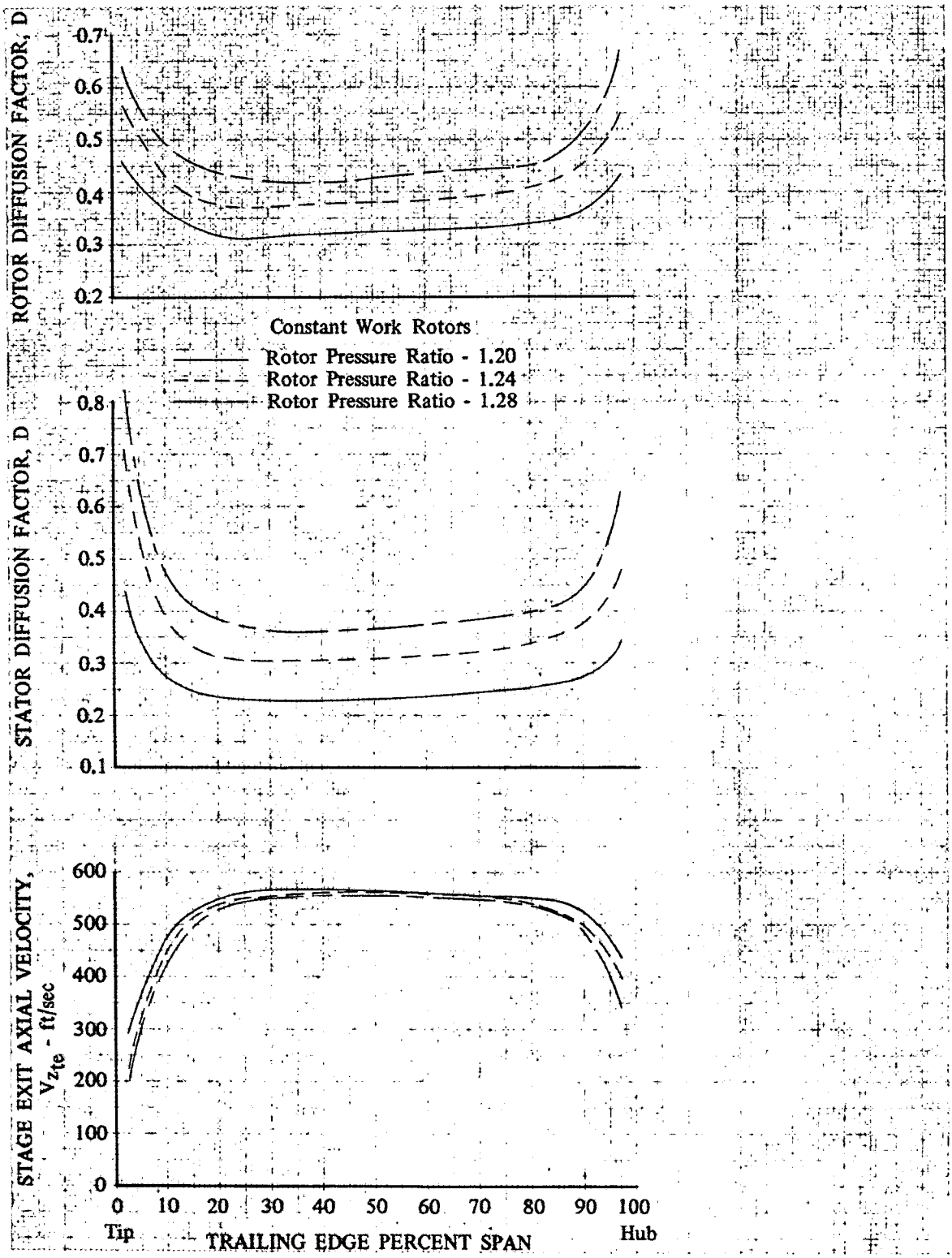

Figure 17. Effect of Pressure Ratio on Constant Work Stages DF 93403

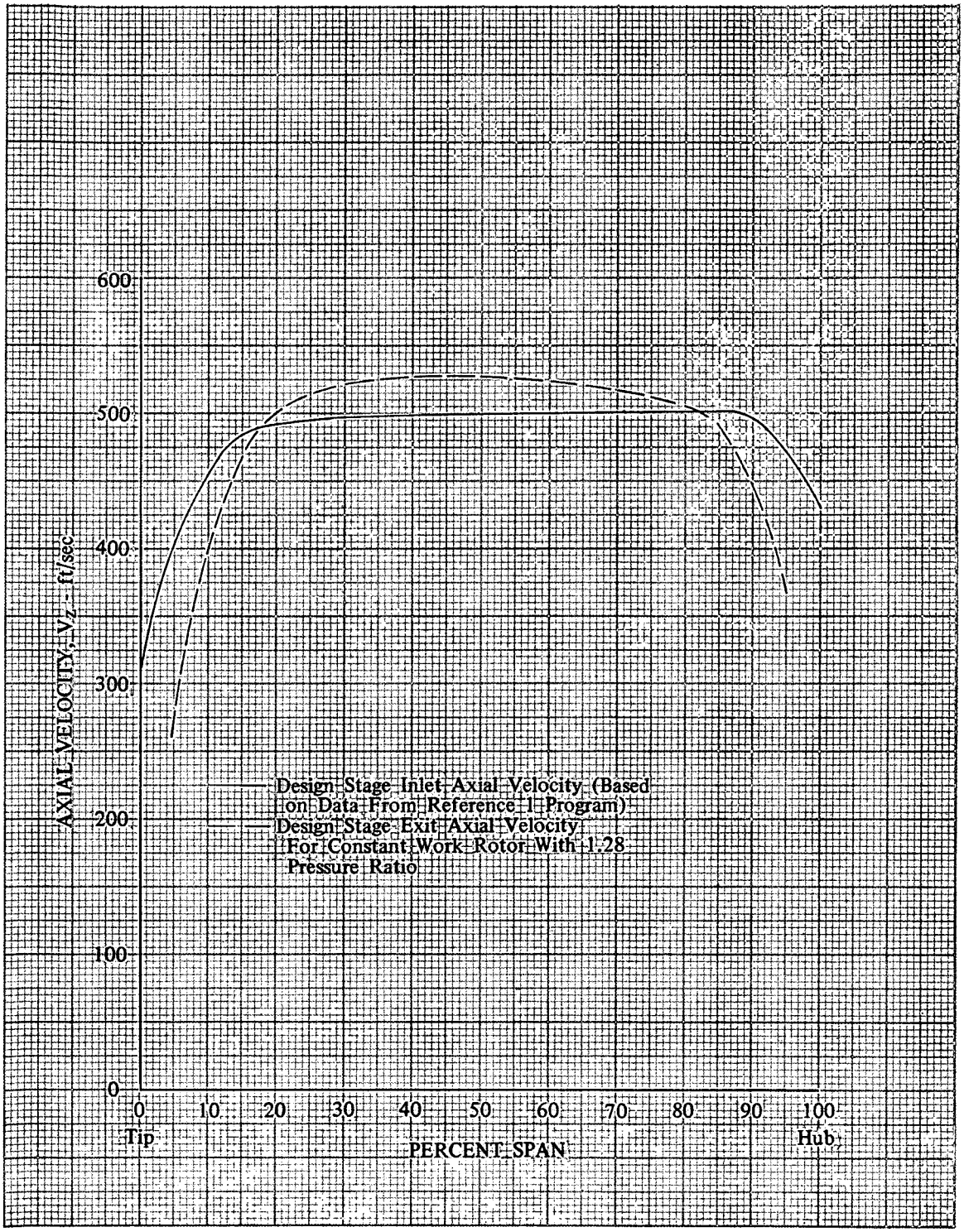

Figure 18. Stage Inlet and Exit Axial Velocity Distributions for Stages D and E DF 93404

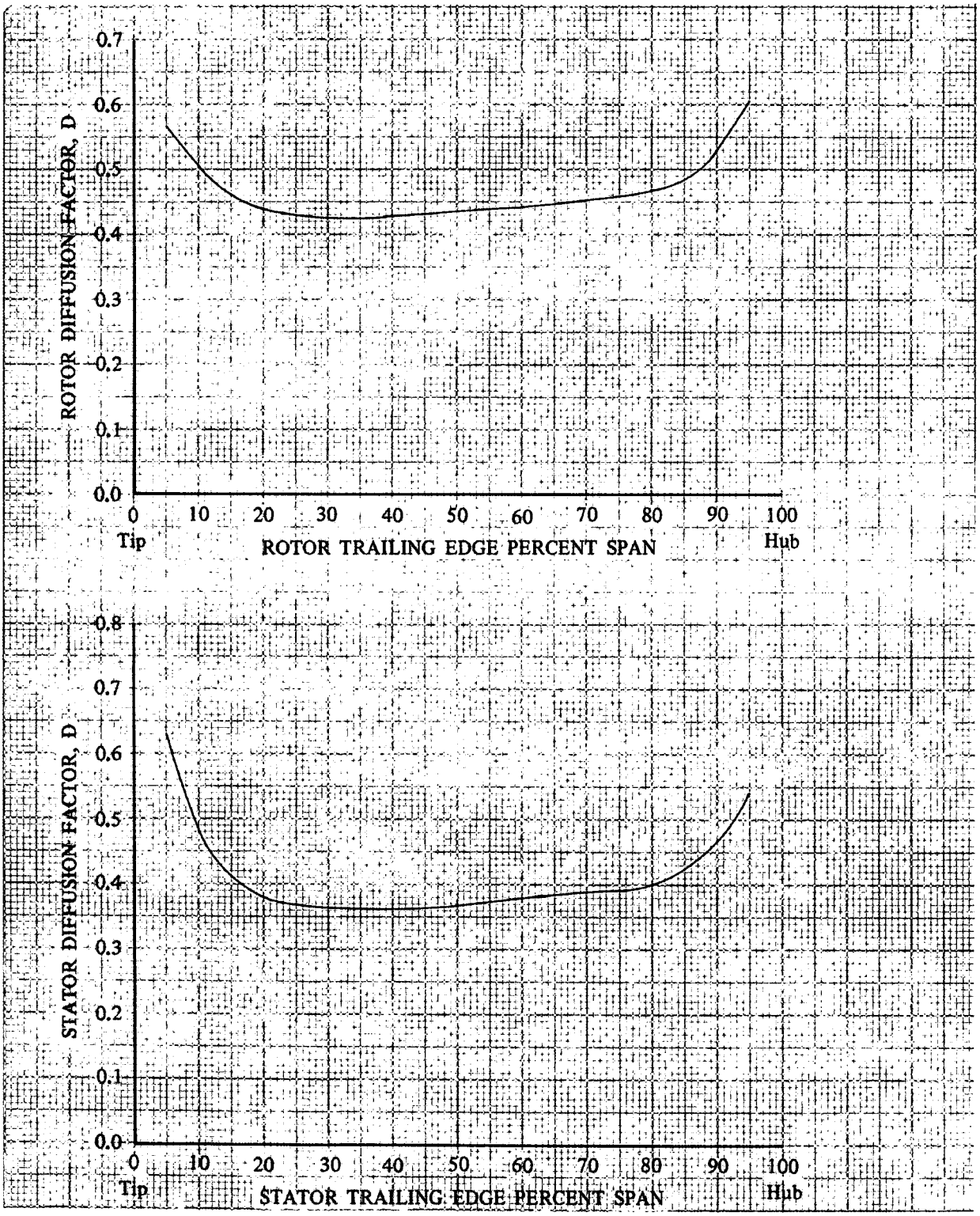

Figure 19. Rotor and Stator Diffusion Factor Distributions for Stages D and E DF 93405

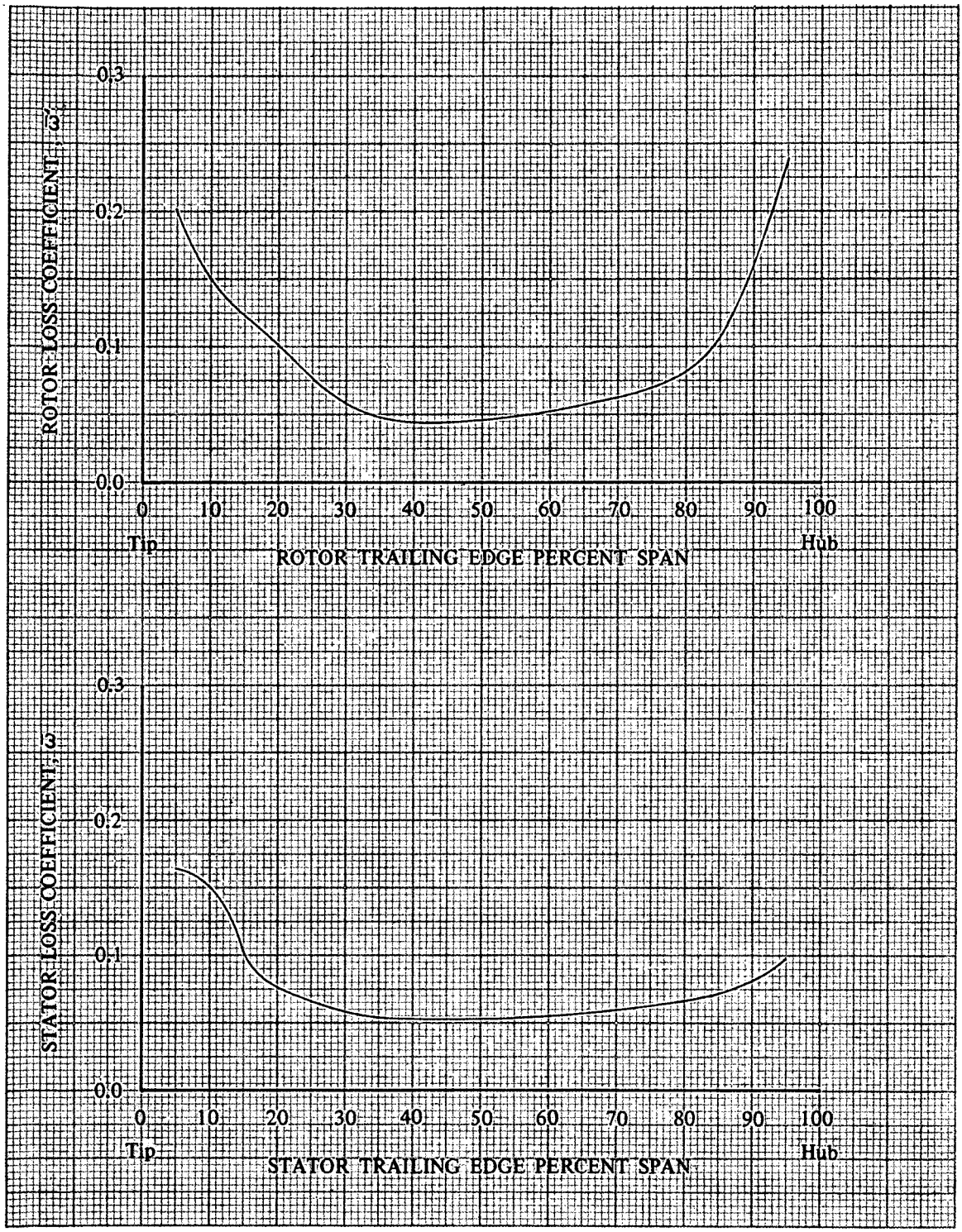

Figure 20. Rotor and Stator Loss Distributions for Stages D and E DF 93406

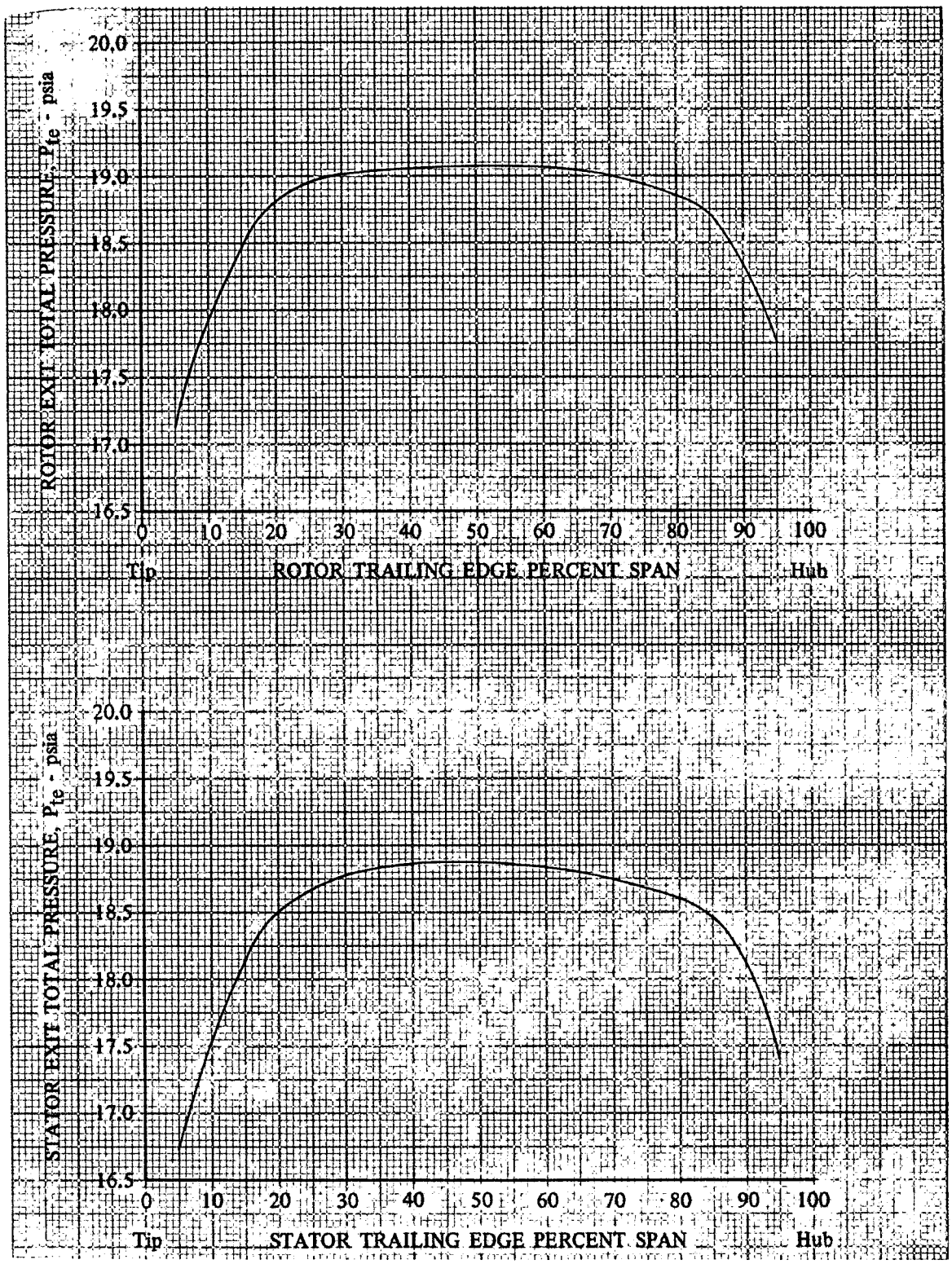

Figure 21. Rotor and Stator Exit Pressure Profiles for Stages D and E DF 93407

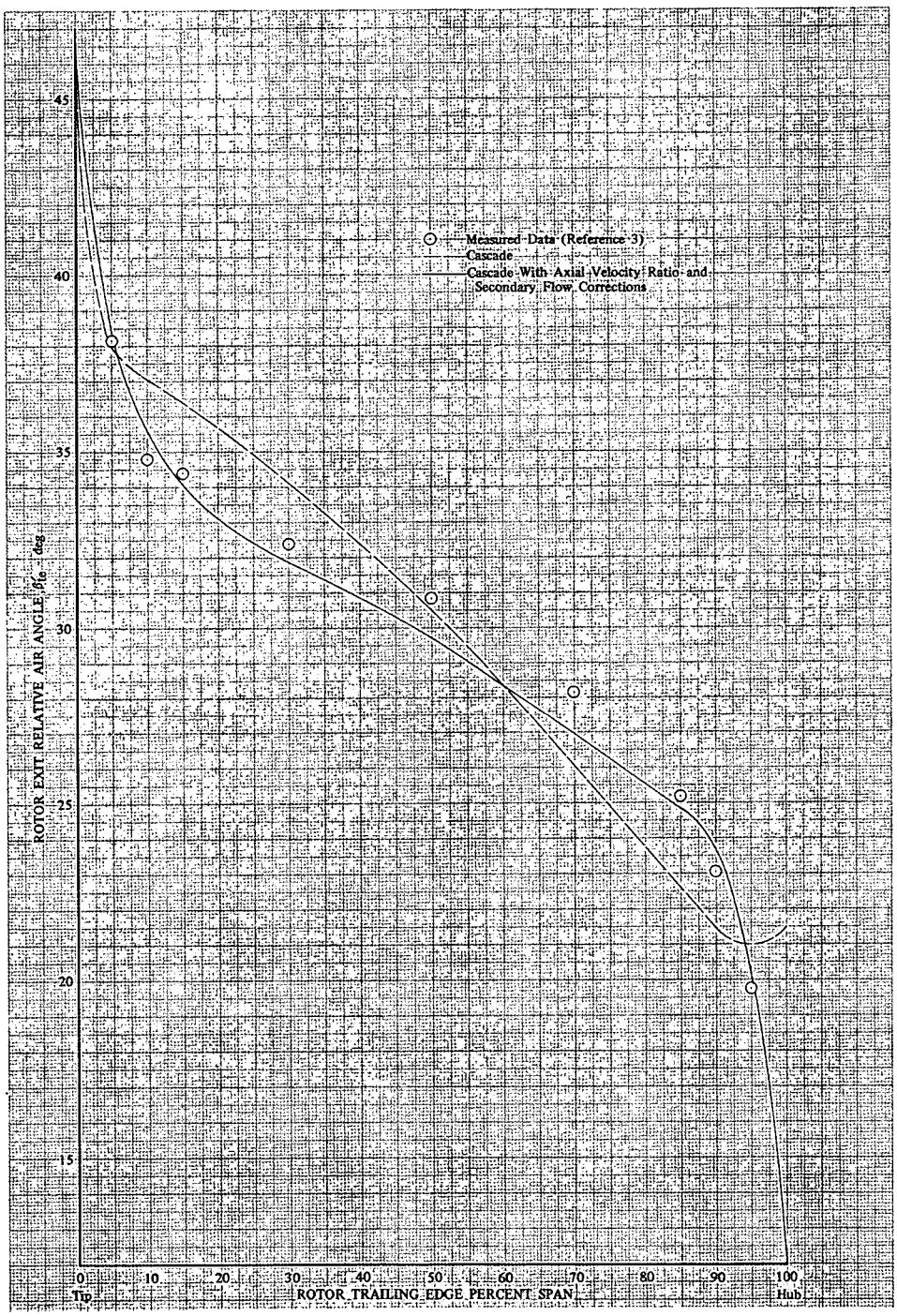

Figure 22. Effect of Axial Velocity Ratio and Secondary Flow Corrections on Rotor Exit Air Angle

DF 93408

9

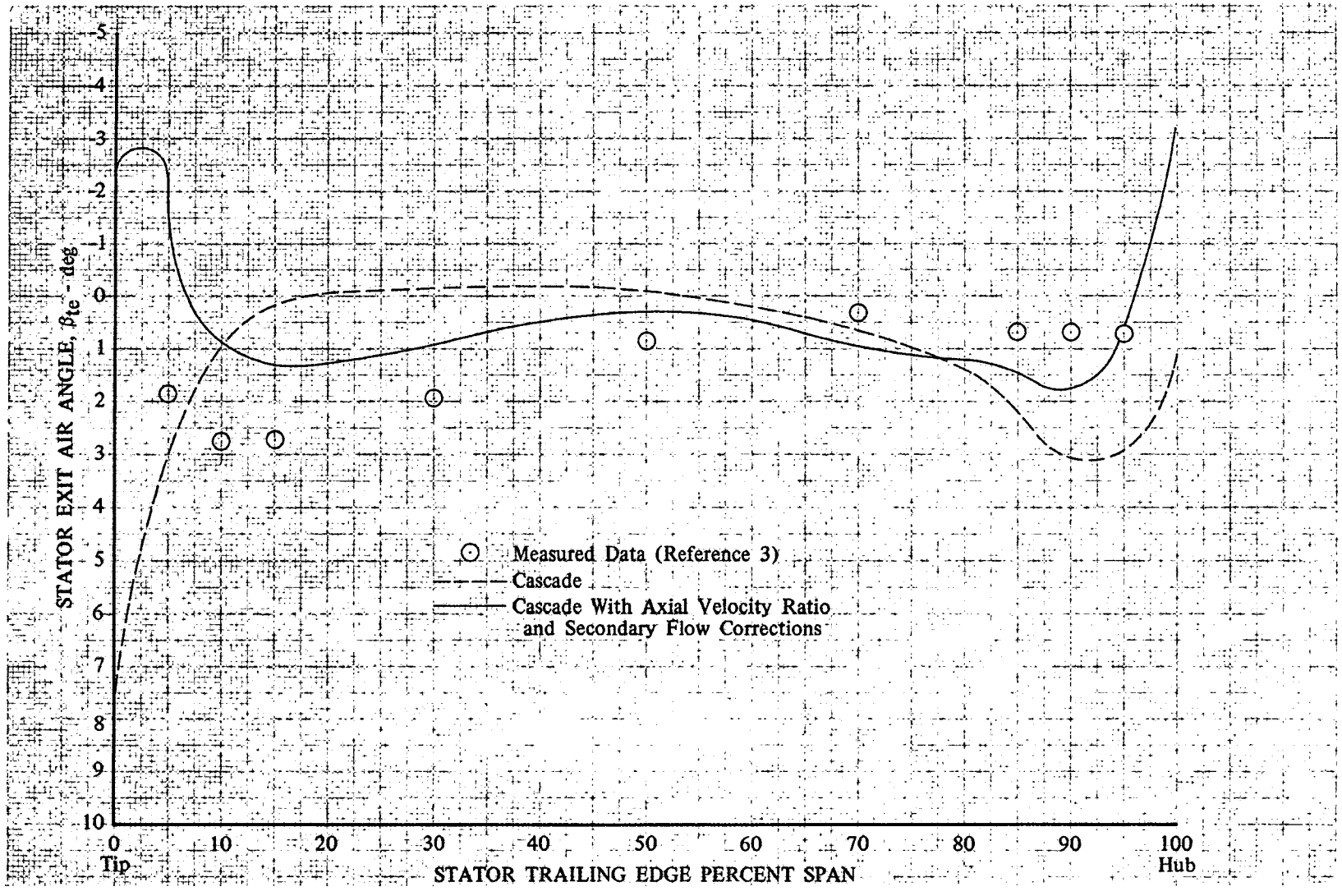

Figure 23. Effect of Axial Velocity Ratio and Secondary Flow Corrections on Stator Exit Air Angle

DF 93409

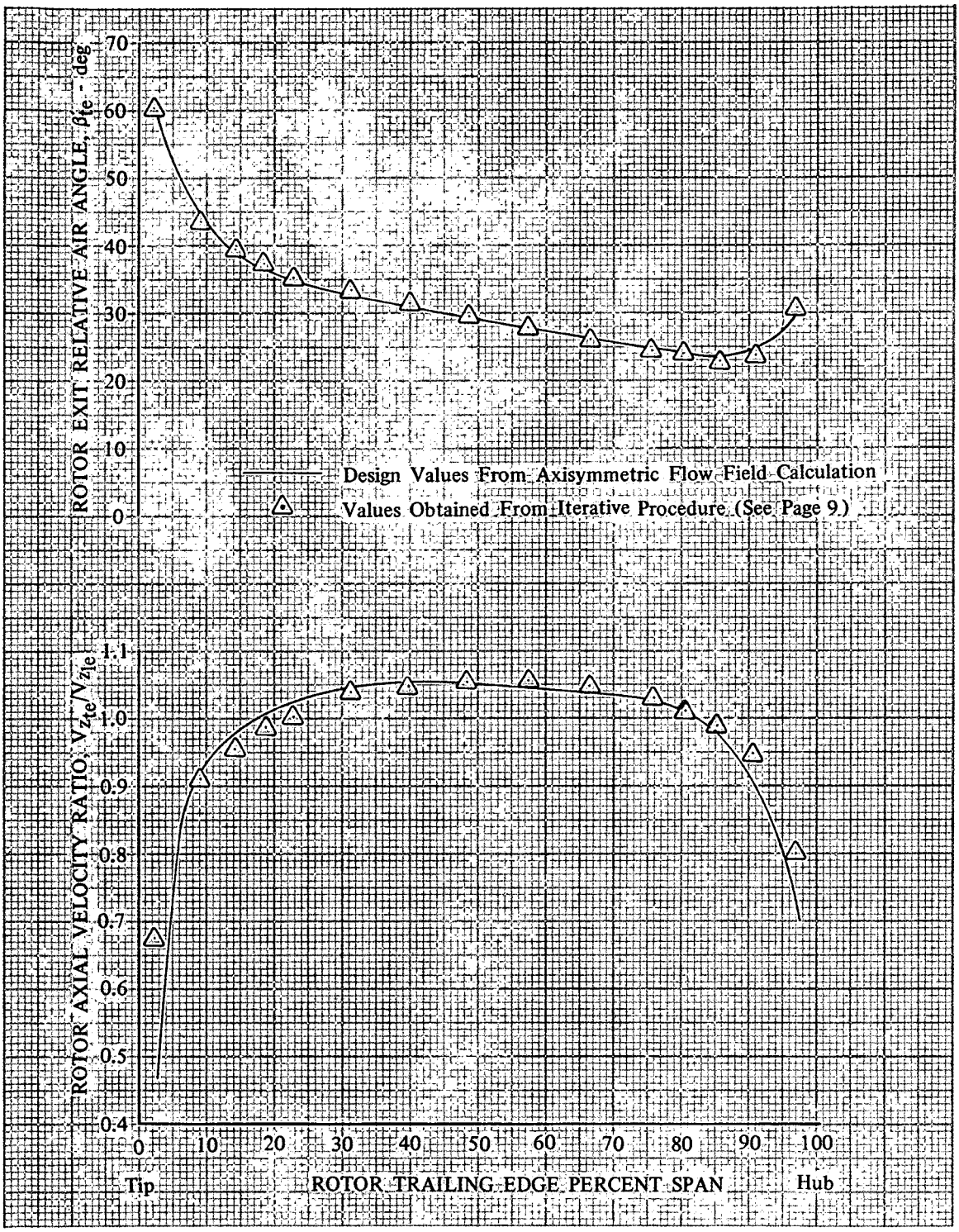

Figure 24. Predicted Values of Rotor Exit Air Angle and Axial Velocity Ratio for Stages D and E DF 93410

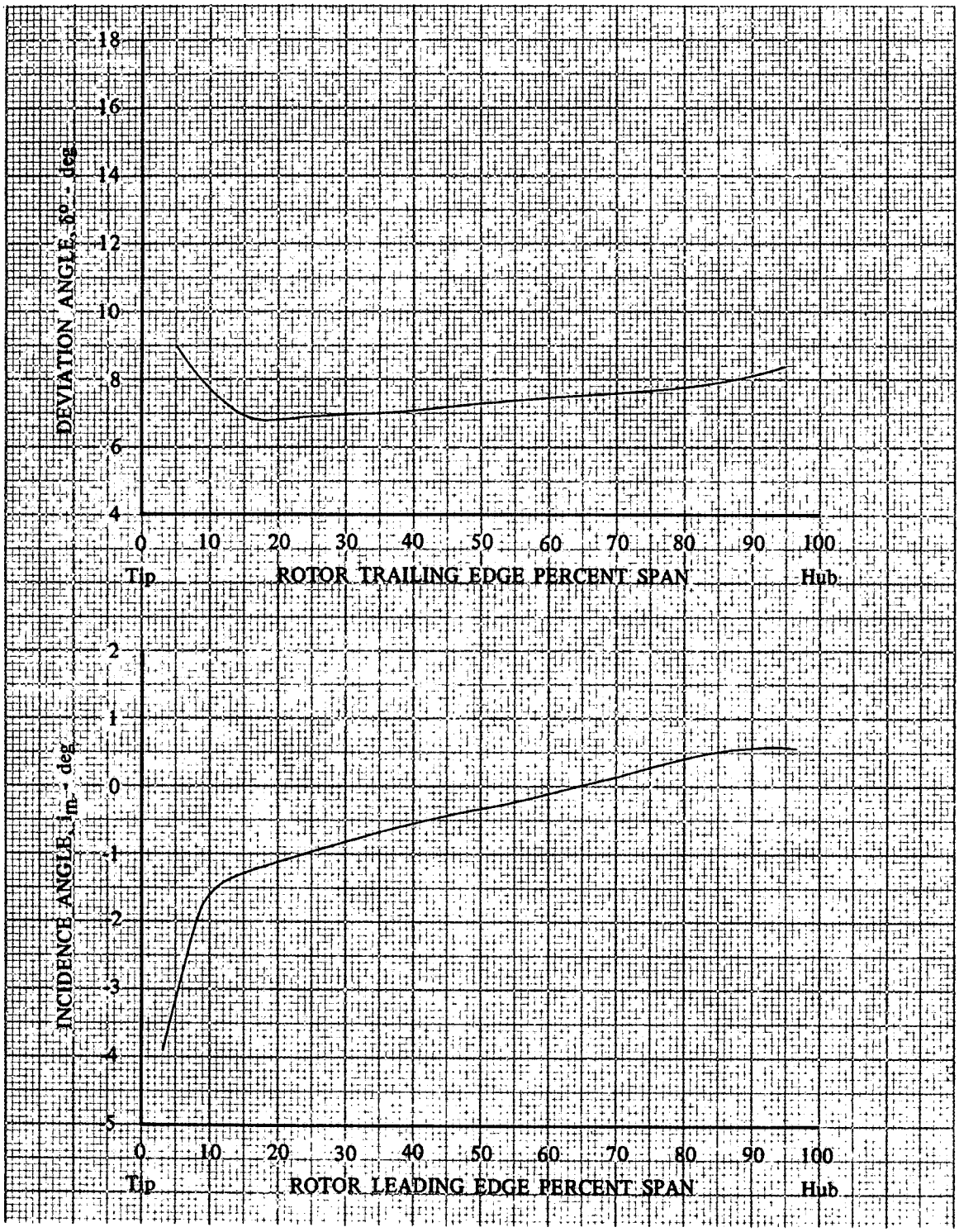

Figure 25. Rotors D and E Incidence and Deviation Angle Distributions DF 93411

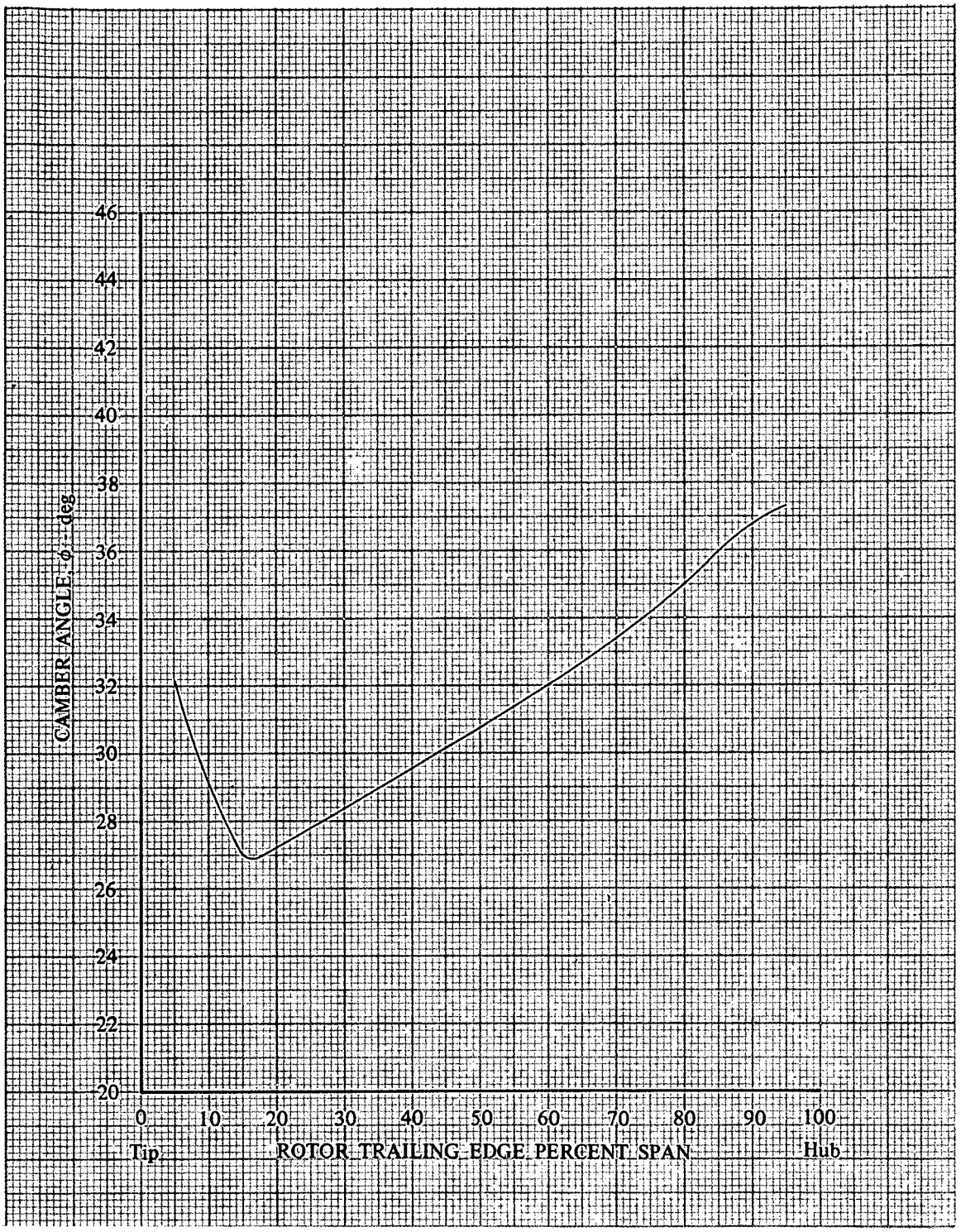

Figure 26. Rotor D Camber Angle Distribution DF 93412

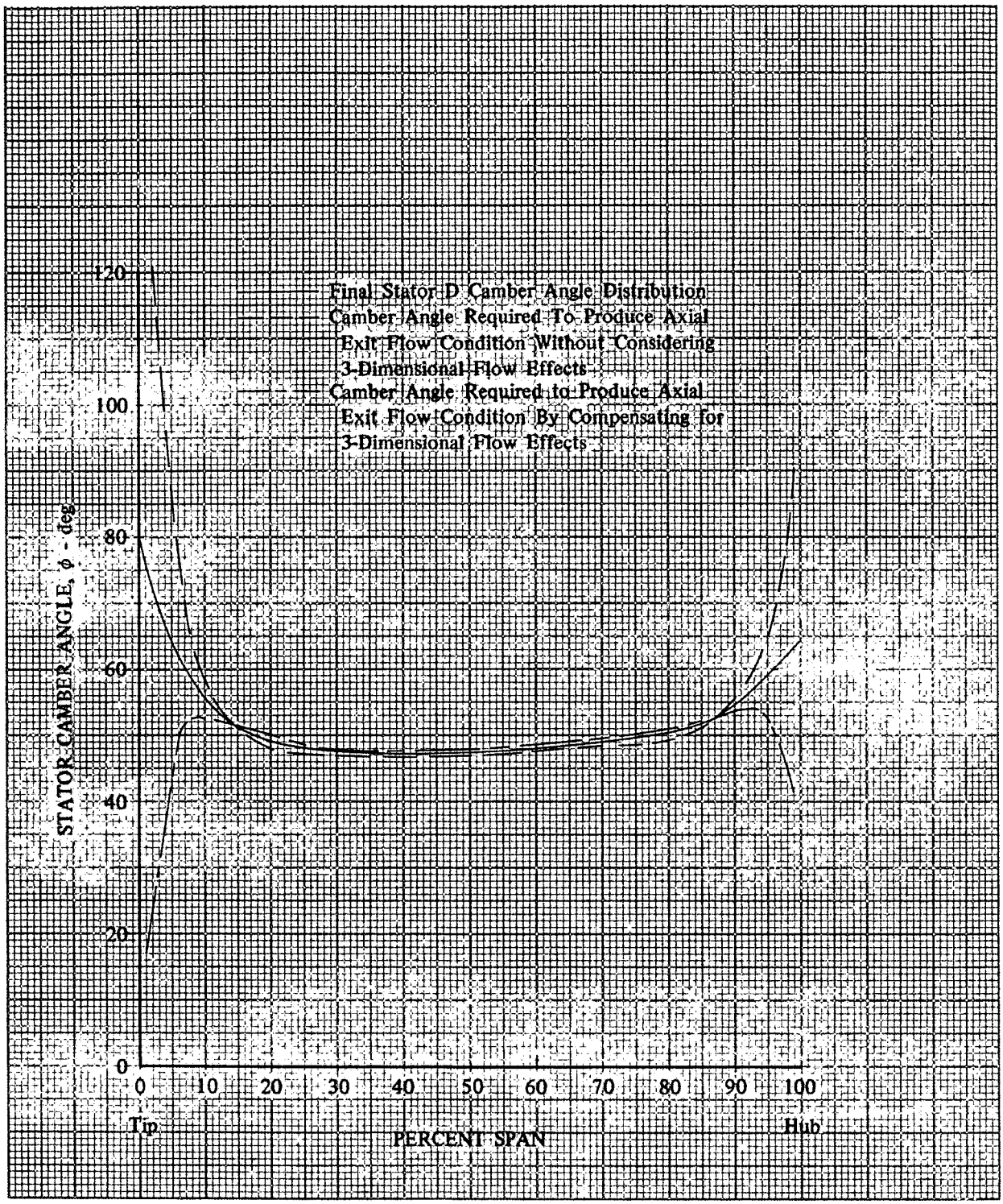

Figure 27. Comparison of Stator Camber Angle Distributions DF 93413

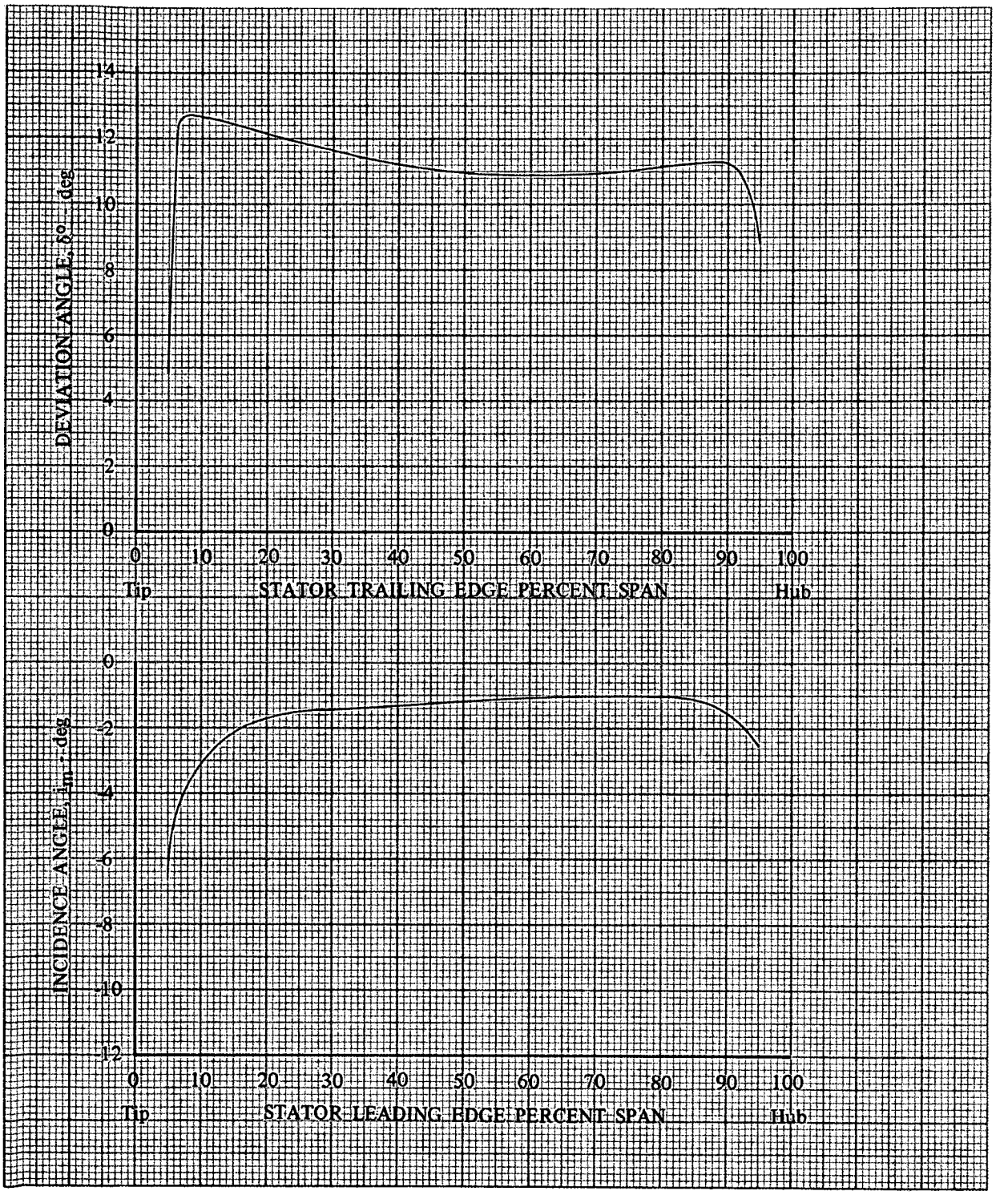

Figure 28. Stators D and E Incidence and Deviation Angle Distributions DF 93414

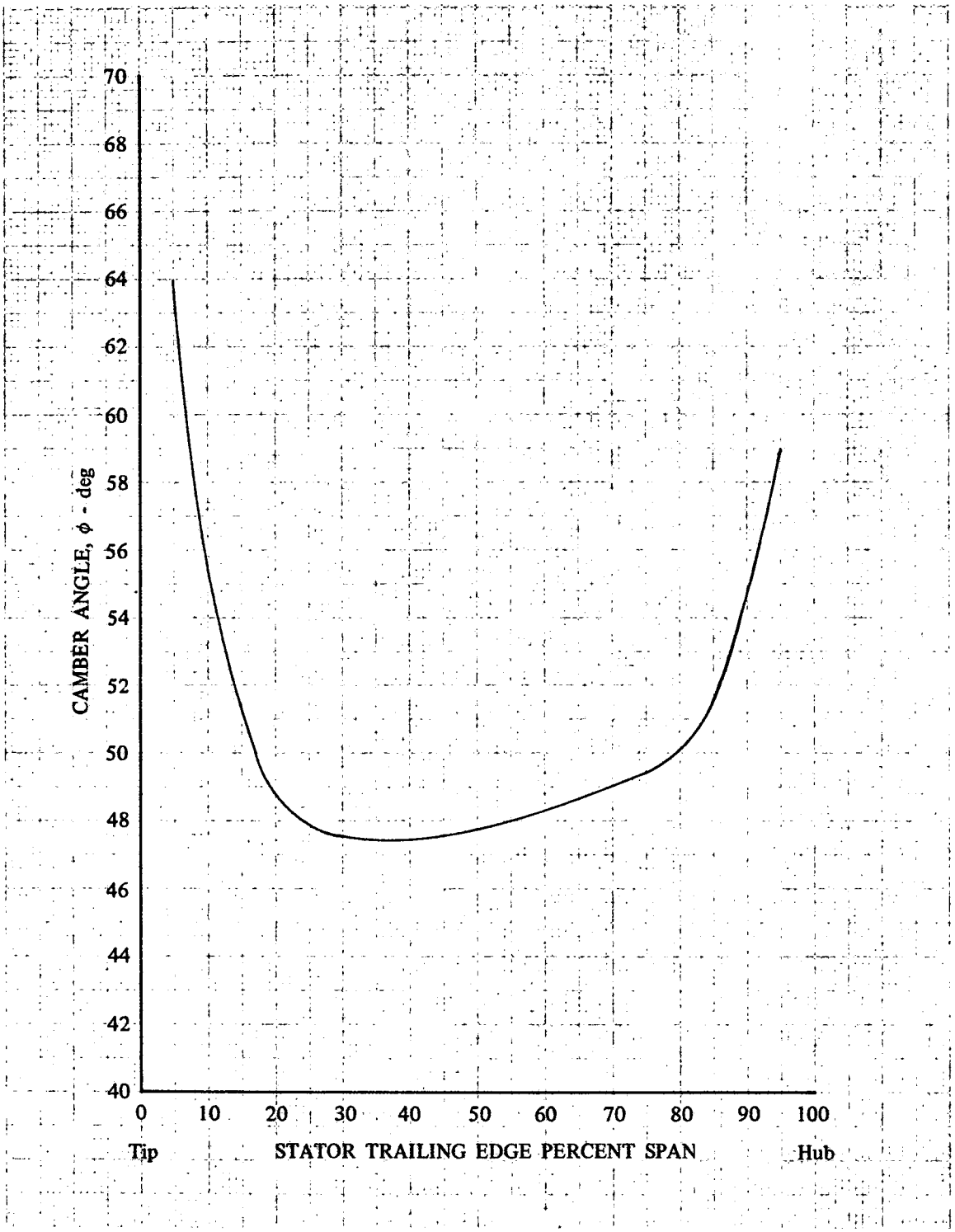

Figure 29. Stator D Camber Angle Distribution DF 93415

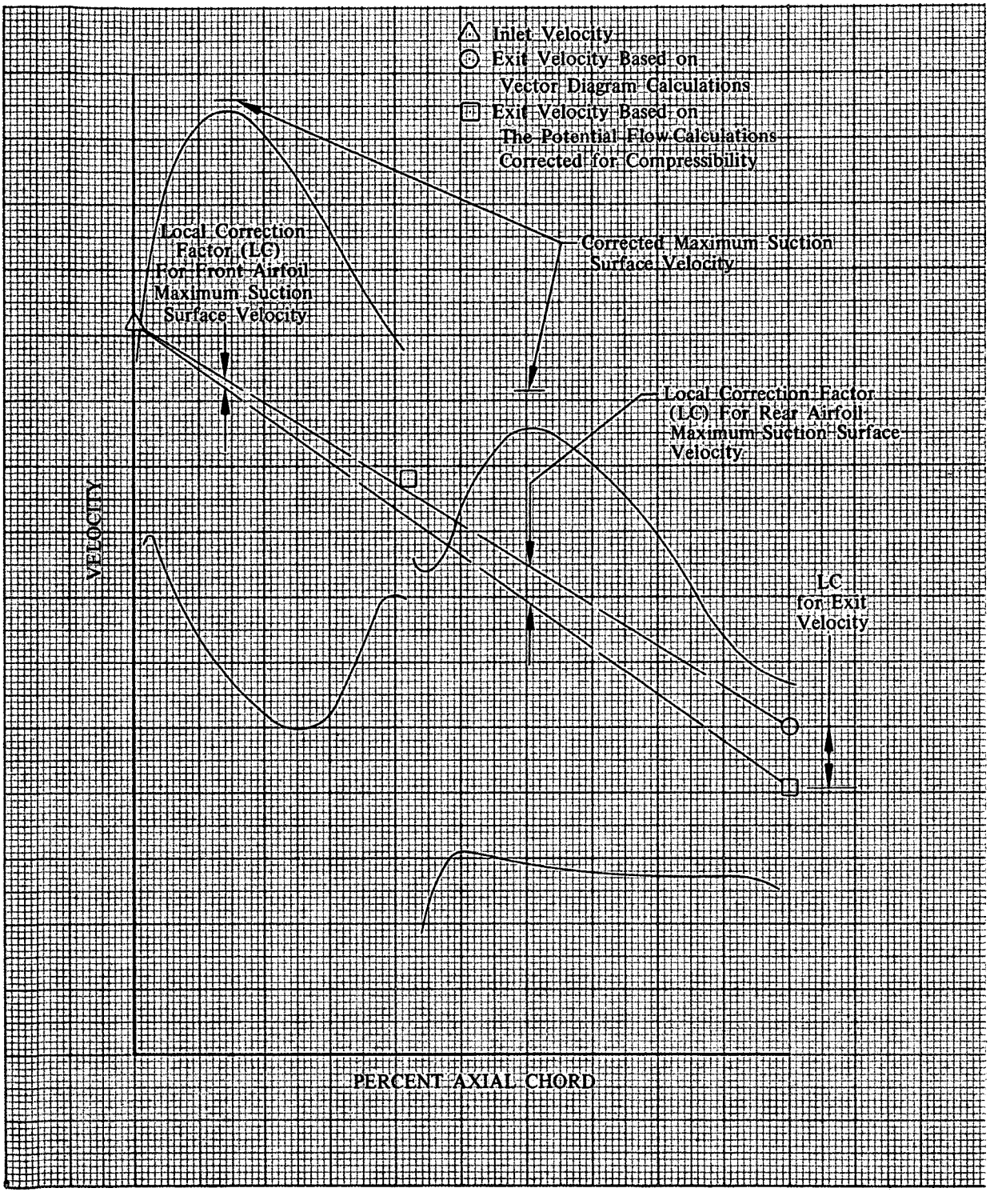

Figure 30. Description of Technique Used to Modify Two-Dimensional Potential Flow Solution for Streamtube Convergence Through the Blade Row DF 93416

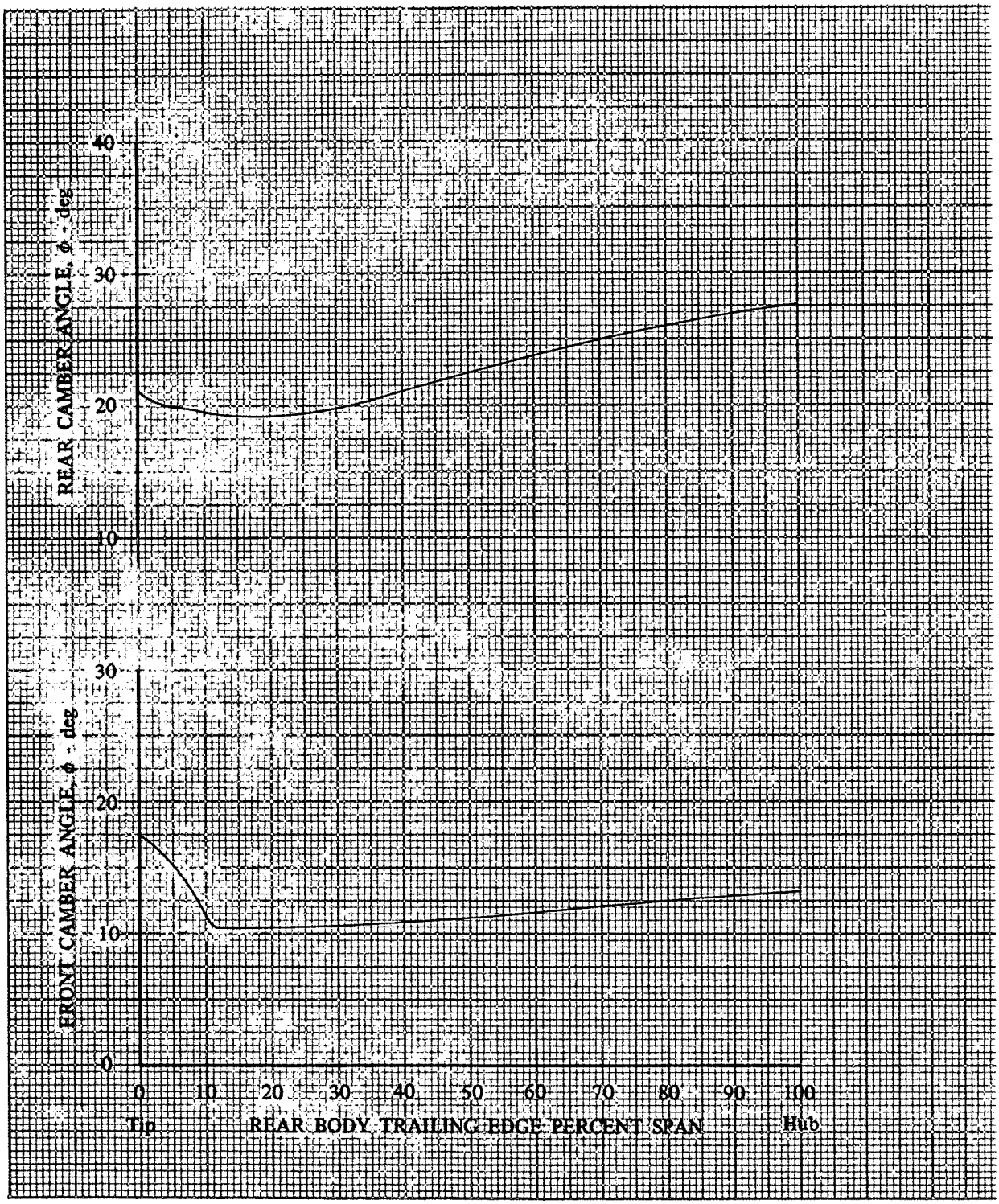

Figure 31. Rotor E Camber Angle Distributions DF 93417

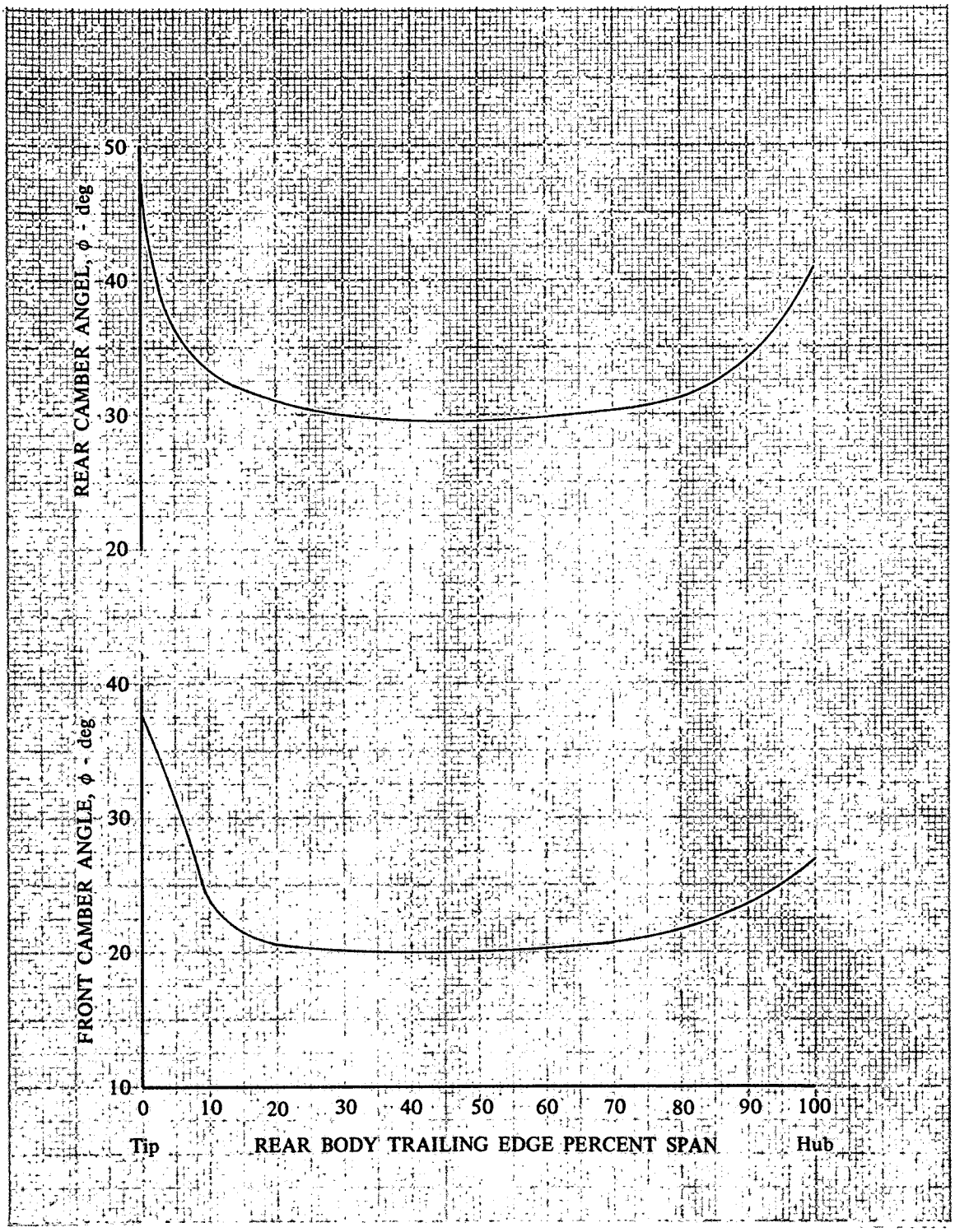

Figure 32. Stator E Camber Angle Distributions DF 93418

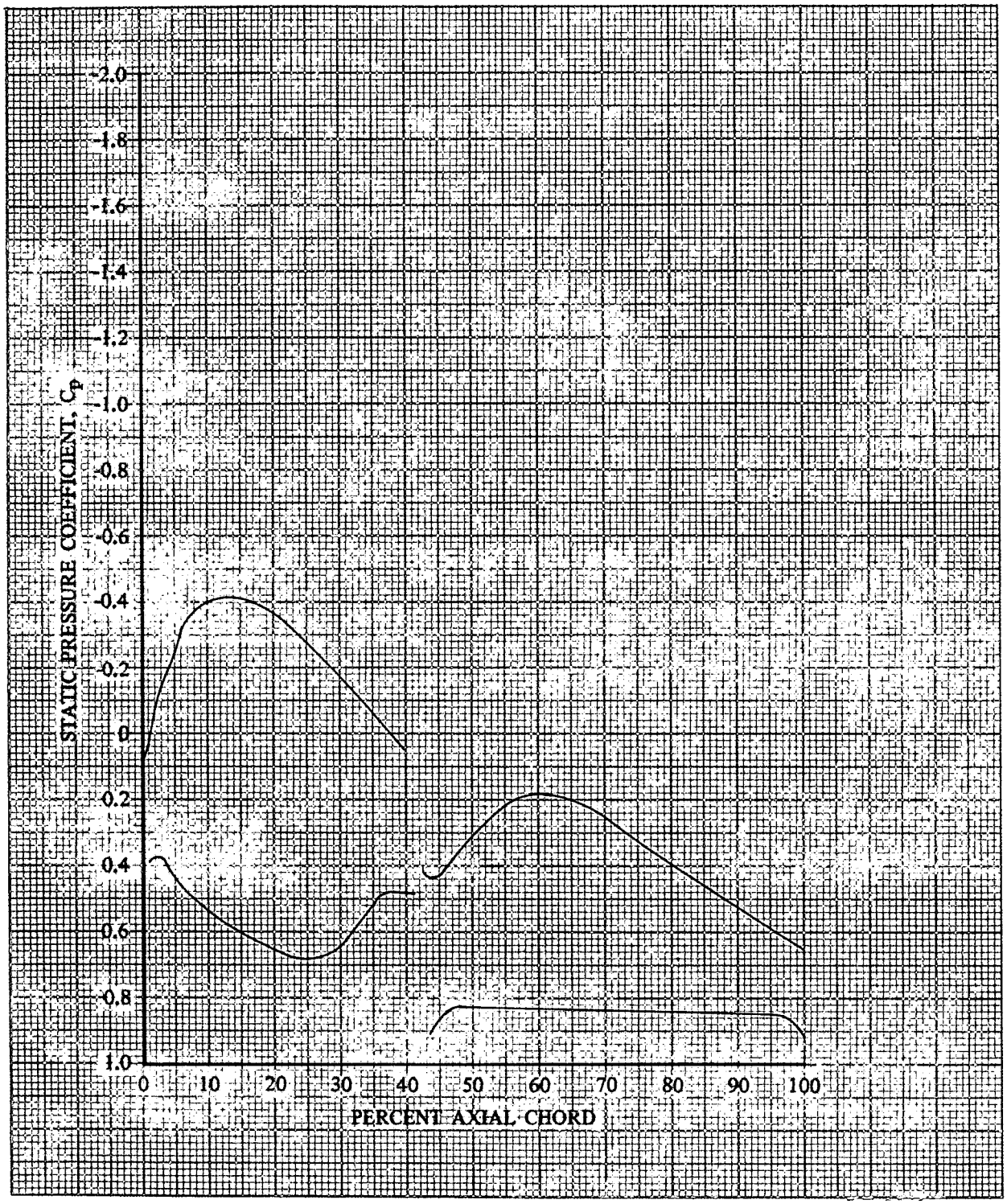

Figure 33. Rotor E Static Pressure Coefficient Distribution, 0% Span From Tip DF 93419

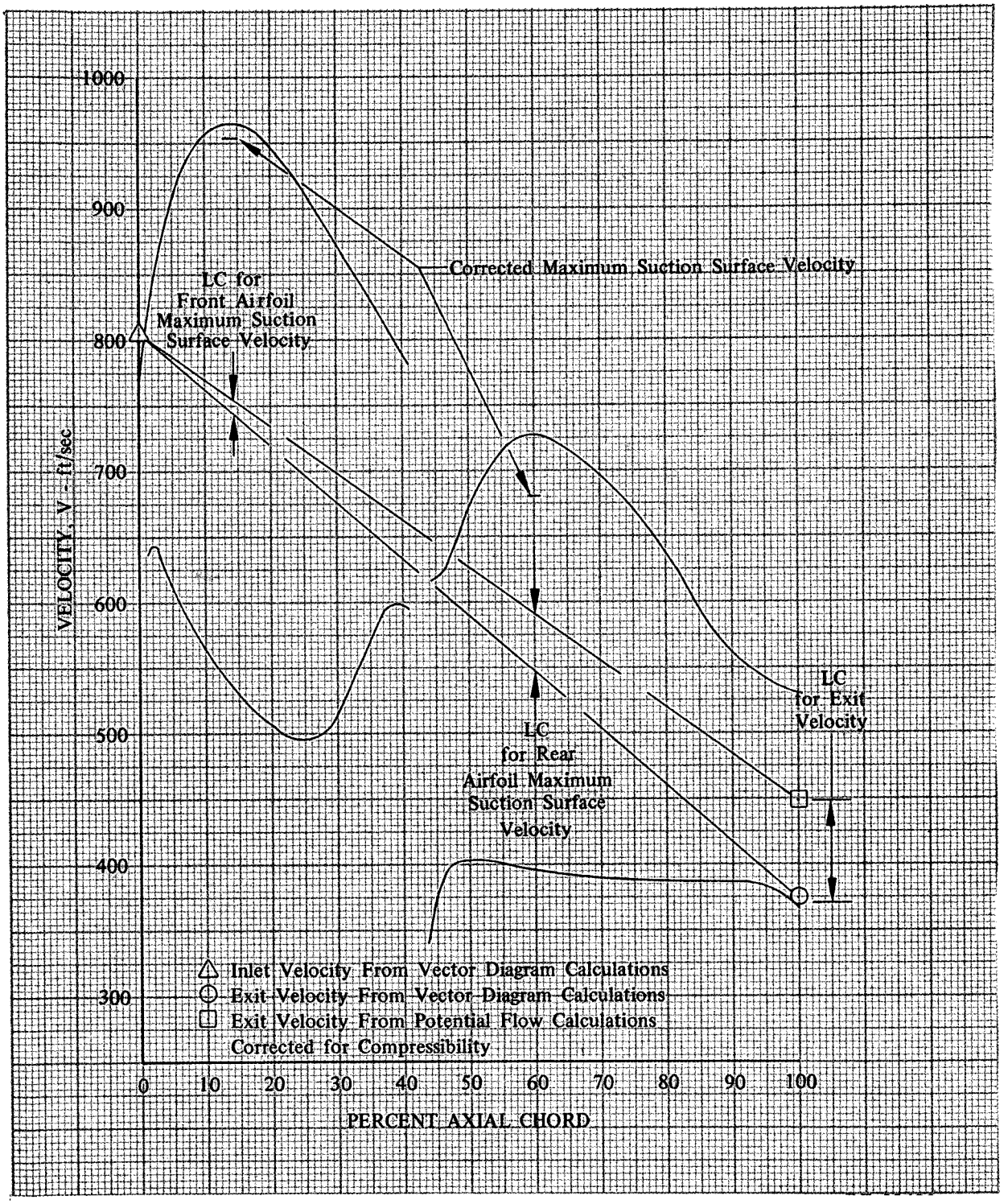

Figure 34. Rotor E Blade Surface Velocities, 0% Span From Tip DF 93420

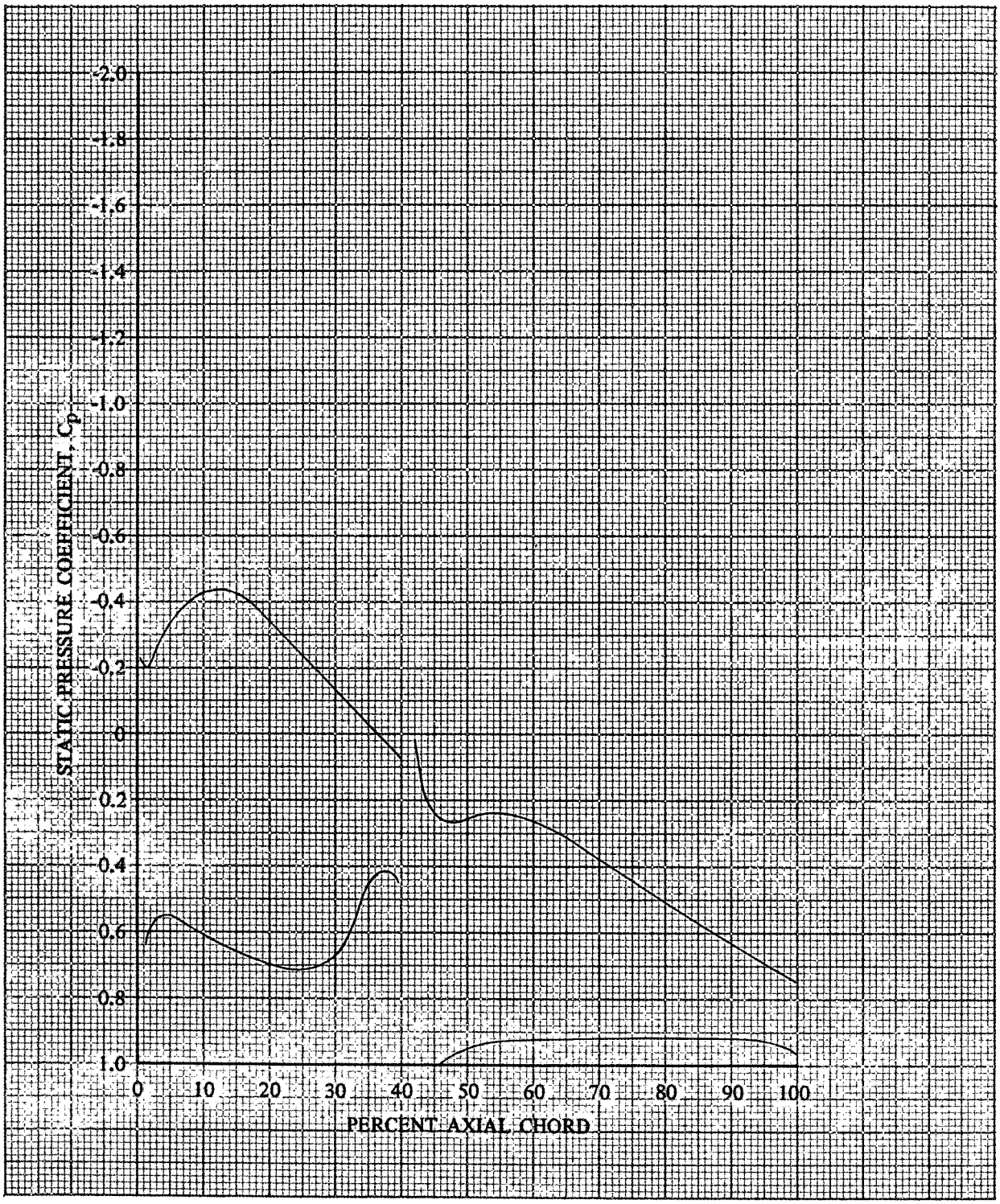

Figure 35. Rotor E Static Pressure Coefficient Distribution, 2.5% Span From Tip DF 93421

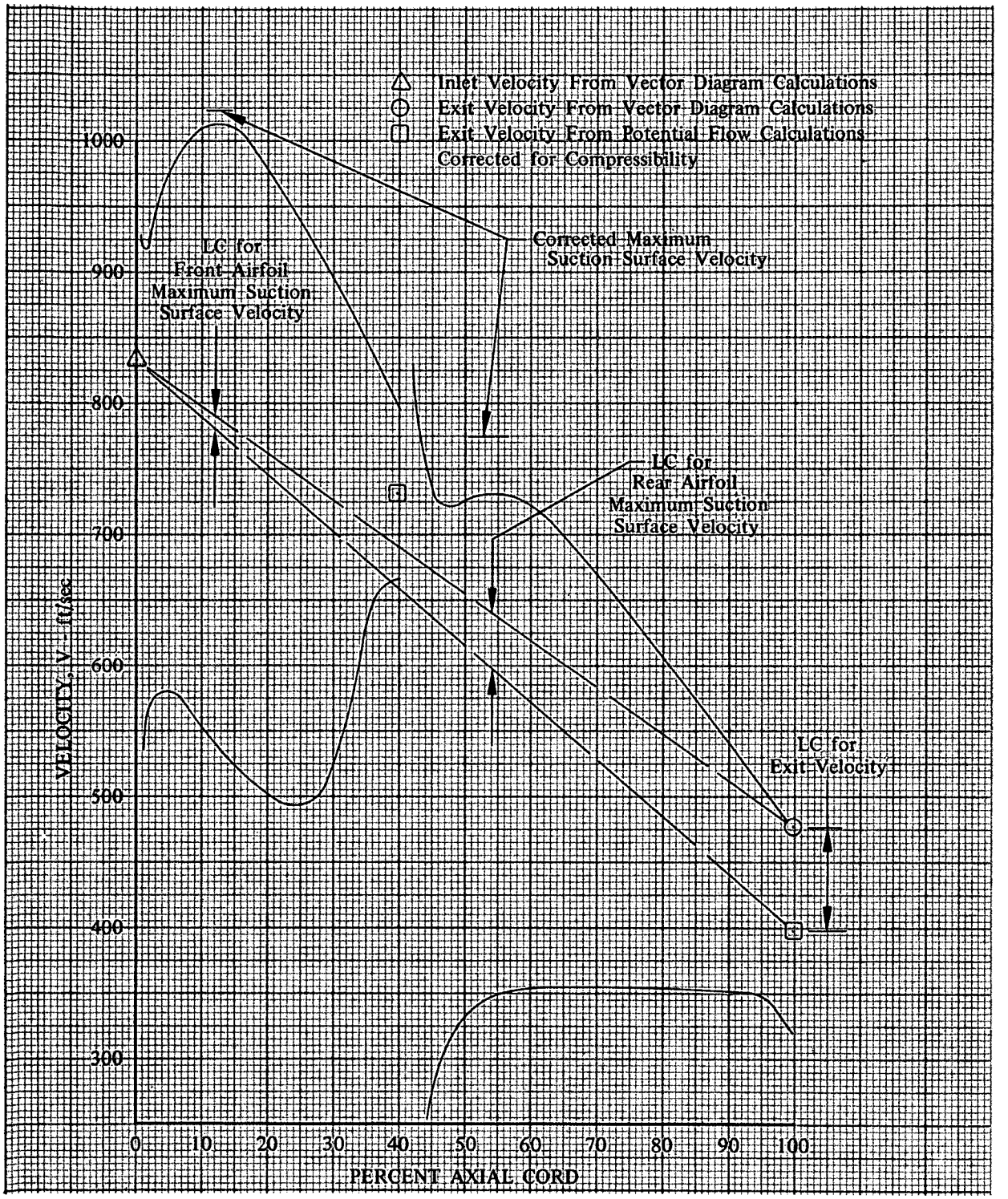

Figure 36. Rotor E Blade Surface Velocities, 2.5% Span From Tip

DF 93422

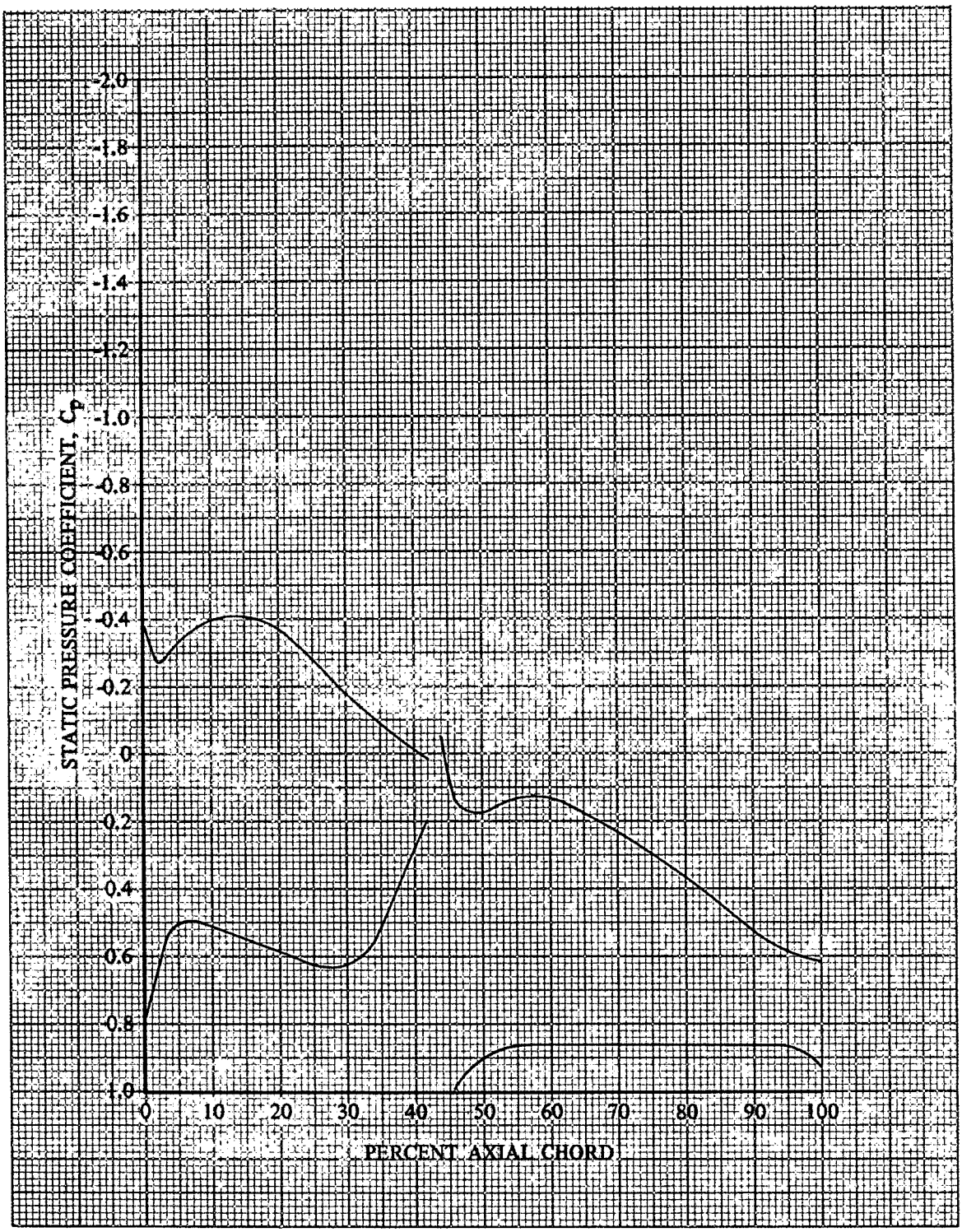

Figure 37. Rotor E Static Pressure Coefficient Distribution, 9.3% Span From Tip DF 93423

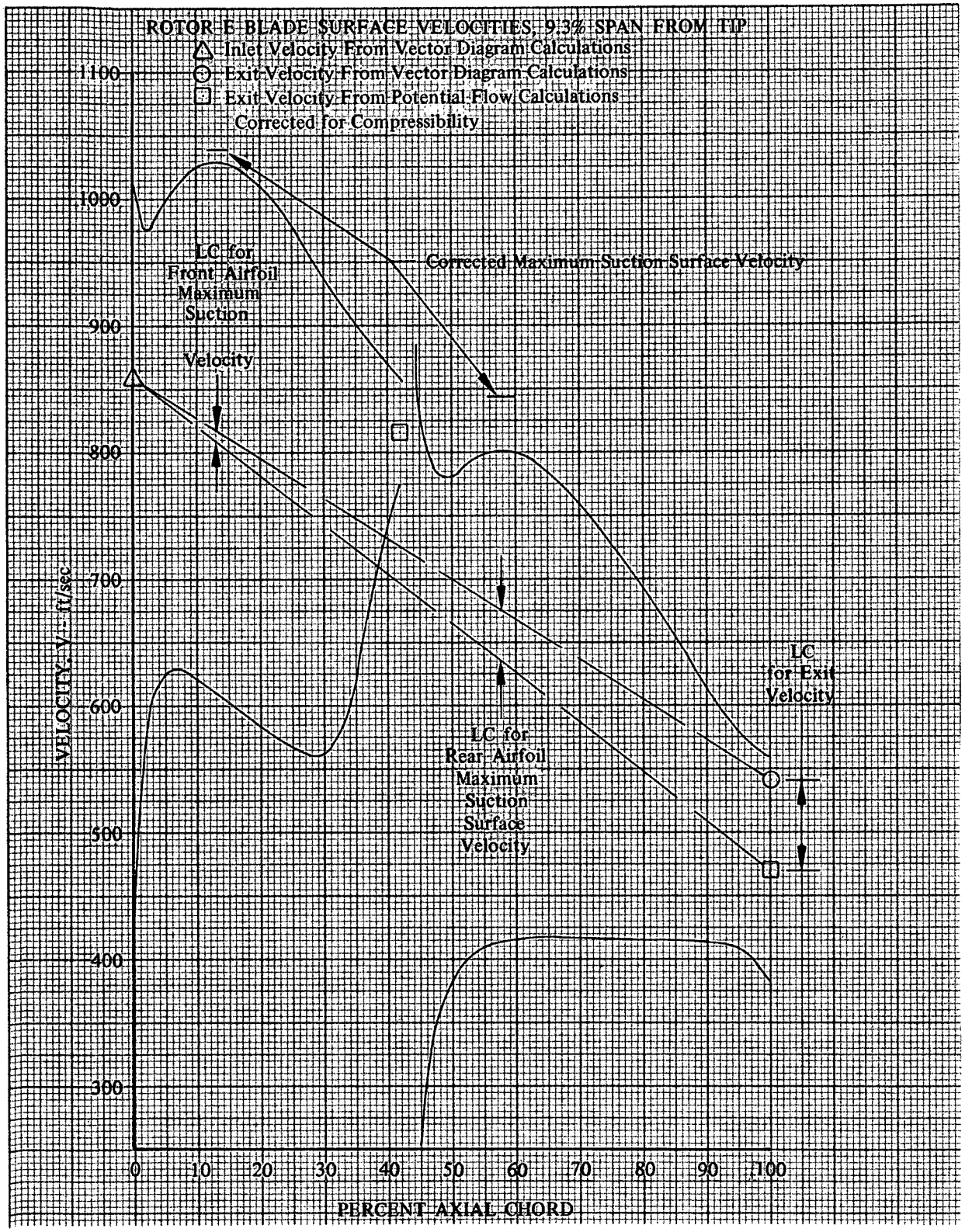

Figure 38. Rotor E Blade Surface Velocities, 9.3% Span From Tip

DF 93424

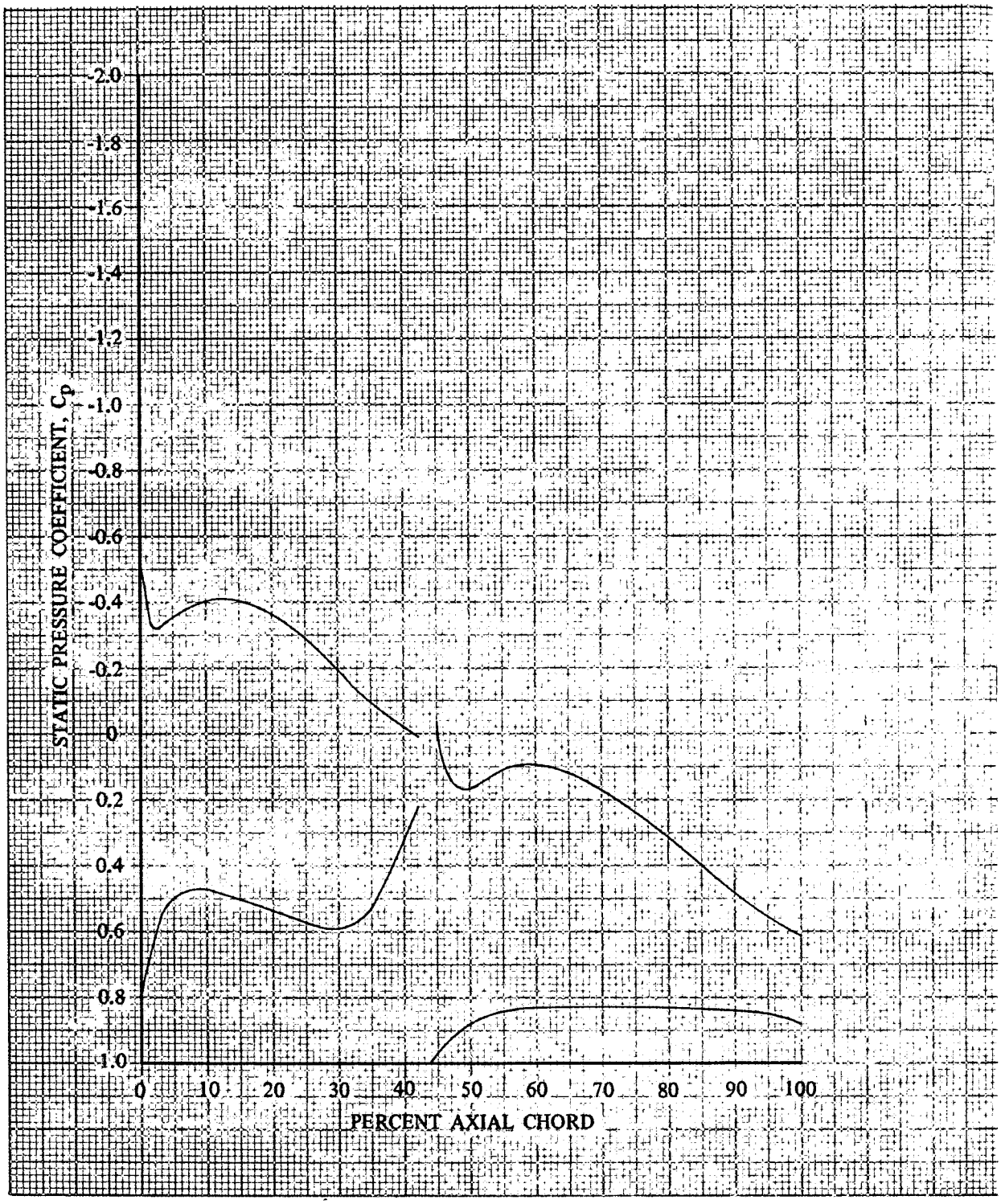

Figure 39. Rotor E Static Pressure Coefficient Distribution, 12.2% Span From Tip DF 93425

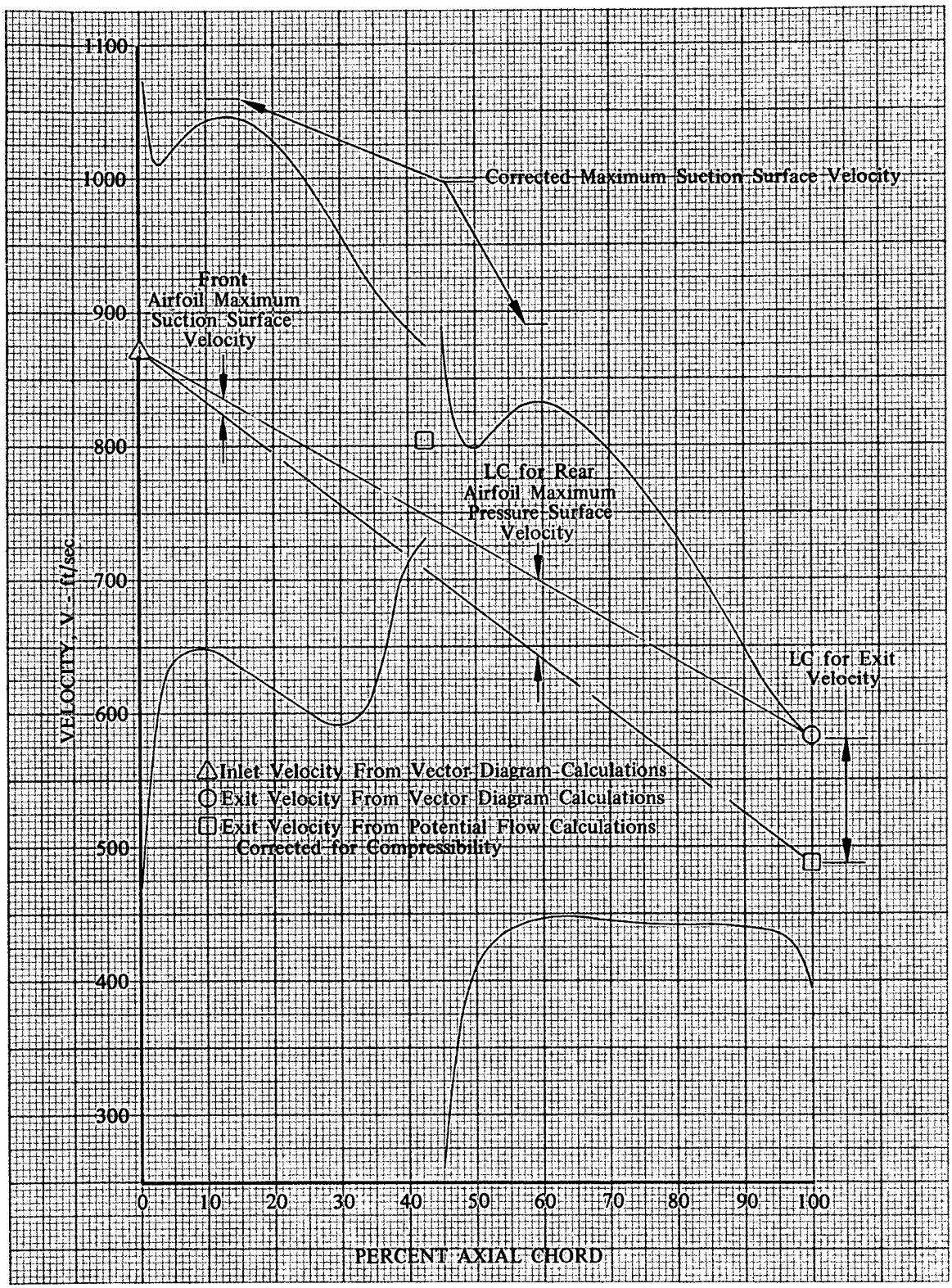

Figure 40. Rotor E Blade Surface Velocities, 12.2% Span From Tip DF 93426

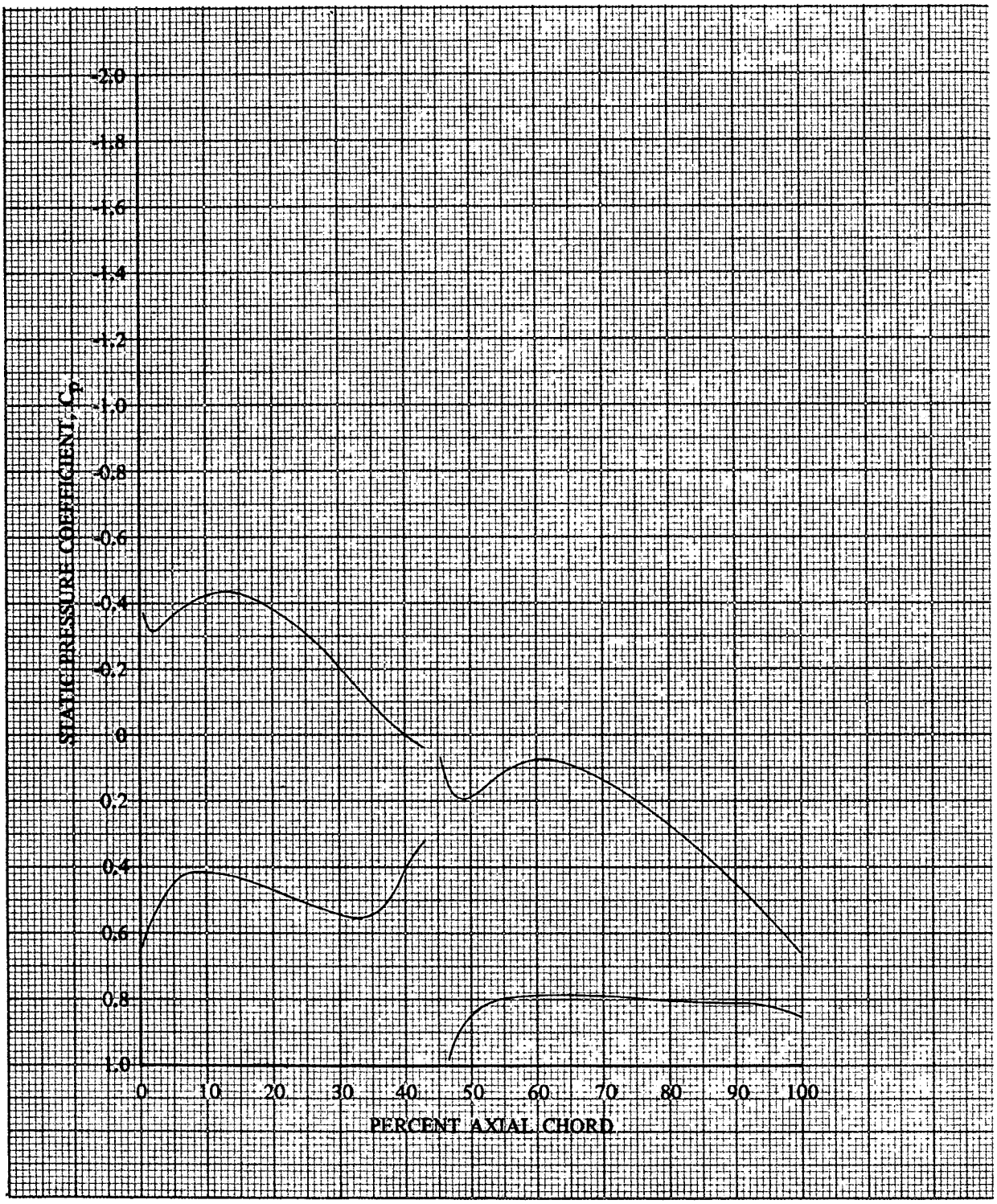

Figure 41. Rotor E Static Pressure Coefficient Distribution, 39.8% Span From Tip DF 93427

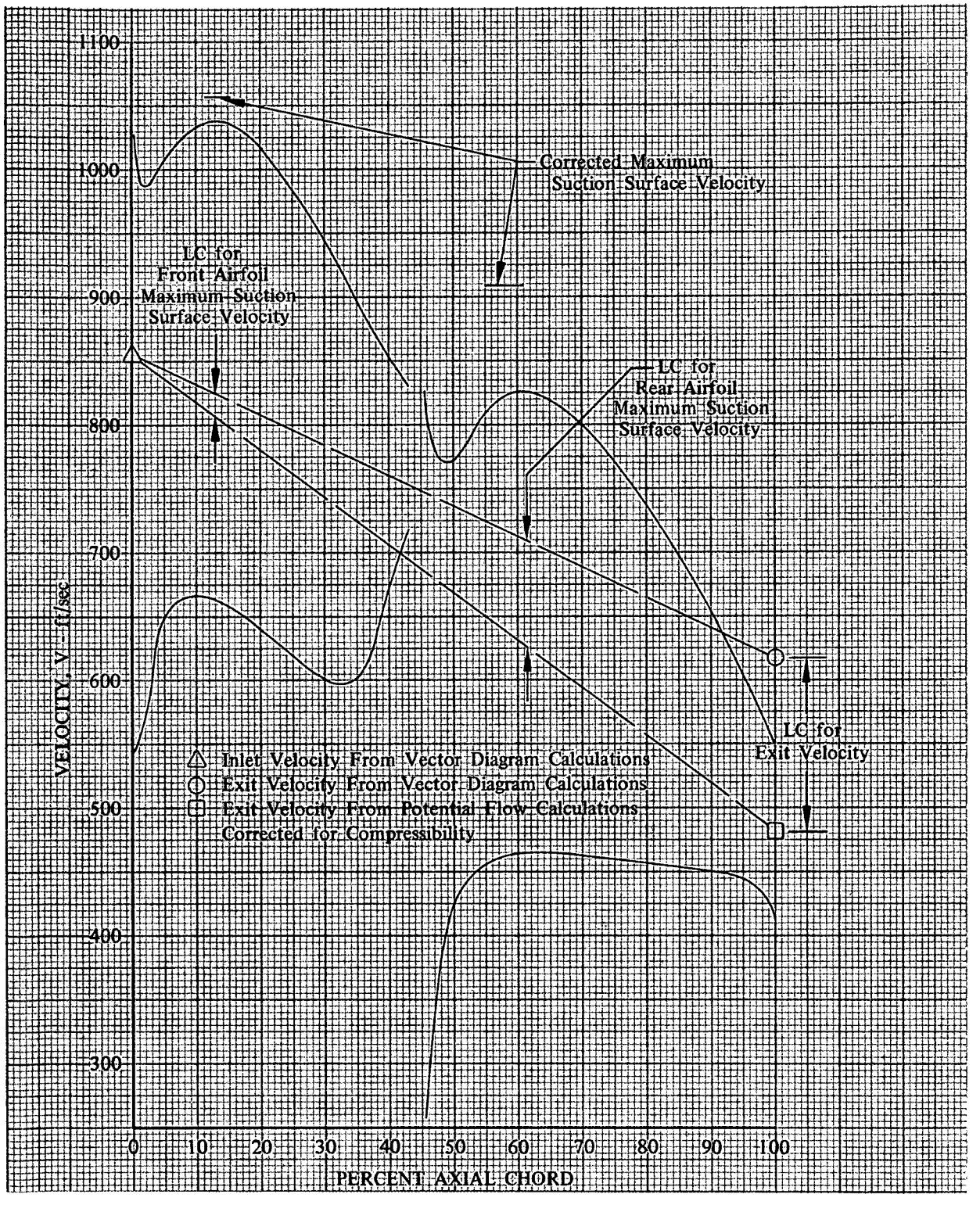

Figure 42. Rotor E Blade Surface Velocities, 39.8% Span From Tip

DF 93428

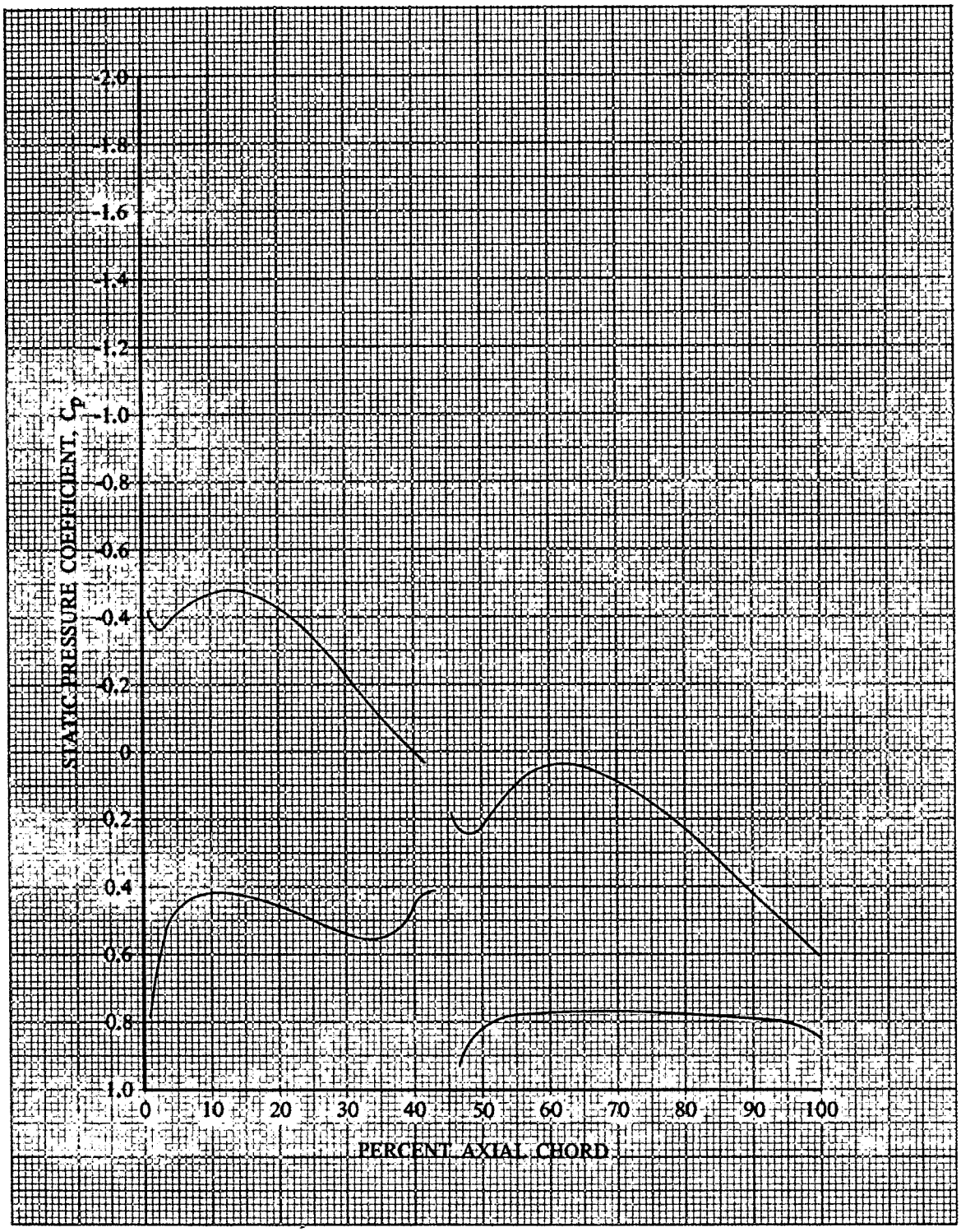

Figure 43. Rotor E Static Pressure Coefficient Distribution, 66.5% Span From Tip DF 93429

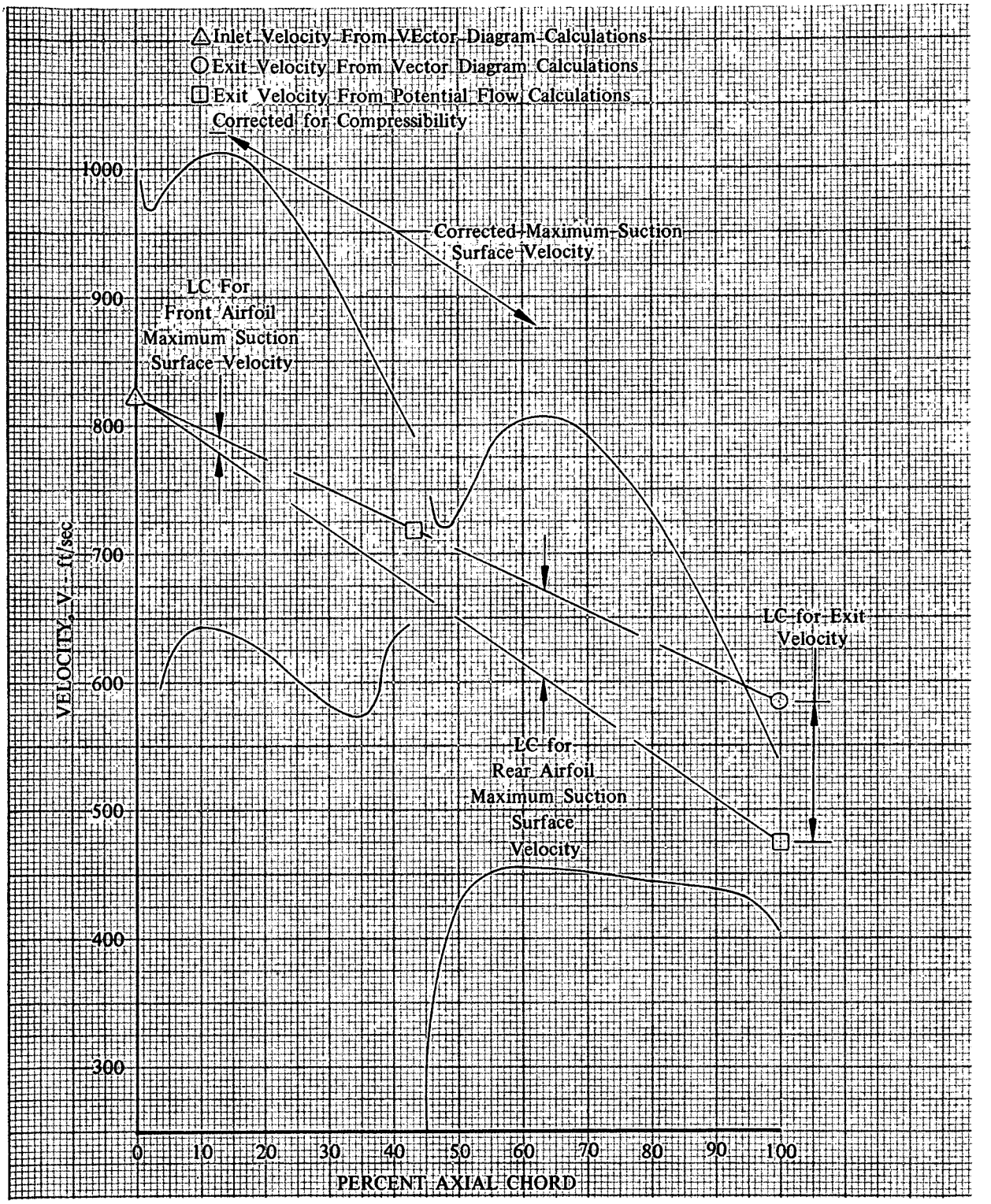

Figure 44. Rotor E Blade Surface Velocities, 66.5% Span From Tip DF 93430

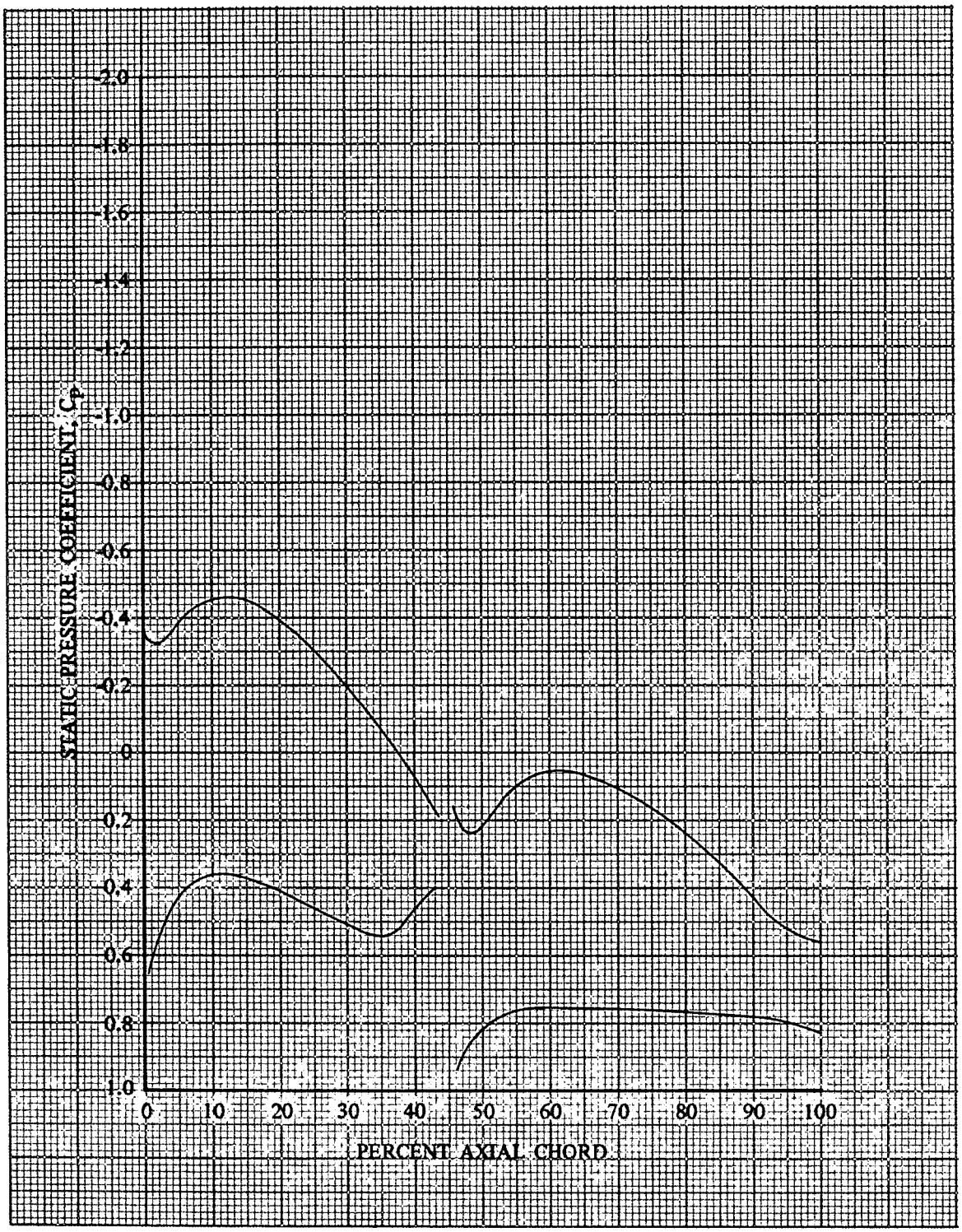

Figure 45. Rotor E Static Pressure Coefficient Distribution, 91.0% Span From Tip DF 93431

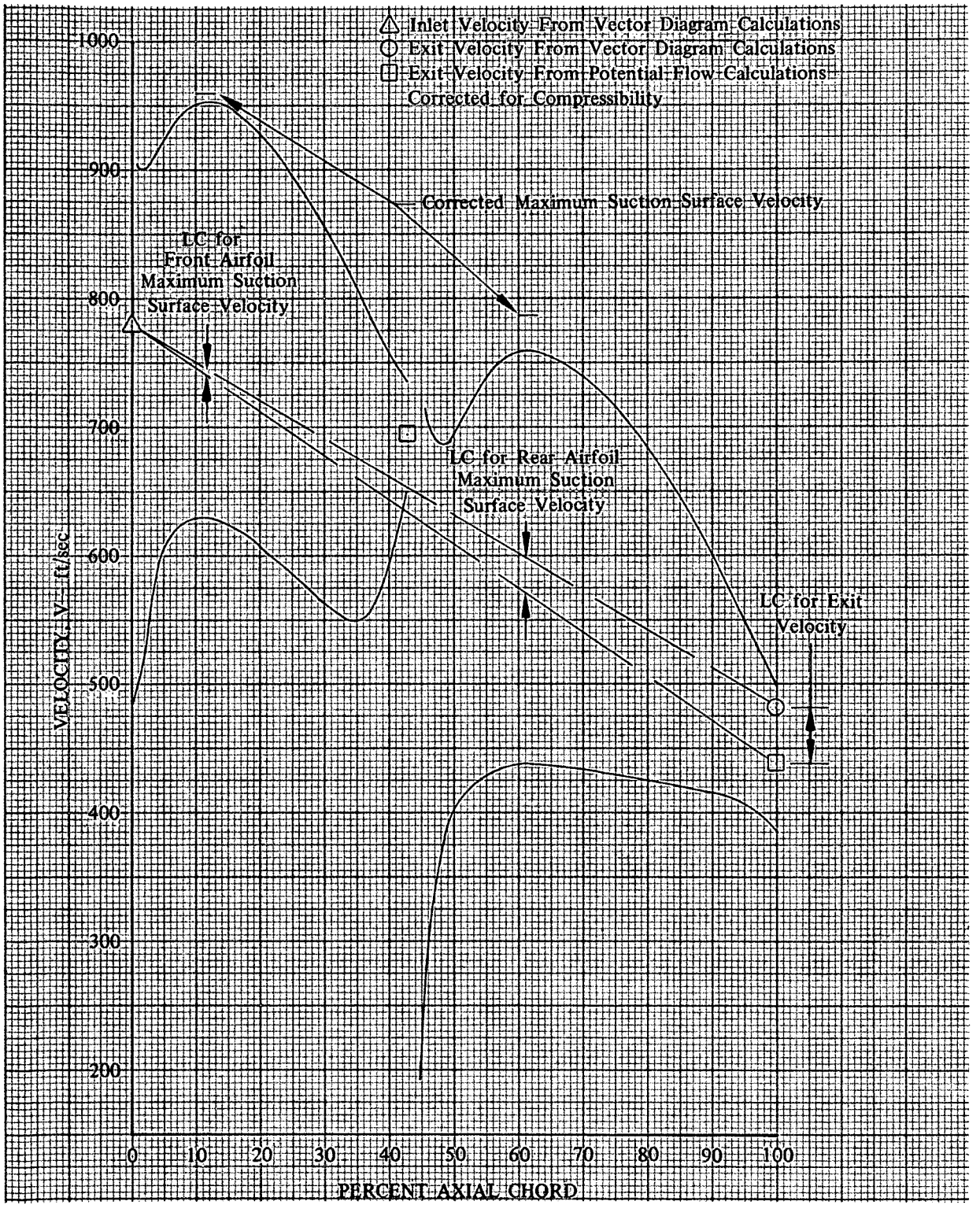

Figure 46. Rotor E Blade Surface Velocities, 91.0% Span From Tip

DF 93432

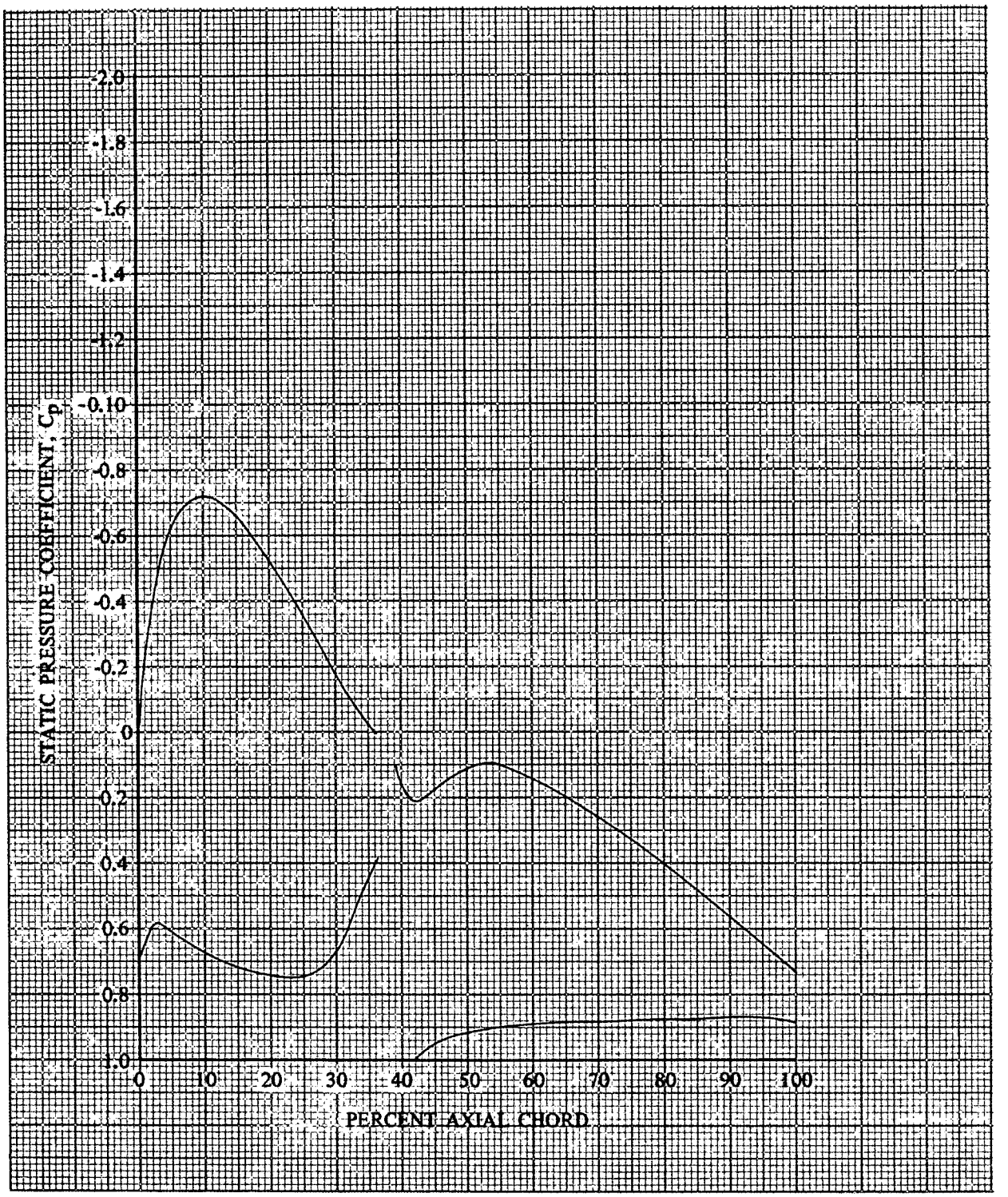

Figure 47. Stator E Static Pressure Coefficient Distribution, 2.5% Span From Tip DF 93433

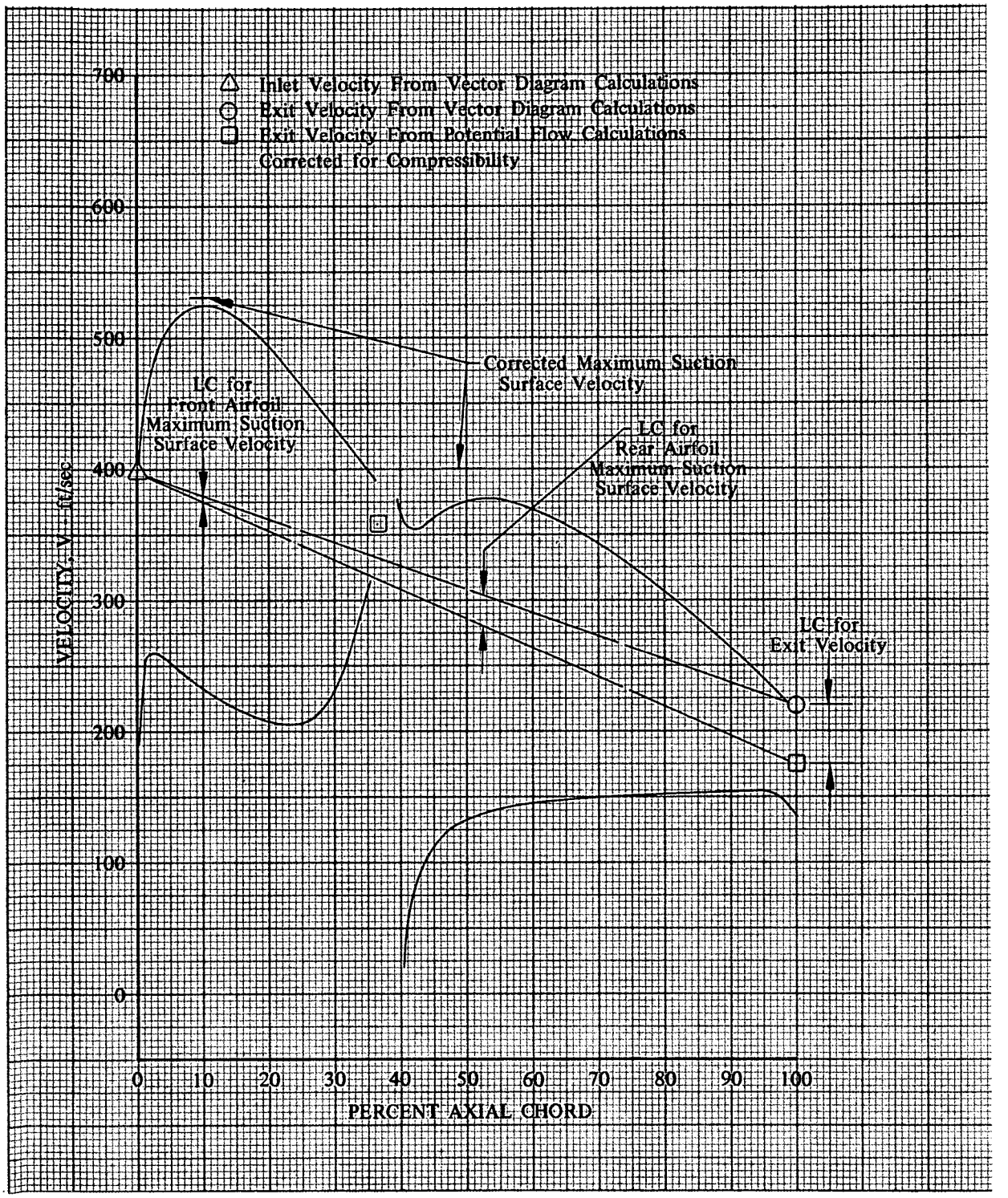

Figure 48. Stator E Vane Surface Velocities, 2.5% Span From Tip

DF 93434

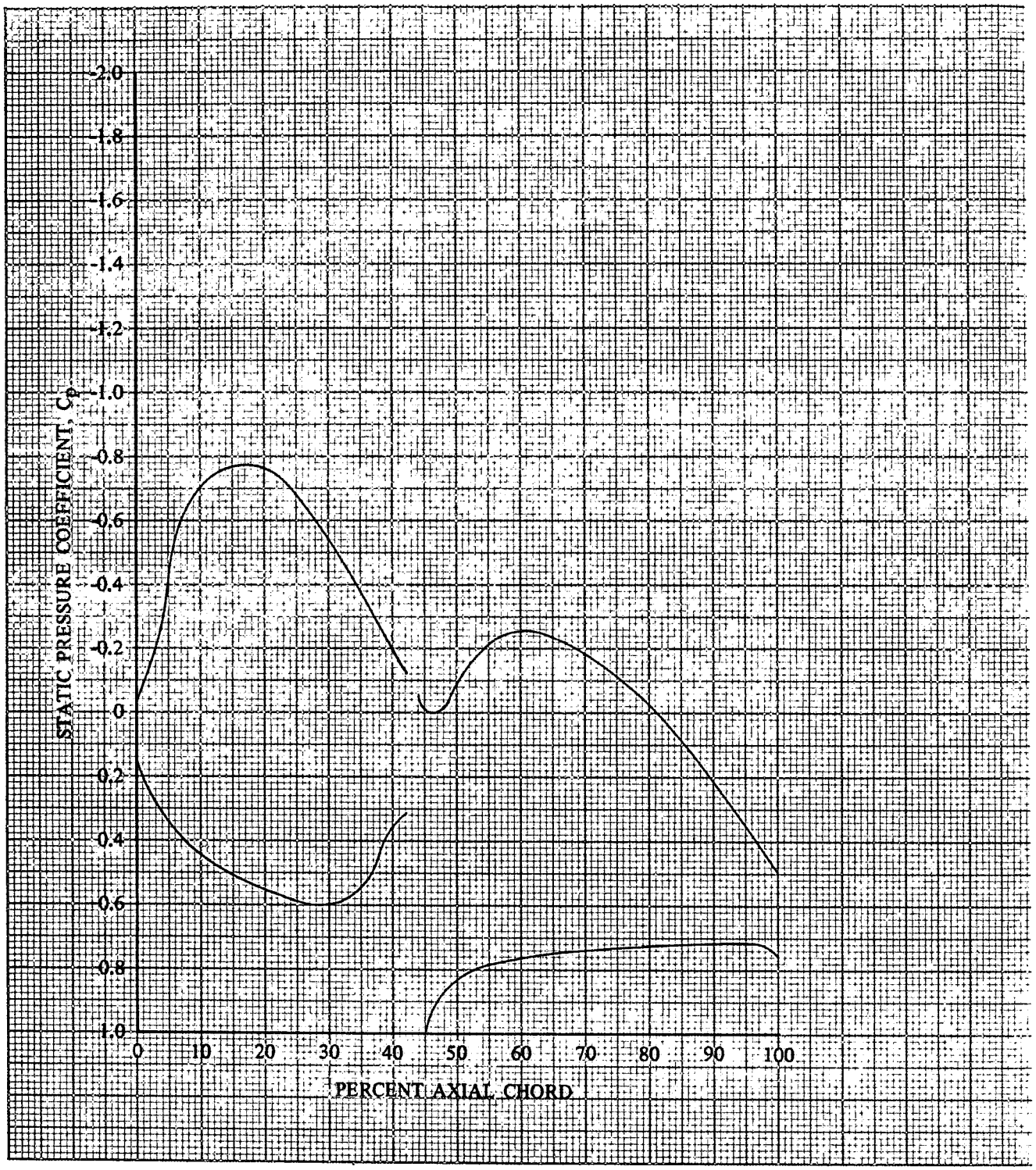

Figure 49. Stator E Static Pressure Coefficient Distribution, 5% Span From Tip DF 93435

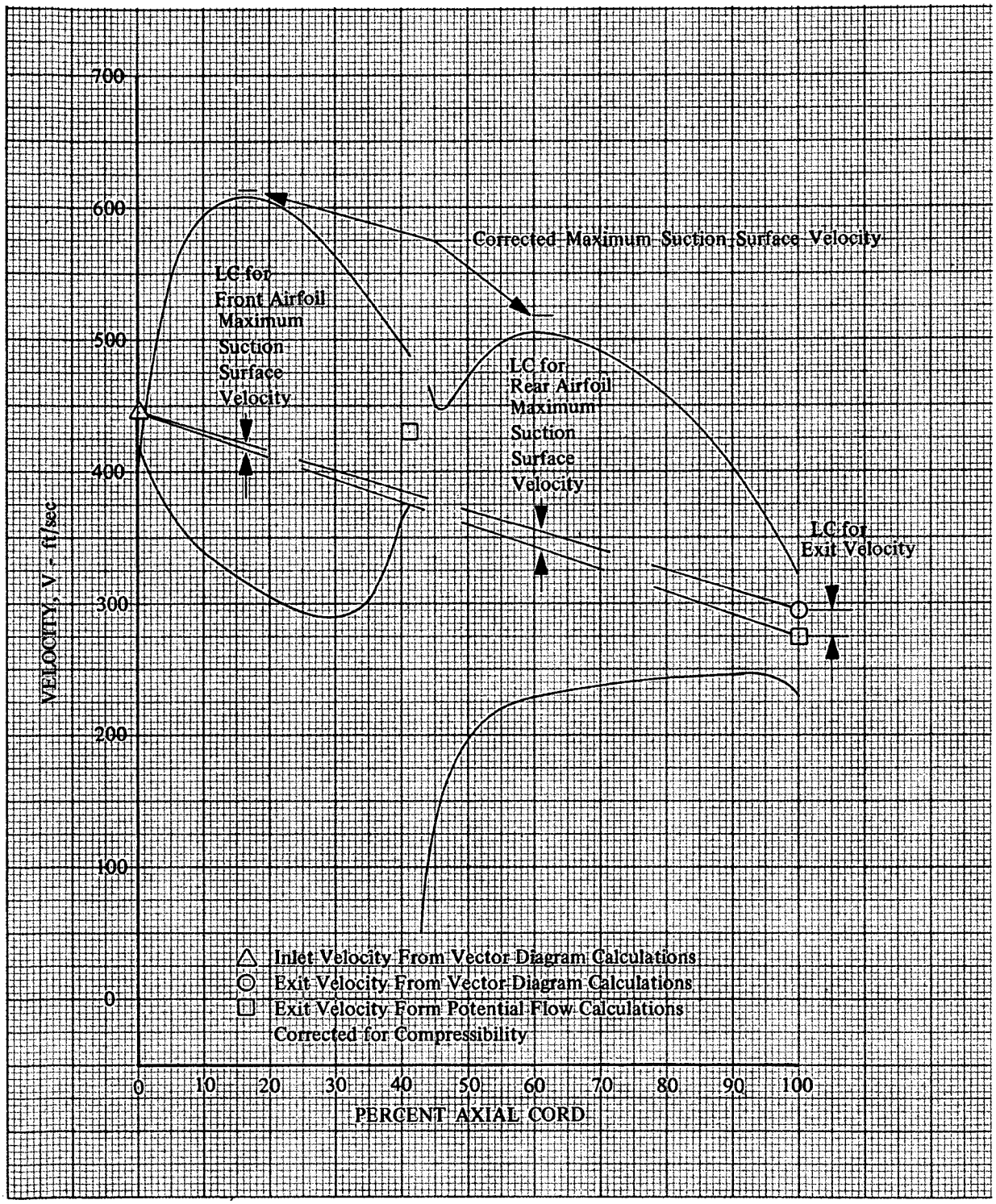

Figure 50. Stator E Vane Surface Velocities, 5% Span From Tip

DF 93436

G

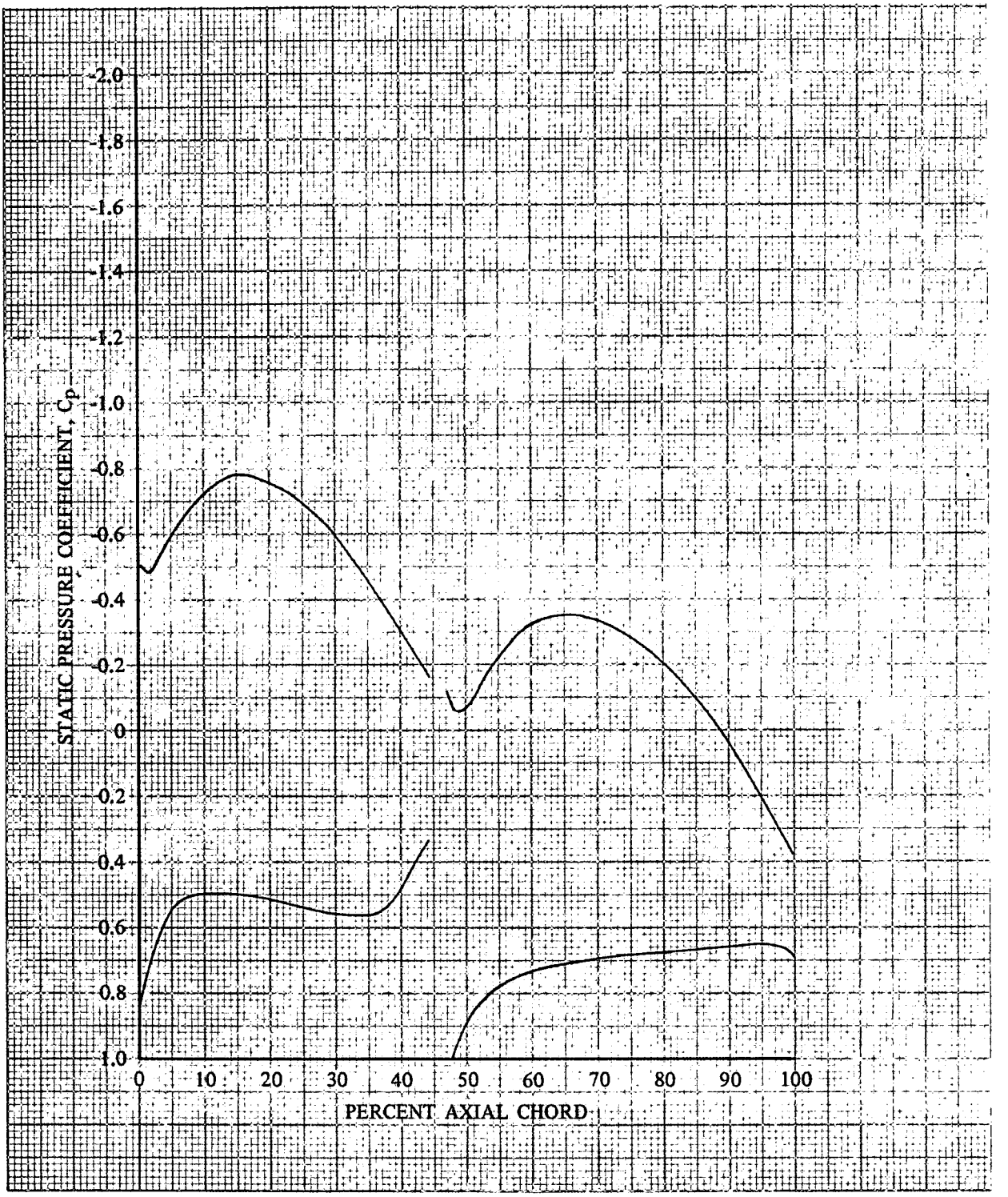

Figure 51. Stator E Static Pressure Coefficient Distribution, 9.1% Span From Tip DF 93437

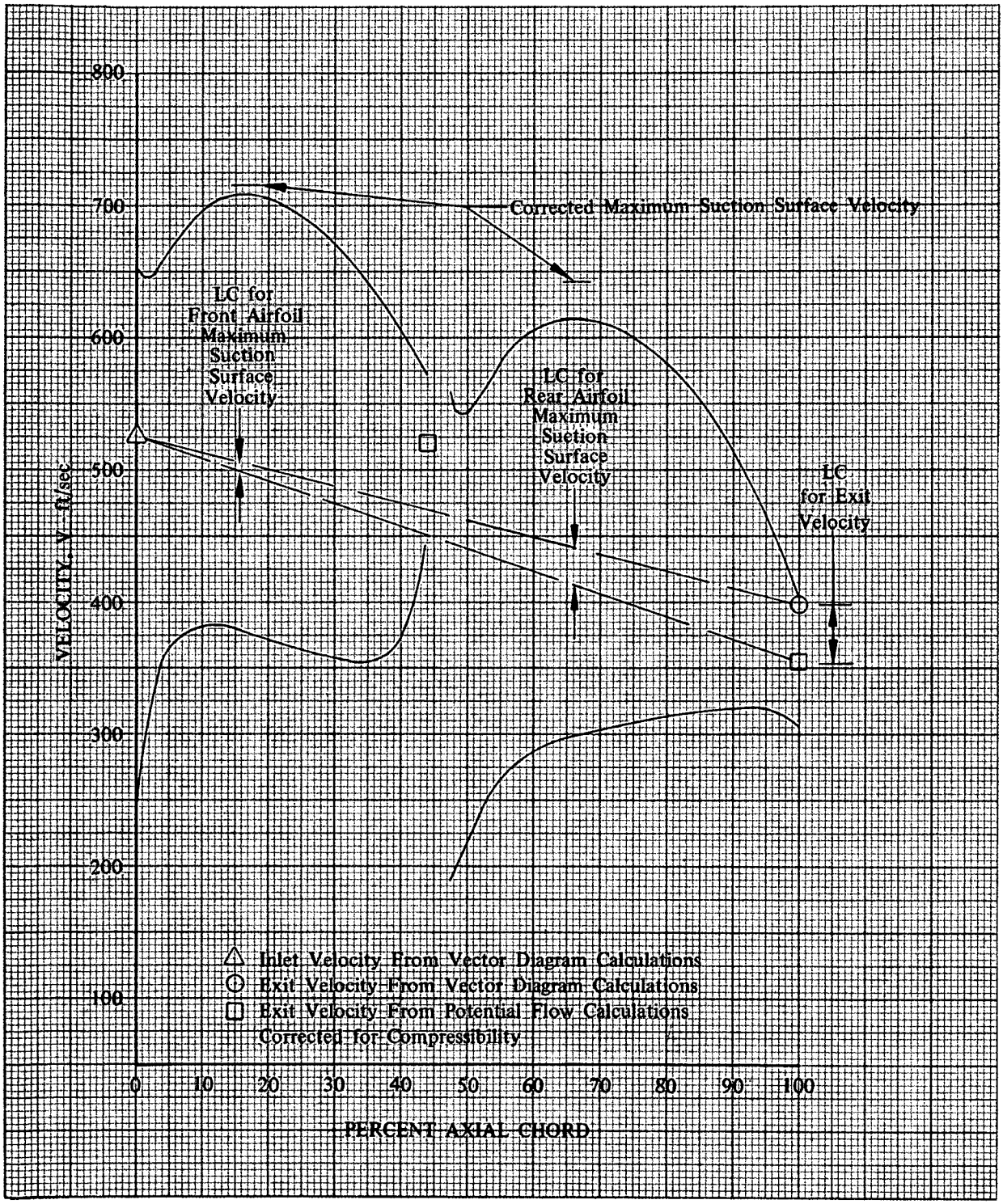

Figure 52. Stator E Vane Surface Velocities, 9.1% Span From Tip DF 93438

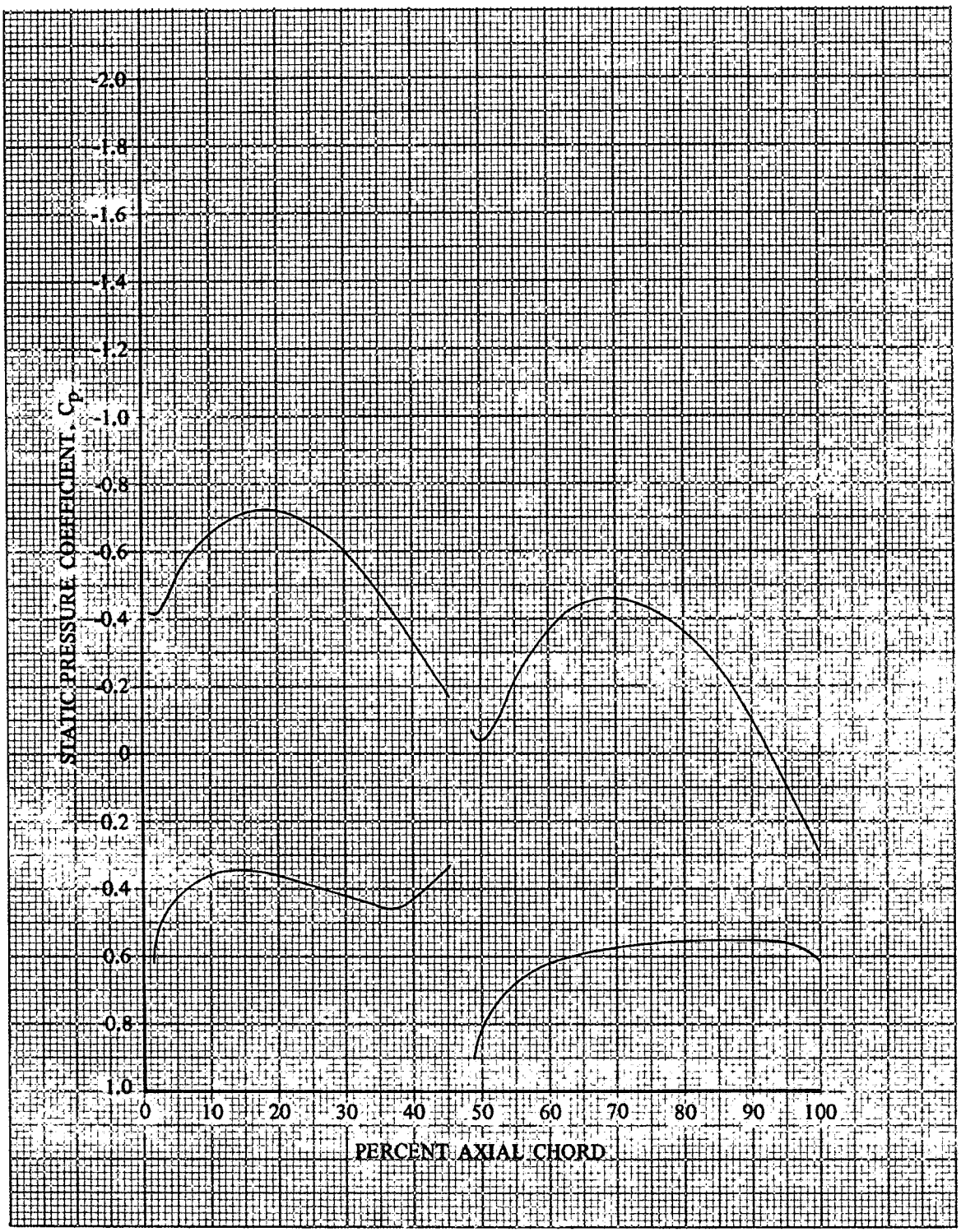

Figure 53. Stator E Static Pressure Coefficient Distribution, 20% Span From Tip DF 93439

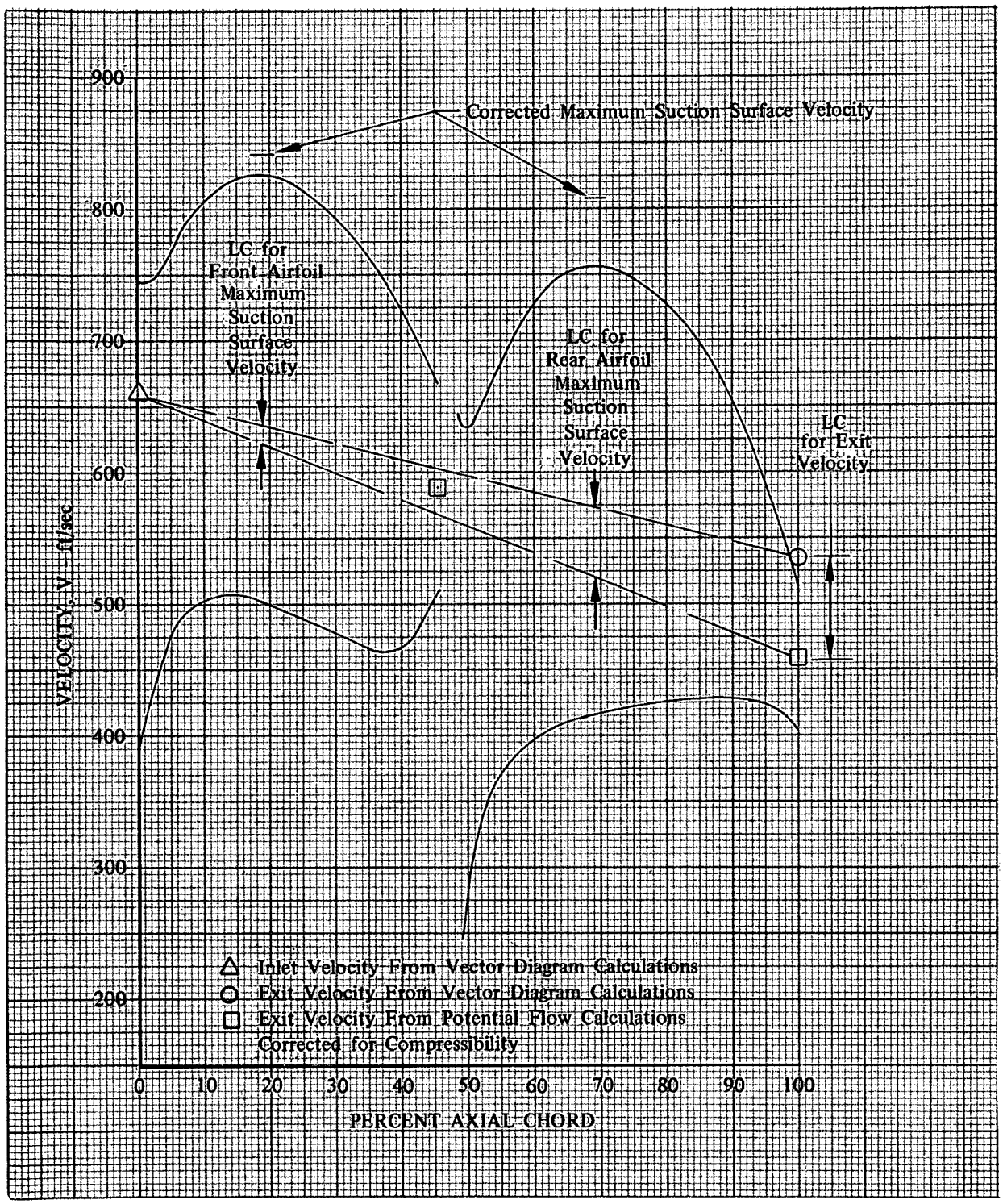

Figure 54. Stator E Vane Surface Velocities, 20% Span From Tip

DF 93440

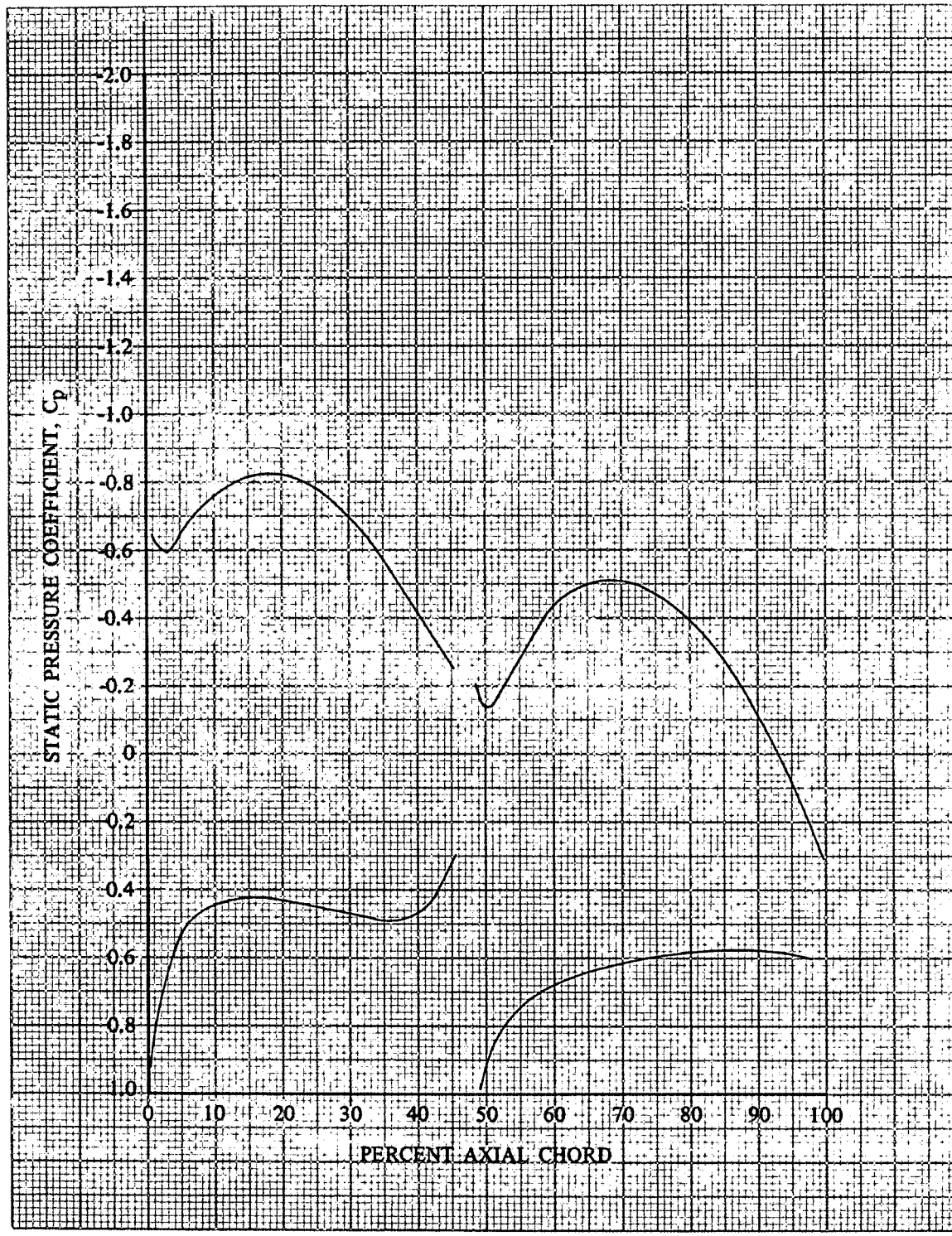

Figure 55. Stator E Static Pressure Coefficient Distribution, 50% Span DF 93441

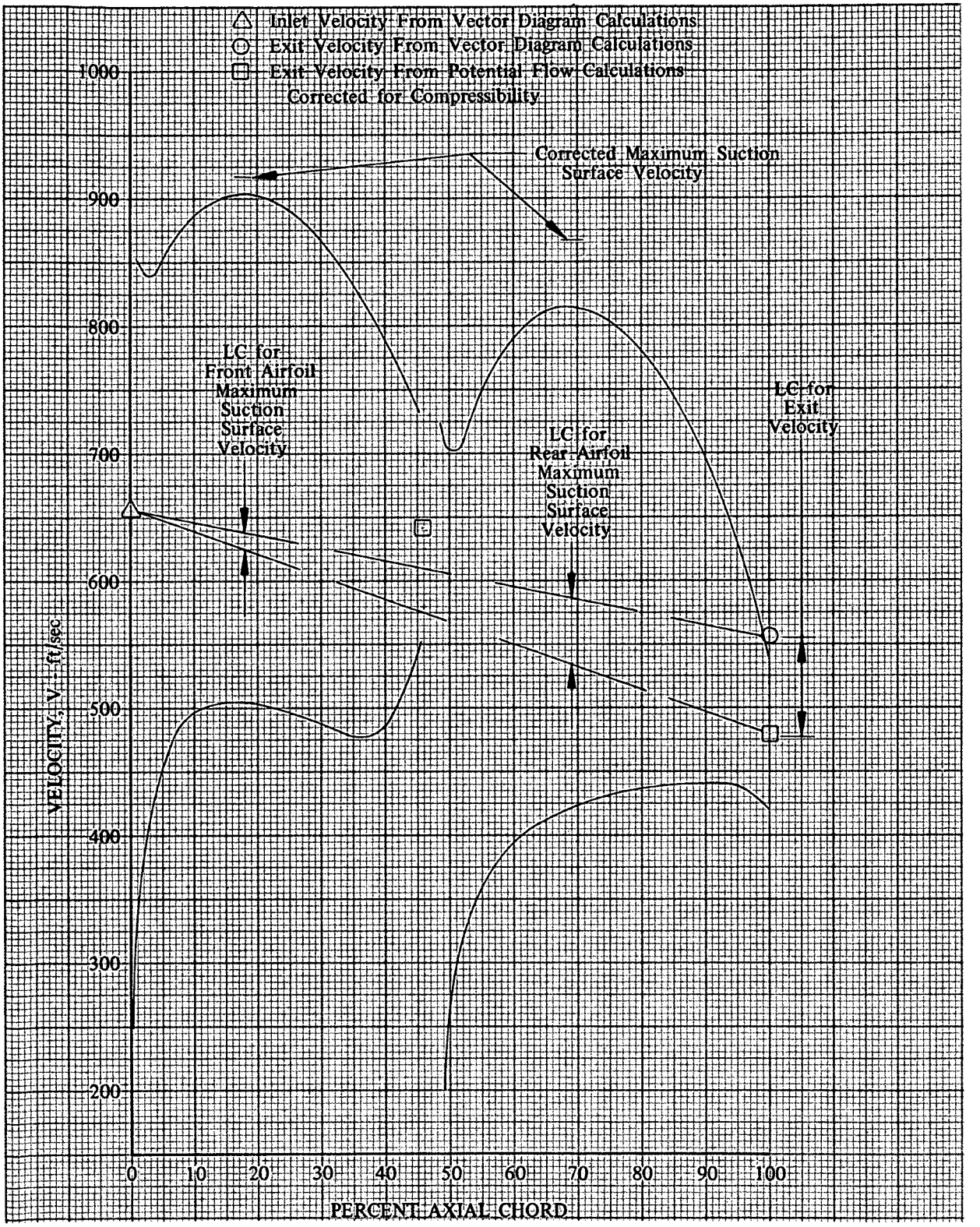

Figure 56. Stator E Vane Surface Velocities, 50% Span DF 93442

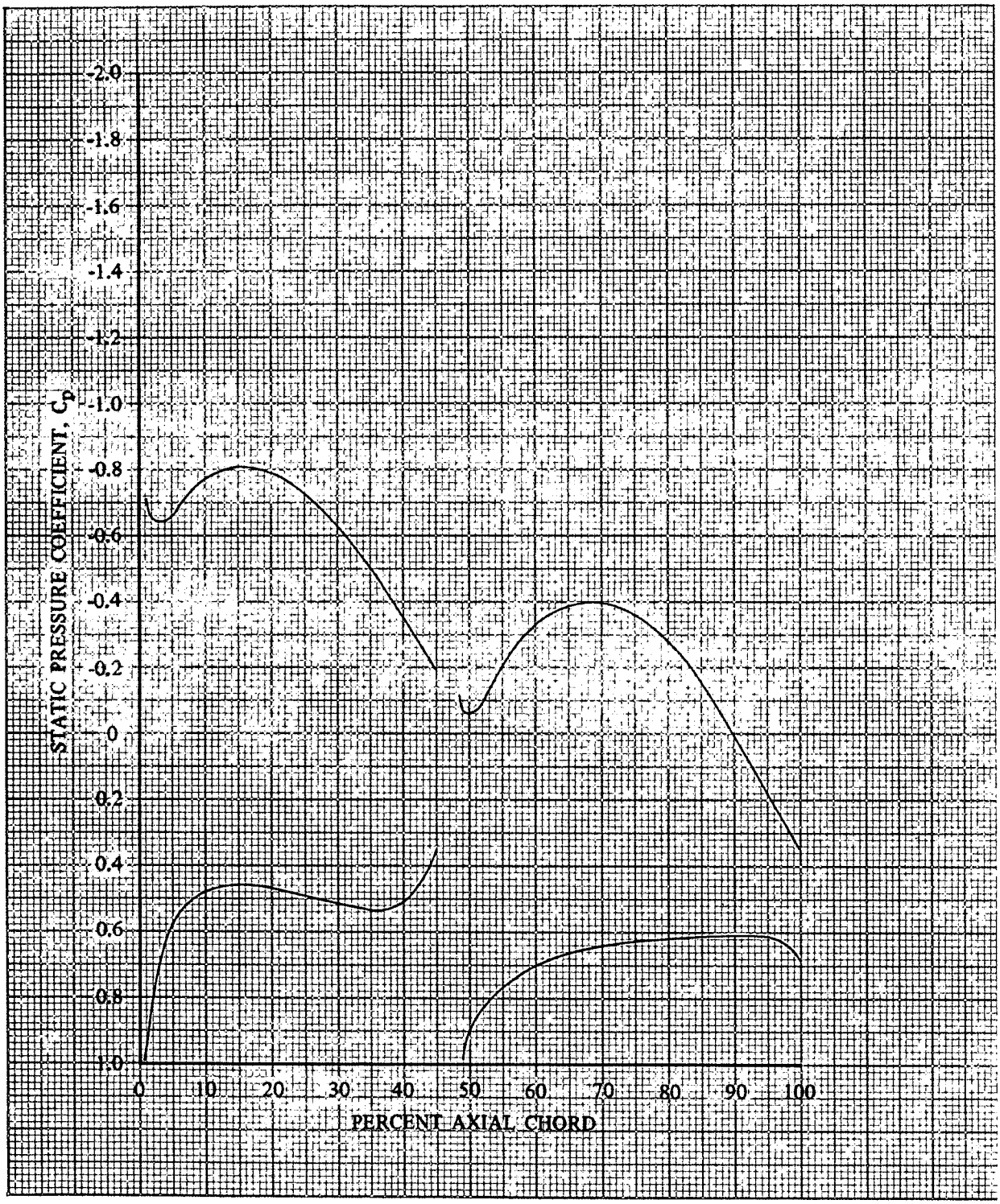

Figure 57. Stator E Static Pressure Coefficient Distribution, 80% Span From Tip DF 93443

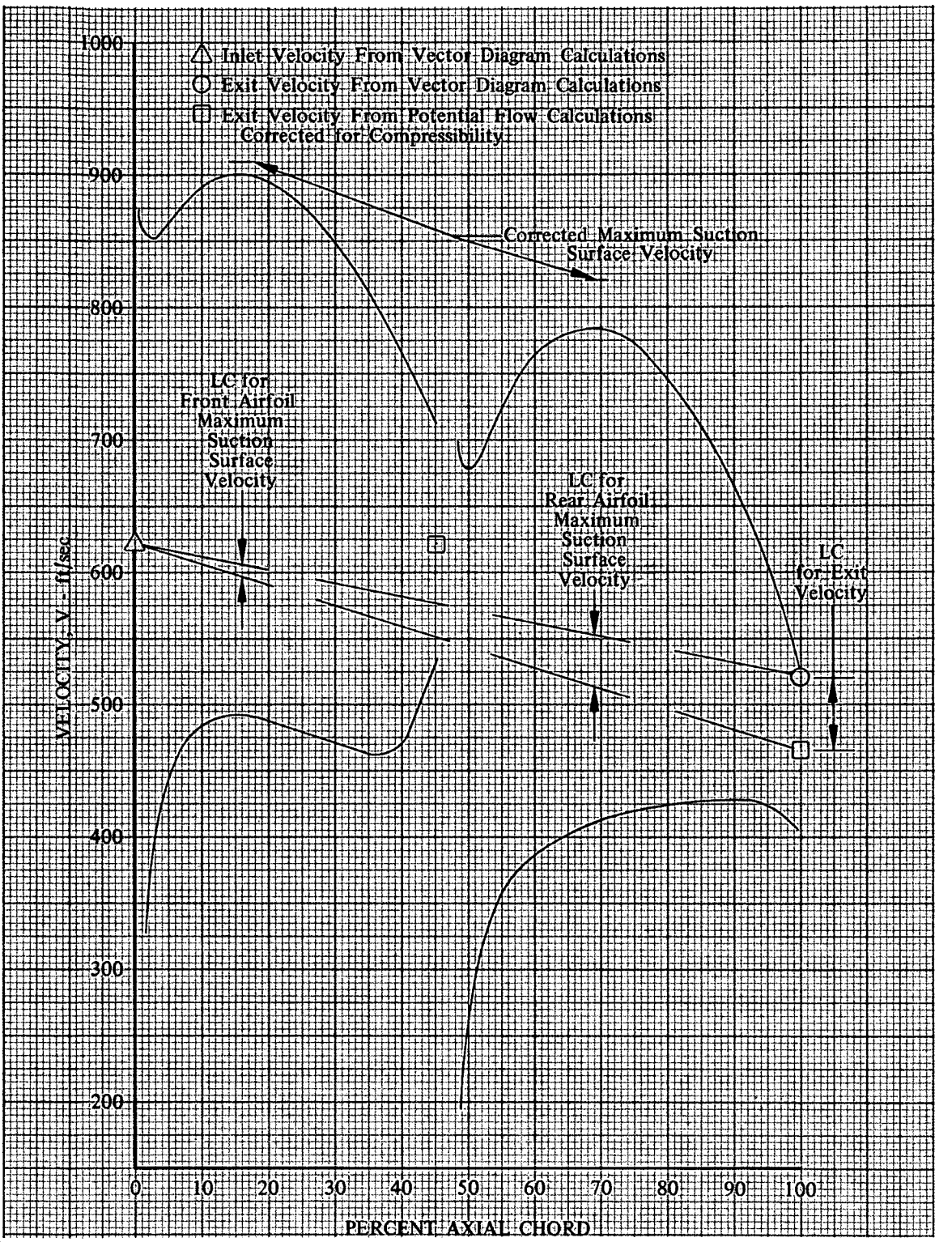

Figure 58. Stator E Vane Surface Velocities, 80% Span From Tip

DF 93444

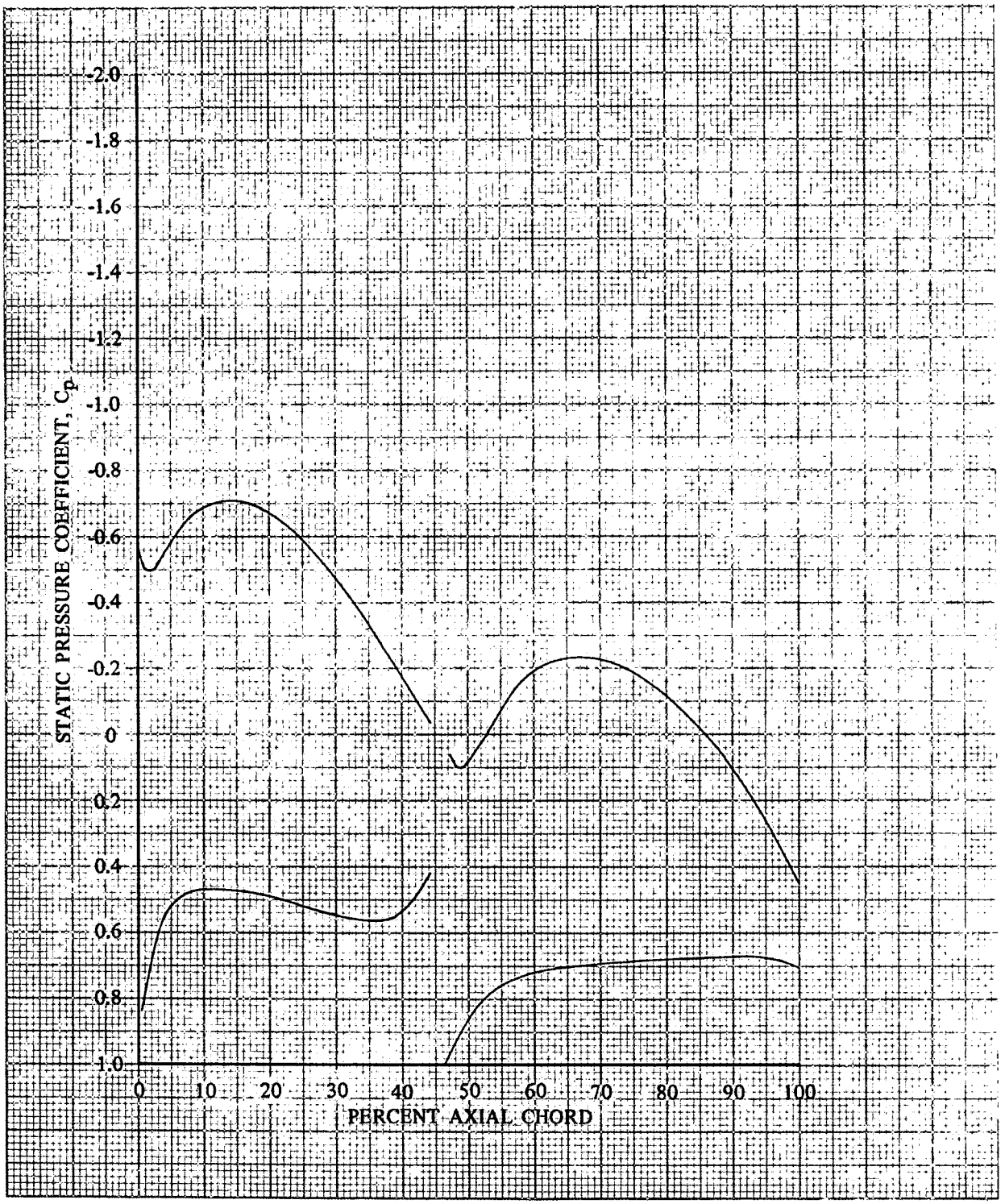

Figure 59. Stator E Static Pressure Coefficient Distribution, 91.1% Span From Tip DF 93445

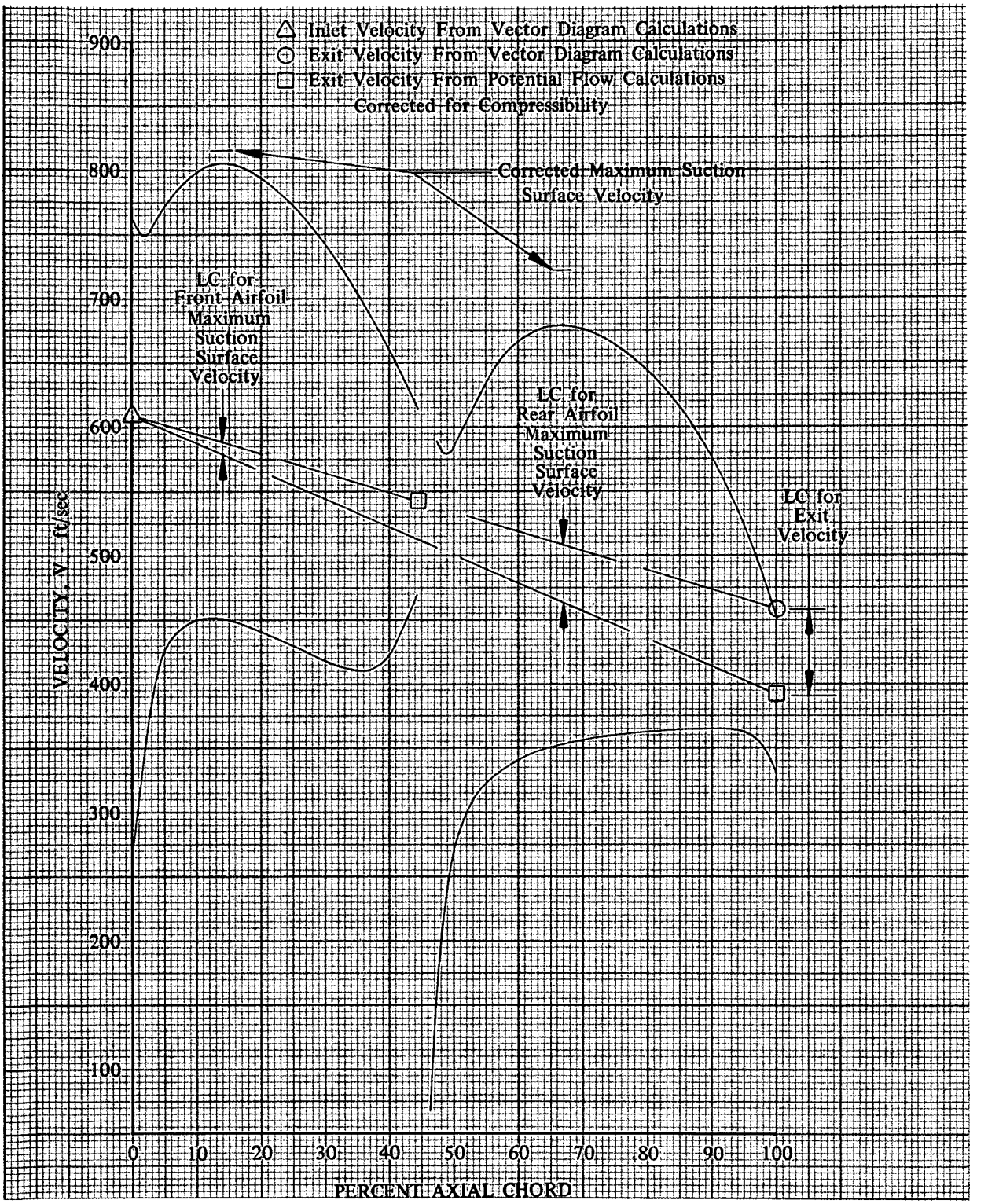

Figure 60. Stator E Vane Surface Velocities, 91.1% Span From Tip

DF 93446

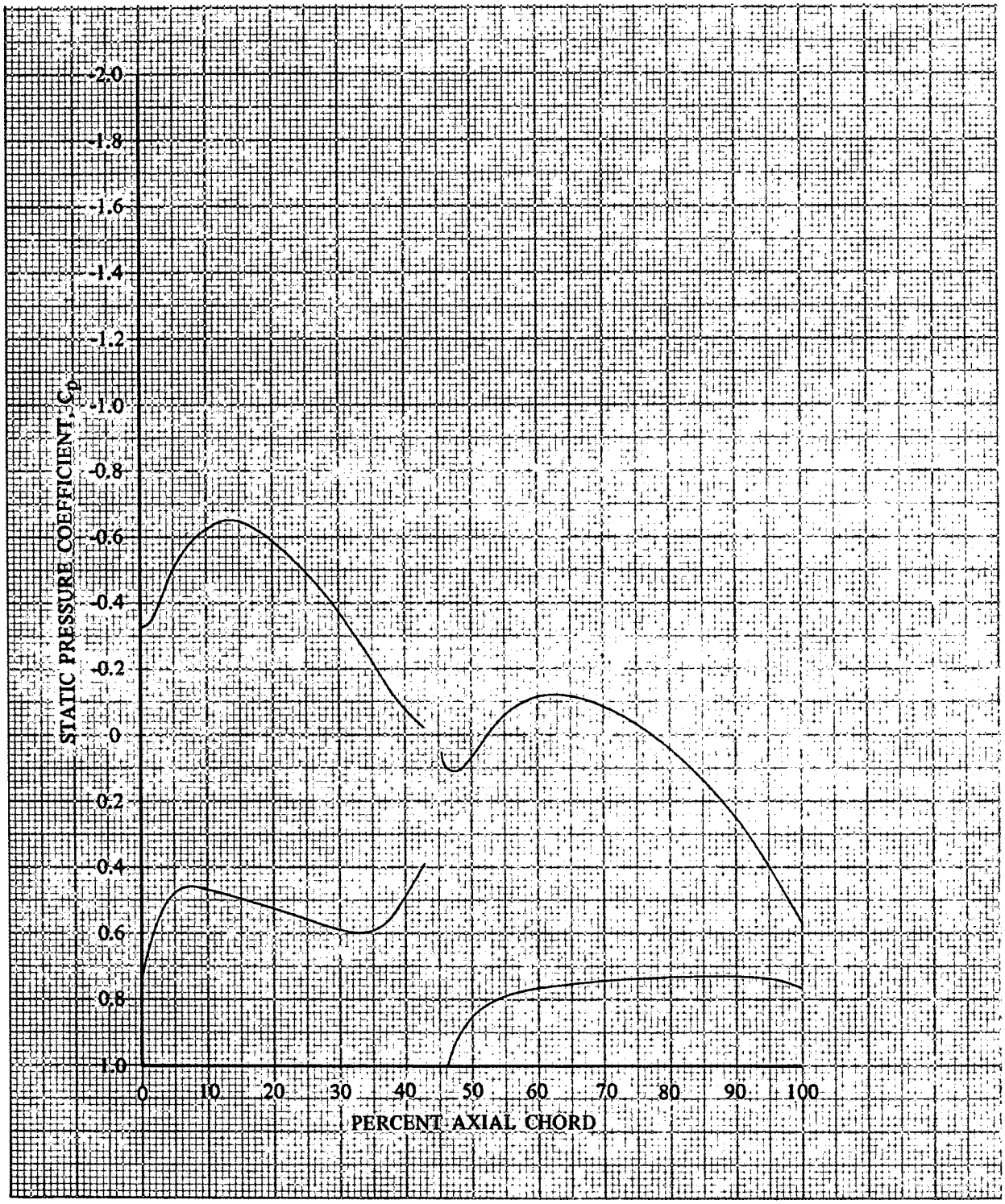

Figure 61. Stator E Static Pressure Coefficient Distribution, 95% Span From Tip DF 93447

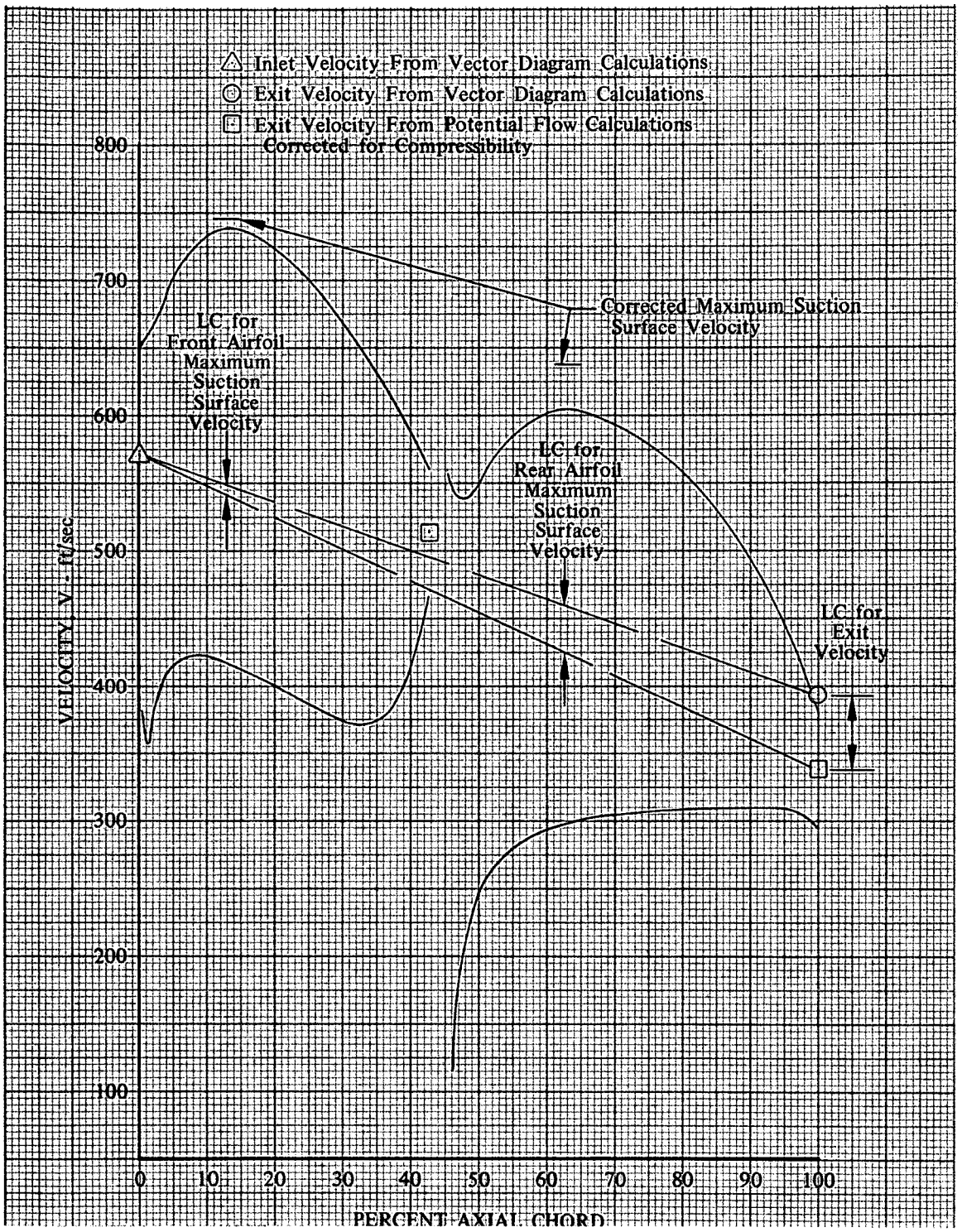

Figure 62. Stator E Vane Surface Velocities, 95% Span From Tip

DF 93448

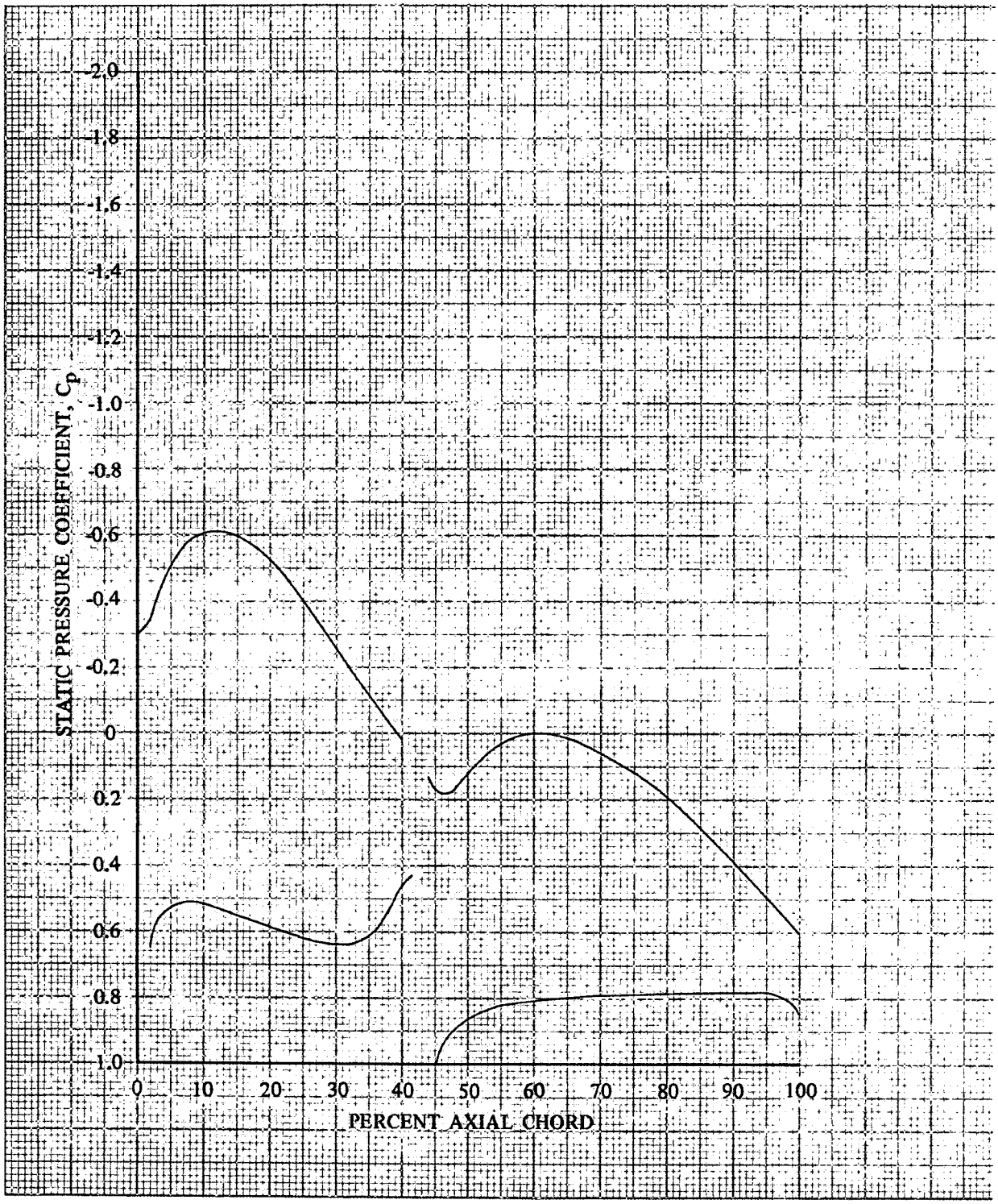

Figure 63. Stator E Static Pressure Coefficient Distribution, 97.5% Span From Tip DF 93449

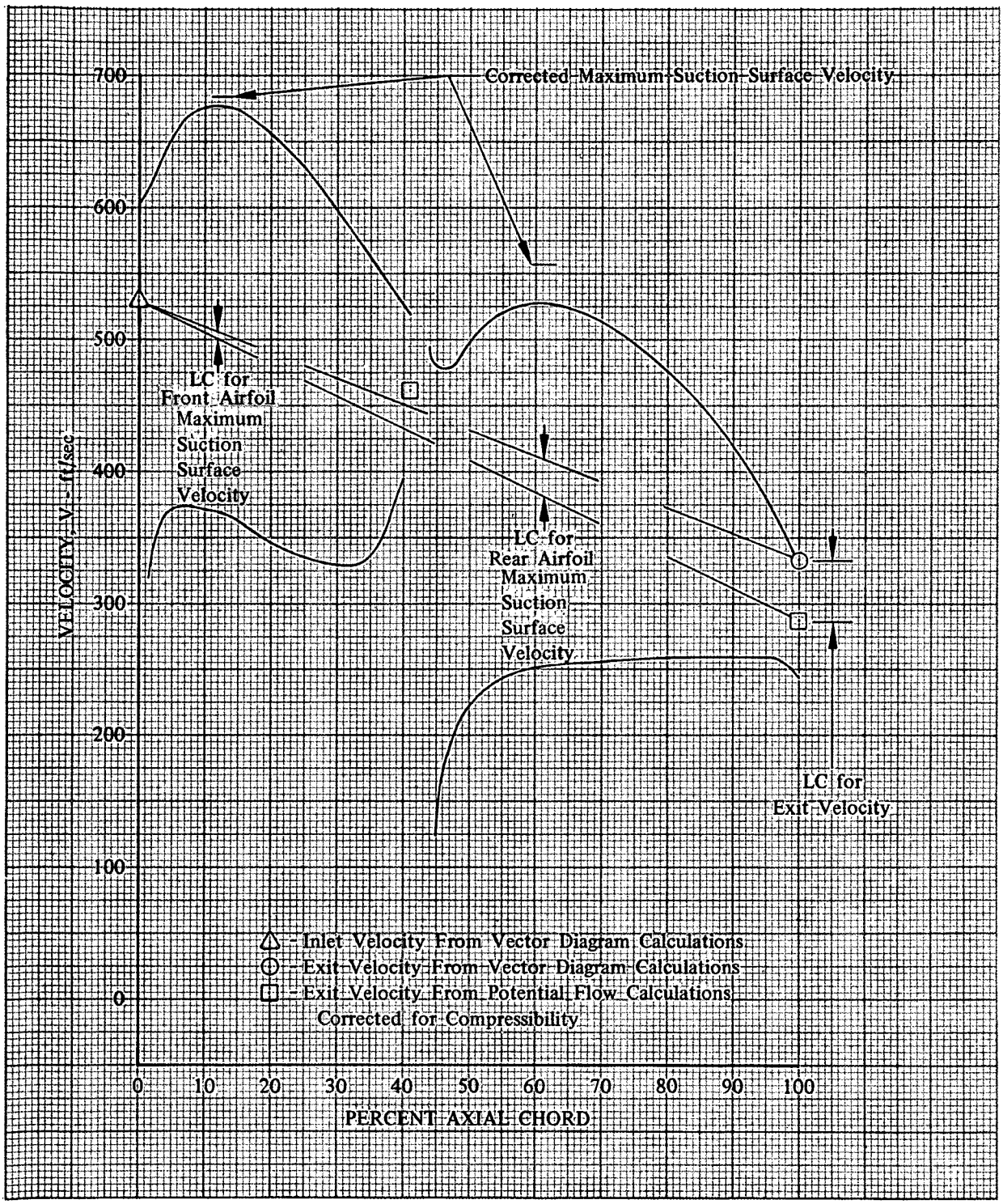

Figure 64. Stator E Blade Surface Velocities, 97.5% Span From Tip

DF 93450

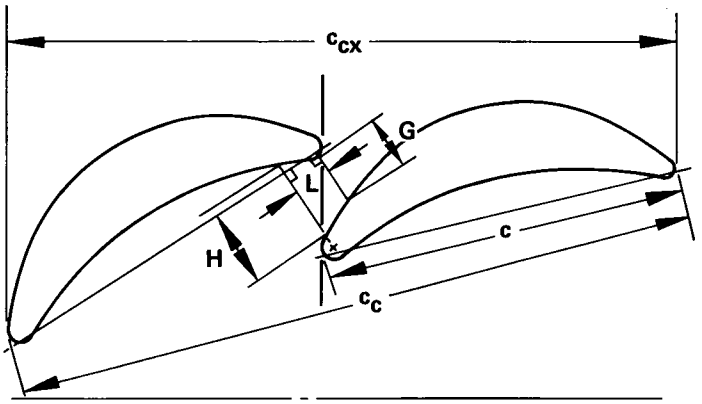

BLADE PASSAGE CONVERGENCE - F = H/G
BLADE PASSAGE GAP RATIO - G/c
BALDE PASSAGE OVERLAP RATIO - L/c
c = INDIVIDUAL AIRFOIL CHORD
c_c = COMBINED OR OVERALL CHORD
c_{cx} = OVERALL AXIAL CHORD

Figure 65. Tandem Airfoil Geometry, Simulated Double-Circular-Arc Airfoils FD 64418

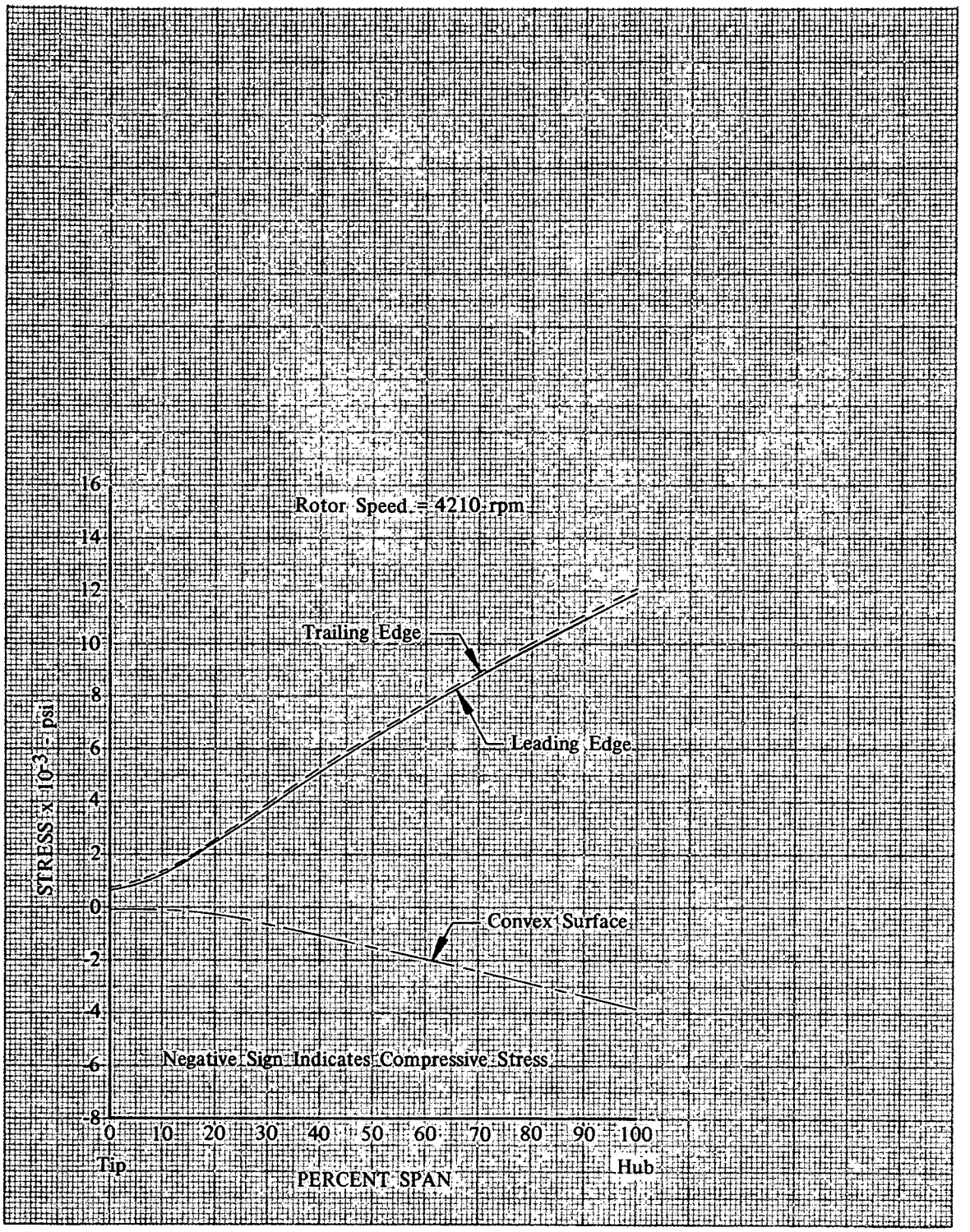

Figure 66. Calculated Rotor D Stress Distribution DF 93451

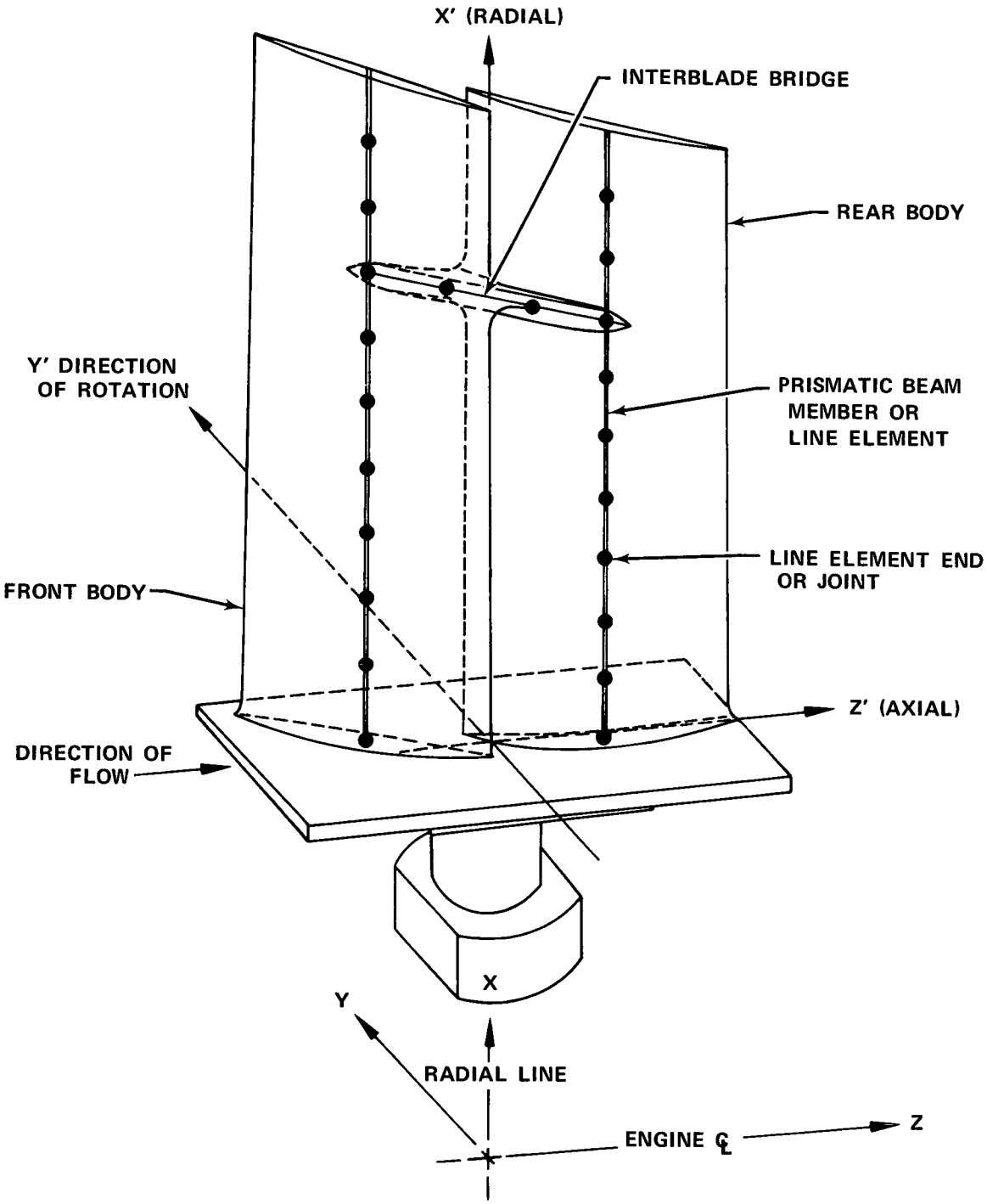

Figure 67. Graphic Description of Tandem Rotor Analytical Model FD 62295A

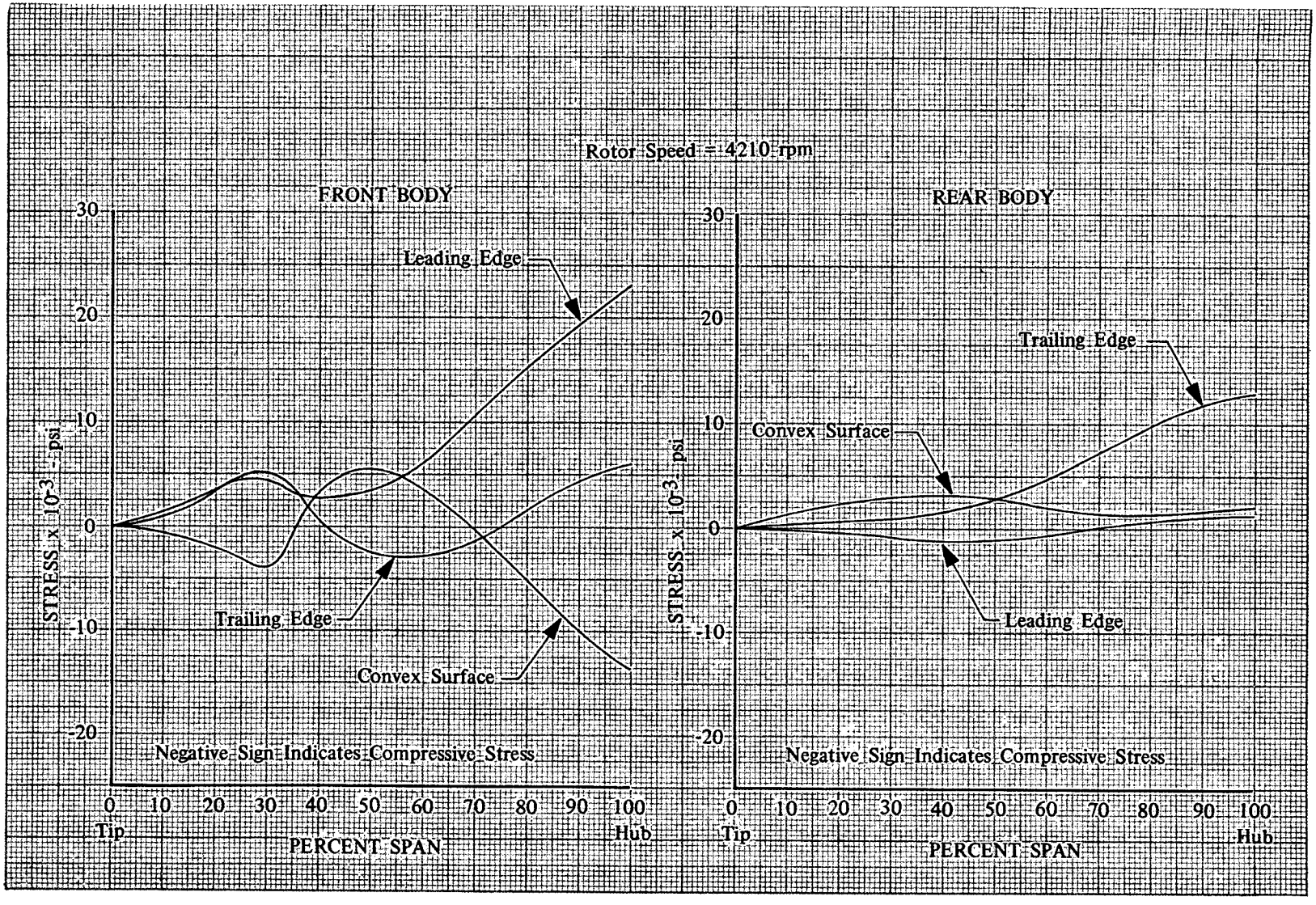

Figure 68. Calculated Rotor E Stress Distributions

DF 93452

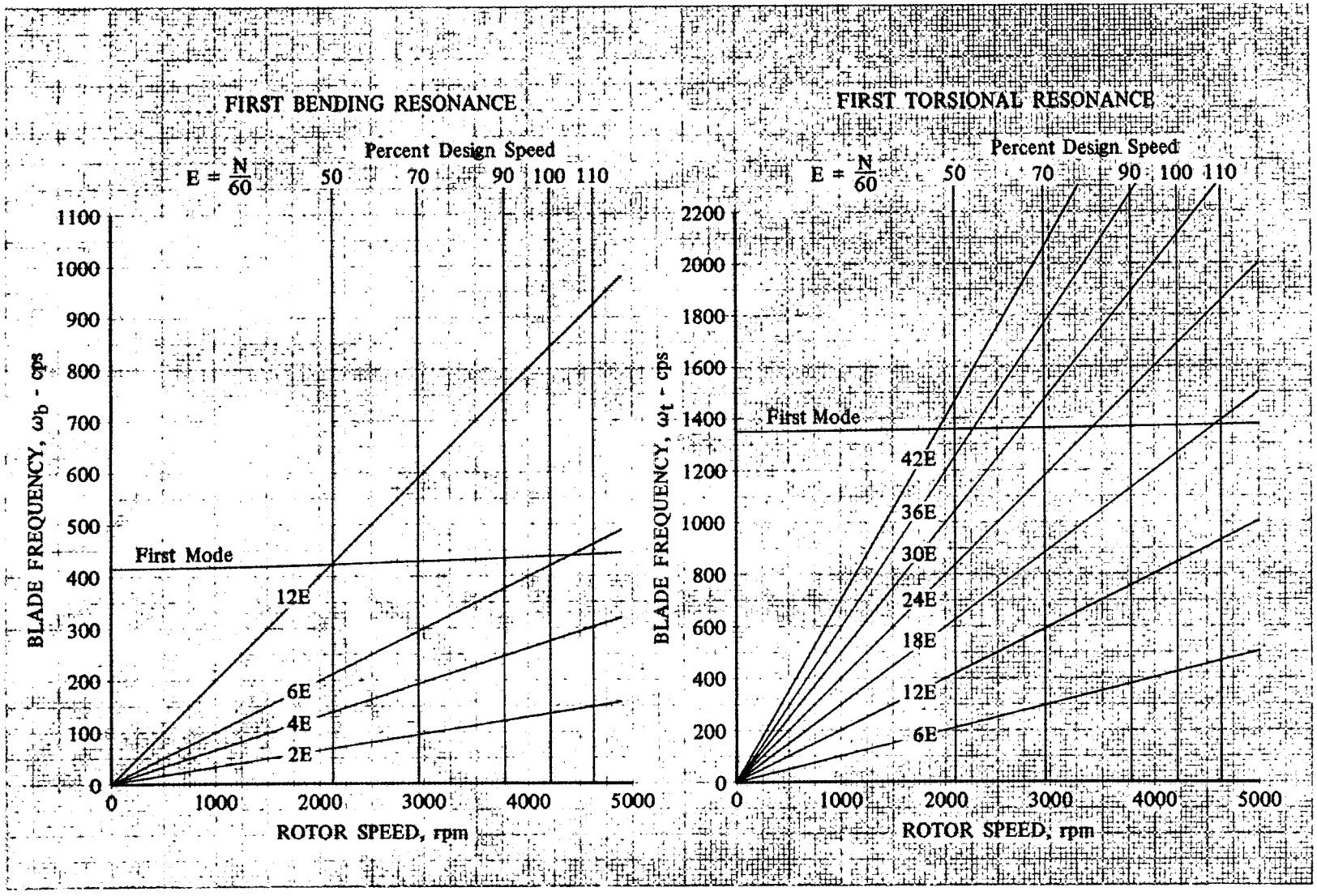

Figure 69. Rotor D Resonance Diagram for First Bending and First Torsional Mode Vibration DF 93453

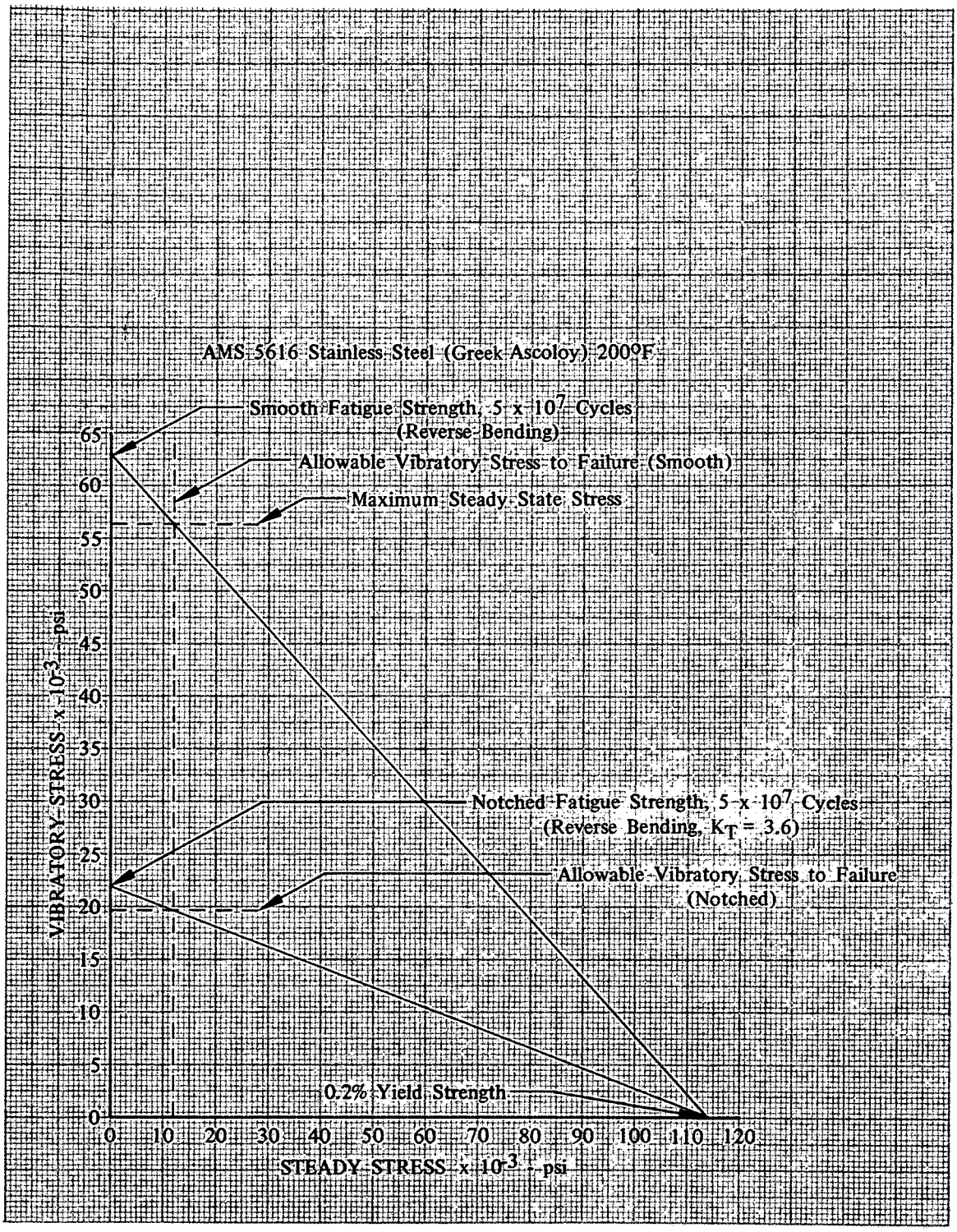

Figure 70. Rotor D Goodman Diagram DF 93454

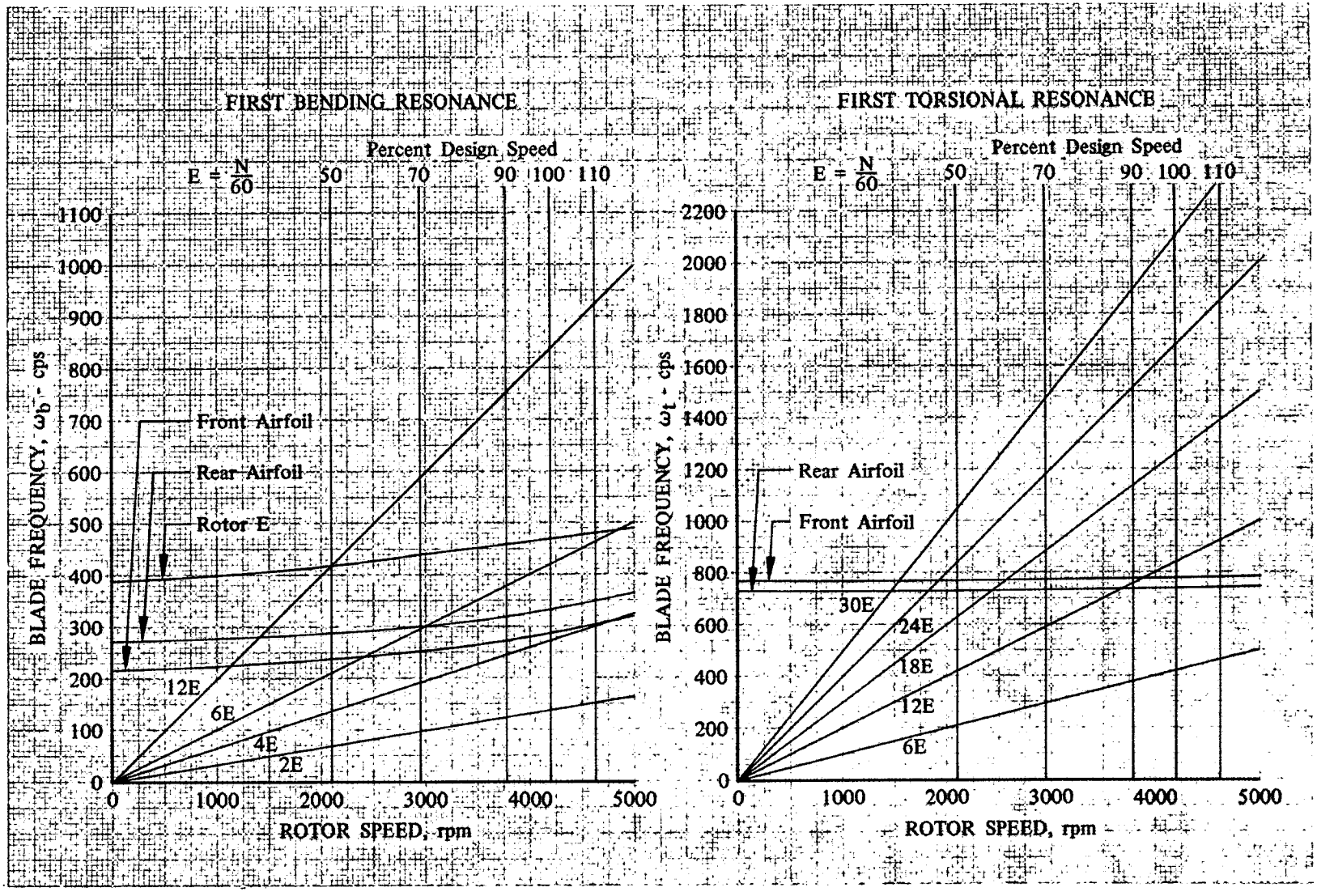

Figure 71. Rotor E Resonance Diagram for First Bending and First Torsional Mode Vibration

DF 93455

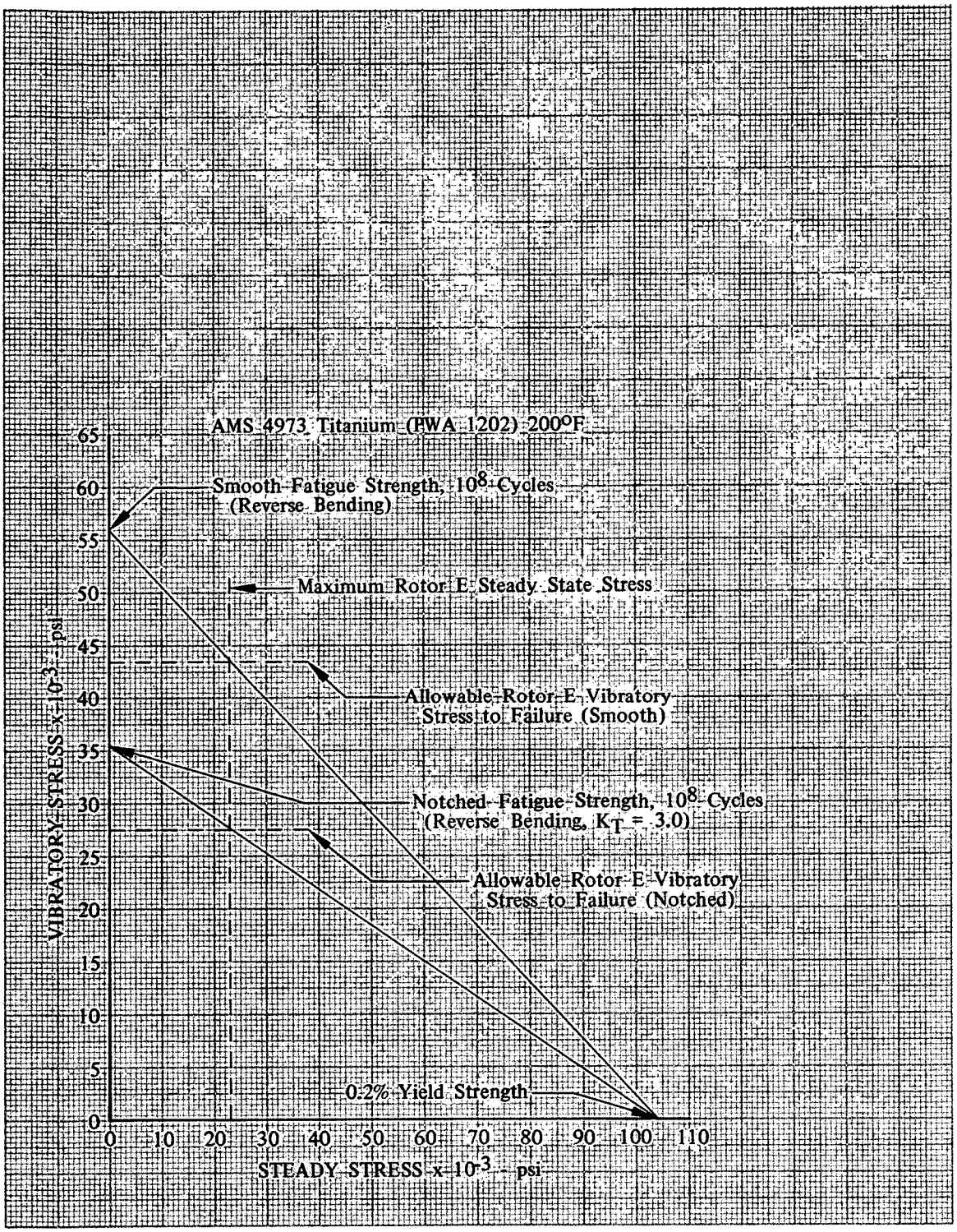

Figure 72. Rotor E Goodman Diagram DF 93456

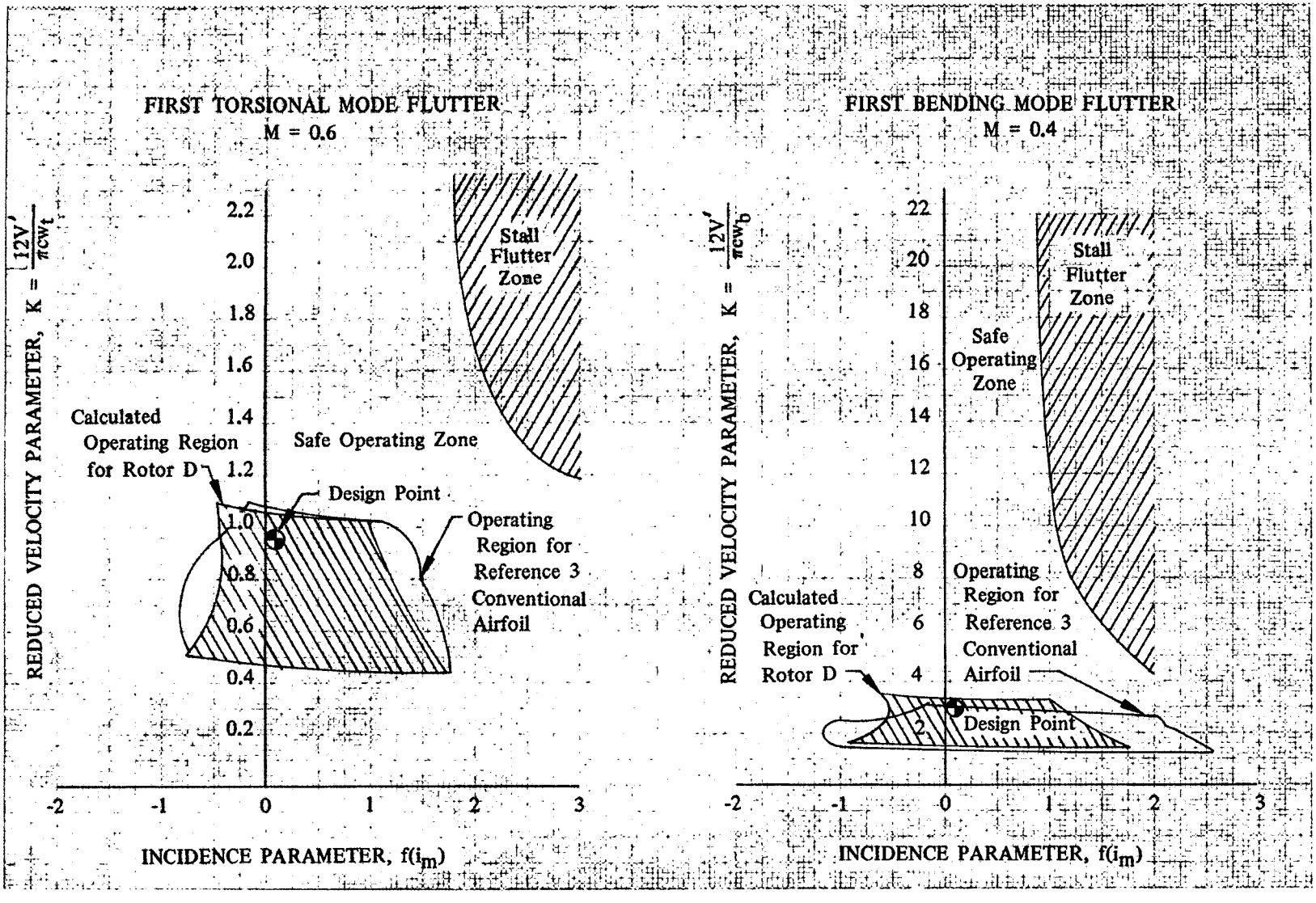

Figure 73. Calculated Rotor D First Bending and First Torsional Mode Flutter Characteristics DF 93457

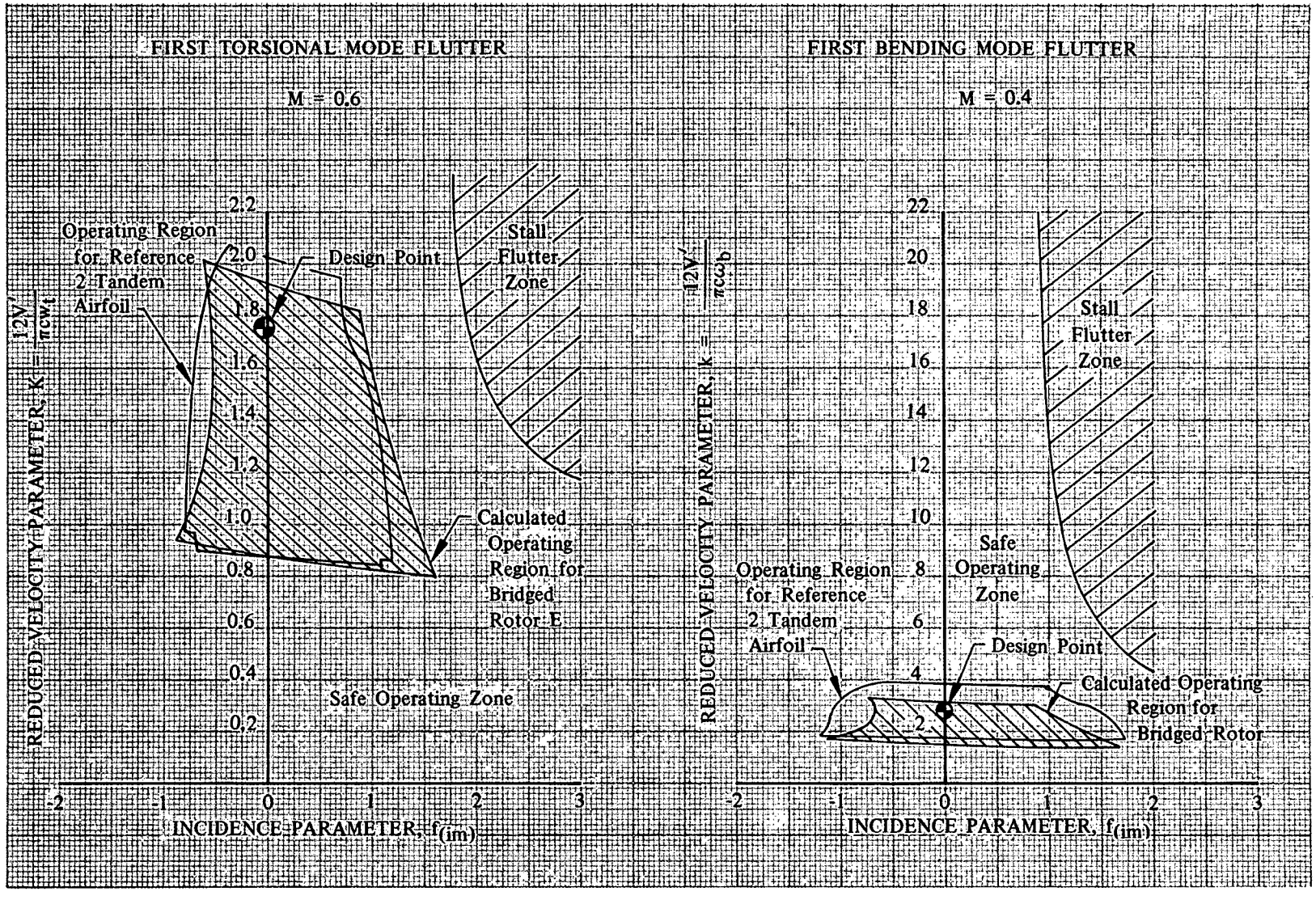

Figure 74. Calculated Rotor E First Bending and First Torsional Mode Flutter Characteristics DF 93458

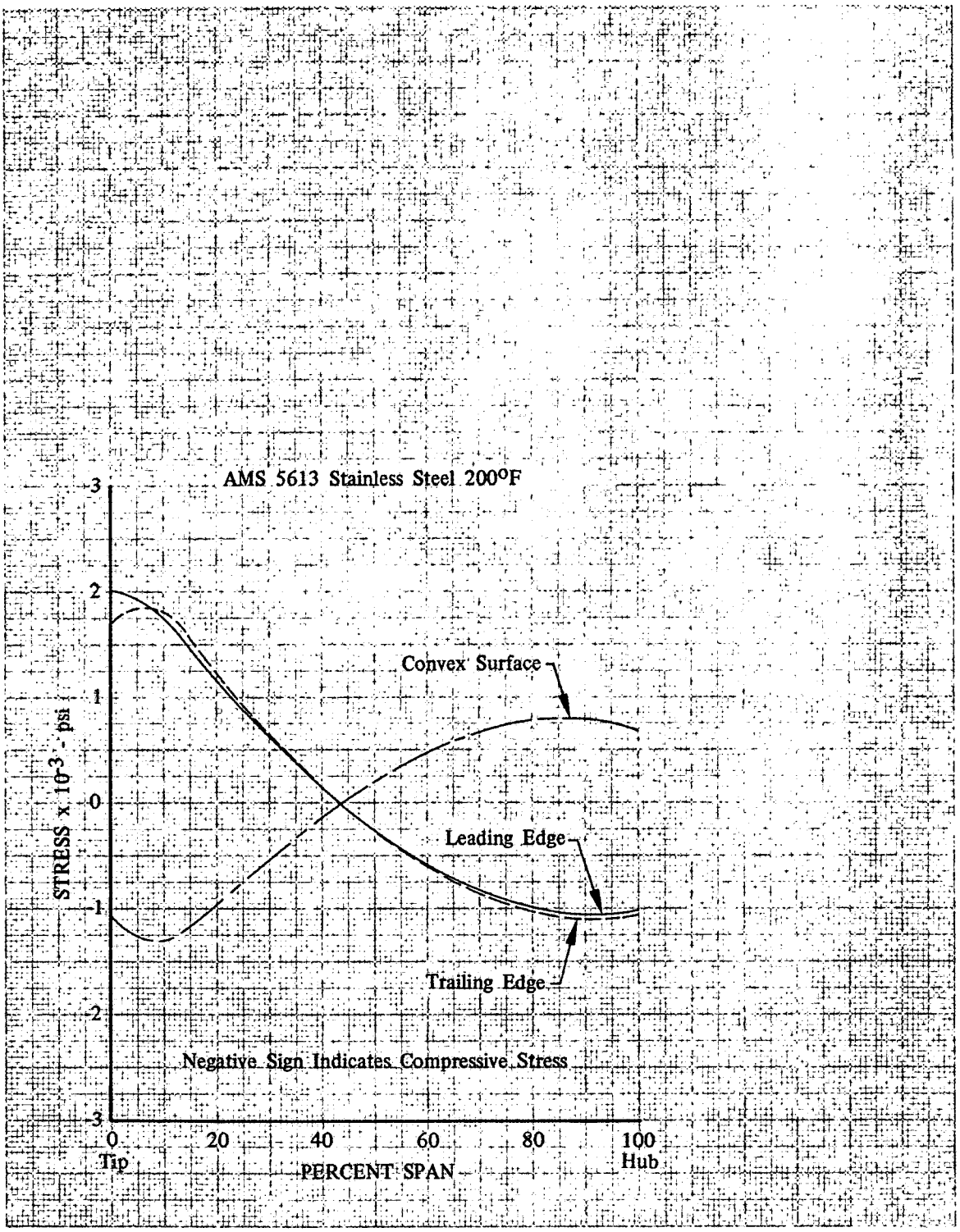

Figure 75. Calculated Stator D Stress Distribution DF 93459

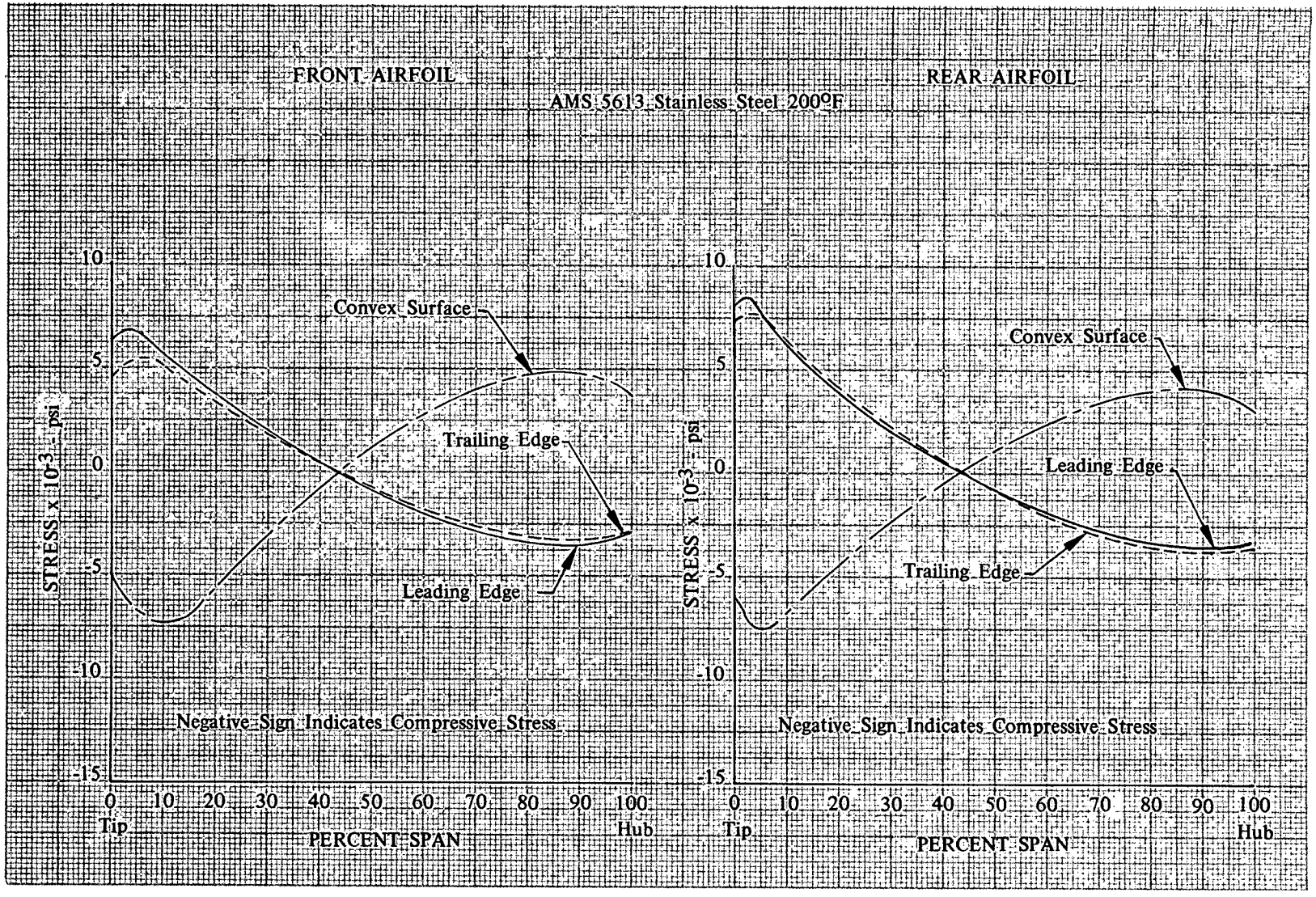

Figure 76. Calculated Stator E Stress Distributions

DF 93460

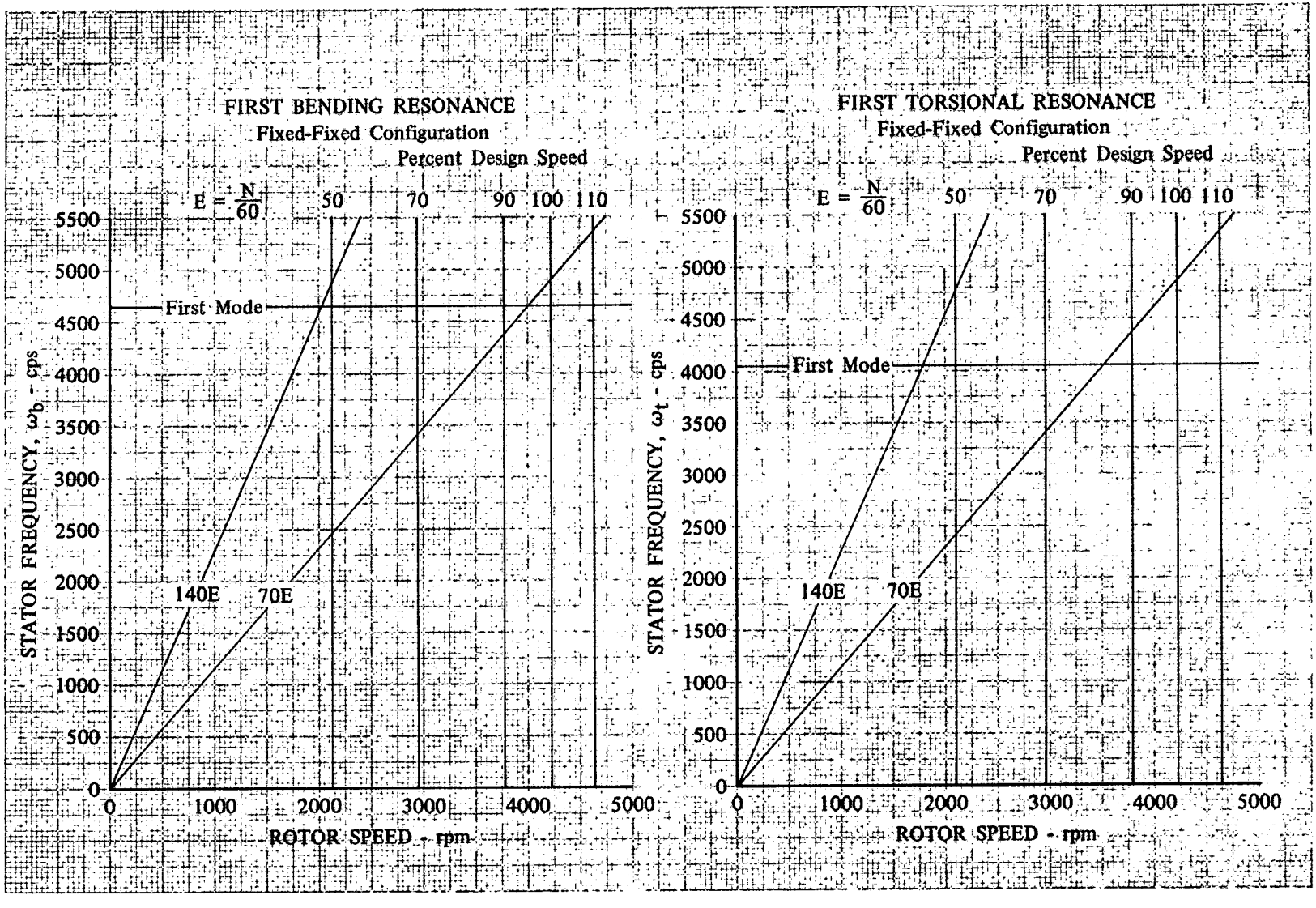

Figure 77. Stator D Resonance Diagram for First Bending and First Torsional Mode Vibration DF 93461

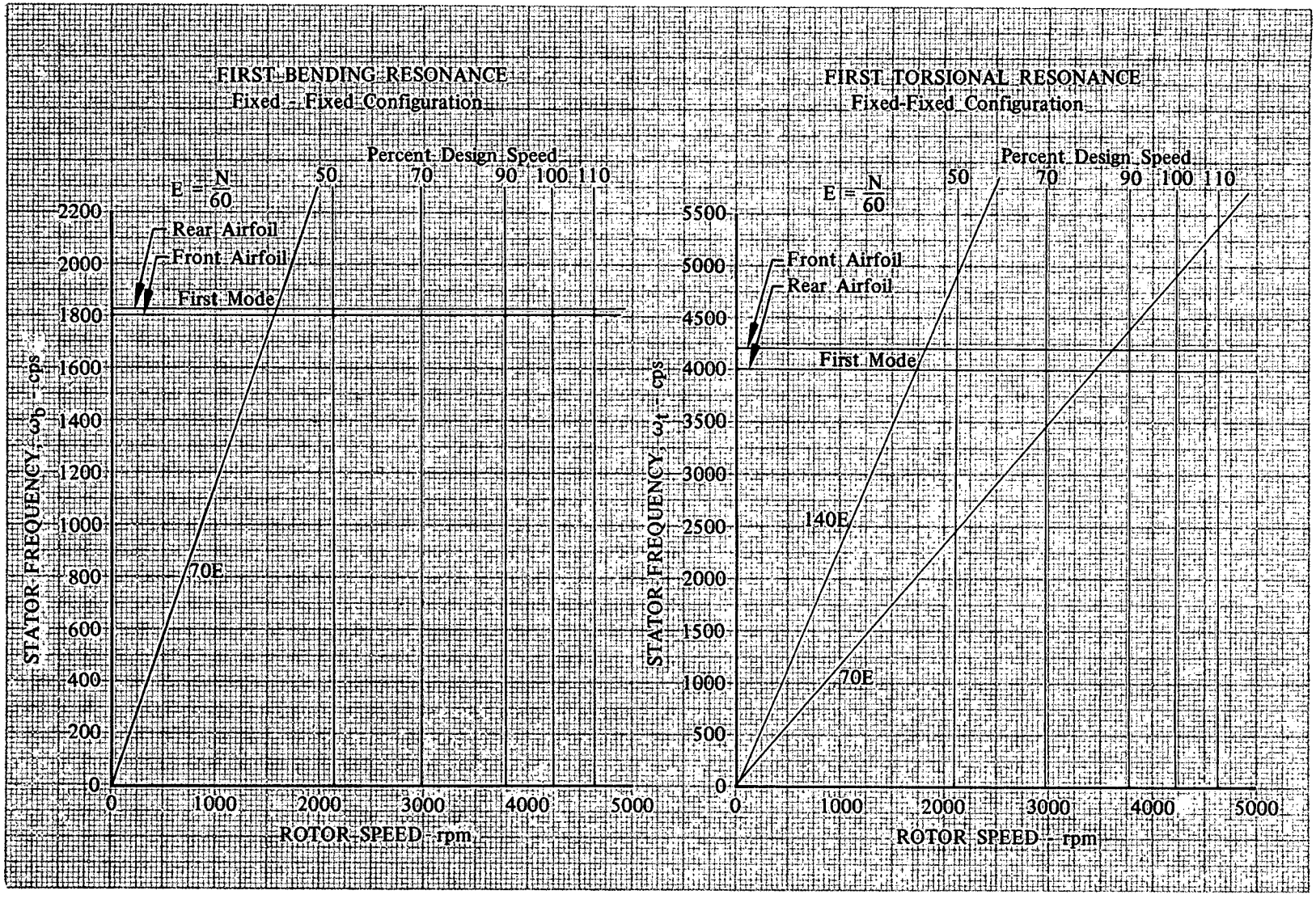

Figure 78. Stator E Resonance Diagram for First Bending and First Torsional Mode Vibration DF 93462

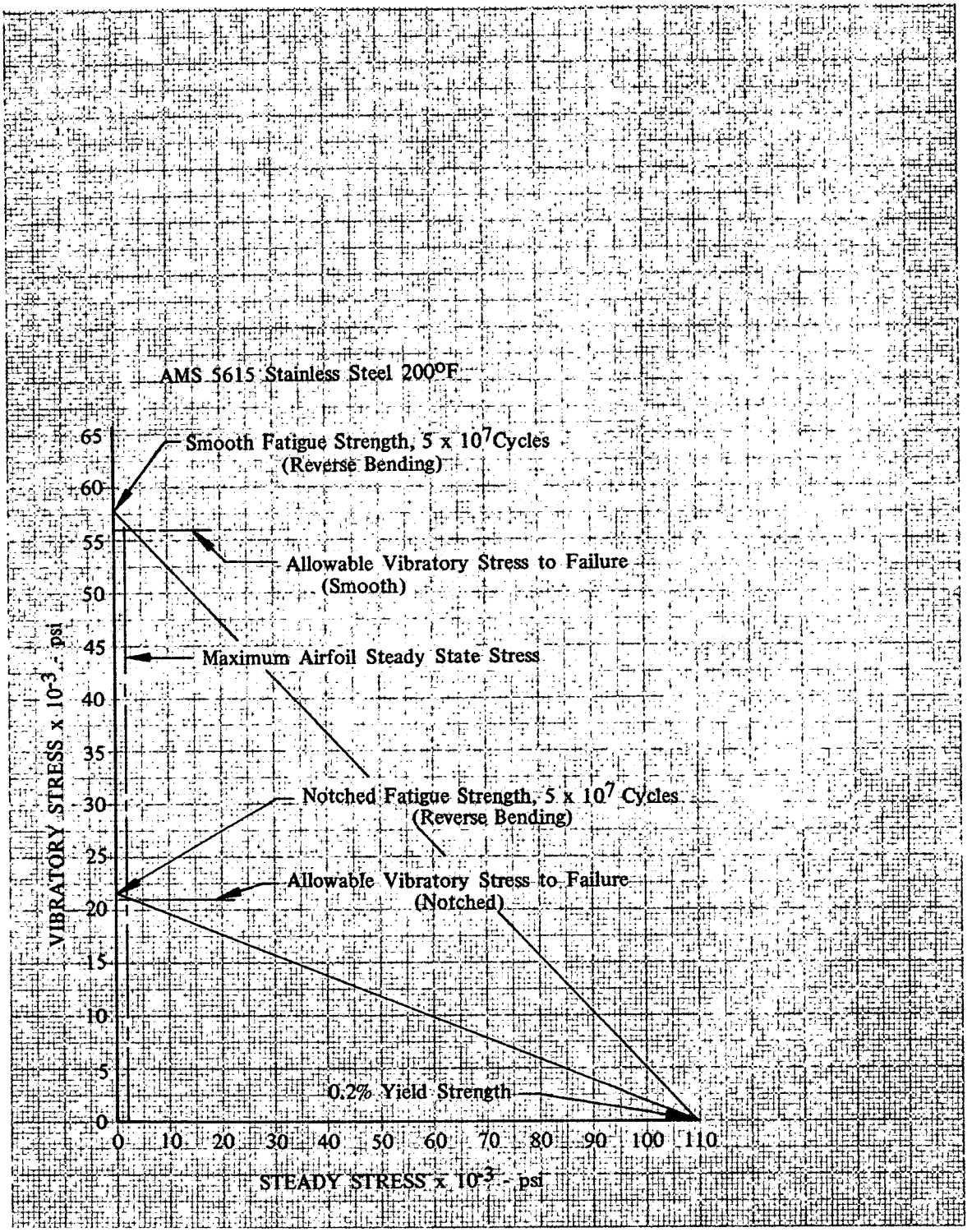

Figure 79. Stator D Goodman Diagram DF 93463

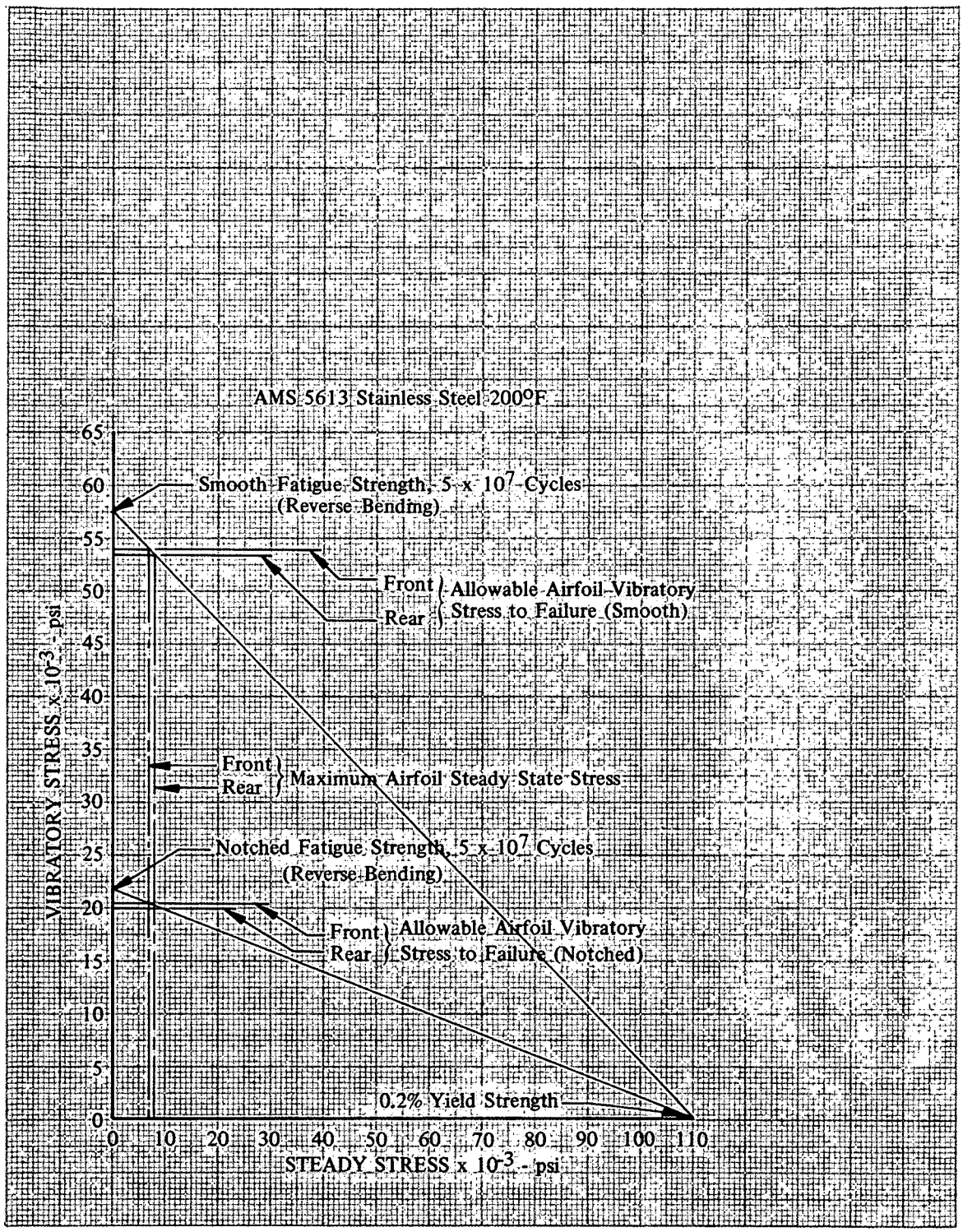

Figure 80. Stator E Goodman Diagram DF 93464

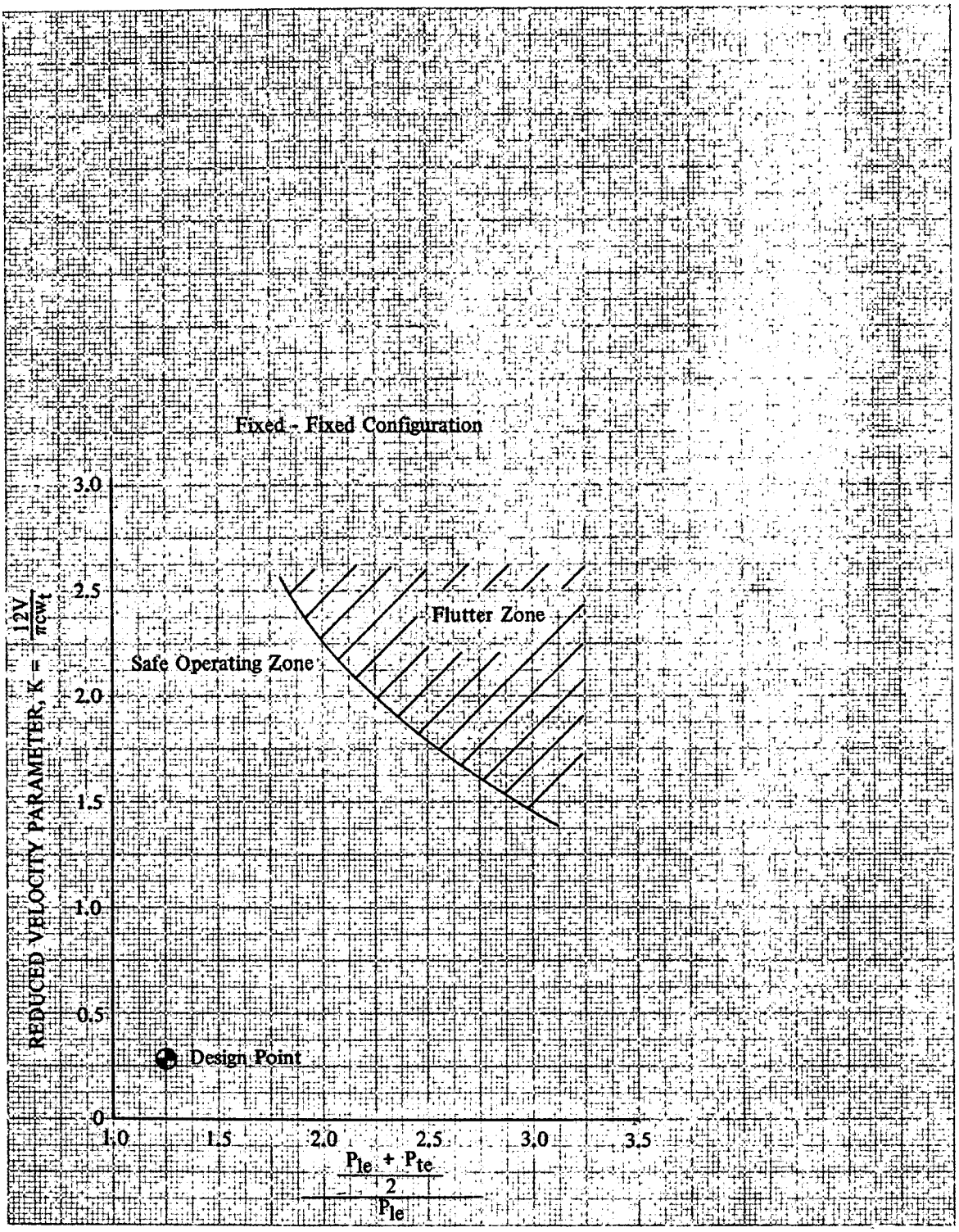

Figure 81. Calculated Stator D First Torsional Mode Flutter Characteristics DF 93465

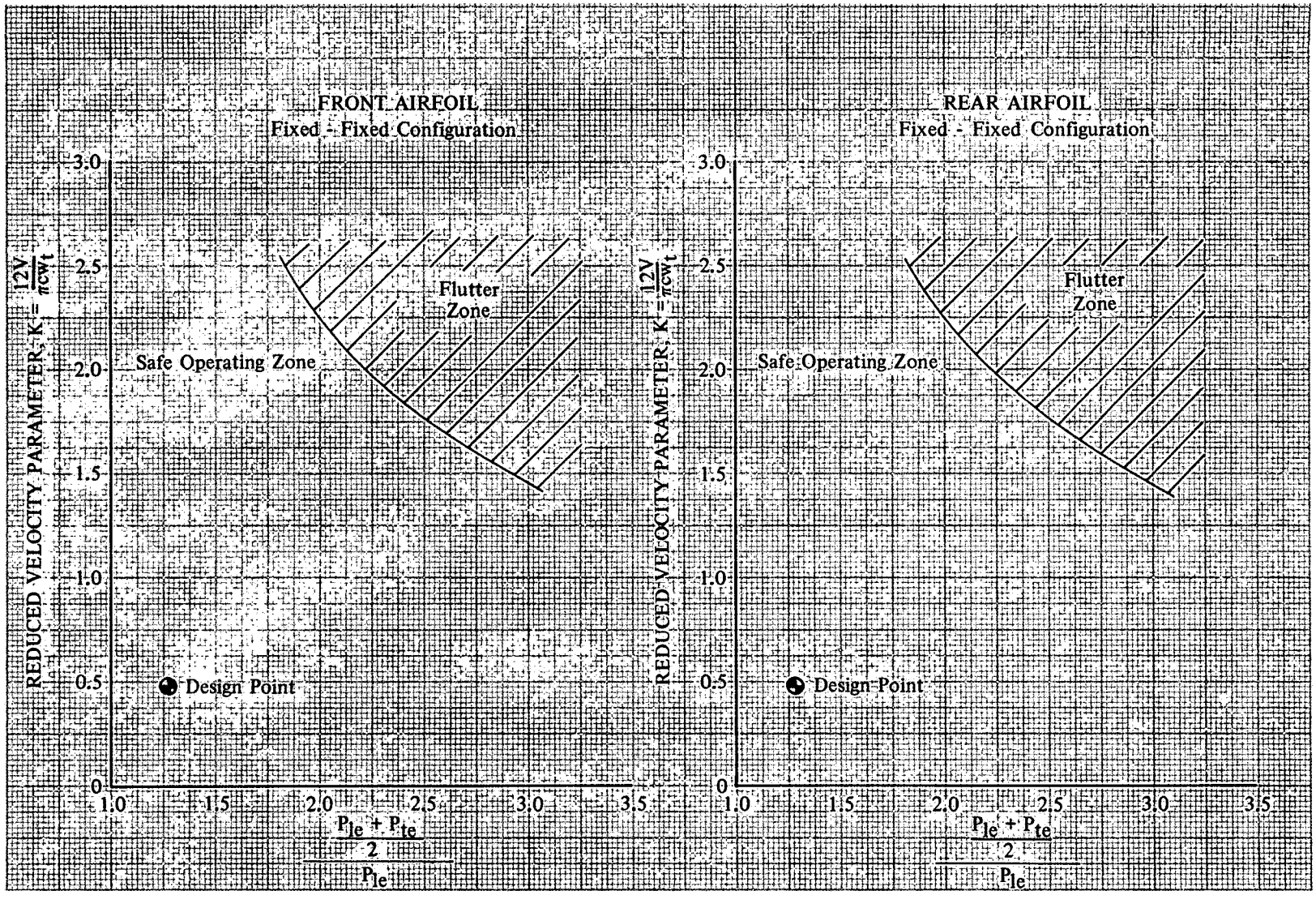

Figure 82. Calculated Stator E First Torsional Mode Flutter Characteristics

DF 93466

APPENDIX A

DEFINITION OF SYMBOLS

AVR	Axial Velocity Ratio ($V_{z_{te}}/V_{z_{le}}$)
a_O	Inlet relative stagnation velocity of sound, ft/sec
c	Chord length, in.
Cp	Static pressure coefficient
d	Diameter, in.
D	Diffusion factor
E	Multiple of rotor frequency
F	Tandem airfoil passage convergence (See figure 61.)
$f(i_m)$	Incidence parameter
G	Tandem airfoil passage gap (te), in. (See figure 61.)
H	Tandem airfoil passage gap (le), in. (See figure 61.)
i_m	Incidence angle, deg
K	Reduced velocity parameter
K_T	Notch factor
L	Tandem airfoil passage overlap, in. (See figure 61.)
LC	Local correction for suction surface velocity (See figure 26.)
M	Mach number
N	Rotor speed, rpm
P	Total pressure, psia
PR	Pressure ratio
p	Static pressure, psia
t	Blade maximum thickness, in.
T	Total temperature, °R
U	Rotor speed, ft/sec
V	Velocity, ft/sec

DEFINITION OF SYMBOLS (Continued)

$\bar{v}$	Secondary velocity, ft/sec
W	Actual flowrate, lb_m/sec
x	Radial direction
y	Tangential direction
z	Axial direction
α	Cone angle (angle of plane tangent to conic surface that approximates the design streamline of revolution), deg
β	Air angle, degrees from axial direction
$\Delta\beta$	Flow turning angle, deg
γ	Ratio of specific heats
$\gamma°$	Blade-chord angle, degrees from axial direction
δ	Ratio of total pressure to NASA standard sea level pressure of 14.694 psia
$\delta°$	Deviation angle, deg
ζ	Absolute vorticity
θ	Ratio of total temperature to NASA standard sea level temperature of 518.7 °R
κ	Blade metal angle, degrees from axial direction
ξ	Absolute vorticity in direction of relative velocity
ρ	Density, lb_f - sec^2/ft^4
σ	Solidity
Φ	Velocity potential
ϕ	Blade camber angle, deg
Ω	Angular velocity vector
ω	Frequency, Hertz
$\bar{\omega}$	Loss coefficient
$\frac{\bar{\omega}\cos\beta te}{2}$	Loss parameter

Subscripts:

a	Axisymmetric calculation value
AVR	Axial velocity ratio
b	Bending
c	Combined or overall
cx	Overall axial
fs	Freestream value
id	Isentropic condition
le	Leading edge
ref	Minimum loss
SF	Secondary flow calculation value
te	Trailing edge
t	Torsional
z	Axial component
θ	Tangential component
2D	Two dimensional

Superscripts:

'	Related to rotor blade
-	Mass average value

DEFINITION OF DESIGN VARIABLES

Incidence Angle:

Rotor: $i_m = \beta'_{le} - \kappa_{le}$ Stator: $i_m = \beta_{le} - \kappa_{le}$

Diffusion Factor:

Rotor: $$D = 1 - \frac{V'_{te}}{V'_{le}} + \frac{d_{te}V_{\theta_{te}} - d_{le}V_{\theta le}}{(d_{le} + d_{te})\sigma V'_{le}}$$

Stator: $$D = 1 - \frac{V_{te}}{V_{le}} - \frac{d_{te}V_{\theta te} - d_{le}V_{\theta le}}{(d_{le} + d_{te})\sigma V_{le}}$$

Deviation Angle:

Rotor: $\delta^\circ = \beta'_{te} - \kappa_{te}$ Stator: $\delta^\circ = \beta_{te} - \kappa_{te}$

Loss Coefficient:

Rotor: $$\bar{\omega}' = \frac{(P'_{te})_{id} - P'_{te}}{\bar{P}'_{le} - P_{le}}$$

where:

$$(P'_{te})_{id} = P'_{le}\left\{1 + \frac{\gamma - 1}{2}\left(\frac{U^2_{te}}{a^2_{Ole}}\right)\left[1 - \left(\frac{d_{le}}{d_{te}}\right)^2\right]\right\}^{\frac{\gamma}{\gamma - 1}}$$

P' is found from $p/P' = \left[1 + \frac{\gamma - 1}{2} M'^2\right]^{\frac{\gamma}{1 - \gamma}}$

Stator: $$\omega = \frac{P_{fs} - P_{te}}{P_{fs} - P_{le}}$$

Static Pressure Coefficient:

$$C_p = \frac{p_L - p_{fs}}{1/2\rho_{fs}V^2_{fs}}$$

Pressure Ratio:

Rotor: $\dfrac{\bar{P}_{rotor\ te}}{\bar{P}_{rotor\ le}}$ Stage: $\dfrac{\bar{P}_{stator\ te}}{\bar{P}_{rotor\ le}}$

Equivalent Flow:

$$\frac{W\sqrt{\theta}}{\delta}$$

Equivalent Rotor Speed:

$$N/\sqrt{\theta}$$

Adiabatic Efficiency:

$$\text{Rotor: } \frac{(PR)^{\frac{\gamma-1}{\gamma}} - 1}{\overline{T}_{te}/518.7 - 1} \qquad \text{Stage: } \frac{(PR)^{\frac{\gamma-1}{\gamma}} - 1}{\overline{T}_{te}/518.7 - 1}$$

APPENDIX B

STAGE D AIRFOIL COORDINATES

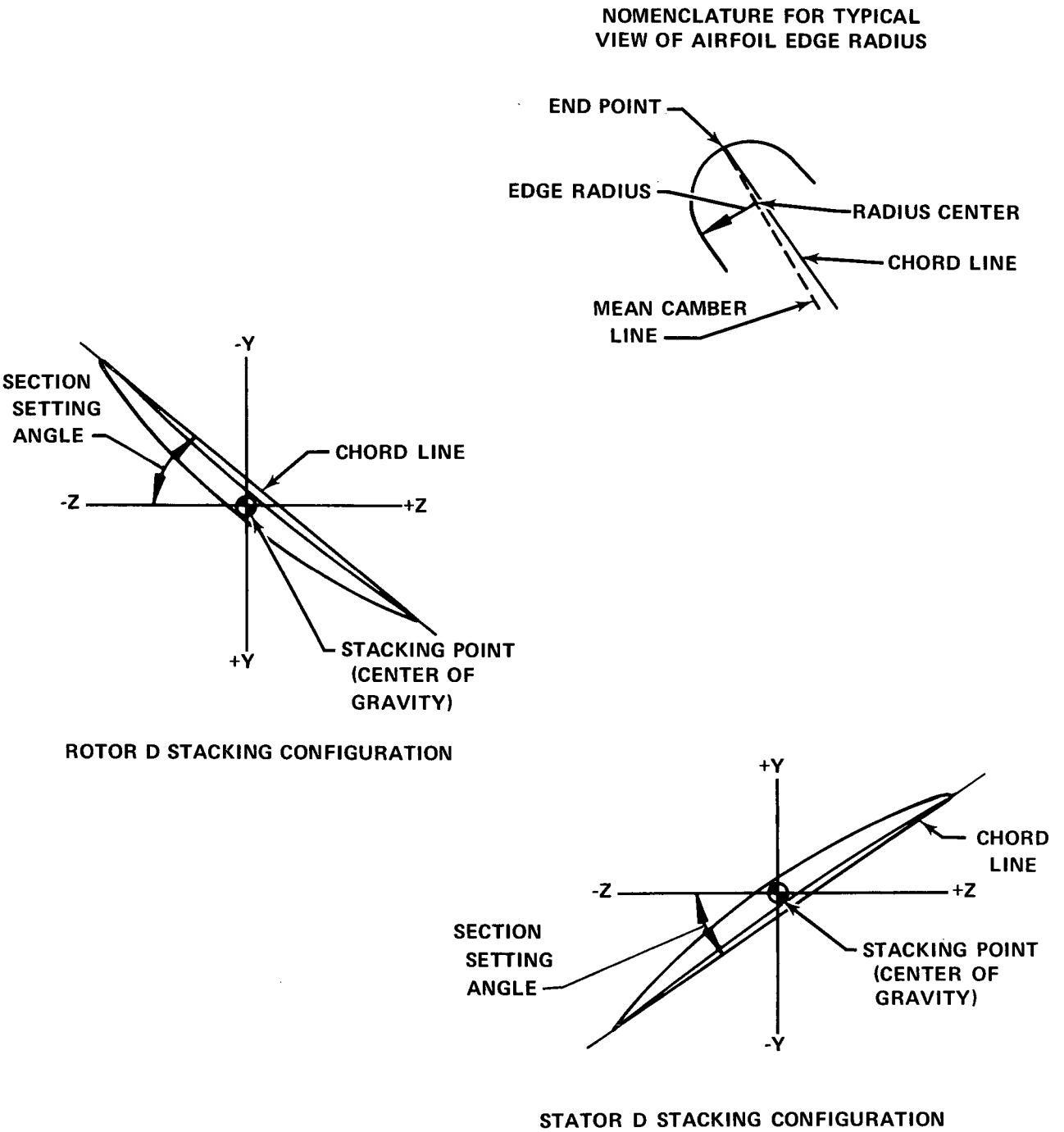

Figure B-1. Stage D Airfoil Coordinates FD 64419

Table B-1. Stage D Airfoil Coordinates

Reproduced from best available copy.

** BLADE SECTION COORDINATES IN TURBOMACHINE ORIENTATION - ROTOR D

NUMBER OF BLADES = 70.0 AXIAL LOCATION OF STACKING LINE IN COMPRESSOR = 19.200 IN.

FRACT. OF SURF.	SECTION 1 FOR XCUT OF 20.4850 IN. SECTION SETTING ANGLE = 63.737 SUCTION SURFACE Z (IN.)	SUCTION SURFACE Y (IN.)	PRESSURE SURFACE Z (IN.)	PRESSURE SURFACE Y (IN.)	SECTION 2 FOR XCUT OF 20.3900 IN. SECTION SETTING ANGLE = 58.096 SUCTION SURFACE Z (IN.)	SUCTION SURFACE Y (IN.)	PRESSURE SURFACE Z (IN.)	PRESSURE SURFACE Y (IN.)	SECTION 3 FOR XCUT OF 20.2900 IN. SECTION SETTING ANGLE = 53.576 SUCTION SURFACE Z (IN.)	SUCTION SURFACE Y (IN.)	PRESSURE SURFACE Z (IN.)	PRESSURE SURFACE Y (IN.)
0.0	-0.4980	-1.1514	-0.4840	-1.1553	-0.6039	-1.0964	-0.5909	-1.1012	-0.6865	-1.0533	-0.6743	-1.0588
0.05	-0.4774	-1.0201	-0.4455	-1.0317	-0.5680	-0.9702	-0.5378	-0.9841	-0.6394	-0.9314	-0.6106	-0.9471
0.12	-0.4363	-0.8400	-0.3842	-0.8616	-0.5079	-0.7973	-0.4582	-0.8227	-0.5654	-0.7642	-0.5177	-0.7926
0.20	-0.3743	-0.6395	-0.3055	-0.6710	-0.4271	-0.6047	-0.3610	-0.6413	-0.4706	-0.5780	-0.4068	-0.6189
0.30	-0.2787	-0.3961	-0.1970	-0.4372	-0.3107	-0.3712	-0.2320	-0.4187	-0.3386	-0.3527	-0.2622	-0.4056
0.40	-0.1671	-0.1601	-0.0802	-0.2074	-0.1802	-0.1455	-0.0962	-0.1999	-0.1937	-0.1355	-0.1118	-0.1961
0.50	-0.0432	0.0695	0.0426	0.0195	-0.0383	0.0730	0.0447	0.0157	-0.0378	0.0737	0.0431	0.0099
0.60	0.0896	0.2937	0.1689	0.2448	0.1126	0.2849	0.1890	0.2289	0.1273	0.2753	0.2018	0.2129
0.70	0.2285	0.5140	0.2966	0.4700	0.2702	0.4910	0.3354	0.4406	0.2998	0.4696	0.3632	0.4134
0.80	0.3706	0.7324	0.4232	0.6970	0.4322	0.6927	0.4821	0.6521	0.4780	0.6572	0.5261	0.6120
0.88	0.4848	0.9075	0.5219	0.8816	0.5635	0.8519	0.5984	0.8222	0.6234	0.8032	0.6567	0.7702
0.95	0.5838	1.0626	0.6052	1.0469	0.6785	0.9908	0.6983	0.9729	0.7517	0.9285	0.7704	0.9087
1.00	0.6536	1.1753	0.6623	1.1679	0.7604	1.0903	0.7682	1.0820	0.8438	1.0170	0.8509	1.0081
L.E. CIRCLE CENTER			-0.4908	-1.1528			-0.5972	-1.0983			-0.6802	-1.0556
T.E. CIRCLE CENTER			0.6577	1.1714			0.7641	1.0859			0.8470	1.0123
	LER = 0.0073		TER = 0.0057		LER = 0.0070		TER = 0.0057		LER = 0.0067		TER = 0.0057	
	CHORD = 2.6054				CHORD = 2.5863				CHORD = 2.5832			

FRACT. OF SURF.	SECTION 4 FOR XCUT OF 20.1200 IN. SECTION SETTING ANGLE = 48.618 SUCTION SURFACE Z (IN.)	SUCTION SURFACE Y (IN.)	PRESSURE SURFACE Z (IN.)	PRESSURE SURFACE Y (IN.)	SECTION 5 FOR XCUT OF 20.0900 IN. SECTION SETTING ANGLE = 46.023 SUCTION SURFACE Z (IN.)	SUCTION SURFACE Y (IN.)	PRESSURE SURFACE Z (IN.)	PRESSURE SURFACE Y (IN.)	SECTION 6 FOR XCUT OF 20.0150 IN. SECTION SETTING ANGLE = 46.812 SUCTION SURFACE Z (IN.)	SUCTION SURFACE Y (IN.)	PRESSURE SURFACE Z (IN.)	PRESSURE SURFACE Y (IN.)
0.0	-0.7724	-1.0063	-0.7614	-1.0124	-0.7820	-1.0004	-0.7712	-1.0066	-0.8004	-0.9877	-0.7899	-0.9941
0.05	-0.7151	-0.8890	-0.6882	-0.9065	-0.7237	-0.8836	-0.6970	-0.9015	-0.7403	-0.8721	-0.7142	-0.8905
0.12	-0.6282	-0.7281	-0.5830	-0.7602	-0.6356	-0.7236	-0.5906	-0.7562	-0.6500	-0.7137	-0.6055	-0.7474
0.20	-0.5202	-0.5494	-0.4590	-0.5955	-0.5263	-0.5458	-0.4653	-0.5927	-0.5383	-0.5379	-0.4779	-0.5864
0.30	-0.3732	-0.3337	-0.2990	-0.3934	-0.3777	-0.3313	-0.3037	-0.3921	-0.3868	-0.3261	-0.3133	-0.3891
0.40	-0.2139	-0.1268	-0.1339	-0.1953	-0.2168	-0.1258	-0.1370	-0.1955	-0.2231	-0.1236	-0.1435	-0.1960
0.50	-0.0435	0.0712	0.0359	-0.0011	-0.0449	0.0706	0.0344	-0.0029	-0.0482	0.0695	0.0311	-0.0070
0.60	0.1367	0.2601	0.2099	0.1894	0.1370	0.2578	0.2102	0.1858	0.1370	0.2528	0.2102	0.1780
0.70	0.3255	0.4399	0.3876	0.3761	0.3278	0.4356	0.3898	0.3707	0.3314	0.4263	0.3936	0.3588
0.80	0.5217	0.6106	0.5686	0.5592	0.5261	0.6040	0.5729	0.5518	0.5340	0.5897	0.5808	0.5354
0.88	0.6831	0.7406	0.7152	0.7033	0.6894	0.7320	0.7215	0.6940	0.7012	0.7131	0.7332	0.6737
0.95	0.8269	0.8458	0.8445	0.8276	0.8351	0.8390	0.8526	0.8165	0.8507	0.8157	0.8681	0.7924
1.00	0.9308	0.9253	0.9372	0.9156	0.9405	0.9128	0.9469	0.9031	0.9591	0.8858	0.9653	0.8759
L.E. CIRCLE CENTER			-0.7667	-1.0089			-0.7763	-1.0031			-0.7949	-0.9904
T.E. CIRCLE CENTER			0.9337	0.9202			0.9433	0.9077			0.9619	0.8806
	LER = 0.0063		TER = 0.0058		LER = 0.0063		TER = 0.0058		LER = 0.0062		TER = 0.0059	
	CHORD = 2.5837				CHORD = 2.5828				CHORD = 2.5785			

Table B-1. Stage D Airfoil Coordinates (Continued)

Reproduced from best available copy.

** BLADE SECTION COORDINATES IN TURBOMACHINE ORIENTATION - ROTOR D

NUMBER OF BLADES = 70.0 AXIAL LOCATION OF STACKING LINE IN COMPRESSOR = 19.200 IN.

SECTION 7 FOR XCUT OF 19.8600 IN.
SECTION SETTING ANGLE = 45.179

FRACT. OF SURF.	SUCTION SURFACE Z (IN.)	SUCTION SURFACE Y (IN.)	PRESSURE SURFACE Z (IN.)	PRESSURE SURFACE Y (IN.)
0.0	-0.8209	-0.9654	-0.8107	-0.9720
0.05	-0.7586	-0.8510	-0.7328	-0.8703
0.12	-0.6655	-0.6945	-0.6213	-0.7301
0.20	-0.5507	-0.5211	-0.4904	-0.5728
0.30	-0.3956	-0.3133	-0.3221	-0.3806
0.40	-0.2285	-0.1157	-0.1489	-0.1933
0.50	-0.0503	0.0714	0.0290	-0.0106
0.60	0.1379	0.2478	0.2112	0.1675
0.70	0.3352	0.4135	0.3978	0.3412
0.80	0.5424	0.5689	0.5896	0.5109
0.88	0.7138	0.6853	0.7461	0.6433
0.95	0.8677	0.7810	0.8852	0.7565
1.00	0.9797	0.8459	0.9858	0.8358
L.E. CIRCLE CENTER			-0.8155	-0.9683
T.E. CIRCLE CENTER			0.9823	0.8407

LER = 0.0061 TER = 0.0059
CHORD = 2.5624

SECTION 8 FOR XCUT OF 19.6700 IN.
SECTION SETTING ANGLE = 43.956

SUCTION SURFACE Z (IN.)	SUCTION SURFACE Y (IN.)	PRESSURE SURFACE Z (IN.)	PRESSURE SURFACE Y (IN.)
-0.8412	-0.9544	-0.8311	-0.9609
-0.7778	-0.8402	-0.7515	-0.8601
-0.6828	-0.6840	-0.6374	-0.7211
-0.5655	-0.5113	-0.5034	-0.5654
-0.4064	-0.3046	-0.3307	-0.3754
-0.2345	-0.1087	-0.1525	-0.1906
-0.0510	0.0759	0.0305	-0.0110
0.1430	0.2489	0.2181	0.1634
0.3462	0.4099	0.4098	0.3328
0.5567	0.5583	0.6043	0.4963
0.7299	0.6680	0.7623	0.6233
0.8848	0.7577	0.9022	0.7318
0.9972	0.8180	1.0032	0.8078
		-0.8359	-0.9572
		0.9998	0.8127

LER = 0.0060 TER = 0.0060
CHORD = 2.5619

SECTION 9 FOR XCUT OF 19.3250 IN.
SECTION SETTING ANGLE = 42.351

SUCTION SURFACE Z (IN.)	SUCTION SURFACE Y (IN.)	PRESSURE SURFACE Z (IN.)	PRESSURE SURFACE Y (IN.)
-0.8599	-0.9397	-0.8500	-0.9463
-0.7960	-0.8258	-0.7688	-0.8471
-0.6999	-0.6703	-0.6526	-0.7105
-0.5812	-0.4987	-0.5162	-0.5576
-0.4198	-0.2939	-0.3404	-0.3715
-0.2451	-0.1009	-0.1591	-0.1910
-0.0580	0.0796	0.0275	-0.0162
0.1405	0.2471	0.2192	0.1527
0.3493	0.4010	0.4156	0.3156
0.5670	0.5410	0.6165	0.4724
0.7470	0.6427	0.7803	0.5935
0.9081	0.7244	0.9257	0.6963
1.0251	0.7785	1.0306	0.7680
		-0.8547	-0.9425
		1.0274	0.7730

LER = 0.0060 TER = 0.0060
CHORD = 2.5586

SECTION 10 FOR XCUT OF 18.8400 IN.
SECTION SETTING ANGLE = 40.554

FRACT. OF SURF.	SUCTION SURFACE Z (IN.)	SUCTION SURFACE Y (IN.)	PRESSURE SURFACE Z (IN.)	PRESSURE SURFACE Y (IN.)
0.0	-0.8864	-0.9176	-0.8758	-0.9249
0.05	-0.8211	-0.8043	-0.7920	-0.8282
0.12	-0.7228	-0.6501	-0.6720	-0.6952
0.20	-0.6011	-0.4803	-0.5313	-0.5466
0.30	-0.4353	-0.2787	-0.3502	-0.3660
0.40	-0.2556	-0.0897	-0.1635	-0.1913
0.50	-0.0629	0.0857	0.0284	-0.0225
0.60	0.1416	0.2470	0.2253	0.1403
0.70	0.3566	0.3936	0.4270	0.2969
0.80	0.5805	0.5250	0.6332	0.4474
0.88	0.7661	0.6190	0.8011	0.5633
0.95	0.9320	0.6929	0.9502	0.6615
1.00	1.0523	0.7410	1.0578	0.7297
L.E. CIRCLE CENTER			-0.8807	-0.9207
T.E. CIRCLE CENTER			1.0545	0.7351

LER = 0.0065 TER = 0.0063
CHORD = 2.5597

SECTION 11 FOR XCUT OF 18.3350 IN.
SECTION SETTING ANGLE = 38.588

SUCTION SURFACE Z (IN.)	SUCTION SURFACE Y (IN.)	PRESSURE SURFACE Z (IN.)	PRESSURE SURFACE Y (IN.)
-0.9136	-0.8934	-0.9022	-0.9016
-0.8470	-0.7808	-0.8158	-0.8075
-0.7465	-0.6276	-0.6922	-0.6781
-0.6216	-0.4597	-0.5473	-0.5340
-0.4513	-0.2613	-0.3609	-0.3592
-0.2663	-0.0767	-0.1688	-0.1908
-0.0678	0.0931	0.0285	-0.0286
0.1428	0.2474	0.2309	0.1271
0.3643	0.3854	0.4380	0.2762
0.5952	0.5066	0.6496	0.4188
0.7857	0.5911	0.8219	0.5281
0.9561	0.6559	0.9748	0.6203
1.0797	0.6968	1.0851	0.6841
		-0.9074	-0.8969
		1.0817	0.6902

LER = 0.0070 TER = 0.0069
CHORD = 2.5587

SECTION 12 FOR XCUT OF 17.8500 IN.
SECTION SETTING ANGLE = 36.969

SUCTION SURFACE Z (IN.)	SUCTION SURFACE Y (IN.)	PRESSURE SURFACE Z (IN.)	PRESSURE SURFACE Y (IN.)
-0.9411	-0.8674	-0.9290	-0.8765
-0.8729	-0.7554	-0.8400	-0.7850
-0.7698	-0.6037	-0.7127	-0.6597
-0.6416	-0.4379	-0.5635	-0.5202
-0.4665	-0.2430	-0.3718	-0.3517
-0.2762	-0.0631	-0.1745	-0.1898
-0.0720	0.1008	0.0281	-0.0347
0.1447	0.2477	0.2358	0.1137
0.3724	0.3768	0.4482	0.2551
0.6095	0.4875	0.6650	0.3895
0.8050	0.5623	0.8416	0.4919
0.9795	0.6175	0.9981	0.5778
1.1059	0.6510	1.1111	0.6369
		-0.9345	-0.8712
		1.1076	0.6436

LER = 0.0076 TER = 0.0076
CHORD = 2.5578

Table B-1. Stage D Airfoil Coordinates (Continued)

** BLADE SECTION COORDINATES IN TURBOMACHINE ORIENTATION - ROTOR D

NUMBER OF BLADES = 70.0 AXIAL LOCATION OF STACKING LINE IN COMPRESSOR = 19.200 IN.

SECTION 13 FOR XCUT OF 17.3900 IN. SECTION SETTING ANGLE = 34.637

FRACT. OF SURF.	SUCTION SURFACE Z (IN.)	SUCTION SURFACE Y (IN.)	PRESSURE SURFACE Z (IN.)	PRESSURE SURFACE Y (IN.)
0.0	-0.9662	-0.8421	-0.9535	-0.8521
0.05	-0.8965	-0.7308	-0.8621	-0.7632
0.12	-0.7911	-0.5803	-0.7315	-0.6416
0.20	-0.6597	-0.4163	-0.5785	-0.5066
0.30	-0.4801	-0.2248	-0.3820	-0.3441
0.40	-0.2848	-0.0493	-0.1799	-0.1885
0.50	-0.0752	0.1088	0.0275	-0.0421
0.60	0.1471	0.2485	0.2400	0.1010
0.70	0.3805	0.3688	0.4572	0.2348
0.80	0.6232	0.4689	0.6789	0.3610
0.88	0.8229	0.5339	0.8592	0.4564
0.95	1.0009	0.5796	1.0191	0.5359
1.00	1.1296	0.6057	1.1344	0.5903
L.E. CIRCLE CENTER			-0.9592	-0.8463
T.E. CIRCLE CENTER			1.1310	0.5977

LER = 0.0081 TER = 0.0081
CHORD = 2.5568

SECTION 14 FOR XCUT OF 16.8850 IN. SECTION SETTING ANGLE = 32.604

FRACT. OF SURF.	SUCTION SURFACE Z (IN.)	SUCTION SURFACE Y (IN.)	PRESSURE SURFACE Z (IN.)	PRESSURE SURFACE Y (IN.)
0.0	-0.9908	-0.8165	-0.9774	-0.8273
0.05	-0.9199	-0.7055	-0.8838	-0.7409
0.12	-0.8123	-0.5557	-0.7500	-0.6229
0.20	-0.6779	-0.3933	-0.5934	-0.4923
0.30	-0.4938	-0.2046	-0.3923	-0.3357
0.40	-0.2933	-0.0335	-0.1854	-0.1865
0.50	-0.0779	0.1188	0.0269	-0.0452
0.60	0.1504	0.2507	0.2443	0.0882
0.70	0.3898	0.3613	0.4665	0.2135
0.80	0.6384	0.4495	0.6932	0.3306
0.88	0.8424	0.5034	0.8776	0.4181
0.95	1.0238	0.5382	1.0410	0.4901
1.00	1.1546	0.5558	1.1588	0.5390
L.E. CIRCLE CENTER			-0.9833	-0.8210
T.E. CIRCLE CENTER			1.1556	0.5471

LER = 0.0087 TER = 0.0088
CHORD = 2.5565

SECTION 15 FOR XCUT OF 16.6250 IN. SECTION SETTING ANGLE = 33.333

FRACT. OF SURF.	SUCTION SURFACE Z (IN.)	SUCTION SURFACE Y (IN.)	PRESSURE SURFACE Z (IN.)	PRESSURE SURFACE Y (IN.)
0.0	-0.9812	-0.8276	-0.9672	-0.8386
0.05	-0.9115	-0.7160	-0.8737	-0.7520
0.12	-0.8058	-0.5650	-0.7405	-0.6335
0.20	-0.6735	-0.4007	-0.5848	-0.5018
0.30	-0.4921	-0.2092	-0.3851	-0.3433
0.40	-0.2939	-0.0349	-0.1800	-0.1917
0.50	-0.0805	0.1206	0.0304	-0.0474
0.60	0.1463	0.2559	0.2457	0.0893
0.70	0.3847	0.3696	0.4658	0.2182
0.80	0.6325	0.4607	0.6905	0.3390
0.88	0.8361	0.5169	0.8733	0.4296
0.95	1.0172	0.5536	1.0354	0.5045
1.00	1.1478	0.5726	1.1523	0.5554
L.E. CIRCLE CENTER			-0.9734	-0.8321
T.E. CIRCLE CENTER			1.1488	0.5637

LER = 0.0090 TER = 0.0090
CHORD = 2.5581

SECTION 16 FOR XCUT OF 16.5200 IN. SECTION SETTING ANGLE = 34.479

FRACT. OF SURF.	SUCTION SURFACE Z (IN.)	SUCTION SURFACE Y (IN.)	PRESSURE SURFACE Z (IN.)	PRESSURE SURFACE Y (IN.)
0.0	-0.9655	-0.8450	-0.9511	-0.8558
0.05	-0.8976	-0.7326	-0.8587	-0.7683
0.12	-0.7945	-0.5800	-0.7271	-0.6480
0.20	-0.6653	-0.4135	-0.5734	-0.5140
0.30	-0.4877	-0.2185	-0.3765	-0.3521
0.40	-0.2931	-0.0401	-0.1743	-0.1966
0.50	-0.0830	0.1199	0.0330	-0.0479
0.60	0.1410	0.2595	0.2452	0.0935
0.70	0.3770	0.3786	0.4624	0.2274
0.80	0.6229	0.4750	0.6842	0.3534
0.88	0.8254	0.5355	0.8648	0.4483
0.95	1.0057	0.5761	1.0250	0.5270
1.00	1.1358	0.5980	1.1407	0.5807
L.E. CIRCLE CENTER			-0.9575	-0.8454
T.E. CIRCLE CENTER			1.1370	0.5890

LER = 0.0091 TER = 0.0091
CHORD = 2.5590

SECTION 17 FOR XCUT OF 16.4250 IN. SECTION SETTING ANGLE = 36.069

FRACT. OF SURF.	SUCTION SURFACE Z (IN.)	SUCTION SURFACE Y (IN.)	PRESSURE SURFACE Z (IN.)	PRESSURE SURFACE Y (IN.)
0.0	-0.9434	-0.8694	-0.9286	-0.8800
0.05	-0.8780	-0.7558	-0.8378	-0.7908
0.12	-0.7785	-0.6011	-0.7086	-0.6680
0.20	-0.6537	-0.4315	-0.5579	-0.5306
0.30	-0.4813	-0.2318	-0.3650	-0.3637
0.40	-0.2918	-0.0479	-0.1671	-0.2027
0.50	-0.0962	0.1182	0.0359	-0.0480
0.60	0.1337	0.2648	0.2440	0.0998
0.70	0.3663	0.3905	0.4571	0.2405
0.80	0.6095	0.4941	0.6749	0.3735
0.88	0.8103	0.5606	0.8526	0.4742
0.95	0.9894	0.6067	1.0104	0.5580
1.00	1.1189	0.6326	1.1244	0.6154
L.E. CIRCLE CENTER			-0.9352	-0.8736
T.E. CIRCLE CENTER			1.1204	0.6236

LER = 0.0092 TER = 0.0091
CHORD = 2.5614

SECTION 18 FOR XCUT OF 16.3250 IN. SECTION SETTING ANGLE = 38.391

FRACT. OF SURF.	SUCTION SURFACE Z (IN.)	SUCTION SURFACE Y (IN.)	PRESSURE SURFACE Z (IN.)	PRESSURE SURFACE Y (IN.)
0.0	-0.9106	-0.9055	-0.8953	-0.9156
0.05	-0.8490	-0.7901	-0.8070	-0.8240
0.12	-0.7549	-0.6323	-0.6816	-0.6971
0.20	-0.6364	-0.4581	-0.5355	-0.5546
0.30	-0.4719	-0.2516	-0.3487	-0.3804
0.40	-0.2898	-0.0597	-0.1570	-0.2113
0.50	-0.0910	0.1153	0.0398	-0.0478
0.60	0.1230	0.2715	0.2417	0.1094
0.70	0.3506	0.4074	0.4488	0.2598
0.80	0.5897	0.5216	0.6610	0.4029
0.88	0.7880	0.5970	0.8344	0.5118
0.95	0.9654	0.6510	0.9887	0.6030
1.00	1.0941	0.6827	1.1004	0.6656
L.E. CIRCLE CENTER			-0.9022	-0.9095
T.E. CIRCLE CENTER			1.0960	0.6737

LER = 0.0093 TER = 0.0092
CHORD = 2.5678

Table B-1. Stage D Airfoil Coordinates (Continued)

Reproduced from best available copy.

** BLADE SECTION COORDINATES IN TURBOMACHINE ORIENTATION - STATOR D

NUMBER OF BLADES = 66.0 AXIAL LOCATION OF STACKING LINE IN COMPRESSOR = 23.293 IN.

SECTION 1 FOR XCUT OF 20.0700 IN. — SECTION SETTING ANGLE = 46.885

FRACT. OF SURF.	SUCTION SURFACE Z (IN.)	SUCTION SURFACE Y (IN.)	PRESSURE SURFACE Z (IN.)	PRESSURE SURFACE Y (IN.)
0.0	-0.7407	-0.9252	-0.6616	-0.9632
0.05	-0.7176	-0.7915	-0.6142	-0.8528
0.12	-0.6613	-0.6182	-0.5340	-0.7078
0.20	-0.5707	-0.4370	-0.4270	-0.5528
0.30	-0.4283	-0.2315	-0.2760	-0.3708
0.40	-0.2621	-0.0443	-0.1108	-0.1975
0.50	-0.0784	0.1297	0.0651	-0.0286
0.60	0.1196	0.2951	0.2495	0.1402
0.70	0.3307	0.4558	0.4410	0.3131
0.80	0.5555	0.6145	0.6395	0.4930
0.88	0.7462	0.7398	0.8038	0.6431
0.95	0.9218	0.8466	0.9520	0.7792
1.00	1.0524	0.9198	1.0605	0.8789
L.E. CIRCLE CENTER			-0.6987	-0.9392
T.E. CIRCLE CENTER			1.0539	0.8988

LER = 0.0442 TER = 0.0210
CHORD = 2.6048

SECTION 2 FOR XCUT OF 20.0350 IN. — SECTION SETTING ANGLE = 41.224

SUCTION SURFACE Z (IN.)	SUCTION SURFACE Y (IN.)	PRESSURE SURFACE Z (IN.)	PRESSURE SURFACE Y (IN.)
-0.8136	-0.8318	-0.7451	-0.8700
-0.7753	-0.7084	-0.6839	-0.7712
-0.7017	-0.5478	-0.5876	-0.6407
-0.5954	-0.3800	-0.4657	-0.5008
-0.4371	-0.1904	-0.2996	-0.3367
-0.2578	-0.0197	-0.1218	-0.1812
-0.0629	0.1360	0.0649	-0.0313
0.1447	0.2801	0.2586	0.1167
0.3633	0.4156	0.4581	0.2660
0.5927	0.5449	0.6633	0.4192
0.7846	0.6438	0.8318	0.5455
0.9590	0.7257	0.9828	0.6591
1.0873	0.7804	1.0927	0.7417
		-0.7767	-0.8462
		1.0875	0.7607

LER = 0.0396 TER = 0.0197
CHORD = 2.5204

SECTION 3 FOR XCUT OF 19.9950 IN. — SECTION SETTING ANGLE = 35.388

SUCTION SURFACE Z (IN.)	SUCTION SURFACE Y (IN.)	PRESSURE SURFACE Z (IN.)	PRESSURE SURFACE Y (IN.)
-0.8832	-0.7421	-0.8251	-0.7801
-0.8307	-0.6282	-0.7512	-0.6921
-0.7410	-0.4797	-0.6401	-0.5754
-0.6199	-0.3245	-0.5042	-0.4500
-0.4467	-0.1502	-0.3237	-0.3032
-0.2549	0.0045	-0.1340	-0.1652
-0.0490	0.1421	0.0630	-0.0339
0.1678	0.2651	0.2658	0.0934
0.3938	0.3756	0.4733	0.2193
0.6279	0.4755	0.6852	0.3458
0.8211	0.5479	0.8580	0.4483
0.9942	0.6048	1.0117	0.5391
1.1203	0.6409	1.1230	0.6045
		-0.8514	-0.7569
		1.1192	0.6225

LER = 0.0350 TER = 0.0184
CHORD = 2.4586

SECTION 4 FOR XCUT OF 19.9520 IN. — SECTION SETTING ANGLE = 29.999

FRACT. OF SURF.	SUCTION SURFACE Z (IN.)	SUCTION SURFACE Y (IN.)	PRESSURE SURFACE Z (IN.)	PRESSURE SURFACE Y (IN.)
0.0	-0.9432	-0.6640	-0.8945	-0.7010
0.05	-0.8790	-0.5581	-0.8102	-0.6223
0.12	-0.7759	-0.4199	-0.6868	-0.5175
0.20	-0.6423	-0.2755	-0.5392	-0.4047
0.30	-0.4563	-0.1146	-0.3466	-0.2732
0.40	-0.2537	0.0259	-0.1465	-0.1508
0.50	-0.0383	0.1474	0.0595	-0.0364
0.60	0.1867	0.2513	0.2703	0.0722
0.70	0.4193	0.3391	0.4849	0.1768
0.80	0.6578	0.4122	0.7029	0.2788
0.88	0.8520	0.4602	0.8796	0.3594
0.95	1.0242	0.4940	1.0359	0.4293
1.00	1.1482	0.5130	1.1486	0.4788
L.E. CIRCLE CENTER			-0.9161	-0.6789
T.E. CIRCLE CENTER			1.1460	0.4959

LER = 0.0309 TER = 0.0172
CHORD = 2.4214

SECTION 5 FOR XCUT OF 19.9020 IN. — SECTION SETTING ANGLE = 24.920

SUCTION SURFACE Z (IN.)	SUCTION SURFACE Y (IN.)	PRESSURE SURFACE Z (IN.)	PRESSURE SURFACE Y (IN.)
-0.9959	-0.5942	-0.9561	-0.6294
-0.9220	-0.4951	-0.8634	-0.5587
-0.8076	-0.3657	-0.7299	-0.4643
-0.6635	-0.2308	-0.5724	-0.3629
-0.4665	-0.0819	-0.3693	-0.2453
-0.2543	0.0456	-0.1602	-0.1375
-0.0305	0.1521	0.0539	-0.0387
0.2021	0.2381	0.2720	0.0522
0.4407	0.3044	0.4931	0.1365
0.6832	0.3518	0.7168	0.2152
0.8786	0.3764	0.8973	0.2747
1.0499	0.3880	1.0562	0.3244
1.1720	0.3903	1.1703	0.3585
		-0.9733	-0.6088
		1.1689	0.3746

LER = 0.0269 TER = 0.0161
CHORD = 2.4001

SECTION 6 FOR XCUT OF 19.8580 IN. — SECTION SETTING ANGLE = 20.136

SUCTION SURFACE Z (IN.)	SUCTION SURFACE Y (IN.)	PRESSURE SURFACE Z (IN.)	PRESSURE SURFACE Y (IN.)
-1.0409	-0.5325	-1.0097	-0.5648
-0.9596	-0.4390	-0.9109	-0.5007
-0.8365	-0.3168	-0.7696	-0.4153
-0.6840	-0.1901	-0.6045	-0.3240
-0.4779	-0.0518	-0.3929	-0.2192
-0.2576	0.0637	-0.1761	-0.1249
-0.0264	0.1561	0.0450	-0.0411
0.2129	0.2251	0.2696	0.0329
0.4571	0.2705	0.4968	0.0976
0.7033	0.2930	0.7259	0.1536
0.8998	0.2947	0.9101	0.1924
1.0704	0.2843	1.0716	0.2221
1.1908	0.2700	1.1871	0.2408
		-1.0229	-0.5463
		1.1868	0.2557

LER = 0.0227 TER = 0.0149
CHORD = 2.3883

Table B-1. Stage D Airfoil Coordinates (Continued)

** BLADE SECTION COORDINATES IN TURBOMACHINE ORIENTATION - STATOR D

NUMBER OF BLADES = 66.0 AXIAL LOCATION OF STACKING LINE IN COMPRESSOR = 23.293 IN.

SECTION 7 FOR XCUT OF 19.7450 IN.
SECTION SETTING ANGLE = 15.963

FRACT. OF SURF.	SUCTION SURFACE Z (IN.)	SUCTION SURFACE Y (IN.)	PRESSURE SURFACE Z (IN.)	PRESSURE SURFACE Y (IN.)
0.0	-1.0728	-0.4842	-1.0498	-0.5114
0.05	-0.9877	-0.3943	-0.9482	-0.4521
0.12	-0.8599	-0.2772	-0.8032	-0.3735
0.20	-0.7024	-0.1565	-0.6338	-0.2903
0.30	-0.4906	-0.0267	-0.4170	-0.1964
0.40	-0.2649	0.0787	-0.1953	-0.1140
0.50	-0.0284	0.1587	0.0308	-0.0435
0.60	0.2158	0.2124	0.2603	0.0151
0.70	0.4642	0.2389	0.4923	0.0619
0.80	0.7134	0.2382	0.7260	0.0967
0.88	0.9109	0.2183	0.9135	0.1160
0.95	1.0807	0.1869	1.0776	0.1266
1.00	1.1997	0.1566	1.1946	0.1306
L.E. CIRCLE CENTER			-1.0592	-0.4961
T.E. CIRCLE CENTER			1.1952	0.1440

LER = 0.0180 TER = 0.0134
CHORD = 2.3749

SECTION 8 FOR XCUT OF 19.6170 IN.
SECTION SETTING ANGLE = 13.451

FRACT. OF SURF.	SUCTION SURFACE Z (IN.)	SUCTION SURFACE Y (IN.)	PRESSURE SURFACE Z (IN.)	PRESSURE SURFACE Y (IN.)
0.0	-1.0867	-0.4598	-1.0746	-0.4752
0.05	-1.0005	-0.3720	-0.9720	-0.4202
0.12	-0.8718	-0.2581	-0.8260	-0.3476
0.20	-0.7140	-0.1413	-0.6559	-0.2711
0.30	-0.5026	-0.0167	-0.4391	-0.1855
0.40	-0.2781	0.0827	-0.2178	-0.1112
0.50	-0.0421	0.1558	0.0084	-0.0486
0.60	0.2019	0.2006	0.2383	0.0012
0.70	0.4504	0.2162	0.4714	0.0379
0.80	0.6995	0.2018	0.7066	0.0608
0.88	0.8967	0.1686	0.8956	0.0690
0.95	1.0658	0.1238	1.0613	0.0687
1.00	1.1839	0.0830	1.1795	0.0640
L.E. CIRCLE CENTER			-1.0794	-0.4665
T.E. CIRCLE CENTER			1.1802	0.0739

LER = 0.0099 TER = 0.0099
CHORD = 2.3432

SECTION 9 FOR XCUT OF 19.3710 IN.
SECTION SETTING ANGLE = 12.457

FRACT. OF SURF.	SUCTION SURFACE Z (IN.)	SUCTION SURFACE Y (IN.)	PRESSURE SURFACE Z (IN.)	PRESSURE SURFACE Y (IN.)
0.0	-1.0945	-0.4320	-1.0829	-0.4477
0.05	-1.0055	-0.3469	-0.9783	-0.3954
0.12	-0.8732	-0.2366	-0.8297	-0.3268
0.20	-0.7117	-0.1241	-0.6570	-0.2549
0.30	-0.4964	-0.0051	-0.4371	-0.1751
0.40	-0.2689	0.0885	-0.2135	-0.1067
0.50	-0.0323	0.1556	0.0134	-0.0498
0.60	0.2105	0.1951	0.2428	-0.0048
0.70	0.4562	0.2065	0.4743	0.0280
0.80	0.7015	0.1894	0.7069	0.0485
0.88	0.8945	0.1550	0.8929	0.0556
0.95	1.0601	0.1100	1.0557	0.0549
1.00	1.1759	0.0694	1.1719	0.0504
L.E. CIRCLE CENTER			-1.0874	-0.4389
T.E. CIRCLE CENTER			1.1724	0.0603

LER = 0.0098 TER = 0.0098
CHORD = 2.3340

SECTION 10 FOR XCUT OF 18.9240 IN.
SECTION SETTING ANGLE = 12.199

FRACT. OF SURF.	SUCTION SURFACE Z (IN.)	SUCTION SURFACE Y (IN.)	PRESSURE SURFACE Z (IN.)	PRESSURE SURFACE Y (IN.)
0.0	-1.0963	-0.4248	-1.0850	-0.4405
0.05	-1.0069	-0.3404	-0.9802	-0.3890
0.12	-0.8740	-0.2312	-0.8314	-0.3215
0.20	-0.7120	-0.1199	-0.6585	-0.2508
0.30	-0.4966	-0.0024	-0.4386	-0.1727
0.40	-0.2692	0.0896	-0.2151	-0.1059
0.50	-0.0328	0.1550	0.0116	-0.0506
0.60	0.2094	0.1930	0.2407	-0.0071
0.70	0.4545	0.2031	0.4718	0.0245
0.80	0.6992	0.1851	0.7043	0.0441
0.88	0.8925	0.1506	0.8908	0.0512
0.95	1.0585	0.1061	1.0542	0.0510
1.00	1.1747	0.0662	1.1708	0.0472
L.E. CIRCLE CENTER			-1.0894	-0.4318
T.E. CIRCLE CENTER			1.1712	0.0570

LER = 0.0098 TER = 0.0098
CHORD = 2.3325

SECTION 11 FOR XCUT OF 18.4670 IN.
SECTION SETTING ANGLE = 12.645

FRACT. OF SURF.	SUCTION SURFACE Z (IN.)	SUCTION SURFACE Y (IN.)	PRESSURE SURFACE Z (IN.)	PRESSURE SURFACE Y (IN.)
0.0	-1.0938	-0.4338	-1.0823	-0.4494
0.05	-1.0050	-0.3486	-0.9779	-0.3969
0.12	-0.8729	-0.2382	-0.8295	-0.3280
0.20	-0.7117	-0.1255	-0.6571	-0.2559
0.30	-0.4969	-0.0062	-0.4376	-0.1759
0.40	-0.2700	0.0877	-0.2144	-0.1074
0.50	-0.0339	0.1549	0.0121	-0.0505
0.60	0.2083	0.1947	0.2411	-0.0053
0.70	0.4534	0.2065	0.4721	0.0280
0.80	0.6983	0.1903	0.7045	0.0494
0.88	0.8920	0.1574	0.8910	0.0579
0.95	1.0583	0.1141	1.0544	0.0590
1.00	1.1748	0.0752	1.1711	0.0562
L.E. CIRCLE CENTER			-1.0868	-0.4407
T.E. CIRCLE CENTER			1.1714	0.0660

LER = 0.0098 TER = 0.0098
CHORD = 2.3340

SECTION 12 FOR XCUT OF 18.0320 IN.
SECTION SETTING ANGLE = 13.087

FRACT. OF SURF.	SUCTION SURFACE Z (IN.)	SUCTION SURFACE Y (IN.)	PRESSURE SURFACE Z (IN.)	PRESSURE SURFACE Y (IN.)
0.0	-1.0909	-0.4443	-1.0793	-0.4597
0.05	-1.0030	-0.3579	-0.9754	-0.4059
0.12	-0.8720	-0.2459	-0.8277	-0.3352
0.20	-0.7117	-0.1314	-0.6558	-0.2613
0.30	-0.4977	-0.0099	-0.4369	-0.1791
0.40	-0.2712	0.0860	-0.2140	-0.1086
0.50	-0.0353	0.1552	0.0122	-0.0498
0.60	0.2070	0.1967	0.2412	-0.0030
0.70	0.4525	0.2102	0.4723	0.0318
0.80	0.6979	0.1954	0.7049	0.0545
0.88	0.8919	0.1635	0.8915	0.0639
0.95	1.0587	0.1210	1.0551	0.0658
1.00	1.1755	0.0826	1.1719	0.0636
L.E. CIRCLE CENTER			-1.0839	-0.4511
T.E. CIRCLE CENTER			1.1722	0.0734

LER = 0.0098 TER = 0.0098
CHORD = 2.3356

Table B-1. Stage D Airfoil Coordinates (Continued)

Reproduced from best available copy.

** BLADE SECTION COORDINATES IN TURBOMACHINE ORIENTATION - STATOR D

NUMBER OF BLADES = 66.0 AXIAL LOCATION OF STACKING LINE IN COMPRESSOR = 23.295 IN.

SECTION 13 FOR XCUT OF 17.5750 IN.
SECTION SETTING ANGLE = 13.419

FRACT. OF SURF.	SUCTION SURFACE Z (IN.)	SUCTION SURFACE Y (IN.)	PRESSURE SURFACE Z (IN.)	PRESSURE SURFACE Y (IN.)
0.0	-1.0883	-0.4541	-1.0764	-0.4694
0.05	-1.0013	-0.3666	-0.9731	-0.4142
0.12	-0.8713	-0.2529	-0.8261	-0.3418
0.20	-0.7120	-0.1365	-0.6549	-0.2658
0.30	-0.4988	-0.0128	-0.4365	-0.1815
0.40	-0.2726	0.0851	-0.2140	-0.1091
0.50	-0.0366	0.1559	0.0121	-0.0488
0.60	0.2060	0.1988	0.2411	-0.0008
0.70	0.4519	0.2132	0.4724	0.0348
0.80	0.6978	0.1990	0.7052	0.0581
0.88	0.8923	0.1673	0.8921	0.0677
0.95	1.0595	0.1248	1.0558	0.0696
1.00	1.1765	0.0862	1.1728	0.0672
L.E. CIRCLE CENTER			-1.0811	-0.4608
T.E. CIRCLE CENTER			1.1731	0.0770

LER = 0.0098 TER = 0.0098
CHORD = 2.3371

SECTION 14 FOR XCUT OF 17.1030 IN.
SECTION SETTING ANGLE = 14.004

FRACT. OF SURF.	SUCTION SURFACE Z (IN.)	SUCTION SURFACE Y (IN.)	PRESSURE SURFACE Z (IN.)	PRESSURE SURFACE Y (IN.)
0.0	-1.0826	-0.4712	-1.0704	-0.4862
0.05	-0.9973	-0.3817	-0.9682	-0.4288
0.12	-0.8693	-0.2653	-0.8226	-0.3532
0.20	-0.7118	-0.1456	-0.6526	-0.2739
0.30	-0.5001	-0.0181	-0.4355	-0.1858
0.40	-0.2747	0.0833	-0.2137	-0.1101
0.50	-0.0389	0.1571	0.0120	-0.0471
0.60	0.2039	0.2024	0.2408	0.0031
0.70	0.4504	0.2185	0.4721	0.0403
0.80	0.6971	0.2053	0.7052	0.0644
0.88	0.8922	0.1738	0.8923	0.0743
0.95	1.0598	0.1313	1.0563	0.0760
1.00	1.1771	0.0924	1.1734	0.0734
L.E. CIRCLE CENTER			-1.0753	-0.4778
T.E. CIRCLE CENTER			1.1738	0.0832

LER = 0.0098 TER = 0.0096
CHORD = 2.3376

SECTION 15 FOR XCUT OF 16.7110 IN.
SECTION SETTING ANGLE = 17.676

FRACT. OF SURF.	SUCTION SURFACE Z (IN.)	SUCTION SURFACE Y (IN.)	PRESSURE SURFACE Z (IN.)	PRESSURE SURFACE Y (IN.)
0.0	-1.0426	-0.5644	-1.0289	-0.5776
0.05	-0.9666	-0.4662	-0.9333	-0.5092
0.12	-0.8504	-0.3363	-0.7959	-0.4183
0.20	-0.7042	-0.2004	-0.6342	-0.3219
0.30	-0.5033	-0.0521	-0.4254	-0.2134
0.40	-0.2849	0.0691	-0.2097	-0.1190
0.50	-0.0526	0.1608	0.0118	-0.0394
0.60	0.1898	0.2214	0.2382	0.0248
0.70	0.4379	0.2499	0.4685	0.0734
0.80	0.6877	0.2461	0.7016	0.1061
0.88	0.8859	0.2199	0.8894	0.1208
0.95	1.0563	0.1804	1.0542	0.1253
1.00	1.1755	0.1428	1.1720	0.1238
L.E. CIRCLE CENTER			-1.0347	-0.5700
T.E. CIRCLE CENTER			1.1723	0.1336

LER = 0.0096 TER = 0.0096
CHORD = 2.3359

SECTION 16 FOR XCUT OF 16.5150 IN.
SECTION SETTING ANGLE = 25.358

FRACT. OF SURF.	SUCTION SURFACE Z (IN.)	SUCTION SURFACE Y (IN.)	PRESSURE SURFACE Z (IN.)	PRESSURE SURFACE Y (IN.)
0.0	-0.9533	-0.7128	-0.9377	-0.7232
0.05	-0.8923	-0.6055	-0.8530	-0.6418
0.12	-0.7966	-0.4601	-0.7305	-0.5314
0.20	-0.6724	-0.3030	-0.5848	-0.4112
0.30	-0.4955	-0.1243	-0.3941	-0.2713
0.40	-0.2960	0.0301	-0.1940	-0.1449
0.50	-0.0772	0.1559	0.0148	-0.0334
0.60	0.1571	0.2499	0.2315	0.0618
0.70	0.4021	0.3104	0.4549	0.1399
0.80	0.6531	0.3364	0.6837	0.2002
0.88	0.8549	0.3325	0.8697	0.2356
0.95	1.0301	0.3113	1.0340	0.2571
1.00	1.1536	0.2861	1.1520	0.2671
L.E. CIRCLE CENTER			-0.9447	-0.7168
T.E. CIRCLE CENTER			1.1514	0.2767

LER = 0.0095 TER = 0.0096
CHORD = 2.3387

SECTION 17 FOR XCUT OF 16.4250 IN.
SECTION SETTING ANGLE = 31.366

FRACT. OF SURF.	SUCTION SURFACE Z (IN.)	SUCTION SURFACE Y (IN.)	PRESSURE SURFACE Z (IN.)	PRESSURE SURFACE Y (IN.)
0.0	-0.8798	-0.8090	-0.8531	-0.8230
0.05	-0.8290	-0.6968	-0.7773	-0.7330
0.12	-0.7477	-0.5423	-0.6672	-0.6092
0.20	-0.6395	-0.3719	-0.5350	-0.4723
0.30	-0.4809	-0.1730	-0.3599	-0.3100
0.40	-0.2970	0.0045	-0.1737	-0.1600
0.50	-0.0903	0.1553	0.0235	-0.0247
0.60	0.1355	0.2752	0.2308	0.0943
0.70	0.3760	0.3615	0.4469	0.1956
0.80	0.6259	0.4131	0.6705	0.2785
0.88	0.8292	0.4293	0.8536	0.3314
0.95	1.0074	0.4254	1.0163	0.3677
1.00	1.1340	0.4125	1.1336	0.3880
L.E. CIRCLE CENTER			-0.8654	-0.8141
T.E. CIRCLE CENTER			1.1320	0.4002

LER = 0.0152 TER = 0.0124
CHORD = 2.3652

SECTION 18 FOR XCUT OF 16.3360 IN.
SECTION SETTING ANGLE = 38.675

FRACT. OF SURF.	SUCTION SURFACE Z (IN.)	SUCTION SURFACE Y (IN.)	PRESSURE SURFACE Z (IN.)	PRESSURE SURFACE Y (IN.)
0.0	-0.7872	-0.9392	-0.7547	-0.9517
0.05	-0.7501	-0.8208	-0.6895	-0.8517
0.12	-0.6878	-0.6549	-0.5940	-0.7124
0.20	-0.6007	-0.4677	-0.4782	-0.5554
0.30	-0.4663	-0.2427	-0.3222	-0.3654
0.40	-0.3030	-0.0351	-0.1530	-0.1856
0.50	-0.1123	0.1485	0.0296	-0.0192
0.60	0.1026	0.3025	0.2249	0.1313
0.70	0.3370	0.4232	0.4318	0.2642
0.80	0.5856	0.5091	0.6488	0.3784
0.88	0.7911	0.5524	0.8286	0.4559
0.95	0.9734	0.5720	0.9895	0.5134
1.00	1.1042	0.5756	1.1063	0.5488
L.E. CIRCLE CENTER			-0.7701	-0.9431
T.E. CIRCLE CENTER			1.1033	0.5620

LER = 0.0176 TER = 0.0136
CHORD = 2.4343

APPENDIX C

STAGE E AIRFOIL COORDINATES

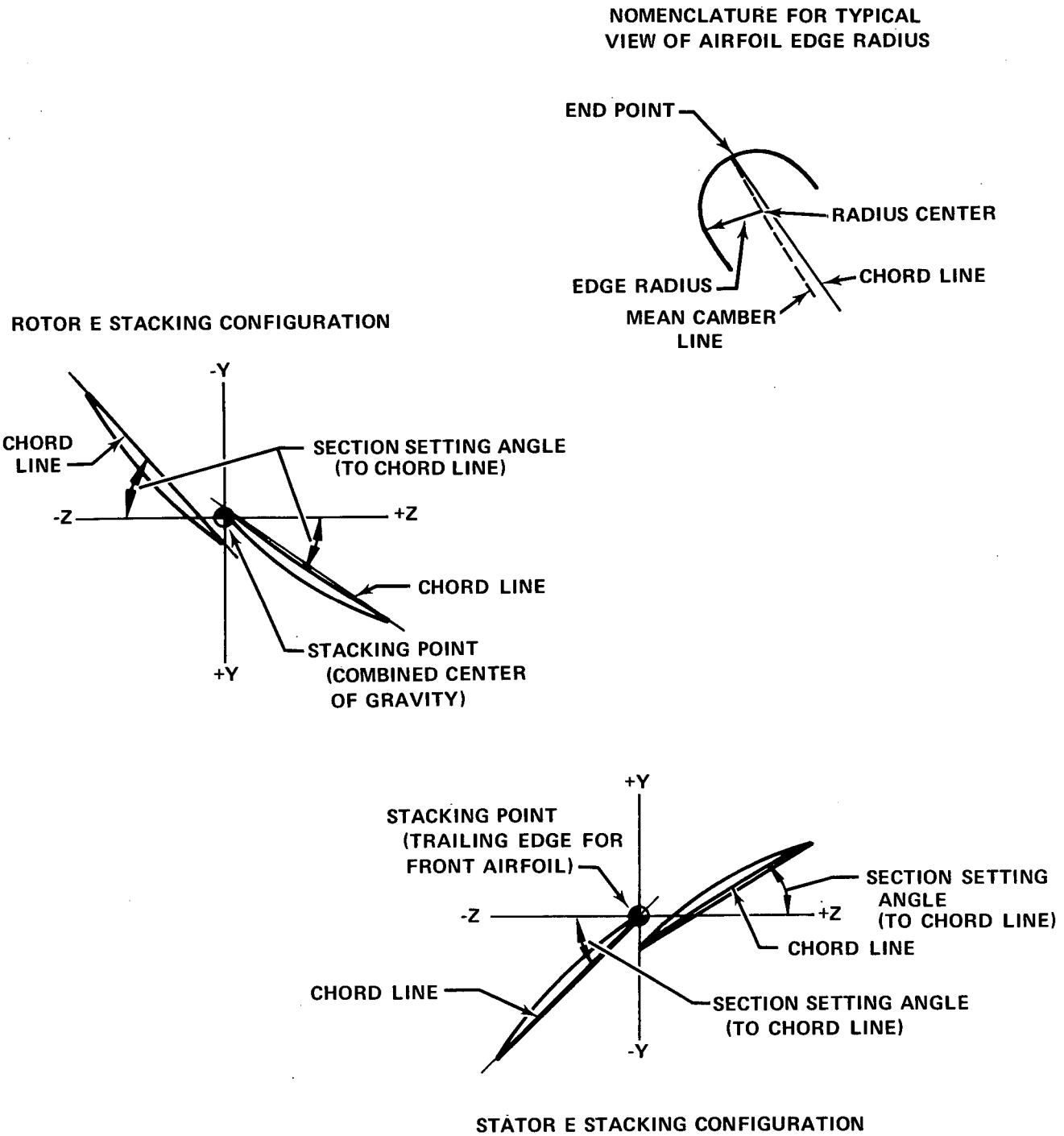

Figure C-1. Stage E Airfoil Coordinates FD 64420

Table C-1. Stage E Airfoil Coordinates

** BLADE SECTION COORDINATES IN TURBOMACHINE ORIENTATION - ROTOR E FRONT AIRFOIL

NUMBER OF BLADES = 70.0 AXIAL LOCATION OF STACKING LINE IN COMPRESSOR = 19.188 IN.

FRACT. OF SURF.	SECTION 1 FOR XCUT OF 20.5350 IN. SECTION SETTING ANGLE = 70.007 SUCTION SURFACE Z IN.	SUCTION SURFACE Y IN.	PRESSURE SURFACE Z IN.	PRESSURE SURFACE Y IN.	SECTION 2 FOR XCUT OF 20.4850 IN. SECTION SETTING ANGLE = 66.948 SUCTION SURFACE Z IN.	SUCTION SURFACE Y IN.	PRESSURE SURFACE Z IN.	PRESSURE SURFACE Y IN.	SECTION 3 FOR XCUT OF 20.3900 IN. SECTION SETTING ANGLE = 62.227 SUCTION SURFACE Z IN.	SUCTION SURFACE Y IN.	PRESSURE SURFACE Z IN.	PRESSURE SURFACE Y IN.
0.0	-0.4460	-0.9390	-0.4148	-0.9446	-0.5002	-0.9299	-0.4717	-0.9366	-0.5901	-0.9152	-0.5661	-0.9232
0.05	-0.4358	-0.8769	-0.4003	-0.8840	-0.4857	-0.8685	-0.4524	-0.8770	-0.5691	-0.8550	-0.5395	-0.8655
0.12	-0.4187	-0.7905	-0.3782	-0.7995	-0.4629	-0.7831	-0.4240	-0.7940	-0.5376	-0.7713	-0.5015	-0.7850
0.20	-0.3954	-0.6925	-0.3507	-0.7036	-0.4335	-0.6863	-0.3898	-0.6996	-0.4988	-0.6766	-0.4571	-0.6934
0.30	-0.3611	-0.5712	-0.3131	-0.5845	-0.3921	-0.5666	-0.3447	-0.5824	-0.4466	-0.5596	-0.4003	-0.5794
0.40	-0.3218	-0.4513	-0.2726	-0.4664	-0.3462	-0.4483	-0.2972	-0.4660	-0.3905	-0.4442	-0.3421	-0.4661
0.50	-0.2780	-0.3329	-0.2294	-0.3492	-0.2961	-0.3317	-0.2477	-0.3505	-0.3308	-0.3304	-0.2826	-0.3534
0.60	-0.2298	-0.2162	-0.1841	-0.2329	-0.2421	-0.2168	-0.1965	-0.2357	-0.2677	-0.2186	-0.2222	-0.2414
0.70	-0.1775	-0.1014	-0.1373	-0.1173	-0.1843	-0.1038	-0.1441	-0.1216	-0.2012	-0.1087	-0.1611	-0.1299
0.80	-0.1214	0.0114	-0.0890	-0.0024	-0.1230	0.0071	-0.0907	-0.0082	-0.1315	-0.0010	-0.0993	-0.0189
0.88	-0.0741	0.1001	-0.0496	0.0888	-0.0716	0.0943	-0.0472	0.0819	-0.0737	0.0836	-0.0494	0.0694
0.95	-0.0310	0.1766	-0.0145	0.1683	-0.0250	0.1694	-0.0087	0.1604	-0.0216	0.1563	-0.0055	0.1463
1.00	0.0007	0.2305	0.0108	0.2248	0.0091	0.2223	0.0190	0.2162	0.0164	0.2076	0.0261	0.2010
L.E. CIRCLE CENTER			-0.4302	-0.9412			-0.4858	-0.9326			-0.5779	-0.9186
T.E. CIRCLE CENTER			0.0056	0.2273			0.0139	0.2190			0.0210	0.2040
LER = 0.0159			TER = 0.0058		LER = 0.0147		TER = 0.0058		LER = 0.0127		TER = 0.0059	
CHORD = 1.2688					CHORD = 1.2759				CHORD = 1.2909			

FRACT. OF SURF.	SECTION 4 FOR XCUT OF 20.2900 IN. SECTION SETTING ANGLE = 58.583 SUCTION SURFACE Z IN.	SUCTION SURFACE Y IN.	PRESSURE SURFACE Z IN.	PRESSURE SURFACE Y IN.	SECTION 5 FOR XCUT OF 20.1200 IN. SECTION SETTING ANGLE = 54.792 SUCTION SURFACE Z IN.	SUCTION SURFACE Y IN.	PRESSURE SURFACE Z IN.	PRESSURE SURFACE Y IN.	SECTION 6 FOR XCUT OF 20.0900 IN. SECTION SETTING ANGLE = 54.372 SUCTION SURFACE Z IN.	SUCTION SURFACE Y IN.	PRESSURE SURFACE Z IN.	PRESSURE SURFACE Y IN.
0.0	-0.6667	-0.9032	-0.6468	-0.9116	-0.7572	-0.8899	-0.7429	-0.8977	-0.7682	-0.8884	-0.7547	-0.8960
0.05	-0.6408	-0.8441	-0.6148	-0.8557	-0.7270	-0.8320	-0.7057	-0.8441	-0.7377	-0.8307	-0.7171	-0.8428
0.12	-0.6030	-0.7619	-0.5696	-0.7776	-0.6833	-0.7517	-0.6537	-0.7692	-0.6935	-0.7506	-0.6644	-0.7683
0.20	-0.5573	-0.6690	-0.5175	-0.6885	-0.6312	-0.6610	-0.5941	-0.6836	-0.6408	-0.6602	-0.6041	-0.6832
0.30	-0.4969	-0.5543	-0.4517	-0.5776	-0.5630	-0.5494	-0.5195	-0.5767	-0.5719	-0.5490	-0.5285	-0.5769
0.40	-0.4330	-0.4415	-0.3852	-0.4671	-0.4916	-0.4397	-0.4447	-0.4700	-0.4997	-0.4397	-0.4529	-0.4707
0.50	-0.3660	-0.3304	-0.3180	-0.3571	-0.4172	-0.3320	-0.3697	-0.3636	-0.4245	-0.3325	-0.3771	-0.3647
0.60	-0.2957	-0.2212	-0.2504	-0.2475	-0.3397	-0.2264	-0.2945	-0.2573	-0.3463	-0.2274	-0.3011	-0.2589
0.70	-0.2224	-0.1141	-0.1823	-0.1383	-0.2593	-0.1230	-0.2192	-0.1511	-0.2651	-0.1245	-0.2251	-0.1532
0.80	-0.1461	-0.0093	-0.1139	-0.0295	-0.1761	-0.0219	-0.1438	-0.0453	-0.1812	-0.0239	-0.1489	-0.0477
0.88	-0.0831	0.0730	-0.0590	0.0572	-0.1076	0.0573	-0.0834	0.0393	-0.1121	0.0548	-0.0879	0.0365
0.95	-0.0266	0.1437	-0.0106	0.1327	-0.0463	0.1253	-0.0304	0.1130	-0.0503	0.1225	-0.0344	0.1100
1.00	0.0145	0.1935	0.0240	0.1865	-0.0018	0.1731	0.0075	0.1656	-0.0053	0.1700	0.0038	0.1624
L.E. CIRCLE CENTER			-0.6565	-0.9069			-0.7497	-0.8933			-0.7612	-0.8918
T.E. CIRCLE CENTER			0.0190	0.1897			0.0026	0.1691			-0.0010	0.1659
LER = 0.0108			TER = 0.0059		LER = 0.0082		TER = 0.0060		LER = 0.0078		TER = 0.0060	
CHORD = 1.3046					CHORD = 1.3159				CHORD = 1.3163			

Table C-1. Stage E Airfoil Coordinates (Continued)

** BLADE SECTION COORDINATES IN TURBOMACHINE ORIENTATION - ROTOR E FRONT AIRFOIL

NUMBER OF BLADES = 70.0 AXIAL LOCATION OF STACKING LINE IN COMPRESSOR = 19.188 IN.

SECTION 7 FOR XCUT OF 20.0150 IN.
SECTION SETTING ANGLE = 53.611

FRACT. OF SURF.	SUCTION SURFACE Z IN.	SUCTION SURFACE Y IN.	PRESSURE SURFACE Z IN.	PRESSURE SURFACE Y IN.
0.0	-0.7891	-0.8863	-0.7772	-0.8935
0.05	-0.7580	-0.8289	-0.7389	-0.8409
0.12	-0.7131	-0.7492	-0.6853	-0.7672
0.20	-0.6597	-0.6594	-0.6240	-0.6832
0.30	-0.5898	-0.5490	-0.5470	-0.5781
0.40	-0.5165	-0.4406	-0.4699	-0.4731
0.50	-0.4400	-0.3344	-0.3926	-0.3682
0.60	-0.3604	-0.2303	-0.3152	-0.2634
0.70	-0.2779	-0.1286	-0.2378	-0.1586
0.80	-0.1926	-0.0292	-0.1603	-0.0541
0.88	-0.1224	0.0486	-0.0982	0.0295
0.95	-0.0596	0.1154	-0.0438	0.1025
1.00	-0.0140	0.1623	-0.0049	0.1545
L.E. CIRCLE CENTER			-0.7829	-0.8895
T.E. CIRCLE CENTER			-0.0097	0.1581

LER = 0.0069 TER = 0.0060
CHORD = 1.3149

SECTION 8 FOR XCUT OF 19.8600 IN.
SECTION SETTING ANGLE = 52.840

SUCTION SURFACE Z IN.	SUCTION SURFACE Y IN.	PRESSURE SURFACE Z IN.	PRESSURE SURFACE Y IN.
-0.8087	-0.8822	-0.7986	-0.8887
-0.7769	-0.8249	-0.7592	-0.8368
-0.7310	-0.7455	-0.7042	-0.7641
-0.6764	-0.6560	-0.6413	-0.6810
-0.6052	-0.5462	-0.5627	-0.5773
-0.5308	-0.4387	-0.4842	-0.4736
-0.4532	-0.3336	-0.4058	-0.3701
-0.3727	-0.2310	-0.3274	-0.2666
-0.2893	-0.1308	-0.2491	-0.1633
-0.2032	-0.0333	-0.1708	-0.0601
-0.1324	0.0429	-0.1082	0.0224
-0.0691	0.1081	-0.0535	0.0945
-0.0232	0.1539	-0.0144	0.1459
		-0.8034	-0.8851
		-0.0191	0.1496

LER = 0.0060 TER = 0.0060
CHORD = 1.3103

SECTION 9 FOR XCUT OF 19.6700 IN.
SECTION SETTING ANGLE = 51.904

SUCTION SURFACE Z IN.	SUCTION SURFACE Y IN.	PRESSURE SURFACE Z IN.	PRESSURE SURFACE Y IN.
-0.8297	-0.8758	-0.8196	-0.8824
-0.7972	-0.8184	-0.7791	-0.8307
-0.7501	-0.7389	-0.7225	-0.7584
-0.6942	-0.6494	-0.6578	-0.6758
-0.6211	-0.5397	-0.5769	-0.5727
-0.5445	-0.4325	-0.4961	-0.4697
-0.4647	-0.3278	-0.4153	-0.3667
-0.3817	-0.2258	-0.3346	-0.2639
-0.2958	-0.1265	-0.2540	-0.1611
-0.2070	-0.0299	-0.1735	-0.0584
-0.1341	0.0453	-0.1092	0.0236
-0.0689	0.1096	-0.0530	0.0954
-0.0216	0.1547	-0.0129	0.1466
		-0.8244	-0.8787
		-0.0176	0.1503

LER = 0.0060 TER = 0.0060
CHORD = 1.3196

SECTION 10 FOR XCUT OF 19.3250 IN.
SECTION SETTING ANGLE = 50.833

FRACT. OF SURF.	SUCTION SURFACE Z IN.	SUCTION SURFACE Y IN.	PRESSURE SURFACE Z IN.	PRESSURE SURFACE Y IN.
0.0	-0.8635	-0.8717	-0.8536	-0.8784
0.05	-0.8306	-0.8139	-0.8120	-0.8271
0.12	-0.7827	-0.7340	-0.7537	-0.7552
0.20	-0.7256	-0.6442	-0.6871	-0.6731
0.30	-0.6507	-0.5343	-0.6038	-0.5706
0.40	-0.5720	-0.4272	-0.5205	-0.4683
0.50	-0.4897	-0.3229	-0.4372	-0.3660
0.60	-0.4039	-0.2216	-0.3538	-0.2638
0.70	-0.3149	-0.1234	-0.2705	-0.1617
0.80	-0.2226	-0.0283	-0.1873	-0.0598
0.88	-0.1467	0.0455	-0.1207	0.0217
0.95	-0.0788	0.1083	-0.0625	0.0930
1.00	-0.0294	0.1522	-0.0209	0.1438
L.E. CIRCLE CENTER			-0.8583	-0.8746
T.E. CIRCLE CENTER			-0.0255	0.1476

LER = 0.0060 TER = 0.0060
CHORD = 1.3306

SECTION 11 FOR XCUT OF 18.8400 IN.
SECTION SETTING ANGLE = 49.342

SUCTION SURFACE Z IN.	SUCTION SURFACE Y IN.	PRESSURE SURFACE Z IN.	PRESSURE SURFACE Y IN.
-0.9007	-0.8620	-0.8909	-0.8689
-0.8668	-0.8040	-0.8475	-0.8183
-0.8175	-0.7239	-0.7867	-0.7475
-0.7586	-0.6340	-0.7172	-0.6666
-0.6810	-0.5244	-0.6303	-0.5655
-0.5993	-0.4178	-0.5435	-0.4645
-0.5136	-0.3145	-0.4567	-0.3635
-0.4242	-0.2145	-0.3699	-0.2625
-0.3311	-0.1180	-0.2832	-0.1615
-0.2345	-0.0250	-0.1966	-0.0606
-0.1549	0.0467	-0.1273	0.0201
-0.0836	0.1075	-0.0667	0.0907
-0.0317	0.1498	-0.0235	0.1412
		-0.8955	-0.8650
		-0.0280	0.1451

LER = 0.0060 TER = 0.0060
CHORD = 1.3435

SECTION 12 FOR XCUT OF 18.3350 IN.
SECTION SETTING ANGLE = 47.882

SUCTION SURFACE Z IN.	SUCTION SURFACE Y IN.	PRESSURE SURFACE Z IN.	PRESSURE SURFACE Y IN.
-0.9356	-0.8482	-0.9260	-0.8553
-0.9011	-0.7901	-0.8809	-0.8056
-0.8506	-0.7100	-0.8179	-0.7361
-0.7900	-0.6203	-0.7459	-0.6567
-0.7101	-0.5111	-0.6559	-0.5573
-0.6258	-0.4054	-0.5659	-0.4580
-0.5371	-0.3033	-0.4760	-0.3586
-0.4442	-0.2050	-0.3861	-0.2591
-0.3474	-0.1106	-0.2963	-0.1597
-0.2469	-0.0203	-0.2065	-0.0602
-0.1638	0.0490	-0.1348	0.0194
-0.0894	0.1073	-0.0720	0.0890
-0.0352	0.1476	-0.0272	0.1388
		-0.9304	-0.8513
		-0.0317	0.1428

LER = 0.0060 TER = 0.0060
CHORD = 1.3521

Table C-1. Stage E Airfoil Coordinates (Continued)

** BLADE SECTION COORDINATES IN TURBOMACHINE ORIENTATION - ROTOR E FRONT AIRFOIL

NUMBER OF BLADES = 70.0 AXIAL LOCATION OF STACKING LINE IN COMPRESSOR = 19.188 IN.

FRACT. OF SURF.	SECTION 13 FOR XCUT OF 17.8500 IN. SECTION SETTING ANGLE = 46.494 SUCTION SURFACE Z IN.	SUCTION SURFACE Y IN.	PRESSURE SURFACE Z IN.	PRESSURE SURFACE Y IN.	SECTION 14 FOR XCUT OF 17.3900 IN. SECTION SETTING ANGLE = 45.450 SUCTION SURFACE Z IN.	SUCTION SURFACE Y IN.	PRESSURE SURFACE Z IN.	PRESSURE SURFACE Y IN.	SECTION 15 FOR XCUT OF 16.8850 IN. SECTION SETTING ANGLE = 44.715 SUCTION SURFACE Z IN.	SUCTION SURFACE Y IN.	PRESSURE SURFACE Z IN.	PRESSURE SURFACE Y IN.
0.0	-0.9640	-0.8290	-0.9545	-0.8363	-0.9844	-0.8101	-0.9750	-0.8175	-0.9983	-0.7916	-0.9891	-0.7991
0.05	-0.9287	-0.7711	-0.9080	-0.7879	-0.9485	-0.7525	-0.9273	-0.7704	-0.9623	-0.7343	-0.9404	-0.7532
0.12	-0.8770	-0.6914	-0.8429	-0.7201	-0.8960	-0.6734	-0.8605	-0.7043	-0.9095	-0.6556	-0.8724	-0.6888
0.20	-0.8150	-0.6024	-0.7685	-0.6425	-0.8329	-0.5851	-0.7843	-0.6286	-0.8460	-0.5679	-0.7950	-0.6148
0.30	-0.7330	-0.4943	-0.6757	-0.5454	-0.7495	-0.4781	-0.6894	-0.5338	-0.7619	-0.4618	-0.6987	-0.5219
0.40	-0.6463	-0.3899	-0.5830	-0.4482	-0.6613	-0.3751	-0.5948	-0.4386	-0.6729	-0.3598	-0.6028	-0.4285
0.50	-0.5551	-0.2895	-0.4904	-0.3509	-0.5683	-0.2762	-0.5004	-0.3431	-0.5790	-0.2622	-0.5075	-0.3346
0.60	-0.4595	-0.1933	-0.3980	-0.2534	-0.4709	-0.1818	-0.4064	-0.2473	-0.4806	-0.1693	-0.4126	-0.2402
0.70	-0.3597	-0.1013	-0.3058	-0.1558	-0.3692	-0.0919	-0.3127	-0.1512	-0.3778	-0.0812	-0.3182	-0.1452
0.80	-0.2560	-0.0139	-0.2137	-0.0580	-0.2635	-0.0069	-0.2193	-0.0547	-0.2708	0.0018	-0.2243	-0.0498
0.88	-0.1703	0.0528	-0.1401	0.0203	-0.1762	0.0576	-0.1448	0.0226	-0.1824	0.0644	-0.1496	0.0269
0.95	-0.0935	0.1086	-0.0758	0.0889	-0.0979	0.1114	-0.0797	0.0905	-0.1032	0.1164	-0.0845	0.0943
1.00	-0.0376	0.1470	-0.0299	0.1379	-0.0409	0.1483	-0.0334	0.1391	-0.0455	0.1518	-0.0381	0.1425
L.E. CIRCLE CENTER			-0.9588	-0.8321			-0.9792	-0.8132			-0.9932	-0.7947
T.E. CIRCLE CENTER			-0.0343	0.1420			-0.0377	0.1432			-0.0424	0.1467
LER = 0.0060 CHORD = 1.3550			TER = 0.0060		LER = 0.0060 CHORD = 1.3541		TER = 0.0060		LER = 0.0060 CHORD = 1.3500		TER = 0.0060	

FRACT. OF SURF.	SECTION 16 FOR XCUT OF 16.6250 IN. SECTION SETTING ANGLE = 45.275 SUCTION SURFACE Z IN.	SUCTION SURFACE Y IN.	PRESSURE SURFACE Z IN.	PRESSURE SURFACE Y IN.	SECTION 17 FOR XCUT OF 16.5200 IN. SECTION SETTING ANGLE = 45.908 SUCTION SURFACE Z IN.	SUCTION SURFACE Y IN.	PRESSURE SURFACE Z IN.	PRESSURE SURFACE Y IN.	SECTION 18 FOR XCUT OF 16.4250 IN. SECTION SETTING ANGLE = 46.742 SUCTION SURFACE Z IN.	SUCTION SURFACE Y IN.	PRESSURE SURFACE Z IN.	PRESSURE SURFACE Y IN.
0.0	-0.9884	-0.7985	-0.9790	-0.8059	-0.9773	-0.8090	-0.9678	-0.8161	-0.9629	-0.8227	-0.9532	-0.8296
0.05	-0.9536	-0.7406	-0.9309	-0.7595	-0.9437	-0.7504	-0.9205	-0.7690	-0.9308	-0.7632	-0.9071	-0.7814
0.12	-0.9024	-0.6610	-0.8638	-0.6944	-0.8941	-0.6697	-0.8546	-0.7028	-0.8833	-0.6813	-0.8426	-0.7138
0.20	-0.8407	-0.5722	-0.7874	-0.6197	-0.8340	-0.5798	-0.7794	-0.6270	-0.8252	-0.5899	-0.7692	-0.6364
0.30	-0.7585	-0.4647	-0.6924	-0.5258	-0.7536	-0.4710	-0.6859	-0.5318	-0.7472	-0.4792	-0.6776	-0.5394
0.40	-0.6710	-0.3615	-0.5979	-0.4315	-0.6677	-0.3665	-0.5927	-0.4362	-0.6632	-0.3730	-0.5862	-0.4423
0.50	-0.5784	-0.2629	-0.5037	-0.3367	-0.5763	-0.2667	-0.4999	-0.3404	-0.5734	-0.2717	-0.4950	-0.3450
0.60	-0.4809	-0.1692	-0.4101	-0.2415	-0.4797	-0.1719	-0.4073	-0.2443	-0.4780	-0.1755	-0.4039	-0.2477
0.70	-0.3787	-0.0805	-0.3168	-0.1459	-0.3782	-0.0824	-0.3150	-0.1480	-0.3774	-0.0849	-0.3128	-0.1504
0.80	-0.2721	0.0028	-0.2239	-0.0500	-0.2721	0.0015	-0.2230	-0.0514	-0.2718	-0.0001	-0.2218	-0.0531
0.88	-0.1838	0.0653	-0.1499	0.0270	-0.1839	0.0644	-0.1495	0.0259	-0.1840	0.0632	-0.1489	0.0247
0.95	-0.1044	0.1171	-0.0853	0.0946	-0.1047	0.1162	-0.0853	0.0937	-0.1048	0.1153	-0.0851	0.0928
1.00	-0.0467	0.1522	-0.0393	0.1430	-0.0469	0.1514	-0.0395	0.1422	-0.0470	0.1506	-0.0396	0.1414
L.E. CIRCLE CENTER			-0.9832	-0.8016			-0.9721	-0.8119			-0.9576	-0.8255
T.E. CIRCLE CENTER			-0.0436	0.1471			-0.0438	0.1463			-0.0440	0.1455
LER = 0.0060 CHORD = 1.3472			TER = 0.0060		LER = 0.0060 CHORD = 1.3460		TER = 0.0060		LER = 0.0060 CHORD = 1.3452		TER = 0.0060	

Table C-1. Stage E Airfoil Coordinates (Continued)

** BLADE SECTION COORDINATES IN TURBOMACHINE CRIENTATION - ROTOR E FRONT AIRFOIL

NUMBER OF BLADES = 70.0 AXIAL LOCATION OF STACKING LINE IN COMPRESSOR = 19.188 IN.

SECTION 19 FOR XCUT OF 16.3250 IN.
SECTION SETTING ANGLE = 47.925

FRACT. OF SURF.	SUCTION SURFACE Z (IN.)	SUCTION SURFACE Y (IN.)	PRESSURE SURFACE Z (IN.)	PRESSURE SURFACE Y (IN.)
0.0	-0.9427	-0.8421	-0.9327	-0.8486
0.05	-0.9128	-0.7813	-0.8882	-0.7988
0.12	-0.8681	-0.6975	-0.8260	-0.7291
0.20	-0.8130	-0.6040	-0.7549	-0.6494
0.30	-0.7381	-0.4908	-0.6662	-0.5498
0.40	-0.6568	-0.3821	-0.5773	-0.4503
0.50	-0.5692	-0.2786	-0.4884	-0.3510
0.60	-0.4756	-0.1804	-0.3993	-0.2520
0.70	-0.3762	-0.0882	-0.3098	-0.1533
0.80	-0.2714	-0.0022	-0.2201	-0.0549
0.88	-0.1839	0.0619	-0.1481	0.0235
0.95	-0.1049	0.1144	-0.0849	0.0919
1.00	-0.0471	0.1499	-0.0396	0.1407
L.E. CIRCLE CENTER			-0.9372	-0.8446
T.E. CIRCLE CENTER			-0.0440	0.1447

LER = 0.0060 TER = 0.0060
CHORD = 1.3449

Table C-1. Stage E Airfoil Coordinates (Continued)

** BLADE SECTION COORDINATES IN TURBOMACHINE ORIENTATION - ROTOR E REAR AIRFOIL

NUMBER OF BLADES = 70.0 AXIAL LOCATION OF STACKING LINE IN COMPRESSOR = 19.188 IN.

SECTION 1 FOR XCUT OF 20.5350 IN.
SECTION SETTING ANGLE = 65.116

FRACT. OF SURF.	SUCTION SURFACE Z IN.	SUCTION SURFACE Y IN.	PRESSURE SURFACE Z IN.	PRESSURE SURFACE Y IN.
0.0	0.0259	-0.0930	0.0372	-0.0980
0.05	0.0432	-0.0331	0.0605	-0.0415
0.12	0.0696	0.0498	0.0937	0.0370
0.20	0.1024	0.1430	0.1325	0.1261
0.30	0.1468	0.2573	0.1820	0.2364
0.40	0.1946	0.3694	0.2322	0.3457
0.50	0.2451	0.4793	0.2827	0.4543
0.60	0.2977	0.5873	0.3335	0.5620
0.70	0.3515	0.6940	0.3846	0.6688
0.80	0.4063	0.7995	0.4358	0.7747
0.88	0.4506	0.8834	0.4766	0.8589
0.95	0.4896	0.9566	0.5122	0.9321
1.00	0.5175	1.0088	0.5375	0.9842
L.E. CIRCLE CENTER			0.0317	-0.0952
T.E. CIRCLE CENTER			0.5273	0.9963
	LER = 0.0062		TER = 0.0159	
	CHORD = 1.2207			

SECTION 2 FOR XCUT OF 20.4850 IN.
SECTION SETTING ANGLE = 61.117

SUCTION SURFACE Z IN.	SUCTION SURFACE Y IN.	PRESSURE SURFACE Z IN.	PRESSURE SURFACE Y IN.
0.0304	-0.0792	0.0414	-0.0848
0.0517	-0.0208	0.0686	-0.0302
0.0834	0.0598	0.1072	0.0457
0.1223	0.1504	0.1520	0.1317
0.1742	0.2613	0.2088	0.2381
0.2293	0.3697	0.2663	0.3435
0.2872	0.4755	0.3241	0.4480
0.3470	0.5792	0.3822	0.5517
0.4084	0.6811	0.4405	0.6543
0.4708	0.7814	0.4988	0.7560
0.5212	0.8606	0.5453	0.8366
0.5655	0.9294	0.5859	0.9068
0.5973	0.9783	0.6148	0.9566
		0.0361	-0.0817
		0.6058	0.9672
LER = 0.0061		TER = 0.0140	
CHORD = 1.2137			

SECTION 3 FOR XCUT OF 20.3900 IN.
SECTION SETTING ANGLE = 54.770

SUCTION SURFACE Z IN.	SUCTION SURFACE Y IN.	PRESSURE SURFACE Z IN.	PRESSURE SURFACE Y IN.
0.0324	-0.0621	0.0428	-0.0684
0.0596	-0.0059	0.0760	-0.0167
0.0997	0.0716	0.1229	0.0552
0.1479	0.1583	0.1771	0.1366
0.2115	0.2640	0.2456	0.2371
0.2783	0.3667	0.3147	0.3366
0.3478	0.4665	0.3841	0.4350
0.4196	0.5635	0.4538	0.5322
0.4930	0.6579	0.5238	0.6284
0.5678	0.7500	0.5938	0.7234
0.6283	0.8220	0.6497	0.7986
0.6817	0.8839	0.6986	0.8639
0.7199	0.9276	0.7334	0.9101
		0.0378	-0.0649
		0.7263	0.9186
LER = 0.0061		TER = 0.0110	
CHORD = 1.2177			

SECTION 4 FOR XCUT OF 20.2900 IN.
SECTION SETTING ANGLE = 49.797

FRACT. OF SURF.	SUCTION SURFACE Z IN.	SUCTION SURFACE Y IN.	PRESSURE SURFACE Z IN.	PRESSURE SURFACE Y IN.
0.0	0.0271	-0.0546	0.0371	-0.0615
0.05	0.0589	0.0000	0.0749	-0.0118
0.12	0.1054	0.0752	0.1283	0.0571
0.20	0.1609	0.1592	0.1899	0.1351
0.30	0.2336	0.2612	0.2676	0.2314
0.40	0.3097	0.3598	0.3459	0.3263
0.50	0.3887	0.4551	0.4248	0.4200
0.60	0.4702	0.5470	0.5042	0.5124
0.70	0.5538	0.6356	0.5838	0.6035
0.80	0.6390	0.7211	0.6636	0.6934
0.88	0.7081	0.7874	0.7275	0.7643
0.95	0.7692	0.8438	0.7835	0.8256
1.00	0.8130	0.8832	0.8234	0.8691
L.E. CIRCLE CENTER			0.0323	-0.0577
T.E. CIRCLE CENTER			0.8179	0.8759
	LER = 0.0061		TER = 0.0088	
	CHORD = 1.2350			

SECTION 5 FOR XCUT OF 20.1200 IN.
SECTION SETTING ANGLE = 44.611

SUCTION SURFACE Z IN.	SUCTION SURFACE Y IN.	PRESSURE SURFACE Z IN.	PRESSURE SURFACE Y IN.
0.0089	-0.0592	0.0185	-0.0666
0.0452	-0.0058	0.0610	-0.0188
0.0980	0.0676	0.1209	0.0474
0.1610	0.1492	0.1901	0.1222
0.2433	0.2478	0.2776	0.2143
0.3294	0.3426	0.3662	0.3049
0.4189	0.4333	0.4556	0.3938
0.5115	0.5200	0.5458	0.4813
0.6067	0.6027	0.6366	0.5671
0.7043	0.6812	0.7281	0.6514
0.7837	0.7412	0.8016	0.7177
0.8542	0.7915	0.8661	0.7748
0.9049	0.8262	0.9123	0.8152
		0.0140	-0.0626
		0.9083	0.8205
LER = 0.0061		TER = 0.0066	
CHORD = 1.2695			

SECTION 6 FOR XCUT OF 20.0900 IN.
SECTION SETTING ANGLE = 44.028

SUCTION SURFACE Z IN.	SUCTION SURFACE Y IN.	PRESSURE SURFACE Z IN.	PRESSURE SURFACE Y IN.
0.0054	-0.0615	0.0149	-0.0689
0.0421	-0.0082	0.0578	-0.0213
0.0956	0.0650	0.1185	0.0447
0.1593	0.1465	0.1885	0.1191
0.2427	0.2448	0.2771	0.2108
0.3299	0.3391	0.3668	0.3008
0.4206	0.4294	0.4575	0.3893
0.5145	0.5156	0.5490	0.4762
0.6112	0.5975	0.6412	0.5615
0.7103	0.6753	0.7341	0.6451
0.7911	0.7345	0.8089	0.7109
0.8628	0.7840	0.8745	0.7675
0.9144	0.8182	0.9215	0.8075
		0.0104	-0.0649
		0.9176	0.8126
LER = 0.0061		TER = 0.0064	
CHORD = 1.2747			

Table C-1. Stage E Airfoil Coordinates (Continued)

** BLADE SECTION COORDINATES IN TURBOMACHINE ORIENTATION - ROTOR E REAR AIRFOIL

NUMBER OF BLADES = 70.0 AXIAL LOCATION OF STACKING LINE IN COMPRESSOR = 19.188 IN.

FRACT. OF SURF.	SECTION 7 FOR XCUT OF 20.0150 IN. SECTION SETTING ANGLE = 42.894 SUCTION SURFACE Z IN.	SUCTION SURFACE Y IN.	PRESSURE SURFACE Z IN.	PRESSURE SURFACE Y IN.	SECTION 8 FOR XCUT OF 19.8600 IN. SECTION SETTING ANGLE = 41.640 SUCTION SURFACE Z IN.	SUCTION SURFACE Y IN.	PRESSURE SURFACE Z IN.	PRESSURE SURFACE Y IN.	SECTION 9 FOR XCUT OF 19.6700 IN. SECTION SETTING ANGLE = 40.545 SUCTION SURFACE Z IN.	SUCTION SURFACE Y IN.	PRESSURE SURFACE Z IN.	PRESSURE SURFACE Y IN.
0.0	-0.0030	-0.0682	0.0064	-0.0757	-0.0115	-0.0765	-0.0024	-0.0841	-0.0108	-0.0742	-0.0017	-0.0820
0.05	0.0346	-0.0150	0.0502	-0.0284	0.0267	-0.0235	0.0421	-0.0375	0.0286	-0.0213	0.0443	-0.0361
0.12	0.0892	0.0580	0.1122	0.0370	0.0821	0.0491	0.1050	0.0271	0.0859	0.0509	0.1093	0.0275
0.20	0.1544	0.1391	0.1838	0.1109	0.1483	0.1297	0.1778	0.0998	0.1541	0.1309	0.1845	0.0991
0.30	0.2397	0.2368	0.2745	0.2017	0.2349	0.2266	0.2699	0.1893	0.2436	0.2270	0.2796	0.1871
0.40	0.3291	0.3305	0.3664	0.2908	0.3258	0.3193	0.3634	0.2771	0.3372	0.3184	0.3759	0.2733
0.50	0.4222	0.4199	0.4595	0.3783	0.4210	0.4075	0.4590	0.3633	0.4348	0.4051	0.4734	0.3578
0.60	0.5187	0.5049	0.5536	0.4641	0.5203	0.4911	0.5558	0.4477	0.5357	0.4870	0.5717	0.4405
0.70	0.6183	0.5855	0.6486	0.5482	0.6230	0.5699	0.6540	0.5303	0.6398	0.5638	0.6710	0.5215
0.80	0.7206	0.6617	0.7445	0.6306	0.7289	0.6440	0.7532	0.6111	0.7470	0.6356	0.7714	0.6006
0.88	0.8041	0.7193	0.8217	0.6953	0.8157	0.6997	0.8335	0.6744	0.8346	0.6894	0.8524	0.6627
0.95	0.8783	0.7674	0.8897	0.7509	0.8930	0.7458	0.9042	0.7288	0.9127	0.7337	0.9237	0.7160
1.00	0.9318	0.8004	0.9384	0.7902	0.9489	0.7772	0.9550	0.7671	0.9691	0.7639	0.9750	0.7536
L.E. CIRCLE CENTER			0.0020	-0.0716			-0.0067	-0.0800			-0.0059	-0.0777
T.E. CIRCLE CENTER			0.9348	0.7951			0.9516	0.7720			0.9717	0.7585
	LER = 0.0060		TER = 0.0061		LER = 0.0060		TER = 0.0059		LER = 0.0060		TER = 0.0059	
	CHORD = 1.2854				CHORD = 1.2941				CHORD = 1.2984			

FRACT. OF SURF.	SECTION 10 FOR XCUT OF 19.3250 IN. SECTION SETTING ANGLE = 38.299 SUCTION SURFACE Z IN.	SUCTION SURFACE Y IN.	PRESSURE SURFACE Z IN.	PRESSURE SURFACE Y IN.	SECTION 11 FOR XCUT OF 18.8400 IN. SECTION SETTING ANGLE = 36.285 SUCTION SURFACE Z IN.	SUCTION SURFACE Y IN.	PRESSURE SURFACE Z IN.	PRESSURE SURFACE Y IN.	SECTION 12 FOR XCUT OF 18.3350 IN. SECTION SETTING ANGLE = 34.134 SUCTION SURFACE Z IN.	SUCTION SURFACE Y IN.	PRESSURE SURFACE Z IN.	PRESSURE SURFACE Y IN.
0.0	-0.0181	-0.0734	-0.0094	-0.0814	-0.0209	-0.0732	-0.0123	-0.0814	-0.0244	-0.0727	-0.0159	-0.0812
0.05	0.0228	-0.0208	0.0387	-0.0367	0.0214	-0.0205	0.0378	-0.0378	0.0192	-0.0203	0.0361	-0.0390
0.12	0.0823	0.0509	0.1066	0.0252	0.0830	0.0511	0.1086	0.0225	0.0827	0.0508	0.1096	0.0192
0.20	0.1534	0.1300	0.1850	0.0949	0.1567	0.1298	0.1904	0.0902	0.1589	0.1287	0.1945	0.0845
0.30	0.2465	0.2247	0.2842	0.1803	0.2535	0.2234	0.2939	0.1733	0.2592	0.2208	0.3018	0.1644
0.40	0.3442	0.3143	0.3848	0.2640	0.3552	0.3115	0.3987	0.2544	0.3647	0.3067	0.4106	0.2423
0.50	0.4462	0.3986	0.4866	0.3458	0.4615	0.3937	0.5048	0.3336	0.4751	0.3861	0.5207	0.3183
0.60	0.5521	0.4776	0.5898	0.4258	0.5720	0.4699	0.6121	0.4109	0.5899	0.4589	0.6320	0.3923
0.70	0.6617	0.5511	0.6942	0.5040	0.6862	0.5399	0.7207	0.4863	0.7087	0.5247	0.7446	0.4642
0.80	0.7745	0.6190	0.7998	0.5802	0.8039	0.6036	0.8304	0.5598	0.8310	0.5834	0.8584	0.5342
0.88	0.8669	0.6691	0.8850	0.6398	0.9002	0.6499	0.9190	0.6171	0.9312	0.6252	0.9502	0.5887
0.95	0.9491	0.7100	0.9601	0.6909	0.9860	0.6870	0.9971	0.6663	1.0203	0.6579	1.0311	0.6354
1.00	1.0086	0.7374	1.0141	0.7269	1.0480	0.7116	1.0531	0.7008	1.0846	0.6790	1.0893	0.6681
L.E. CIRCLE CENTER			-0.0134	-0.0770			-0.0162	-0.0769			-0.0197	-0.0765
T.E. CIRCLE CENTER			1.0109	0.7319			1.0501	0.7060			1.0864	0.6733
	LER = 0.0060		TER = 0.0060		LER = 0.0060		TER = 0.0060		LER = 0.0060		TER = 0.0060	
	CHORD = 1.3172				CHORD = 1.3348				CHORD = 1.3483			

Table C-1. Stage E Airfoil Coordinates (Continued)

** BLADE SECTION COORDINATES IN TURBOMACHINE CRIENTATION - ROTOR E REAR AIRFOIL

NUMBER OF BLADES = 70.0 AXIAL LOCATION OF STACKING LINE IN COMPRESSOR = 19.188 IN.

FRACT. OF SURF.	SECTION 13 FOR XCUT OF 17.8500 IN. SECTION SETTING ANGLE = 32.105 SUCTION SURFACE Z IN.	SUCTION SURFACE Y IN.	PRESSURE SURFACE Z IN.	PRESSURE SURFACE Y IN.	SECTION 14 FOR XCUT OF 17.3900 IN. SECTION SETTING ANGLE = 30.096 SUCTION SURFACE Z IN.	SUCTION SURFACE Y IN.	PRESSURE SURFACE Z IN.	PRESSURE SURFACE Y IN.	SECTION 15 FOR XCUT OF 16.8850 IN. SECTION SETTING ANGLE = 27.749 SUCTION SURFACE Z IN.	SUCTION SURFACE Y IN.	PRESSURE SURFACE Z IN.	PRESSURE SURFACE Y IN.
0.0	-0.0269	-0.0725	-0.0186	-0.0811	-0.0303	-0.0695	-0.0222	-0.0782	-0.0349	-0.0616	-0.0271	-0.0706
0.05	0.0175	-0.0203	0.0349	-0.0404	0.0149	-0.0178	0.0324	-0.0392	0.0111	-0.0107	0.0287	-0.0336
0.12	0.0825	0.0502	0.1104	0.0156	0.0811	0.0519	0.1096	0.0145	0.0787	0.0577	0.1075	0.0172
0.20	0.1605	0.1272	0.1976	0.0784	0.1608	0.1276	0.1987	0.0746	0.1601	0.1314	0.1985	0.0737
0.30	0.2635	0.2175	0.3079	0.1551	0.2660	0.2157	0.3115	0.1476	0.2678	0.2166	0.3136	0.1422
0.40	0.3720	0.3009	0.4196	0.2296	0.3771	0.2964	0.4256	0.2184	0.3814	0.2936	0.4301	0.2082
0.50	0.4856	0.3773	0.5327	0.3020	0.4934	0.3693	0.5412	0.2869	0.5005	0.3620	0.5479	0.2718
0.60	0.6038	0.4462	0.6471	0.3722	0.6145	0.4340	0.6581	0.3531	0.6242	0.4214	0.6671	0.3328
0.70	0.7262	0.5073	0.7627	0.4403	0.7398	0.4902	0.7762	0.4169	0.7520	0.4715	0.7875	0.3913
0.80	0.8522	0.5606	0.8797	0.5062	0.8686	0.5377	0.8956	0.4784	0.8832	0.5119	0.9091	0.4473
0.88	0.9552	0.5974	0.9740	0.5574	0.9737	0.5692	0.9920	0.5259	0.9901	0.5372	1.0072	0.4903
0.95	1.0468	0.6253	1.0572	0.6010	1.0671	0.5921	1.0770	0.5662	1.0847	0.5541	1.0936	0.5265
1.00	1.1129	0.6426	1.1170	0.6314	1.1344	0.6056	1.1380	0.5942	1.1527	0.5632	1.1556	0.5516
L.E. CIRCLE CENTER			-0.0223	-0.0763			-0.0257	-0.0733			-0.0304	-0.0656
T.E. CIRCLE CENTER			1.1143	0.6368			1.1355	0.5997			1.1534	0.5572
LER = 0.0060 CHORD = 1.3538			TER = 0.0060		LER = 0.0060 CHORD = 1.3542		TER = 0.0060		LER = 0.0060 CHORD = 1.3496		TER = 0.0060	

FRACT. OF SURF.	SECTION 16 FOR XCUT OF 16.6250 IN. SECTION SETTING ANGLE = 27.753 SUCTION SURFACE Z IN.	SUCTION SURFACE Y IN.	PRESSURE SURFACE Z IN.	PRESSURE SURFACE Y IN.	SECTION 17 FOR XCUT OF 16.5200 IN. SECTION SETTING ANGLE = 28.308 SUCTION SURFACE Z IN.	SUCTION SURFACE Y IN.	PRESSURE SURFACE Z IN.	PRESSURE SURFACE Y IN.	SECTION 18 FOR XCUT OF 16.4250 IN. SECTION SETTING ANGLE = 29.160 SUCTION SURFACE Z IN.	SUCTION SURFACE Y IN.	PRESSURE SURFACE Z IN.	PRESSURE SURFACE Y IN.
0.0	-0.0361	-0.0546	-0.0284	-0.0636	-0.0363	-0.0517	-0.0286	-0.0607	-0.0365	-0.0497	-0.0288	-0.0587
0.05	0.0101	-0.0042	0.0279	-0.0278	0.0098	-0.0015	0.0277	-0.0252	0.0096	0.0004	0.0277	-0.0235
0.12	0.0779	0.0634	0.1072	0.0216	0.0774	0.0660	0.1071	0.0237	0.0768	0.0678	0.1070	0.0252
0.20	0.1594	0.1364	0.1986	0.0767	0.1586	0.1389	0.1985	0.0787	0.1574	0.1408	0.1982	0.0802
0.30	0.2670	0.2208	0.3139	0.1438	0.2656	0.2234	0.3135	0.1458	0.2636	0.2258	0.3128	0.1478
0.40	0.3805	0.2971	0.4304	0.2089	0.3783	0.3003	0.4295	0.2113	0.3752	0.3036	0.4281	0.2143
0.50	0.4991	0.3650	0.5480	0.2719	0.4961	0.3690	0.5465	0.2752	0.4918	0.3737	0.5441	0.2796
0.60	0.6224	0.4242	0.6666	0.3329	0.6184	0.4293	0.6643	0.3374	0.6128	0.4358	0.6607	0.3438
0.70	0.7496	0.4743	0.7863	0.3919	0.7446	0.4810	0.7829	0.3981	0.7377	0.4898	0.7780	0.4069
0.80	0.8800	0.5152	0.9069	0.4489	0.8741	0.5237	0.9023	0.4571	0.8658	0.5355	0.8958	0.4689
0.88	0.9862	0.5410	1.0041	0.4930	0.9795	0.5514	0.9984	0.5033	0.9704	0.5658	0.9906	0.5177
0.95	1.0802	0.5586	1.0895	0.5306	1.0729	0.5708	1.0829	0.5428	1.0630	0.5879	1.0738	0.5599
1.00	1.1478	0.5683	1.1508	0.5568	1.1401	0.5819	1.1434	0.5706	1.1297	0.6010	1.1334	0.5897
L.E. CIRCLE CENTER			-0.0316	-0.0586			-0.0319	-0.0557			-0.0320	-0.0536
T.E. CIRCLE CENTER			1.1485	0.5623			1.1410	0.5760			1.1308	0.5951
LER = 0.0060 CHORD = 1.3455			TER = 0.0060		LER = 0.0060 CHORD = 1.3441		TER = 0.0060		LER = 0.0060 CHORD = 1.3435		TER = 0.0060	

Table C-1. Stage E Airfoil Coordinates (Continued)

** BLADE SECTION COORDINATES IN TURBOMACHINE ORIENTATION - ROTOR E REAR AIRFOIL

NUMBER OF BLADES = 70.0 AXIAL LOCATION OF STACKING LINE IN COMPRESSOR = 19.188 IN.

SECTION 19 FOR XCUT OF 16.3250 IN.
SECTION SETTING ANGLE = 30.465

FRACT. OF SURF.	SUCTION SURFACE Z (IN.)	SUCTION SURFACE Y (IN.)	PRESSURE SURFACE Z (IN.)	PRESSURE SURFACE Y (IN.)
0.0	-0.0365	-0.0486	-0.0288	-0.0577
0.05	0.0092	0.0013	0.0276	-0.0227
0.12	0.0759	0.0687	0.1068	0.0260
0.20	0.1557	0.1421	0.1976	0.0813
0.30	0.2605	0.2281	0.3115	0.1499
0.40	0.3705	0.3074	0.4257	0.2180
0.50	0.4853	0.3797	0.5403	0.2857
0.60	0.6045	0.4447	0.6553	0.3529
0.70	0.7275	0.5023	0.7706	0.4196
0.80	0.8538	0.5523	0.8864	0.4860
0.88	0.9570	0.5866	0.9792	0.5388
0.95	1.0487	0.6125	1.0607	0.5848
1.00	1.1148	0.6286	1.1190	0.6175
L.E. CIRCLE CENTER			-0.0320	-0.0526
T.E. CIRCLE CENTER			1.1161	0.6228

LER = 0.0060 TER = 0.0060
CHORD = 1.3440

Table C-1. Stage E Airfoil Coordinates (Continued)

** BLADE SECTION COORDINATES IN TURBOMACHINE ORIENTATION - STATOR E FRONT AIRFOIL

NUMBER OF BLADES = 66.0 AXIAL LOCATION OF STACKING LINE IN COMPRESSOR = 23.276 IN.

FRACT. OF SURF.	SECTION 1 FOR XCUT OF 20.1990 IN. SECTION SETTING ANGLE = 75.491 SUCTION SURFACE Z (IN.)	SUCTION SURFACE Y (IN.)	PRESSURE SURFACE Z (IN.)	PRESSURE SURFACE Y (IN.)	SECTION 2 FOR XCUT OF 20.1560 IN. SECTION SETTING ANGLE = 73.596 SUCTION SURFACE Z (IN.)	SUCTION SURFACE Y (IN.)	PRESSURE SURFACE Z (IN.)	PRESSURE SURFACE Y (IN.)	SECTION 3 FOR XCUT OF 20.1140 IN. SECTION SETTING ANGLE = 65.397 SUCTION SURFACE Z (IN.)	SUCTION SURFACE Y (IN.)	PRESSURE SURFACE Z (IN.)	PRESSURE SURFACE Y (IN.)
0.0	-0.3901	-1.5309	-0.2134	-1.5699	-0.5426	-1.3509	-0.4034	-1.3864	-0.6676	-1.1985	-0.5591	-1.2308
0.05	-0.3996	-1.4573	-0.2242	-1.4912	-0.5400	-1.2832	-0.3986	-1.3176	-0.6553	-1.1355	-0.5419	-1.1702
0.10	-0.4055	-1.3552	-0.2321	-1.3831	-0.5302	-1.1894	-0.3867	-1.2228	-0.6327	-1.0487	-0.5140	-1.0865
0.20	-0.4028	-1.2394	-0.2321	-1.2619	-0.5111	-1.0835	-0.3667	-1.1160	-0.6002	-0.9512	-0.4777	-0.9918
0.30	-0.3875	-1.0950	-0.2210	-1.1125	-0.4770	-0.9525	-0.3335	-0.9840	-0.5508	-0.8314	-0.4267	-0.8745
0.40	-0.3612	-0.9499	-0.1998	-0.9642	-0.4335	-0.8220	-0.2930	-0.8528	-0.4932	-0.7131	-0.3704	-0.7576
0.50	-0.3258	-0.8024	-0.1702	-0.8160	-0.3822	-0.6907	-0.2464	-0.7213	-0.4289	-0.5955	-0.3098	-0.6404
0.60	-0.2805	-0.6525	-0.1367	-0.6652	-0.3226	-0.5585	-0.1969	-0.5877	-0.3575	-0.4784	-0.2473	-0.5215
0.70	-0.2254	-0.4991	-0.1016	-0.5101	-0.2547	-0.4248	-0.1467	-0.4505	-0.2790	-0.3613	-0.1844	-0.3994
0.80	-0.1615	-0.3409	-0.0660	-0.3496	-0.1795	-0.2883	-0.0963	-0.3087	-0.1944	-0.2434	-0.1217	-0.2735
0.88	-0.1045	-0.2098	-0.0375	-0.2165	-0.1144	-0.1763	-0.0562	-0.1912	-0.1227	-0.1477	-0.0719	-0.1696
0.95	-0.0506	-0.0912	-0.0130	-0.0960	-0.0542	-0.0757	-0.0216	-0.0851	-0.0571	-0.0625	-0.0289	-0.0758
1.00	-0.0098	-0.0039	0.0041	-0.0073	-0.0092	-0.0022	0.0027	-0.0072	-0.0087	-0.0007	0.0015	-0.0070
L.E. CIRCLE CENTER			-0.3018	-1.5506			-0.4726	-1.3674			-0.6126	-1.2122
T.E. CIRCLE CENTER			-0.0031	-0.0065			-0.0036	-0.0054			-0.0040	-0.0045
LER = -0.0904 CHORD = 1.4894			TER = 0.0072		LER = 0.0718 CHORD = 1.5188		TER = 0.0065		LER = 0.0567 CHORD = 1.4150		TER = 0.0061	

FRACT. OF SURF.	SECTION 4 FOR XCUT OF 20.0700 IN. SECTION SETTING ANGLE = 57.394 SUCTION SURFACE Z (IN.)	SUCTION SURFACE Y (IN.)	PRESSURE SURFACE Z (IN.)	PRESSURE SURFACE Y (IN.)	SECTION 5 FOR XCUT OF 20.0350 IN. SECTION SETTING ANGLE = 51.710 SUCTION SURFACE Z (IN.)	SUCTION SURFACE Y (IN.)	PRESSURE SURFACE Z (IN.)	PRESSURE SURFACE Y (IN.)	SECTION 6 FOR XCUT OF 20.0199 IN. SECTION SETTING ANGLE = 49.477 SUCTION SURFACE Z (IN.)	SUCTION SURFACE Y (IN.)	PRESSURE SURFACE Z (IN.)	PRESSURE SURFACE Y (IN.)
0.0	-0.7755	-1.0618	-0.6936	-1.0910	-0.8460	-0.9685	-0.7814	-0.9955	-0.8725	-0.9322	-0.8144	-0.9583
0.05	-0.7548	-1.0030	-0.6657	-1.0376	-0.8199	-0.9126	-0.7468	-0.9469	-0.8445	-0.8774	-0.7774	-0.9116
0.10	-0.7214	-0.9223	-0.6244	-0.9636	-0.7795	-0.8360	-0.6970	-0.8794	-0.8014	-0.8024	-0.7244	-0.8466
0.20	-0.6774	-0.8322	-0.5743	-0.8797	-0.7281	-0.7508	-0.6380	-0.8028	-0.7472	-0.7191	-0.6621	-0.7727
0.30	-0.6149	-0.7223	-0.5080	-0.7754	-0.6571	-0.6476	-0.5618	-0.7074	-0.6730	-0.6185	-0.5823	-0.6807
0.40	-0.5453	-0.6150	-0.4382	-0.6714	-0.5796	-0.5478	-0.4832	-0.6121	-0.5926	-0.5215	-0.5004	-0.5888
0.50	-0.4697	-0.5096	-0.3655	-0.5671	-0.4967	-0.4506	-0.4026	-0.5165	-0.5070	-0.4276	-0.4168	-0.4967
0.60	-0.3880	-0.4060	-0.2916	-0.4613	-0.4083	-0.3562	-0.3213	-0.4197	-0.4160	-0.3368	-0.3327	-0.4034
0.70	-0.3004	-0.3039	-0.2177	-0.3530	-0.3146	-0.2644	-0.2401	-0.3209	-0.3201	-0.2490	-0.2487	-0.3083
0.80	-0.2076	-0.2027	-0.1442	-0.2416	-0.2164	-0.1747	-0.1594	-0.2195	-0.2197	-0.1637	-0.1652	-0.2108
0.88	-0.1300	-0.1218	-0.0859	-0.1498	-0.1348	-0.1039	-0.0953	-0.1362	-0.1367	-0.0969	-0.0989	-0.1308
0.95	-0.0597	-0.0506	-0.0353	-0.0673	-0.0614	-0.0424	-0.0396	-0.0614	-0.0621	-0.0392	-0.0413	-0.0591
1.00	-0.0083	0.0005	0.0005	-0.0069	-0.0080	0.0014	-0.0002	-0.0069	-0.0079	0.0017	-0.0005	-0.0068
L.E. CIRCLE CENTER			-0.7334	-1.0732			-0.8124	-0.9788			-0.8421	-0.9422
T.E. CIRCLE CENTER			-0.0044	-0.0038			-0.0047	-0.0033			-0.0048	-0.0031
LER = 0.0436 CHORD = 1.3437			TER = 0.0058		LER = 0.0352 CHORD = 1.3074		TER = 0.0057		LER = 0.0320 CHORD = 1.2959		TER = 0.0057	

Table C-1. Stage E Airfoil Coordinates (Continued)

** BLADE SECTION COORDINATES IN TURBOMACHINE ORIENTATION - STATOR E FRONT AIRFOIL

NUMBER OF BLADES = 66.0 AXIAL LOCATION OF STACKING LINE IN COMPRESSOR = 23.276 IN.

FRACT. OF SURF.	SECTION 7 FOR XCUT OF 19.9950 IN. SECTION SETTING ANGLE = 46.098 SUCTION SURFACE Z (IN.)	SUCTION SURFACE Y (IN.)	PRESSURE SURFACE Z (IN.)	PRESSURE SURFACE Y (IN.)	SECTION 8 FOR XCUT OF 19.9520 IN. SECTION SETTING ANGLE = 41.145 SUCTION SURFACE Z (IN.)	SUCTION SURFACE Y (IN.)	PRESSURE SURFACE Z (IN.)	PRESSURE SURFACE Y (IN.)	SECTION 9 FOR XCUT OF 19.9020 IN. SECTION SETTING ANGLE = 36.707 SUCTION SURFACE Z (IN.)	SUCTION SURFACE Y (IN.)	PRESSURE SURFACE Z (IN.)	PRESSURE SURFACE Y (IN.)
0.0	-0.9115	-0.8774	-0.8630	-0.9019	-0.9659	-0.7963	-0.9309	-0.8185	-1.0112	-0.7215	-0.9873	-0.7413
0.05	-0.8805	-0.8241	-0.8225	-0.8580	-0.9310	-0.7453	-0.8856	-0.7785	-0.9730	-0.6727	-0.9384	-0.7049
0.12	-0.8336	-0.7515	-0.7648	-0.7968	-0.8788	-0.6761	-0.8217	-0.7228	-0.9167	-0.6065	-0.8697	-0.6540
0.20	-0.7755	-0.6711	-0.6978	-0.7271	-0.8151	-0.5999	-0.7482	-0.6592	-0.8485	-0.5340	-0.7912	-0.5960
0.30	-0.6966	-0.5744	-0.6126	-0.6403	-0.7299	-0.5088	-0.6557	-0.5799	-0.7581	-0.4481	-0.6927	-0.5236
0.40	-0.6119	-0.4817	-0.5259	-0.5535	-0.6392	-0.4225	-0.5623	-0.5007	-0.6624	-0.3675	-0.5939	-0.4513
0.50	-0.5222	-0.3926	-0.4379	-0.4665	-0.5438	-0.3406	-0.4683	-0.4214	-0.5623	-0.2921	-0.4947	-0.3790
0.60	-0.4275	-0.3072	-0.3496	-0.3786	-0.4438	-0.2632	-0.3741	-0.3414	-0.4579	-0.2222	-0.3956	-0.3064
0.70	-0.3281	-0.2255	-0.2616	-0.2891	-0.3397	-0.1905	-0.2802	-0.2603	-0.3496	-0.1578	-0.2967	-0.2331
0.80	-0.2247	-0.1470	-0.1740	-0.1976	-0.2319	-0.1222	-0.1867	-0.1777	-0.2381	-0.0989	-0.1980	-0.1589
0.88	-0.1394	-0.0863	-0.1044	-0.1226	-0.1434	-0.0704	-0.1123	-0.1103	-0.1468	-0.0556	-0.1194	-0.0987
0.95	-0.0631	-0.0343	-0.0439	-0.0556	-0.0645	-0.0271	-0.0476	-0.0504	-0.0657	-0.0203	-0.0509	-0.0454
1.00	-0.0077	0.0022	-0.0009	-0.0068	-0.0074	0.0028	-0.0015	-0.0068	-0.0072	0.0034	-0.0021	-0.0068
L.E. CIRCLE CENTER			-0.8858	-0.8868			-0.9469	-0.8051			-0.9979	-0.7297
T.E. CIRCLE CENTER			-0.0049	-0.0028			-0.0052	-0.0024			-0.0054	-0.0021
LER = 0.0274 CHORD = 1.2810			TER = 0.0057		LER = 0.0209 CHORD = 1.2640		TER = 0.0057		LER = 0.0157 CHORD = 1.2521		TER = 0.0058	

FRACT. OF SURF.	SECTION 10 FOR XCUT OF 19.8380 IN. SECTION SETTING ANGLE = 32.793 SUCTION SURFACE Z (IN.)	SUCTION SURFACE Y (IN.)	PRESSURE SURFACE Z (IN.)	PRESSURE SURFACE Y (IN.)	SECTION 11 FOR XCUT OF 19.7450 IN. SECTION SETTING ANGLE = 29.739 SUCTION SURFACE Z (IN.)	SUCTION SURFACE Y (IN.)	PRESSURE SURFACE Z (IN.)	PRESSURE SURFACE Y (IN.)	SECTION 12 FOR XCUT OF 19.6170 IN. SECTION SETTING ANGLE = 28.099 SUCTION SURFACE Z (IN.)	SUCTION SURFACE Y (IN.)	PRESSURE SURFACE Z (IN.)	PRESSURE SURFACE Y (IN.)
0.0	-1.0462	-0.6523	-1.0310	-0.6695	-1.0647	-0.5933	-1.0541	-0.6075	-1.0713	-0.5607	-1.0621	-0.5725
0.05	-1.0057	-0.6053	-0.9796	-0.6362	-1.0231	-0.5478	-1.0023	-0.5766	-1.0288	-0.5165	-1.0096	-0.5434
0.12	-0.9463	-0.5419	-0.9078	-0.5896	-0.9623	-0.4866	-0.9295	-0.5335	-0.9667	-0.4570	-0.9361	-0.5027
0.20	-0.8748	-0.4727	-0.8257	-0.5365	-0.8893	-0.4201	-0.8462	-0.4844	-0.8926	-0.3926	-0.8519	-0.4564
0.30	-0.7804	-0.3914	-0.7229	-0.4703	-0.7931	-0.3427	-0.7418	-0.4235	-0.7952	-0.3178	-0.7466	-0.3988
0.40	-0.6811	-0.3161	-0.6201	-0.4044	-0.6919	-0.2717	-0.6370	-0.3630	-0.6931	-0.2495	-0.6411	-0.3415
0.50	-0.5773	-0.2467	-0.5170	-0.3387	-0.5862	-0.2074	-0.5319	-0.3029	-0.5867	-0.1882	-0.5353	-0.2846
0.60	-0.4694	-0.1836	-0.4139	-0.2731	-0.4764	-0.1502	-0.4266	-0.2433	-0.4764	-0.1340	-0.4293	-0.2281
0.70	-0.3579	-0.1270	-0.3109	-0.2072	-0.3630	-0.1002	-0.3209	-0.1839	-0.3628	-0.0874	-0.3231	-0.1720
0.80	-0.2432	-0.0769	-0.2079	-0.1409	-0.2465	-0.0578	-0.2151	-0.1248	-0.2462	-0.0484	-0.2167	-0.1162
0.88	-0.1497	-0.0415	-0.1257	-0.0876	-0.1515	-0.0293	-0.1303	-0.0776	-0.1513	-0.0233	-0.1315	-0.0723
0.95	-0.0657	-0.0139	-0.0538	-0.0407	-0.0673	-0.0084	-0.0561	-0.0364	-0.0672	-0.0058	-0.0567	-0.0341
1.00	-0.0069	0.0039	-0.0026	-0.0069	-0.0067	0.0042	-0.0030	-0.0070	-0.0066	0.0042	-0.0031	-0.0071
L.E. CIRCLE CENTER			-1.0373	-0.6598			-1.0583	-0.5996			-1.0658	-0.5659
T.E. CIRCLE CENTER			-0.0056	-0.0019			-0.0057	-0.0017			-0.0057	-0.0017
LER = 0.0116 CHORD = 1.2411			TER = 0.0059		LER = 0.0090 CHORD = 1.2255		TER = 0.0060		LER = 0.0076 CHORD = 1.2144		TER = 0.0060	

Table C-1. Stage E Airfoil Coordinates (Continued)

** BLADE SECTION COORDINATES IN TURBOMACHINE ORIENTATION - STATOR E FRONT AIRFOIL

NUMBER OF BLADES = 66.0 AXIAL LOCATION OF STACKING LINE IN COMPRESSOR = 23.276 IN.

FRACT. OF SURF.	SECTION 13 FOR XCUT OF 19.3710 IN. SECTION SETTING ANGLE = 26.778 SUCTION SURFACE Z (IN.)	SUCTION SURFACE Y (IN.)	PRESSURE SURFACE Z (IN.)	PRESSURE SURFACE Y (IN.)	SECTION 14 FOR XCUT OF 18.9240 IN. SECTION SETTING ANGLE = 26.340 SUCTION SURFACE Z (IN.)	SUCTION SURFACE Y (IN.)	PRESSURE SURFACE Z (IN.)	PRESSURE SURFACE Y (IN.)	SECTION 15 FOR XCUT OF 18.4670 IN. SECTION SETTING ANGLE = 26.574 SUCTION SURFACE Z (IN.)	SUCTION SURFACE Y (IN.)	PRESSURE SURFACE Z (IN.)	PRESSURE SURFACE Y (IN.)
0.0	-1.0801	-0.5373	-1.0730	-0.5470	-1.0828	-0.5286	-1.0758	-0.5382	-1.0801	-0.5328	-1.0731	-0.5423
0.05	-1.0366	-0.4942	-1.0197	-0.5196	-1.0389	-0.4859	-1.0224	-0.5113	-1.0366	-0.4897	-1.0199	-0.5149
0.12	-0.9732	-0.4363	-0.9450	-0.4813	-0.9752	-0.4286	-0.9475	-0.4736	-0.9734	-0.4319	-0.9454	-0.4766
0.20	-0.8977	-0.3739	-0.8596	-0.4377	-0.8993	-0.3668	-0.8619	-0.4306	-0.8979	-0.3695	-0.8602	-0.4330
0.30	-0.7998	-0.3016	-0.7529	-0.3832	-0.8001	-0.2953	-0.7548	-0.3771	-0.7992	-0.2974	-0.7535	-0.3788
0.40	-0.6955	-0.2360	-0.6460	-0.3289	-0.6963	-0.2305	-0.6477	-0.3237	-0.6958	-0.2320	-0.6467	-0.3248
0.50	-0.5880	-0.1773	-0.5391	-0.2748	-0.5886	-0.1727	-0.5405	-0.2705	-0.5883	-0.1737	-0.5398	-0.2712
0.60	-0.4770	-0.1258	-0.4321	-0.2209	-0.4773	-0.1222	-0.4331	-0.2175	-0.4772	-0.1227	-0.4327	-0.2178
0.70	-0.3628	-0.0817	-0.3250	-0.1671	-0.3630	-0.0790	-0.3257	-0.1647	-0.3630	-0.0792	-0.3255	-0.1647
0.80	-0.2460	-0.0453	-0.2178	-0.1136	-0.2461	-0.0435	-0.2183	-0.1120	-0.2461	-0.0435	-0.2182	-0.1119
0.88	-0.1510	-0.0217	-0.1320	-0.0709	-0.1510	-0.0206	-0.1323	-0.0700	-0.1510	-0.0206	-0.1322	-0.0698
0.95	-0.0670	-0.0052	-0.0568	-0.0336	-0.0670	-0.0048	-0.0569	-0.0333	-0.0670	-0.0047	-0.0569	-0.0332
1.00	-0.0065	0.0042	-0.0031	-0.0071	-0.0065	0.0042	-0.0031	-0.0071	-0.0065	0.0042	-0.0031	-0.0071
L.E. CIRCLE CENTER			-1.0758	-0.5416			-1.0785	-0.5329			-1.0758	-0.5370
T.E. CIRCLE CENTER			-0.0057	-0.0017			-0.0057	-0.0017			-0.0057	-0.0017
LER = 0.0061 CHORD = 1.2106			TER = 0.0060		LER = 0.0060 CHORD = 1.2091		TER = 0.0060		LER = 0.0060 CHORD = 1.2085		TER = 0.0060	

FRACT. OF SURF.	SECTION 16 FOR XCUT OF 18.0320 IN. SECTION SETTING ANGLE = 26.945 SUCTION SURFACE Z (IN.)	SUCTION SURFACE Y (IN.)	PRESSURE SURFACE Z (IN.)	PRESSURE SURFACE Y (IN.)	SECTION 17 FOR XCUT OF 17.5750 IN. SECTION SETTING ANGLE = 27.369 SUCTION SURFACE Z (IN.)	SUCTION SURFACE Y (IN.)	PRESSURE SURFACE Z (IN.)	PRESSURE SURFACE Y (IN.)	SECTION 18 FOR XCUT OF 17.1030 IN. SECTION SETTING ANGLE = 28.317 SUCTION SURFACE Z (IN.)	SUCTION SURFACE Y (IN.)	PRESSURE SURFACE Z (IN.)	PRESSURE SURFACE Y (IN.)
0.0	-1.0770	-0.5399	-1.0698	-0.5493	-1.0735	-0.5481	-1.0663	-0.5575	-1.0664	-0.5670	-1.0590	-0.5761
0.05	-1.0340	-0.4963	-1.0170	-0.5212	-1.0311	-0.5039	-1.0138	-0.5287	-1.0248	-0.5217	-1.0070	-0.5461
0.12	-0.9714	-0.4377	-0.9429	-0.4821	-0.9691	-0.4446	-0.9401	-0.4886	-0.9640	-0.4609	-0.9341	-0.5044
0.20	-0.8965	-0.3745	-0.8581	-0.4376	-0.8948	-0.3805	-0.8558	-0.4432	-0.8909	-0.3951	-0.8505	-0.4571
0.30	-0.7983	-0.3013	-0.7519	-0.3823	-0.7973	-0.3063	-0.7501	-0.3868	-0.7945	-0.3188	-0.7458	-0.3986
0.40	-0.6954	-0.2351	-0.6456	-0.3275	-0.6948	-0.2390	-0.6442	-0.3310	-0.6931	-0.2494	-0.6407	-0.3407
0.50	-0.5882	-0.1760	-0.5390	-0.2731	-0.5880	-0.1790	-0.5380	-0.2757	-0.5870	-0.1874	-0.5353	-0.2834
0.60	-0.4773	-0.1243	-0.4322	-0.2191	-0.4773	-0.1264	-0.4316	-0.2209	-0.4769	-0.1329	-0.4295	-0.2269
0.70	-0.3631	-0.0802	-0.3252	-0.1655	-0.3633	-0.0817	-0.3248	-0.1667	-0.3632	-0.0864	-0.3234	-0.1709
0.80	-0.2463	-0.0440	-0.2180	-0.1123	-0.2464	-0.0449	-0.2178	-0.1130	-0.2465	-0.0479	-0.2169	-0.1157
0.88	-0.1512	-0.0208	-0.1322	-0.0700	-0.1513	-0.0213	-0.1321	-0.0704	-0.1514	-0.0231	-0.1315	-0.0720
0.95	-0.0670	-0.0048	-0.0569	-0.0333	-0.0671	-0.0050	-0.0569	-0.0334	-0.0672	-0.0057	-0.0566	-0.0341
1.00	-0.0065	0.0042	-0.0031	-0.0071	-0.0065	0.0042	-0.0031	-0.0071	-0.0066	0.0041	-0.0030	-0.0072
L.E. CIRCLE CENTER			-1.0726	-0.5440			-1.0691	-0.5522			-1.0619	-0.5709
T.E. CIRCLE CENTER			-0.0057	-0.0017			-0.0057	-0.0017			-0.0057	-0.0018
LER = 0.0060 CHORD = 1.2088			TER = 0.0060		LER = 0.0060 CHORD = 1.2094		TER = 0.0060		LER = 0.0060 CHORD = 1.2118		TER = 0.0060	

Table C-1. Stage E Airfoil Coordinates (Continued)

** BLADE SECTION COORDINATES IN TURBOMACHINE ORIENTATION - STATOR E FRONT AIRFOIL

NUMBER OF BLADES = 66.0 AXIAL LOCATION OF STACKING LINE IN COMPRESSOR = 23.276 IN.

FRACT. OF SURF.	SECTION 19 FOR XCUT OF 16.7110 IN. SECTION SETTING ANGLE = 34.070 SUCTION SURFACE Z (IN.)	SUCTION SURFACE Y (IN.)	PRESSURE SURFACE Z (IN.)	PRESSURE SURFACE Y (IN.)	SECTION 20 FOR XCUT OF 16.5150 IN. SECTION SETTING ANGLE = 43.734 SUCTION SURFACE Z (IN.)	SUCTION SURFACE Y (IN.)	PRESSURE SURFACE Z (IN.)	PRESSURE SURFACE Y (IN.)	SECTION 21 FOR XCUT OF 16.4250 IN. SECTION SETTING ANGLE = 50.505 SUCTION SURFACE Z (IN.)	SUCTION SURFACE Y (IN.)	PRESSURE SURFACE Z (IN.)	PRESSURE SURFACE Y (IN.)
0.0	-1.0159	-0.6771	-1.0069	-0.6866	-0.9079	-0.8460	-0.8900	-0.8579	-0.8233	-0.9628	-0.7991	-0.9768
0.05	-0.9800	-0.6268	-0.9582	-0.6502	-0.8785	-0.7899	-0.8476	-0.8130	-0.7994	-0.9032	-0.7614	-0.9262
0.12	-0.9255	-0.5586	-0.8899	-0.5996	-0.8344	-0.7130	-0.7880	-0.7503	-0.7629	-0.8207	-0.7084	-0.8553
0.20	-0.8592	-0.4840	-0.8114	-0.5422	-0.7799	-0.6275	-0.7195	-0.6790	-0.7169	-0.7281	-0.6475	-0.7746
0.30	-0.7705	-0.3963	-0.7127	-0.4714	-0.7054	-0.5248	-0.6332	-0.5906	-0.6530	-0.6155	-0.5706	-0.6742
0.40	-0.6758	-0.3153	-0.6134	-0.4017	-0.6240	-0.4275	-0.5460	-0.5033	-0.5818	-0.5073	-0.4928	-0.5748
0.50	-0.5753	-0.2416	-0.5133	-0.3330	-0.5360	-0.3364	-0.4578	-0.4172	-0.5034	-0.4042	-0.4138	-0.4766
0.60	-0.4697	-0.1756	-0.4126	-0.2654	-0.4415	-0.2522	-0.3686	-0.3323	-0.4176	-0.3074	-0.3336	-0.3797
0.70	-0.3594	-0.1177	-0.3111	-0.1991	-0.3408	-0.1758	-0.2785	-0.2488	-0.3246	-0.2178	-0.2524	-0.2842
0.80	-0.2451	-0.0684	-0.2090	-0.1339	-0.2344	-0.1076	-0.1872	-0.1667	-0.2249	-0.1360	-0.1698	-0.1902
0.88	-0.1511	-0.0353	-0.1267	-0.0826	-0.1457	-0.0592	-0.1134	-0.1022	-0.1407	-0.0767	-0.1027	-0.1162
0.95	-0.0674	-0.0110	-0.0544	-0.0385	-0.0657	-0.0217	-0.0482	-0.0467	-0.0640	-0.0295	-0.0433	-0.0526
1.00	-0.0069	0.0036	-0.0024	-0.0073	-0.0073	0.0024	-0.0012	-0.0076	-0.0076	0.0016	-0.0003	-0.0077
L.E. CIRCLE CENTER			-1.0111	-0.6811			-0.8981	-0.8506			-0.8103	-0.9682
T.E. CIRCLE CENTER			-0.0055	-0.0022			-0.0051	-0.0031			-0.0047	-0.0037
	LER = 0.0070		TER = 0.0060		LER = 0.0108		TER = 0.0059		LER = 0.0141		TER = 0.0060	
	CHORD = 1.2262				CHORD = 1.2480				CHORD = 1.2768			

FRACT. OF SURF.	SECTION 22 FOR XCUT OF 16.3360 IN. SECTION SETTING ANGLE = 58.613 SUCTION SURFACE Z (IN.)	SUCTION SURFACE Y (IN.)	PRESSURE SURFACE Z (IN.)	PRESSURE SURFACE Y (IN.)
0.0	-0.7132	-1.1075	-0.6803	-1.1243
0.05	-0.6960	-1.0436	-0.6487	-1.0666
0.12	-0.6691	-0.9545	-0.6042	-0.9858
0.20	-0.6341	-0.8534	-0.5531	-0.8934
0.30	-0.5837	-0.7288	-0.4886	-0.7783
0.40	-0.5256	-0.6072	-0.4229	-0.6640
0.50	-0.4596	-0.4894	-0.3559	-0.5509
0.60	-0.3853	-0.3768	-0.2875	-0.4390
0.70	-0.3026	-0.2708	-0.2179	-0.3284
0.80	-0.2118	-0.1721	-0.1468	-0.2195
0.83	-0.1336	-0.0989	-0.0887	-0.1338
0.95	-0.0615	-0.0394	-0.0368	-0.0599
1.00	-0.0080	0.0005	0.0008	-0.0079
L.E. CIRCLE CENTER			-0.6957	-0.1138
T.E. CIRCLE CENTER			-0.0043	-0.0044
	LER = 0.0186		TER = 0.0061	
	CHORD = 1.3319			

Table C-1. Stage E Airfoil Coordinates (Continued)

** BLADE SECTION COORDINATES IN TURBOMACHINE ORIENTATION - STATOR E REAR AIRFOIL

NUMBER OF BLADES = 66.0 AXIAL LOCATION OF STACKING LINE IN COMPRESSOR = 23.276 IN.

FRACT. OF SURF.	SECTION 1 FOR XCUT OF 20.1990 IN. SECTION SETTING ANGLE = 56.240 SUCTION SURFACE Z (IN.)	SUCTION SURFACE Y (IN.)	PRESSURE SURFACE Z (IN.)	PRESSURE SURFACE Y (IN.)	SECTION 2 FOR XCUT OF 20.1560 IN. SECTION SETTING ANGLE = 49.444 SUCTION SURFACE Z (IN.)	SUCTION SURFACE Y (IN.)	PRESSURE SURFACE Z (IN.)	PRESSURE SURFACE Y (IN.)	SECTION 3 FOR XCUT OF 20.1140 IN. SECTION SETTING ANGLE = 42.489 SUCTION SURFACE Z (IN.)	SUCTION SURFACE Y (IN.)	PRESSURE SURFACE Z (IN.)	PRESSURE SURFACE Y (IN.)
0.0	0.0013	-0.2587	0.0167	-0.2664	0.0017	-0.2426	0.0149	-0.2511	0.0020	-0.2283	0.0134	-0.2374
0.05	0.0139	-0.1776	0.0507	-0.2013	0.0228	-0.1725	0.0541	-0.1975	0.0303	-0.1673	0.0569	-0.1933
0.12	0.0383	-0.0673	0.1001	-0.1102	0.0580	-0.0775	0.1103	-0.1224	0.0746	-0.0851	0.1188	-0.1316
0.20	0.0750	0.0549	0.1589	-0.0059	0.1056	0.0271	0.1762	-0.0364	0.1314	0.0047	0.1908	-0.0609
0.30	0.1329	0.2032	0.2356	0.1256	0.1751	0.1530	0.2612	0.0722	0.2108	0.1118	0.2827	0.0283
0.40	0.2033	0.3479	0.3160	0.2590	0.2550	0.2746	0.3489	0.1823	0.2987	0.2138	0.3767	0.1188
0.50	0.2858	0.4900	0.4001	0.3949	0.3447	0.3926	0.4395	0.2946	0.3947	0.3114	0.4728	0.2110
0.60	0.3800	0.6311	0.4884	0.5326	0.4439	0.5085	0.5333	0.4084	0.4983	0.4057	0.5715	0.3044
0.70	0.4858	0.7729	0.5813	0.6702	0.5525	0.6235	0.6309	0.5223	0.6094	0.4979	0.6730	0.3978
0.80	0.6041	0.9152	0.6791	0.8073	0.6711	0.7377	0.7322	0.6357	0.7283	0.5879	0.7775	0.4910
0.88	0.7082	1.0289	0.7607	0.9159	0.7736	0.8279	0.8161	0.7256	0.8294	0.6579	0.8632	0.5647
0.95	0.8065	1.1275	0.8346	1.0096	0.8689	0.9056	0.8913	0.8031	0.9222	0.7175	0.9398	0.6283
1.00	0.8809	1.1972	0.8887	1.0755	0.9403	0.9601	0.9462	0.8577	0.9911	0.7588	0.9954	0.6730
L.E. CIRCLE CENTER			0.0097	-0.2612			0.0091	-0.2457			0.0085	-0.2318
T.E. CIRCLE CENTER			0.8806	1.1361			0.9398	0.9087			0.9902	0.7158
	LER = 0.0088		TER = 0.0611		LER = 0.0080		TER = 0.0514		LER = 0.0074		TER = 0.0431	
	CHORD = 1.7164				CHORD = 1.5422				CHORD = 1.4148			

FRACT. OF SURF.	SECTION 4 FOR XCUT OF 20.0700 IN. SECTION SETTING ANGLE = 35.240 SUCTION SURFACE Z (IN.)	SUCTION SURFACE Y (IN.)	PRESSURE SURFACE Z (IN.)	PRESSURE SURFACE Y (IN.)	SECTION 5 FOR XCUT OF 20.0350 IN. SECTION SETTING ANGLE = 29.765 SUCTION SURFACE Z (IN.)	SUCTION SURFACE Y (IN.)	PRESSURE SURFACE Z (IN.)	PRESSURE SURFACE Y (IN.)	SECTION 6 FOR XCUT OF 20.0199 IN. SECTION SETTING ANGLE = 27.532 SUCTION SURFACE Z (IN.)	SUCTION SURFACE Y (IN.)	PRESSURE SURFACE Z (IN.)	PRESSURE SURFACE Y (IN.)
0.0	0.0023	-0.2146	0.0120	-0.2243	0.0025	-0.2048	0.0111	-0.2148	0.0026	-0.2008	0.0107	-0.2110
0.05	0.0370	-0.1617	0.0594	-0.1886	0.0415	-0.1572	0.0610	-0.1848	0.0432	-0.1553	0.0616	-0.1831
0.12	0.0894	-0.0938	0.1264	-0.1388	0.0994	-0.0939	0.1314	-0.1428	0.1033	-0.0949	0.1334	-0.1441
0.20	0.1545	-0.0140	0.2038	-0.0816	0.1701	-0.0259	0.2126	-0.0948	0.1762	-0.0303	0.2159	-0.0997
0.30	0.2427	0.0762	0.3019	-0.0097	0.2644	0.0530	0.3149	-0.0345	0.2728	0.0442	0.3199	-0.0439
0.40	0.3379	0.1607	0.4016	0.0632	0.3646	0.1255	0.4184	0.0264	0.3750	0.1122	0.4249	0.0123
0.50	0.4396	0.2399	0.5027	0.1373	0.4703	0.1922	0.5231	0.0881	0.4822	0.1739	0.5309	0.0693
0.60	0.5473	0.3148	0.6057	0.2123	0.5808	0.2536	0.6291	0.1504	0.5939	0.2301	0.6382	0.1266
0.70	0.6607	0.3861	0.7109	0.2872	0.6959	0.3106	0.7369	0.2125	0.7097	0.2815	0.7470	0.1837
0.80	0.7801	0.4540	0.8183	0.3618	0.8156	0.3632	0.8464	0.2742	0.8295	0.3281	0.8573	0.2403
0.88	0.8799	0.5057	0.9059	0.4207	0.9147	0.4020	0.9352	0.3228	0.9283	0.3618	0.9467	0.2848
0.95	0.9705	0.5486	0.9837	0.4715	1.0038	0.4334	1.0140	0.3647	1.0168	0.3886	1.0258	0.3231
1.00	1.0371	0.5778	1.0400	0.5072	1.0688	0.4541	1.0707	0.3940	1.0812	0.4060	1.0828	0.3499
L.E. CIRCLE CENTER			0.0080	-0.2186			0.0077	-0.2090			0.0076	-0.2052
T.E. CIRCLE CENTER			1.0358	0.5424			1.0671	0.4240			1.0794	0.3779
	LER = 0.0070		TER = 0.0355		LER = 0.0067		TER = 0.0302		LER = 0.0066		TER = 0.0282	
	CHORD = 1.3212				CHORD = 1.2710				CHORD = 1.2549			

Table C-1. Stage E Airfoil Coordinates (Continued)

** BLADE SECTION COORDINATES IN TURBOMACHINE ORIENTATION - STATOR E REAR AIRFOIL

NUMBER OF BLADES = 66.0 AXIAL LOCATION OF STACKING LINE IN COMPRESSOR = 23.276 IN.

FRACT. OF SURF.	SECTION 7 FOR XCUT OF 19.9950 IN. SECTION SETTING ANGLE = 24.060 SUCTION SURFACE Z (IN.)	SUCTION SURFACE Y (IN.)	PRESSURE SURFACE Z (IN.)	PRESSURE SURFACE Y (IN.)	SECTION 8 FOR XCUT OF 19.9520 IN. SECTION SETTING ANGLE = 18.756 SUCTION SURFACE Z (IN.)	SUCTION SURFACE Y (IN.)	PRESSURE SURFACE Z (IN.)	PRESSURE SURFACE Y (IN.)	SECTION 9 FOR XCUT OF 19.9020 IN. SECTION SETTING ANGLE = 13.760 SUCTION SURFACE Z (IN.)	SUCTION SURFACE Y (IN.)	PRESSURE SURFACE Z (IN.)	PRESSURE SURFACE Y (IN.)
0.0	0.0027	-0.1947	0.0102	-0.2050	0.0029	-0.1850	0.0094	-0.1957	0.0030	-0.1755	0.0086	-0.1864
0.05	0.0458	-0.1522	0.0626	-0.1803	0.0496	-0.1470	0.0639	-0.1755	0.0530	-0.1413	0.0651	-0.1702
0.12	0.1091	-0.0961	0.1363	-0.1459	0.1176	-0.0971	0.1405	-0.1476	0.1252	-0.0969	0.1442	-0.1480
0.20	0.1853	-0.0366	0.2210	-0.1067	0.1986	-0.0449	0.2283	-0.1161	0.2106	-0.0512	0.2348	-0.1233
0.30	0.2855	0.0313	0.3275	-0.0577	0.3041	0.0134	0.3385	-0.0770	0.3210	-0.0016	0.3484	-0.0931
0.40	0.3907	0.0923	0.4348	-0.0085	0.4138	0.0641	0.4492	-0.0381	0.4349	0.0397	0.4622	-0.0637
0.50	0.5003	0.1466	0.5429	0.0412	0.5269	0.1074	0.5604	0.0007	0.5514	0.0730	0.5763	-0.0349
0.60	0.6137	0.1949	0.6519	0.0909	0.6430	0.1438	0.6722	0.0392	0.6700	0.0983	0.6908	-0.0068
0.70	0.7305	0.2377	0.7623	0.1404	0.7615	0.1737	0.7849	0.0772	0.7901	0.1161	0.8058	0.0203
0.80	0.8506	0.2751	0.8739	0.1892	0.8821	0.1973	0.8985	0.1143	0.9112	0.1266	0.9213	0.0463
0.88	0.9490	0.3011	0.9641	0.2275	0.9798	0.2115	0.9900	0.1432	1.0085	0.1297	1.0141	0.0662
0.95	1.0367	0.3208	1.0438	0.2604	1.0662	0.2206	1.0706	0.1678	1.0938	0.1286	1.0955	0.0828
1.00	1.1001	0.3331	1.1011	0.2833	1.1283	0.2251	1.1284	0.1848	1.1547	0.1256	1.1539	0.0942
L.E. CIRCLE CENTER			0.0074	-0.1992			0.0070	-0.1898			0.0068	-0.1805
T.E. CIRCLE CENTER			1.0981	0.3081			1.1261	0.2049			1.1523	0.1099
	LER = 0.0065		TER = 0.0250		LER = 0.0063		TER = 0.0203		LER = 0.0062		TER = 0.0158	
	CHORD = 1.2345				CHORD = 1.2132				CHORD = 1.2038			

FRACT. OF SURF.	SECTION 10 FOR XCUT OF 19.8380 IN. SECTION SETTING ANGLE = 9.117 SUCTION SURFACE Z (IN.)	SUCTION SURFACE Y (IN.)	PRESSURE SURFACE Z (IN.)	PRESSURE SURFACE Y (IN.)	SECTION 11 FOR XCUT OF 19.7450 IN. SECTION SETTING ANGLE = 5.261 SUCTION SURFACE Z (IN.)	SUCTION SURFACE Y (IN.)	PRESSURE SURFACE Z (IN.)	PRESSURE SURFACE Y (IN.)	SECTION 12 FOR XCUT OF 19.6170 IN. SECTION SETTING ANGLE = 3.668 SUCTION SURFACE Z (IN.)	SUCTION SURFACE Y (IN.)	PRESSURE SURFACE Z (IN.)	PRESSURE SURFACE Y (IN.)
0.0	0.0032	-0.1659	0.0080	-0.1770	0.0033	-0.1572	0.0075	-0.1684	0.0033	-0.1573	0.0073	-0.1685
0.05	0.0560	-0.1348	0.0660	-0.1641	0.0582	-0.1283	0.0666	-0.1577	0.0586	-0.1284	0.0665	-0.1577
0.12	0.1320	-0.0951	0.1474	-0.1468	0.1370	-0.0917	0.1495	-0.1436	0.1380	-0.0921	0.1496	-0.1439
0.20	0.2213	-0.0551	0.2405	-0.1279	0.2294	-0.0557	0.2445	-0.1289	0.2313	-0.0568	0.2448	-0.1299
0.30	0.3362	-0.0131	0.3571	-0.1056	0.3480	-0.0195	0.3634	-0.1126	0.3510	-0.0220	0.3643	-0.1150
0.40	0.4540	0.0198	0.4738	-0.0847	0.4690	0.0067	0.4825	-0.0985	0.4734	0.0021	0.4842	-0.1031
0.50	0.5738	0.0436	0.5906	-0.0652	0.5917	0.0229	0.6017	-0.0866	0.5974	0.0154	0.6044	-0.0941
0.60	0.6949	0.0586	0.7077	-0.0469	0.7152	0.0291	0.7210	-0.0767	0.7221	0.0177	0.7247	-0.0879
0.70	0.8167	0.0650	0.8249	-0.0301	0.8387	0.0253	0.8403	-0.0690	0.8466	0.0092	0.8452	-0.0846
0.80	0.9384	0.0628	0.9423	-0.0148	0.9612	0.0118	0.9597	-0.0635	0.9699	-0.0101	0.9656	-0.0842
0.88	1.0354	0.0551	1.0364	-0.0037	1.0581	-0.0059	1.0551	-0.0605	1.0669	-0.0332	1.0620	-0.0858
0.95	1.1197	0.0440	1.1189	0.0051	1.1417	-0.0263	1.1386	-0.0591	1.1504	-0.0589	1.1462	-0.0887
1.00	1.1794	0.0336	1.1778	0.0108	1.2005	-0.0436	1.1982	-0.0588	1.2089	-0.0803	1.2063	-0.0916
L.E. CIRCLE CENTER			0.0065	-0.1710			0.0063	-0.1625			0.0062	-0.1626
T.E. CIRCLE CENTER			1.1773	0.0223			1.1982	-0.0510			1.2067	-0.0857
	LER = 0.0061		TER = 0.0115		LER = 0.0060		TER = 0.0077		LER = 0.0060		TER = 0.0059	
	CHORD = 1.2040				CHORD = 1.2109				CHORD = 1.2148			

Table C-1. Stage E Airfoil Coordinates (Continued)

** BLADE SECTION COORDINATES IN TURBOMACHINE ORIENTATION - STATOR E REAR AIRFOIL

NUMBER OF BLADES = 66.0 AXIAL LOCATION OF STACKING LINE IN COMPRESSOR = 23.276 IN.

FRACT. OF SURF.	SECTION 13 FOR XCUT OF 19.3710 IN. SECTION SETTING ANGLE = 3.711 SUCTION SURFACE Z (IN.)	SUCTION SURFACE Y (IN.)	PRESSURE SURFACE Z (IN.)	PRESSURE SURFACE Y (IN.)
0.0	0.0034	-0.1551	0.0073	-0.1662
0.05	0.0585	-0.1267	0.0663	-0.1560
0.12	0.1377	-0.0910	0.1491	-0.1427
0.20	0.2305	-0.0562	0.2440	-0.1291
0.30	0.3496	-0.0217	0.3629	-0.1144
0.40	0.4712	0.0023	0.4822	-0.1024
0.50	0.5945	0.0159	0.6016	-0.0931
0.60	0.7185	0.0187	0.7213	-0.0865
0.70	0.8423	0.0107	0.8412	-0.0828
0.80	0.9650	-0.0080	0.9611	-0.0819
0.88	1.0618	-0.0307	1.0571	-0.0833
0.95	1.1450	-0.0561	1.1410	-0.0860
1.00	1.2034	-0.0772	1.2010	-0.0888
L.E. CIRCLE CENTER			0.0062	-0.1603
T.E. CIRCLE CENTER			1.2013	-0.0828
	LER = 0.0060		TER = 0.0060	
	CHORD = 1.2096			

FRACT. OF SURF.	SECTION 14 FOR XCUT OF 18.9240 IN. SECTION SETTING ANGLE = 3.482 SUCTION SURFACE Z (IN.)	SUCTION SURFACE Y (IN.)	PRESSURE SURFACE Z (IN.)	PRESSURE SURFACE Y (IN.)
0.0	0.0035	-0.1562	0.0072	-0.1674
0.05	0.0589	-0.1287	0.0663	-0.1580
0.12	0.1383	-0.0941	0.1492	-0.1459
0.20	0.2314	-0.0605	0.2442	-0.1334
0.30	0.3505	-0.0272	0.3632	-0.1199
0.40	0.4721	-0.0042	0.4824	-0.1088
0.50	0.5951	0.0086	0.6018	-0.1002
0.60	0.7188	0.0110	0.7214	-0.0941
0.70	0.8423	0.0029	0.8411	-0.0905
0.80	0.9647	-0.0156	0.9608	-0.0894
0.88	1.0612	-0.0378	1.0566	-0.0903
0.95	1.1442	-0.0625	1.1404	-0.0925
1.00	1.2026	-0.0832	1.2002	-0.0948
			0.0062	-0.1615
			1.2005	-0.0888
	LER = 0.0060		TER = 0.0060	
	CHORD = 1.2084			

FRACT. OF SURF.	SECTION 15 FOR XCUT OF 18.4670 IN. SECTION SETTING ANGLE = 3.470 SUCTION SURFACE Z (IN.)	SUCTION SURFACE Y (IN.)	PRESSURE SURFACE Z (IN.)	PRESSURE SURFACE Y (IN.)
0.0	0.0035	-0.1546	0.0072	-0.1659
0.05	0.0591	-0.1275	0.0663	-0.1568
0.12	0.1386	-0.0934	0.1493	-0.1451
0.20	0.2318	-0.0602	0.2443	-0.1331
0.30	0.3509	-0.0276	0.3633	-0.1201
0.40	0.4724	-0.0049	0.4825	-0.1094
0.50	0.5953	0.0077	0.6019	-0.1010
0.60	0.7188	0.0101	0.7214	-0.0949
0.70	0.8422	0.0022	0.8411	-0.0911
0.80	0.9644	-0.0159	0.9607	-0.0896
0.88	1.0609	-0.0375	1.0565	-0.0901
0.95	1.1439	-0.0617	1.1403	-0.0917
1.00	1.2024	-0.0819	1.2001	-0.0935
			0.0062	-0.1599
			1.2003	-0.0875
	LER = 0.0060		TER = 0.0060	
	CHORD = 1.2083			

FRACT. OF SURF.	SECTION 16 FOR XCUT OF 18.0320 IN. SECTION SETTING ANGLE = 3.542 SUCTION SURFACE Z (IN.)	SUCTION SURFACE Y (IN.)	PRESSURE SURFACE Z (IN.)	PRESSURE SURFACE Y (IN.)
0.0	0.0035	-0.1525	0.0072	-0.1637
0.05	0.0591	-0.1254	0.0664	-0.1548
0.12	0.1387	-0.0914	0.1494	-0.1431
0.20	0.2318	-0.0583	0.2444	-0.1312
0.30	0.3510	-0.0257	0.3634	-0.1182
0.40	0.4724	-0.0030	0.4826	-0.1075
0.50	0.5953	0.0097	0.6020	-0.0990
0.60	0.7188	0.0122	0.7216	-0.0927
0.70	0.8421	0.0046	0.8412	-0.0887
0.80	0.9644	-0.0131	0.9609	-0.0869
0.88	1.0609	-0.0345	1.0566	-0.0870
0.95	1.1440	-0.0583	1.1404	-0.0883
1.00	1.2025	-0.0783	1.2002	-0.0899
L.E. CIRCLE CENTER			0.0063	-0.1578
T.E. CIRCLE CENTER			1.2004	-0.0839
	LER = 0.0060		TER = 0.0060	
	CHORD = 1.2085			

FRACT. OF SURF.	SECTION 17 FOR XCUT OF 17.5750 IN. SECTION SETTING ANGLE = 3.649 SUCTION SURFACE Z (IN.)	SUCTION SURFACE Y (IN.)	PRESSURE SURFACE Z (IN.)	PRESSURE SURFACE Y (IN.)
0.0	0.0035	-0.1525	0.0072	-0.1638
0.05	0.0590	-0.1252	0.0664	-0.1545
0.12	0.1385	-0.0908	0.1494	-0.1424
0.20	0.2316	-0.0573	0.2444	-0.1300
0.30	0.3508	-0.0242	0.3635	-0.1166
0.40	0.4723	-0.0011	0.4828	-0.1056
0.50	0.5953	0.0119	0.6022	-0.0968
0.60	0.7190	0.0146	0.7219	-0.0904
0.70	0.8424	0.0070	0.8416	-0.0862
0.80	0.9648	-0.0107	0.9614	-0.0844
0.88	1.0614	-0.0321	1.0572	-0.0846
0.95	1.1446	-0.0560	1.1410	-0.0860
1.00	1.2031	-0.0760	1.2009	-0.0877
			0.0063	-0.1579
			1.2011	-0.0817
	LER = 0.0060		TER = 0.0060	
	CHORD = 1.2093			

FRACT. OF SURF.	SECTION 18 FOR XCUT OF 17.1030 IN. SECTION SETTING ANGLE = 4.327 SUCTION SURFACE Z (IN.)	SUCTION SURFACE Y (IN.)	PRESSURE SURFACE Z (IN.)	PRESSURE SURFACE Y (IN.)
0.0	0.0034	-0.1535	0.0074	-0.1647
0.05	0.0584	-0.1247	0.0664	-0.1538
0.12	0.1374	-0.0883	0.1493	-0.1397
0.20	0.2302	-0.0526	0.2443	-0.1252
0.30	0.3492	-0.0171	0.3634	-0.1095
0.40	0.4708	0.0080	0.4827	-0.0965
0.50	0.5941	0.0226	0.6023	-0.0861
0.60	0.7182	0.0266	0.7222	-0.0785
0.70	0.8422	0.0200	0.8421	-0.0734
0.80	0.9652	0.0028	0.9621	-0.0711
0.88	1.0622	-0.0185	1.0582	-0.0711
0.95	1.1458	-0.0425	1.1422	-0.0725
1.00	1.2045	-0.0626	1.2022	-0.0743
			0.0063	-0.1588
			1.2024	-0.0683
	LER = 0.0060		TER = 0.0060	
	CHORD = 1.2116			

Table C-1. Stage E Airfoil Coordinates (Continued)

** BLADE SECTION COORDINATES IN TURBOMACHINE ORIENTATION - STATOR E REAR AIRFOIL

NUMBER OF BLADES = 66.0 AXIAL LOCATION OF STACKING LINE IN COMPRESSOR = 23.276 IN.

FRACT. OF SURF.	SECTION 19 FOR XCUT OF 16.7110 IN. SECTION SETTING ANGLE = 7.140 SUCTION SURFACE Z (IN.)	SUCTION SURFACE Y (IN.)	PRESSURE SURFACE Z (IN.)	PRESSURE SURFACE Y (IN.)	SECTION 20 FOR XCUT OF 16.5150 IN. SECTION SETTING ANGLE = 14.400 SUCTION SURFACE Z (IN.)	SUCTION SURFACE Y (IN.)	PRESSURE SURFACE Z (IN.)	PRESSURE SURFACE Y (IN.)	SECTION 21 FOR XCUT OF 16.4250 IN. SECTION SETTING ANGLE = 20.240 SUCTION SURFACE Z (IN.)	SUCTION SURFACE Y (IN.)	PRESSURE SURFACE Z (IN.)	PRESSURE SURFACE Y (IN.)
0.0	0.0031	-0.1614	0.0081	-0.1721	0.0027	-0.1766	0.0093	-0.1864	0.0025	-0.1866	0.0103	-0.1956
0.05	0.0564	-0.1273	0.0667	-0.1559	0.0511	-0.1341	0.0657	-0.1610	0.0466	-0.1379	0.0645	-0.1633
0.12	0.1336	-0.0838	0.1493	-0.1347	0.1222	-0.0784	0.1454	-0.1270	0.1124	-0.0733	0.1415	-0.1198
0.20	0.2250	-0.0403	0.2441	-0.1126	0.2079	-0.0208	0.2374	-0.0906	0.1930	-0.0050	0.2307	-0.0724
0.30	0.3435	0.0042	0.3634	-0.0882	0.3210	0.0415	0.3539	-0.0487	0.3011	0.0710	0.3443	-0.0170
0.40	0.4656	0.0374	0.4834	-0.0675	0.4399	0.0924	0.4718	-0.0111	0.4164	0.1358	0.4599	0.0341
0.50	0.5902	0.0591	0.6039	-0.0505	0.5631	0.1312	0.5911	0.0223	0.5376	0.1885	0.5773	0.0808
0.60	0.7163	0.0690	0.7249	-0.0372	0.6896	0.1576	0.7114	0.0511	0.6635	0.2287	0.6965	0.1226
0.70	0.8428	0.0672	0.8462	-0.0277	0.8181	0.1716	0.8328	0.0753	0.7927	0.2562	0.8172	0.1593
0.80	0.9685	0.0537	0.9678	-0.0218	0.9472	0.1730	0.9551	0.0949	0.9239	0.2709	0.9393	0.1909
0.88	1.0679	0.0345	1.0651	-0.0199	1.0503	0.1651	1.0533	0.1071	1.0295	0.2732	1.0378	0.2124
0.95	1.1534	0.0117	1.1503	-0.0201	1.1397	0.1517	1.1396	0.1153	1.1217	0.2685	1.1245	0.2285
1.00	1.2135	-0.0080	1.2111	-0.0214	1.2029	0.1384	1.2013	0.1197	1.1873	0.2612	1.1867	0.2384
L.E. CIRCLE CENTER			0.0064	-0.1663			0.0068	-0.1810			0.0071	-0.1905
T.E. CIRCLE CENTER			1.2113	-0.0145			1.2007	0.1292			1.1853	0.2498
	LER = 0.0060		TER = 0.0069		LER = 0.0060		TER = 0.0094		LER = 0.0060		TER = 0.0115	
	CHORD = 1.2273				CHORD = 1.2490				CHORD = 1.2754			

FRACT. OF SURF.	SECTION 22 FOR XCUT OF 16.3360 IN. SECTION SETTING ANGLE = 27.685 SUCTION SURFACE Z (IN.)	SUCTION SURFACE Y (IN.)	PRESSURE SURFACE Z (IN.)	PRESSURE SURFACE Y (IN.)
0.0	0.0022	-0.1984	0.0116	-0.2063
0.05	0.0497	-0.1419	0.0628	-0.1654
0.12	0.0993	-0.0658	0.1359	-0.1095
0.20	0.1728	0.0162	0.2212	-0.0479
0.30	0.2737	0.1101	0.3304	0.0254
0.40	0.3838	0.1932	0.4425	0.0943
0.50	0.5018	0.2644	0.5572	0.1586
0.60	0.6264	0.3232	0.6743	0.2178
0.70	0.7561	0.3691	0.7938	0.2715
0.80	0.8896	0.4019	0.9153	0.3196
0.88	0.9983	0.4185	1.0138	0.3540
0.95	1.0941	0.4259	1.1009	0.3811
1.00	1.1626	0.4272	1.1635	0.3987
L.E. CIRCLE CENTER			0.0075	-0.2016
T.E. CIRCLE CENTER			1.1612	0.4129
	LER = 0.0062		TER = 0.0144	
	CHORD = 1.3277			

APPENDIX D

REFERENCES

1. Brent, J. A., J. G. Cheatham, and A. W. Nilsen, "Single-Stage Experimental Evaluation of Tandem-Airfoil Rotor and Stator Blading for Compressors, Part I - Analysis and Design of Stages A, B, and C," NASA CR-120803, PWA™ FR-4667, June 1972.

2. Brent, J. A., and D. R. Clemmons, "Single-Stage Experimental Evaluation of Tandem-Airfoil Rotor and Stator Blading for Compressors, Part III - Data and Performance for Stage C," NASA CR-120938, PWA FR-5028, August 1972.

3. Brent, J. A., "Single-Stage Experimental Evaluation of Tandem-Airfoil Rotor and Stator Blading for Compressors, Part II - Data and Performance for Stage A," NASA CR-120804, PWA FR-4719, July 1972.

4. Linder, C. G., and B. A. Jones, "Single-Stage Experimental Evaluation of Slotted Rotor and Stator Blading, Part V - Data and Performance for Slotted Rotor 3 - Slotted Stator 2," NASA CR-54548, PWA FR-2285, August 1967.

5. Linder, C. G., and B. A. Jones, "Single-Stage Experimental Evaluation of Slotted Rotor and Stator Blading, Part VIII - Data and Performance for Slotted Stator 3," NASA CR-54551, PWA FR-2288, October 1967.

6. Miller, M. L., and G. Seren, "Single-Stage Experimental Evaluation of Boundary Layer Blowing Techniques for High Lift Stator Blades, Part III - Data and Performance of Single-Slotted 0.65 Hub Diffusion Factor Stator," NASA CR-54566, Allison EDR-5759, June 1968.

7. Carmody, R. H., and G. Seren, "Single-Stage Experimental Evaluation of Boundary Layer Blowing Techniques for High Lift Stator Blades, Part IV - Data and Performance of Double-Slotted 0.75 Hub Diffusion Factor Stator," NASA CR-54567, Allison EDR-5861, August 1968.

8. Horn, R. A., Jr., G. Seren, and R. H. Carmody, "Single-Stage Experimental Evaluation of Boundary Layer Bleed Techniques for High Lift Stator Blades, Part IV - Data and Performance of Triple-Slotted 0.75 Hub Diffusion Factor Stator," NASA CR-54572, Allison EDR-5944, August 1969.

9. Brent, J. A., and B. A. Jones, "Single-Stage Experimental Evaluation of Compressor Blading with Slots and Vortex Generators, Part II - Data and Performance for Stage 5 Without Slots or Vortex Generators," NASA CR-72634, PWA FR-3481, March 1970.

10. Brent, J. A., "Single-Stage Experimental Evaluation of Compressor Blading with Slots and Vortex Generators, Part IV - Supplemental Data for Stage 4," NASA CR-72778, PWA FR-4135, December 1970.

11. "Aerodynamic Design of Axial Flow Compressor" (Revised), NASA SP-36, 1965.

12. Brent, J. A., "Single-Stage Experimental Evaluation of Compressor Blading with Slots and Vortex Generators, Part V - Final Report," NASA CR-72793, PWA FR-4541, March 1972.

13. Smith, Austin G., "On the Generation of the Streamwise Component of Vorticity for Flows in Rotating Passages," The Aeronautical Quarterly, 8, 1957.

14. Dixon, S. L., "Secondary Vorticity in Axial Compressor Blade Rows, "presented at Pennsylvania State Symposium, September 1970.

15. Sanger, N. L., "Analytical Study of the Effects of Geometric Changes on the Flow Characteristics of Tandem-Bladed Compressor Stators," NACA TND-6264, March 1971.

16. Railly, J. W., and El-Sarha, M. E., "Ackeret Method for the Design of Tandem Cascades," The Engineer, 25 June 1965, Pages 1085-1089.

17. Linnemann, H., "Tandem Grid In a Single-Stage Axial Blower," Translated from Konstrucktion by Redstone Scientific Information Center (RSIC) No. 276, 21 September 1964.

18. Giesing, J. P., "Extension of the Douglas Neumann Program to Problems of Lifting, Infinite Cascades," (Revised), Douglas Aircraft Report No. LB 31653, 2 July 1964.

19. Lieblein, S., "Loss and Stall Analysis of Compressor Cascades," Journal of Basic Engineering, September 1969, Pages 387-400.